

UNCLASSIFIED

AD NUMBER
AD378020
CLASSIFICATION CHANGES
TO:                    unclassified
FROM:                confidential
LIMITATION CHANGES
TO: Approved for public release, distribution unlimited
FROM: Controlling DoD Organization: Space and Missile Systems Organization, Los Angeles, CA 90045.
AUTHORITY
31 Dec 1978 per Group-4, DoDD 5200.10 document marking; SAMSO [USAF] ltr dtd 16 Aug 1973

THIS PAGE IS UNCLASSIFIED

# **SECURITY**

---

# **MARKING**

**The classified or limited status of this report applies to each page, unless otherwise marked.**

**Separate page printouts MUST be marked accordingly.**

---

**THIS DOCUMENT CONTAINS INFORMATION AFFECTING THE NATIONAL DEFENSE OF THE UNITED STATES WITHIN THE MEANING OF THE ESPIONAGE LAWS, TITLE 18, U.S.C., SECTIONS 793 AND 794. THE TRANSMISSION OR THE REVELATION OF ITS CONTENTS IN ANY MANNER TO AN UNAUTHORIZED PERSON IS PROHIBITED BY LAW.**

**NOTICE:** When government or other drawings, specifications or other data are used for any purpose other than in connection with a definitely related government procurement operation, the U. S. Government thereby incurs no responsibility, nor any obligation whatsoever; and the fact that the Government may have formulated, furnished, or in any way supplied the said drawings, specifications, or other data is not to be regarded by implication or otherwise as in any manner licensing the holder or any other person or corporation, or conveying any rights or permission to manufacture, use or sell any patented invention that may in any way be related thereto.

AD-378 020

CONTRACT AF 04(09)-150  
SSLV-5 No. 9 POST  
FIRING FLIGHT TEST  
REPORT (FINAL EVALUATION  
REPORT) AND MOL-EFT  
FINAL FLIGHT TEST REPORT (U)

December 1966

DOWNGRADED AT 3 YEAR INTERVALS;  
DECLASSIFIED AFTER 12 YEARS

DOD DIR 5200.10

APPROVED BY:

*R. C. Lea*

R. C. Lea  
Technical Director, Titan IIIC

Martin Company  
Denver, Colorado

Aerospace Division of Martin-Marietta Corporation

CONFIDENTIAL

NOTICE: This document contains information affecting the national defense of the United States, within the meaning of the Espionage Laws, Title 18, USC, Section 793 and 794, the transmission or revelation of which in any manner to an unauthorized person is prohibited by law.

FOREWORD

This document is submitted in compliance with Item I, Exhibit A, Task 5.13 of Contract AF 04(695)-150 in accordance with Contractor Specification SSS-TIII-010-DRD, Program 624A Data Requirements Document, Revision 3, dated 15 April 1963, Line Item 1K-62 (SSLV-5 No. 9 Post Firing Flight Test Report) and Line Item 3C-4 (MOL-EFT Final Flight Test Report).



CONTENTS

	<u>Page</u>
FOREWORD . . . . .	ii
CONTENTS . . . . .	iii
SUMMARY . . . . .	1
1.0 INTRODUCTION . . . . .	5
2.0 CONCLUSIONS . . . . .	6
3.0 TEST RESULTS . . . . .	7
3.1 System Evaluation . . . . .	7
3.1.1 Pre-Countdown . . . . .	7
3.1.2 Countdown . . . . .	7
3.1.3 Flight . . . . .	8
3.2 Airborne Subsystem Evaluation . . . . .	69
3.2.1 Propulsion . . . . .	69
3.2.2 Guidance and Controls . . . . .	191
3.2.3 Airborne Electrical and MDS . . . . .	202
3.2.4 Tracking and Flight Safety . . . . .	206
3.2.5 Instrumentation . . . . .	210
3.2.6 Vehicle Environmental Analysis . . . . .	212
3.2.7 Payload . . . . .	259
3.3 Ground Equipment . . . . .	279
3.3.1 Mechanical AGE . . . . .	279
3.3.2 Electrical AGE . . . . .	288
Addendum (Core & Vehicle Postflight Weight Data) . . . . .	A-1 through A-17

### SUMMARY

Program 624A, Standard Space Launch Vehicle C-9 (MOL/HSQ) was launched from Complex 40 at the Eastern Test Range on 3 November 1966 at 13:50:42.20 GMT (08:50:42.20 EST). This vehicle was the sixth test of the Titan IIIC configuration and the tenth test of 624A program.

The flight test was conducted according to Flight Plan VI. The payload consisted of a MOL simulated laboratory containing 11 experiments and the MOL configuration Gemini capsule using a heat shield containing an egress hatch. The countdown for the vehicle was picked up at T-615 minutes and proceeded without incident until T-30 minutes. A hold was called at that time to evaluate abnormally high winds aloft and their effect on the Gemini wind load constraint ( $Q$ -Alpha) of 4500 lb/deg/ft<sup>2</sup>. During the 1 hour and 45 second hold, it was necessary to repressurize the Stage I oxidizer tank due to decaying pressures resulting from the 44°F ambient temperature. The count was resumed and proceeded until T-3 minutes when another hold lasting 6 minutes was called to evaluate the latest meteorological data. The count was resumed and the vehicle was launched from Pad 40 at 13:50:42.20 GMT (08:50 EST).

Stage 0 operation was satisfactory with accelerations slightly lower than predicted. Stage 0/I separation was normal and airborne staging cameras recording that event were recovered.

Maximum aerodynamic loads occurred at 58 seconds and max  $Q$ -Alpha occurred at 55 seconds. Max  $Q$ -Alpha was approximately 3200 lb-deg/ft<sup>2</sup>, well below the Gemini constraint of 4500 lb-deg/ft<sup>2</sup>.

Stage I operation was satisfactory with acceleration levels higher than predicted. "POGO" oscillations were minimal, approximately 0.1 g's zero-to-peak at 87FSL + 100 seconds. Shutdown was by oxidizer exhaustion. An unexplained transient on the S/A 2 pitch actuator was noted during the engine shutdown transient. Stage I/II separation was normal.

Stage II operation was normal with accelerations slightly lower than predicted. Shutdown was by oxidizer exhaustion. Stage II/III separation was normal.

Stage III first burn operation was normal with accelerations slightly higher than predicted. Shutdown was by velocity-to-be gained with a burn time of 12.799 seconds less than predicted.

Gemini separation was normal and was achieved at an altitude of 523,273 feet to evaluate re-entry effects on the modified heat shield. Re-entry occurred at approximately 400,000 feet and the spacecraft was successfully recovered.

However, the retro operation of the vehicle following spacecraft release left the transtage/sim lab vehicle with a pitch down rate rather than the predicted pitch up rate. Analysis indicates that all retro motors fired normally but torques created by retro motor plume impingement upon adjacent skin surfaces more than compensated for the pitch up torque created by the non-symmetrical arrangement of the motors (3 on top, 2 on the bottom) and the ACS pitch up thrust. Consequently after retro motor burnout the ACS activity to orient the vehicle to a 90 degree pitch up attitude for transtage second burn was considerably longer than scheduled.

The unscheduled ACS activity resulted in throat erosion of 3 ACS nozzles (roll #2, 4 & 8) and excessive propellant line temperatures on the yaw/roll modules from heat soak-back. In addition, all orbital ACS maneuvers required considerably more than scheduled activity due to the reduction of control authority that resulted from ACS nozzle plume impingement forces acting on the relatively long moment arm for this vehicle configuration (distance between vehicle CG and location of the ACS modules). As a result of the additional ACS activities, several peculiarities in the ACS were observed following Gemini separation culminating in loss of vehicle attitude control due to ACS propellant depletion on the 4th and final orbit.

Transtage second burn following Gemini separation was satisfactory. Accelerations were slightly higher than predicted.

During the coast period between second and third burns, ACS back up mode activity was observed, a result of reduced ACS control authority from ACS nozzle plume impingement as previously discussed.

Transtage third burn was satisfactory. Accelerations were slightly lower than predicted. A near circular orbit of 165 by 168 nautical miles was achieved. Following third burn, OV1-6 and OV4-1 (transmitter and receiver) satellites were ejected.

Data indicate more than scheduled ACS activity to control the vehicle at satellite release and to accomplish planned maneuvers following third burn FS2. As previously discussed, the additional activity was a result of reduced ACS control authority due to the normal ACS nozzle plume impingement forces acting on an unusually long moment arm created as a result of the transtage/MOL configuration CG location. The transtage/MOL configuration places the CG approximately 13.3 feet forward of the ACS modules compared to approximately 2 feet forward for other T-IIIC vehicle/payload configurations.

The greater than scheduled ACS activity in both routine maneuvers and as a result of the residual pitch down rates following Gemini separation resulted in excessive propellant temperatures for all ACS modules from heat soak-back. The excessive temperatures in turn caused the oxidizer to vaporize, drastically shifting ACS nozzle mixture ratio during pulsing. As a result chamber pressures were considerably reduced, particularly on the yaw 7 nozzle. Fuel flow was increased due to the reduced chamber back-pressure and more pulses were required at the reduced chamber pressures to produce the required impulses. This inefficient operation plus the additional ACS activity needed due to reduced control authority from plume impingement resulted in ACS propellant exhaustion during the 4th and final orbit and precluded the final planned maneuver which was to impart pitch and roll rates to the vehicle prior to disabling the booster.

Lab support of the experiments was completely satisfactory and results of the 11 experiments have been satisfactory except for the ORBIS LOW experiment (ionospheric sounding experiment), the Corner Reflectors experiment, and the micro-meteoroid detector experiment. None of the experiment failures was attributed to the booster behavior or lab support.

## 1.0 INTRODUCTION

On 3 November 1966, the sixth Titan IIIC standard space launch vehicle flight test was made at the AFETR. Launch of this vehicle C-9 (AF Serial No. 66-002), was from Complex 40 at 13:50:42:20 Greenwich Mean Time (08:50:42:20 EST).

Vehicle 9 consisted of a core vehicle with two United Technology Center solid rocket motors (SRM 11 and SRM 12) positioned parallel to the core in the yaw plane. The flight test was conducted according to Flight Plan VI.

The purpose of the mission was to inject the unmanned Gemini spacecraft into a sub-orbital trajectory which would result in the Gemini spacecraft impacting near Ascension Island. After separation of the Gemini spacecraft it was planned to pitch up the transtage and the Manned Orbiting Laboratory (MOL). The second transtage burn would then produce a transfer orbit having an apogee of 160 n. mi. Upon reaching apogee, a third firing of the transtage main engines would circularize the orbit at approximately 160 n. mi. The OV1-6, OV4-1R, and OV4-1T satellite would then be injected into orbit. Vehicle attitude control was to be maintained for 4 orbits following orbit circularization. At the end of the 4th orbit a pitch and roll rate was to be imparted to the vehicle after which vehicle control was to be disabled.

## **2.0 CONCLUSIONS**

### **2.1 Data Evaluation**

2.1.1 Vehicle SSLV-5 No. 9 performance was satisfactory. No major hardware problems were identified.

2.1.2 Vehicle attitude control at retro-fire following Gemini separation and during the coast periods was less effective than predicted due to plume impingement forces which were not considered in the pre-flight predictions. As a result, ACS propellant exhaustion occurred during the final orbit and several ACS peculiarities were observed.

2.1.3 MML Sim Lab support of the various experiments and satellites was completely satisfactory.

### **2.2 Detailed Test Objectives**

All primary and secondary test objectives for the flight of vehicle C-9 were met. The objectives are described in Aerospace Corporation Report No. T. O.R. -569 (6116-50)-9 Program 624A System Test Objectives for Titan IIIC-9 (AF Serial No. 66-002), Volume I, August, 1966. Determination of accomplishment of each objective is based on the definitions outlined in paragraph 3.1 of that report.

### 3.0 TEST RESULTS

#### 3.1 System Evaluation

##### 3.1.1 Pre-Countdown

The core vehicle with the simulated laboratory was received at Cape Kennedy on the 18th and 20th of August 1966. The core vehicle erection was completed on 21 August 1966. The simulated laboratory was mated to the core on 24 August 1966. Power was applied to the core on 31 August 1966. The vehicle was moved to the SAE on 21 September 1966, and to the launch pad on 27 Sept. 1966. The Gemini "B" spacecraft was mated to the booster on 3 October 1966. The launch CST was conducted on 28 October 1966. A more detailed description of the pre-countdown activities associated with the payload is given in the payload section of this report.

##### 3.1.2 Countdown

The countdown for the vehicle was picked up at T-615 minutes and proceeded without incident until T-30 minutes. A hold was called at that time to evaluate the high winds aloft and their effects on the Gemini wind load constraint (Q-Alpha) of  $4500 \text{ lb/deg/ft}^2$ . During the 1 hour and 45 second hold, it was necessary to repressurize the Stage I oxidizer tank due to decaying pressures resulting from the  $44^\circ \text{F}$  ambient temperature. The count was resumed and proceeded until T-3 minutes when another hold lasting 6 minutes was called to evaluate the latest meteorological data. The count was resumed and the vehicle was launched from Pad 40 at 13:50:42.20 GMT (08:50 EST).



### 3.1.3 Flight

#### 3.1.3.1 Flight Sequence of Events

The flight sequence of events is summarized in Table 1 and significant performance parameters for the various stages are presented in Table 2.

Caution should be exercised when using the various stage performance numbers given in Table 2 and in the sections for performance. Estimate of vehicle performance contained in this report are derived primarily by means of analytical evaluation of differences between predicted and observed axial accelerations and velocity gained within the various phases of flight. For comparative purposes, observed and predicted average values of longitudinal thrust, weight decay rate and effective specific impulse are listed in Table 2. The "quick-look" analytical techniques used in deriving vehicle performance characteristics from trajectory data requires the use of such averages or effective values. Caution should be used in comparing these values to transient or steady state values derived from telemetered internal propulsion system data. Thrust histories are presented based on observed axial accelerations from the IGS and average weight decay rates derived from propellant sensor data.

#### 3.1.3.2 Aerodynamic Environment

##### 3.1.3.2.1 Observed Wind Data

The CKAFS atmospheric sounding data, obtained approximately 30 minutes before liftoff, is presented in Figures 1 and 2. The wind speed profile is presented as a function of altitude in Figure 1 and the wind direction, also a function of altitude, is presented in Figure 2.

A wind sounding taken 3 hours before liftoff showed a maximum wind speed of approximately 150 knots which caused considerable concern in that it was felt that if a launch was attempted in this severe wind environment the Gemini structural constraints might be exceeded. The wind sounding taken 30 minutes before liftoff indicated the maximum wind

0-100000

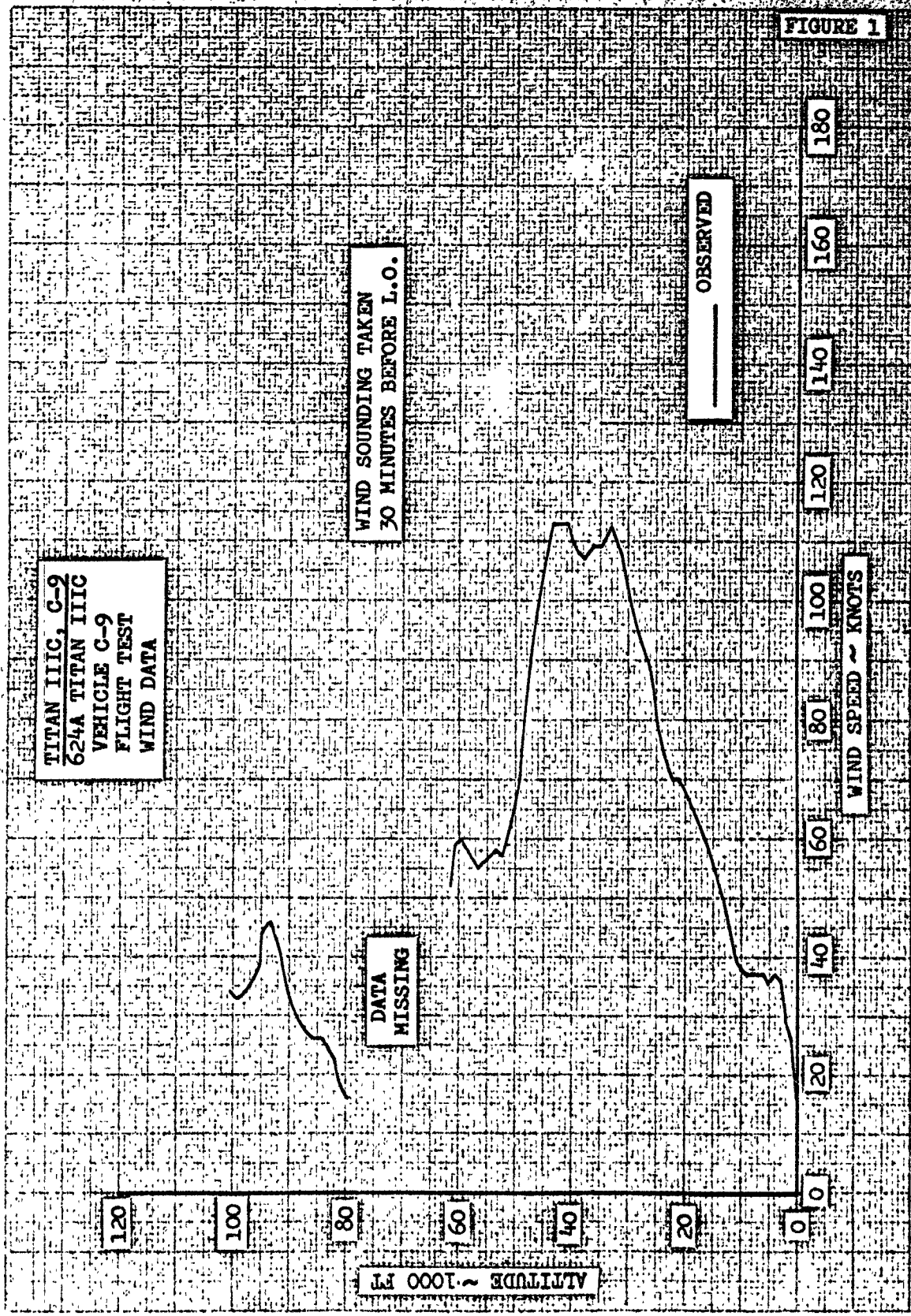


FIGURE 1

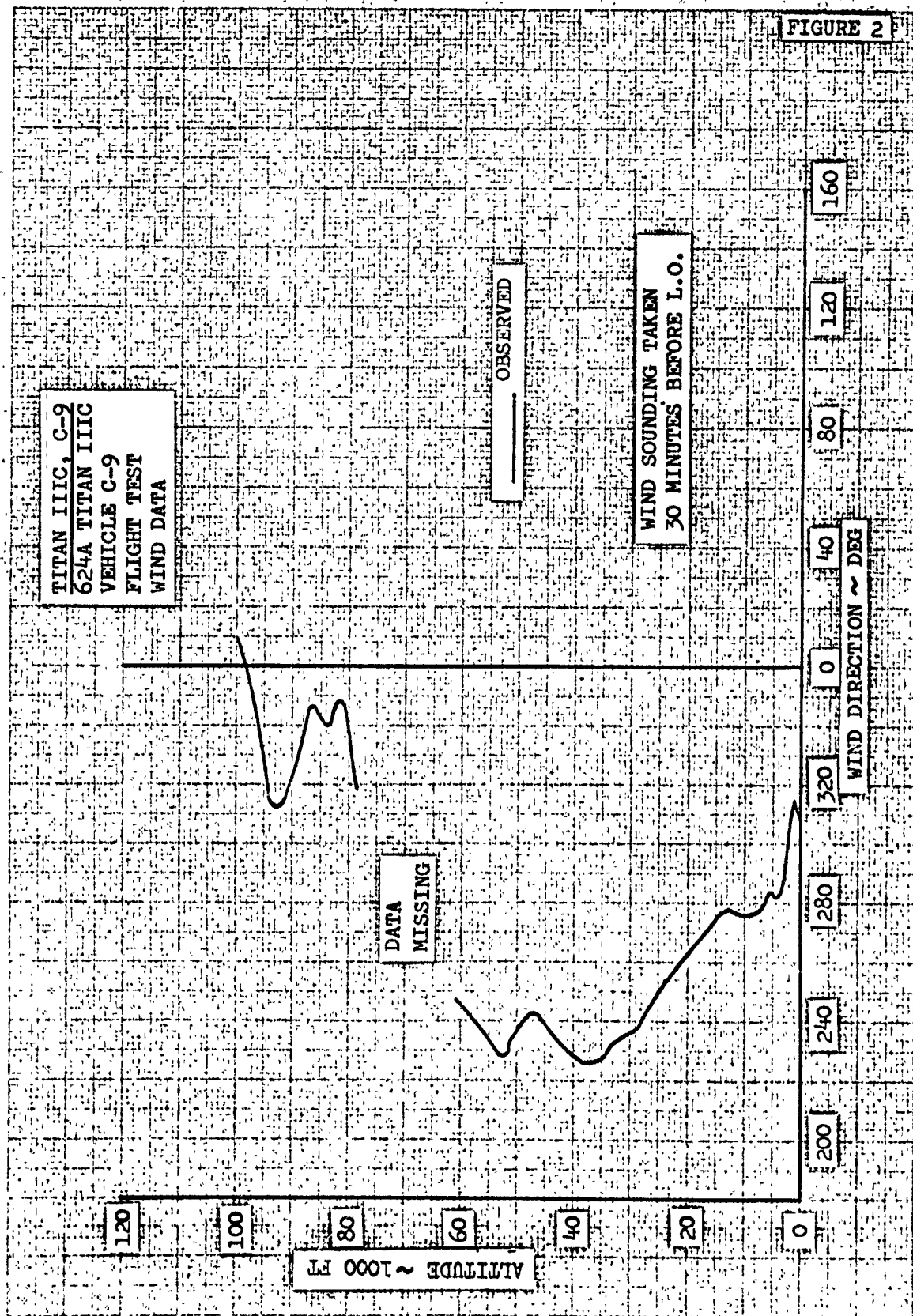


FIGURE 2

TABLE 1

11

TITAN IIIC VEHICLE C-9  
FLIGHT SEQUENCE OF EVENTS

EVENT	OBSERVED ZULU TIME (HR, MIN, SEC)	OBSERVED LIFTOFF TIME (SEC)	PREDICTED LIFTOFF TIME (SEC)
IGS GO Inertial	13:50:38.876	-3.323	-3.0
SRM Ignition (T-0	13:50:41.83	-0.370	-0.25
Liftoff	13:50:42.20	0	0
Start Roll Program	13:50:48.977	6.777	5
End Roll Program	13:50:51.977	9.777	9
Start Pitch	13:50:53.177	10.977	10
MDS S/D Enable	13:51:02.732	20.532	20
A/P GC #1 (Load Relief In)	13:51:22.731	40.531	40
Remove A/P GC #1 (Load Relief Out)	13:52:03.731	81.531	81
A/P GC #2	13:52:03.742	81.542	81
Operate TPS Power Switch and Enable Stage I Engine Start	13:52:03.742	81.542	81
Start Stage I Engine (81FS-1)	13:52:32.382	110.182	108
Disable SRM ISDS	13:52:32.382	110.182	108
MDS SRM Bypass	13:52:32.382	110.182	108
TCA Cover Separation Ordnance	13:52:32.382	110.182	108
Start Staging Camera	13:52:32.382	110.182	108
Remove TCA Cover Separation Ordnance	13:52:37.387	115.187	113
Remove A/P GC #2	13:52:44.429	122.229	120
A/P GC #3	13:52:44.429	122.229	120
Stage O/I Separation Ordnance	13:52:44.429	122.229	120
Start 12.5 Seconds Time Delay for Staging Camera Ejection	13:52:44.429	122.229	120
Remove A/P GC #3	13:53:37.732	175.532	175

TABLE 1 (Cont.)

12

EVENT	OBSERVED ZULU TIME (HR, MIN, SEC)	OBSERVED LIFTOFF TIME (SEC)	PREDICTED LIFTOFF TIME (SEC)
A/P GO #3A	13:53:37.731	175.531	175
Remove A/P GC 3A	13:54:34.731	232.531	232
A/P GC #4	13:54:34.781	232.581	232
Disable Stage I ISDS	13:54:45.732	243.532	243
Enable TCPS S/D	13:54:45.732	243.532	243
MDS Sensor Bypass	13:55:00.377	258.177	259
Enable A/P GC #5	13:55:00.377	258.177	259
Interrupt GC #4 (Within A/P)	13:55:00.377	258.177	259
Enable Stage I/II Separation	13:55:00.377	258.177	259
S/D Stage I Engine (87FS-2)	13:55:00.377	258.177	259
Start Stage II Engine (91FS-1)	13:55:00.377	258.177	259
Pressurize Stage III Tanks	13:55:00.377	258.177	259
Safe Stage I - Destruct Initiators	13:55:00.377	258.177	259
Disable Stage II ISDS (Backup)	13:55:22.731	280.531	280
S.C. GC	13:55:22.731	280.531	280
Remove A/P GC #4	13:56:36.731	354.531	354
Stage II S/D Enable	13:58:31.396	459.196	461
S/D Stage II (91FS-2)	13:58:31.396	459.196	461
Bypass Stage II MDS Sensors	13:58:31.396	459.196	461
Enable ACS	13:58:31.396	459.196	461
PS & Stage III HS	13:58:31.396	459.196	461
Disable Stage II ISDS	13:58:31.396	459.196	461
Pressurize Stage III Tanks	13:58:31.396	459.196	461
S.C. GC	13:58:21.396	459.196	461
Clear Discrete Matrix	13:58:23.396	461.196	463
Clear Discrete Matrix	13:58:25.395	463.195	465
Clear Discrete Matrix	13:58:25.395	463.195	465
Start Reset Discrete Matrix	13:58:27.394	465.194	467
Hold T/M Transmitters On	13:58:29.393	467.193	469

TABLE 1 (Cont.)

EVENT	OBSERVED ZULU TIME (HR, MIN, SEC)	OBSERVED LIFTOFF TIME (SEC)	PREDICTED LIFTOFF TIME (SEC)
Maintain MDS S/D Enable	13:58:29.393	467.193	469
Maintain PS, Stage III HS	13:58:29.393	467.193	469
Stage III Tank Pressurization	13:58:29.393	467.193	469
Apply Power to Discrete Arming Buss #2	13:58:29.393	467.193	469
Stage II/III Separation Ordnance	13:58:31.392	469.192	471
Remove A/P GC #5	13:58:31.392	469.192	471
Disable ISDS	13:58:31.392	469.192	471
Maintain Power to Discrete Arming Buss #2	13:58:31.392	469.192	471
Stage III Start (138FS-1(1))	13:58:34.409	472.209	474
A/P GC #7 and Unlatch Engine	13:58:34.409	472.209	474
Disable ACS	13:58:34.409	472.209	474
Enable Stage III Tank Pressurization (Backup)	13:58:34.409	472.209	474
Signal to Zero G Prop. Experiment	13:58:34.409	472.209	474
A/P GC #8 (Remove A/P GC #7)	14:02:24.732	702.532	702
Pitch Roll Mix	14:02:24.732	702.532	702
Stage III S/D (138FS-2(1))	14:03:42.009	779.809	783
Enable ACS	14:03:42.009	779.809	783
Disable Stage III Tank Pressurization (Backup)	14:03:42.009	779.809	783
Remove Signal to Zero G Prop. Experiment	14:03:42.009	779.809	783
Pitch Roll Mix	14:03:42.009	779.809	783
Remove PS & Stage III HS, and Disable Stage III Tank Pressurization System	14:03:44.391	782.191	785

TABLE 1 (Cont.)

14

EVENT	OBSERVED ZULU TIME (HR, MIN, SEC)	OBSERVED LIFTOFF TIME (SEC)	PREDICTED LIFTOFF TIME (SEC)
Remove A/P GC #8 and Latch Engine	14:03:44.391	782.191	785
Gemini Spacecraft Separation	14:04:12.437	810.237	813
Remove S.C. GC	14:04:12.394	810.194	813
P/L MDS Disable	14:04:15.393	813.193	816
A/P GC #4 (No Effect on Coast Control A/P)	14:04:15.393	813.193	816
Turn on ACS Nozzle Heaters	14:04:15.393	813.193	816
Arm TPS Ordnance Buss	14:04:15.393	813.193	816
Enable Lab Sequencer	14:04:15.393	813.193	816
Stage III Retro-thrust	14:04:15.438	813.238	816
PS & Stage III HS, and Enable Stage III Tank Pressuriza- tion System	14:04:26.391	824.191	827
Remove Gemini Spacecraft Sep. Signal	14:04:26.391	824.191	827
Remove A/P GC #4	14:04:26.393	824.193	827
Turn Off ACS Heaters	14:04:26.393	824.193	827
Stage III Start (138FS-1(2))	14:04:46.459	844.259	845
A/P GC #8 and Unlatch Engine	14:04:46.459	844.259	845
Disable ACS	14:04:46.459	844.259	845
Enable Stage III Tank Pressuri- zation System	14:04:46.459	844.259	845
Signal to Zero G Prop. Experiment	14:04:46.459	844.259	845
S.C. GC	14:04:46.459	844.259	845
Lab Signal #1	14:04:46.459	844.259	845
Open Doors for HTTC and ORBIS	14:04:46.459	844.259	845
Stage III S,D (138FS-2(2))	14:05:29.126	886.926	889

TABLE 1 (Cont.)

15

EVENT	OBSERVED ZULU TIME (HR, MIN, SEC)	OBSERVED LIFTOFF TIME (SEC)	PREDICTED LIFTOFF TIME (SEC)
Enable ACS	14:05:29.126	886.926	889
Disable Stage III Tank Pressurization System	14:05:29.126	886.926	889
Remove Signal to Zero G Prop. Experiment	14:05:29.126	886.926	889
Remove PS & Stage III HS	14:05:31.391	889.191	891
Remove A/P GC #8 and latch Engine	14:05:31.391	889.191	891
Turn Off Command Control Receivers	14:05:31.393	889.193	891
Turn Off MDS	14:05:31.393	889.193	891
Turn On ACS Heaters	14:05:31.393	889.193	891
Remove Pitch Roll Mix	14:05:31.393	889.193	891
Remove S.C. GC	14:05:31.394	889.194	891
PS & Stage III HS	14:43:32.429	3170.229	3180
S.C. GC	14:43:32.435	3170.235	3180
Start Stage III Engine (138FS-1(3) )	14:43:44.436	3182.236	3192
Unlatch Engine	14:43:44.436	3182.236	3192
Disable ACS	14:43:44.436	3182.236	3192
Enable Stage III Tank Pressurization System	14:43:44.436	3182.236	3192
Signal to Zero G Prop. Experiment	14:43:44.436	3182.236	3192
A/P GC #8	14:43:44.436	3182.236	3192
Pitch Roll Mix	14:43:44.436	3182.236	3192
Lab Signal #2	14:43:44.436	3182.236	3192
HTTC Pump Start Signal	14:43:44.436	3182.236	3192
Enable OV-1 Eject	14:43:44.436	3182.236	3192
Stage III S/D (138FS-2(3))	14:43:50.576	3188.376	3198
Enable ACS	14:43:50.576	3188.376	3198



TABLE 1 (Cont.)

EVENT	OBSERVED ZULU TIME (HR, MIN, SEC)	OBSERVED LIFTOFF TIME (SEC)	PREDICTED LIFTOFF TIME (SEC)
Disable Stage III Tank Pressurization System	14:43:50.576	3188.376	3198
Remove Signal to Zero G Prop. Experiment	14:43:50.576	3188.376	3198
Pitch Roll Mix	14:43:50.576	3188.376	3198
Remove PS & Stage III HS	14:43:53.391	3191.191	3200
Latch Engine	14:43:53.391	3191.191	3200
Remove S.C. GC	14:43:53.394	3191.194	3200
Lab Signal #3	14:44:01.491	3199.291	3208
Arm Lab 25V Buss	14:44:01.491	3199.291	3208
Activate Biocell	14:44:01.491	3199.291	3208
Turn On Recorder, Switch Low Power Transmitter Output to Multiplexer	14:44:01.491	3199.291	3208
Switch LOW Transmitters to Command Mode	14:44:01.491	3199.291	3208
Turn SSB & PCm Transmitters Off	14:44:01.491	3199.291	3208
Turn Zero G Prop Experiment Electronics Off	14:44:01.491	3199.291	3208
Switch LOW T/M to Command Mode	14:44:01.491	3199.291	3208
S.C. GC	14:45:36.481	3294.281	3303
Lab Signal #4	14:46:11.491	3329.291	3338
OV-1 Eject Signal	14:46:11.491	3329.291	3338
Enable OV-4 Eject	14:46:11.491	3329.291	3338
Remove S.C. GC	14:46:11.494	3329.294	3338
S.C. GC	14:47:16.481	3394.281	3403
Lab Signal #5	14:47:48.491	3426.291	3435
OV-4T Eject Signal	14:47:48.491	3426.291	3435
Remove S.C. GC	14:47:51.481	3429.281	3438
S.C. GC	14:47:57.481	3435.281	3444

TABLE 1 (Cont.)

17

EVENT	OBSERVED ZULU TIME (HR, MIN, SEC)	OBSERVED LIFTOFF TIME (SEC)	PREDICTED LIFTOFF TIME (SEC)
Lab Signal #6	14:48:06.491	3444.291	3453
OV-4R Eject Signal	14:48:06.491	3444.291	3453
Remove S.C. GC	14:48:09.531	3447.331	3456
Remove Pitch Roll Mix	14:48:09.482	3447.282	3456
Remove A/P GC #8	14:48:09.482	3447.282	3456
Lab Signal #9	15:14:20.491	5018.291	5027
Fuel Cell Purge On	15:14:20.491	5018.291	5027
Lab Signal #10	15:14:36.491	5034.291	5043
Fuel Cell Purge Off	15:14:36.491	5034.291	5043

CONFIDENTIAL

18

TABLE 2  
SIGNIFICANT VEHICLE PERFORMANCE CHARACTERISTICS

	OBSERVED	PREDICTED	CMV/PRED
<u>Stage 0</u>			
(U) 1. Gross Weight at Liftoff lb	1,420,671	1,420,669	2.0
2. Axial Acceleration at Liftoff + 1 sec g's	1.526	1.606	-0.060
3. Time to 87FS-1 sec	110.162	109.550	0.632
4. Velocity at 87FS-1 ft/sec	5,482	5,427	23
5. Altitude at 87FS-1 ft	123,168	123,604	-636
<u>Stage 0/I</u>			
(U) 1. Time to SRM Staging sec	122.229	121.600	0.629
2. Gross Weight at 87FS-1 lb	564,123	564,121	2.0
3. Stage Burning Time (87FS-1 to SRM Staging) sec	12.047	12.050	-0.003
4. Velocity at SRM Staging in ft/sec	5,918	5,829	69
5. Altitude at SRM Staging ft	146,978	146,013	1,037
<u>Stage I</u>			
(C) 1. Time to 87FS-2 sec	258.200	259.649	-1.649
2. Gross Weight after SRM Staging lb	367,188	367,166	2.2
3. Average Weight Decay Rate lb/sec	1,699.35	1,670.03	29.32
4. Average Longitudinal Thrust (Vac) lb	489,557	479,557	9,570

CONFIDENTIAL

CONFIDENTIAL

19

TABLE 2 (Cont.)

	OBSERVED	PREDICTED	OBS V-PRED
5. Average Effective Specific Impulse (Vac) sec	268.21	267.25	0.96
6. Outage lb	538. (F)	503	17
7. Stage Burning Time (from SRM Staging to 87FS-2) sec	135.971	138.25	-2.279
8. Total Stage I Burning Time sec	148.018	150.30	-2.282
9. Velocity at 87FS-2/91FS-1 ft/sec	13,878	13,747	131
10. Velocity Gained During Stage Operation ft/sec	7,960	7,918	42
11. Altitude at 87FS-2/91FS-1 ft	395,422	392,590	2,832
<u>Stage II</u>			
(C) 1. Time to 91FS-2 sec	459.195	459.171	0.025
2. Gross Weight at 91FS-1 lb	119,682	119,929	-247
3. Average Weight Decay Rate lb/sec	328.48	333.15	-4.67
4. Average Longitudinal Thrust (Vac) lb	103,755	103,876	-121
5. Average Effective Specific Impulse (Vac) sec	315.87	311.60	4.27
6. Outage lb	403 (F)	209	194
7. Stage Burning Time sec	200.996	199.32	1.676
8. Velocity Gained During Stage Operation ft/sec	7,428	7,447	-19
9. Velocity at 91FS-2 ft/sec	21,306	21,194	112
10. Altitude at 91FS-2 ft	642,090	639,772	2,318

CONFIDENTIAL

TABLE 2 (Cont.)

Stage III		OBSERVED	PREDICTED	OBSV-PRED
<u>First Burn</u>				
1.	Time to 138FS-1(1) sec	472.198	473.001	-0.803
2.	Time to 138FS-2(1) sec	779.809	793.406	-13.597
3.	Duration of Propellant Settling Mode sec	13.013	13.830	-0.817
4.	Gross Weight at 138FS-1(1) lb	46,735	46,715	20
5.	Average Weight Decay Rate lb/sec	53.83	53.17	0.66
6.	Average Longitudinal Thrust (Vac) lb	16,430	16,068	362
7.	Average Effective Specific Impulse (Vac) sec	305.22	302.22	3.00
8.	Stage Burning Time sec	307.600	320.41	-12.81
9.	Velocity at 138FS-1(1) ft/sec	21,301	21,189	112
10.	Velocity at 138FS-2(1) ft/sec	25,691	25,693	-2.0
11.	Altitude at 138FS-2(1) ft	548,120	548,026	94
<u>Second Burn</u>				
1.	Time to 138FS-1(2) sec	844.259	854.001	-9.742
2.	Time to 138FS-2(2) sec	886.926	897.250	-10.32--
3.	Gross Weight at 138FS-1(2) lb	25,463	25,407	56
4.	Average Weight Decay Rate lb/sec	53.83	52.51	1.32

TABLE 2 (Cont.)

	OBSERVED	PREDICTED	OBSV-PRED
5. Average Longitudinal Thrust (Vac) lb	16,420	15,803	617
6. Average Effective Specific Impulse (Vac) sec	305.04	300.96	4.08
7. Stage Burning Time sec	42.667	43.249	-0.582
8. Velocity at 138FS-1(2) ft/sec	25,753	25,746	7.0
9. Velocity at 138FS-2(2) ft/sec	25,795	25,793	2.0
10. Altitude at 138FS-2(2) ft	479,430	482,342	-2,912
<u>Third Burn</u>			
1. Time to 138FS-1(3) sec	3,182.236	3,186.001	-3.765
2. Time to 138FS-2(3) sec	3,188.376	3,191.813	-3.437
3. Gross Weight at 138FS-1(3) lb	23,103	23,047	56
4. Average Weight Decay Rate lb/sec	53.83	55.01	-1.18
5. Average Longitudinal Thrust (Vac) lb	16,180	16,362	-182
6. Average Effective Specific Impulse (Vac) sec	300.58	297.42	3.16
7. Stage Burning Time sec	6.140	5.812	0.328
8. Velocity at 138FS-1(3) ft/sec	25,222	25,228	-6.0
9. Velocity at 138FS-2(3) ft/sec	25,363	25,365	-2.0
10. Altitude at 138FS-2(3) ft	971,883	971,390	493
11. Outage lb	135 (0)	103	32

TABLE 3

## TITAN IIIC VEHICLE 9 ORBITAL DATA

<u>Gemini Ejection</u>		PREDICTED	OBSERVED
Inertial Velocity	ft/sec	25,721.906	25,721.947
Altitude	ft	523,394.25	523,273.25
Flight Path Angle	deg	-1.8035	-1.8036
<u>Transfer Orbit</u>			
Perigee Ht	n. mi.	76.60	78
Apogee Ht	n. mi.	167.92	166
Period	min	88.96	88.9
Eccentricity		0.0128	0.0122
Inclination	deg	32.88	32.9
<u>Final Orbit</u>			
Perigee Ht	n. mi.	160.13	165
Apogee Ht	n. mi.	162.34	168
Period	min	90.41	90.6
Eccentricity		0.00031	0.00042
Inclination	deg	32.86	32.843

### 3.1.3.2.1 Observed Wind Data - (Cont.)

speed was down to approximately 110 knots, shown in Figure 1, and clearly showed that the winds aloft were diminishing and the launch could be undertaken. The wind direction profile, shown in Figure 2, shows a predominately tailwind which is typical of winds usually experienced at the AFETR.

### 3.1.3.2.2 Aerodynamic Parameters

Trajectory characteristics related to the portion of flight occurring in the sensible atmosphere have been computed by combining vehicle position, velocity, and attitude data from the ACED airborne guidance computer with the CKAFS atmospheric sounding data discussed above. These trajectory characteristics (relative wind velocity, mach number, dynamic pressure,  $q$ -alpha, and total angle of attack) are presented below.

#### 3.1.3.2.2.1 Relative Wind Velocity

The observed relative wind velocity history is presented with the predicted in Figure 3 and shows the the observed initially low and then rising above the predicted data in Stage 0 operation.

#### 3.1.3.2.2.2 Mach Number

Figure 4 presents a comparison of the observed and planned Mach number during Stage 0. Although Stage 0 gained velocity at a greater-than predicted rate, the actual altitude profile was generally lower than expected which resulted in the observed Mach number history being nearly identical to the predicted. Analysis of Figure 4 indicates that no difference can be seen between the predicted and observed until late in Stage 0 flight when the observed can be seen rising above the predicted.

A comparison of predicted and observed Mach number histories during Stage I operation is presented in Figure 5. Due to the higher-than-predicted velocity profile throughout the Stage I operation, the observed Mach number history is high.



FIGURE 3

TITAN IIIC, C-9  
624A TITAN IIIC  
VEHICLE C-9  
FLIGHT TEST  
STAGE 0

— PREDICTED  
- - - OBSERVED

RELATIVE WIND VELOCITY ~ 1000 FT/SEC

6  
5  
4  
3  
2  
1  
0

0 20 40 60 80 100 120

TIME ~ SECONDS FROM L.O.

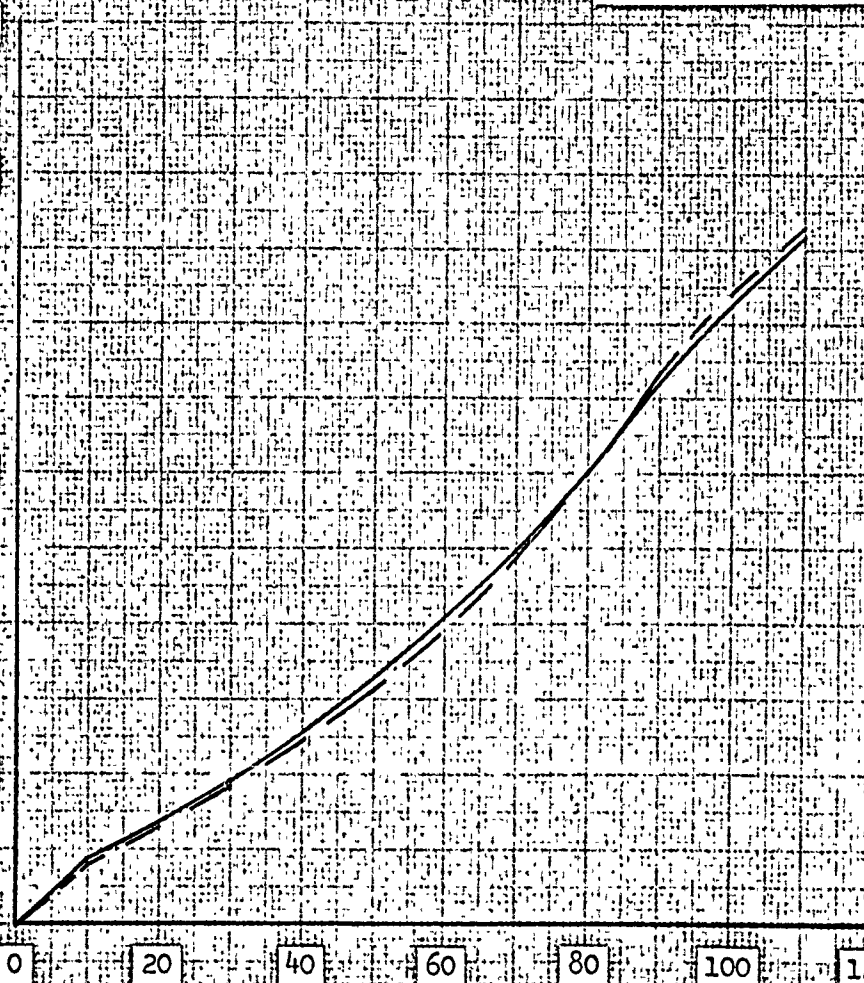
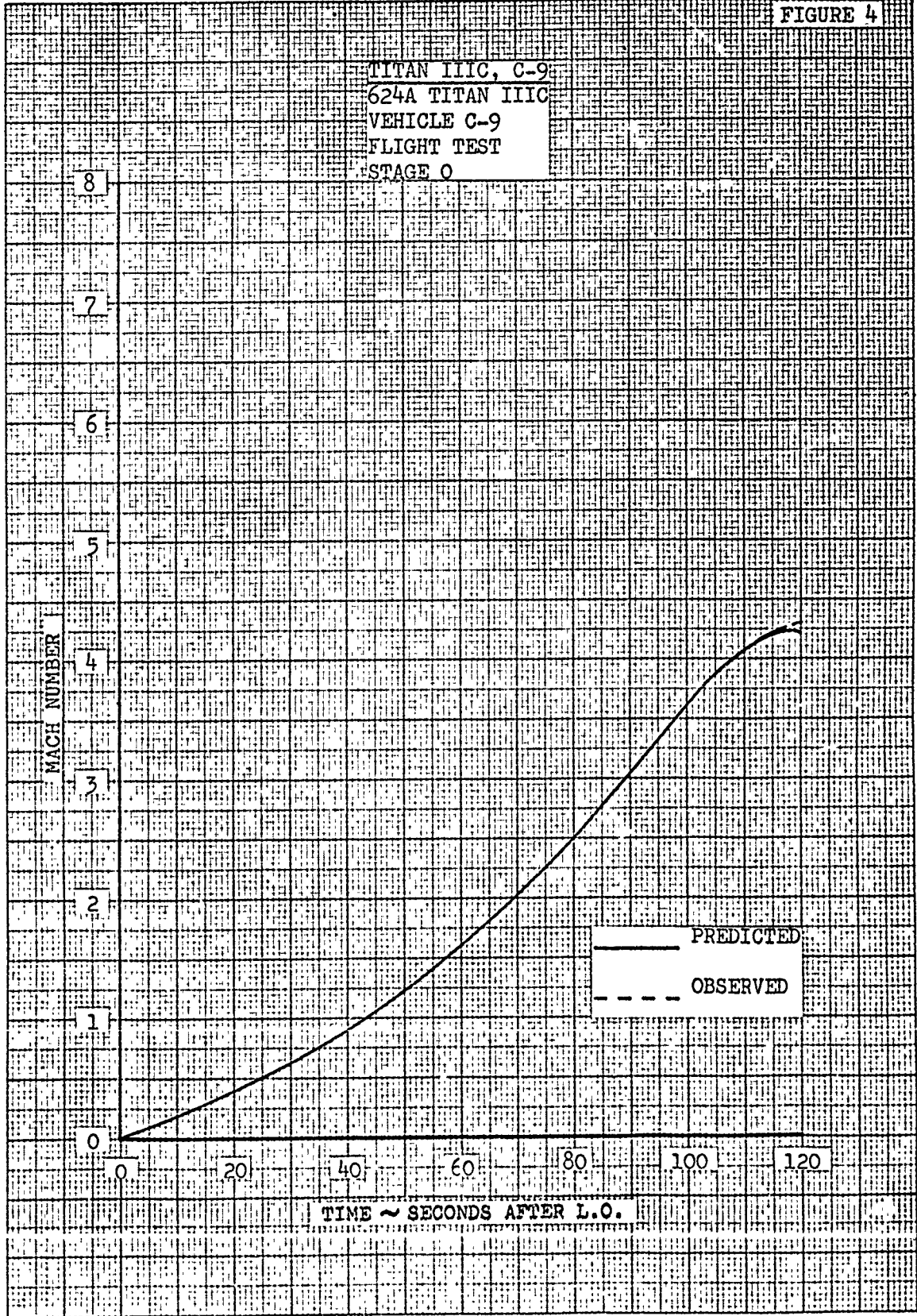


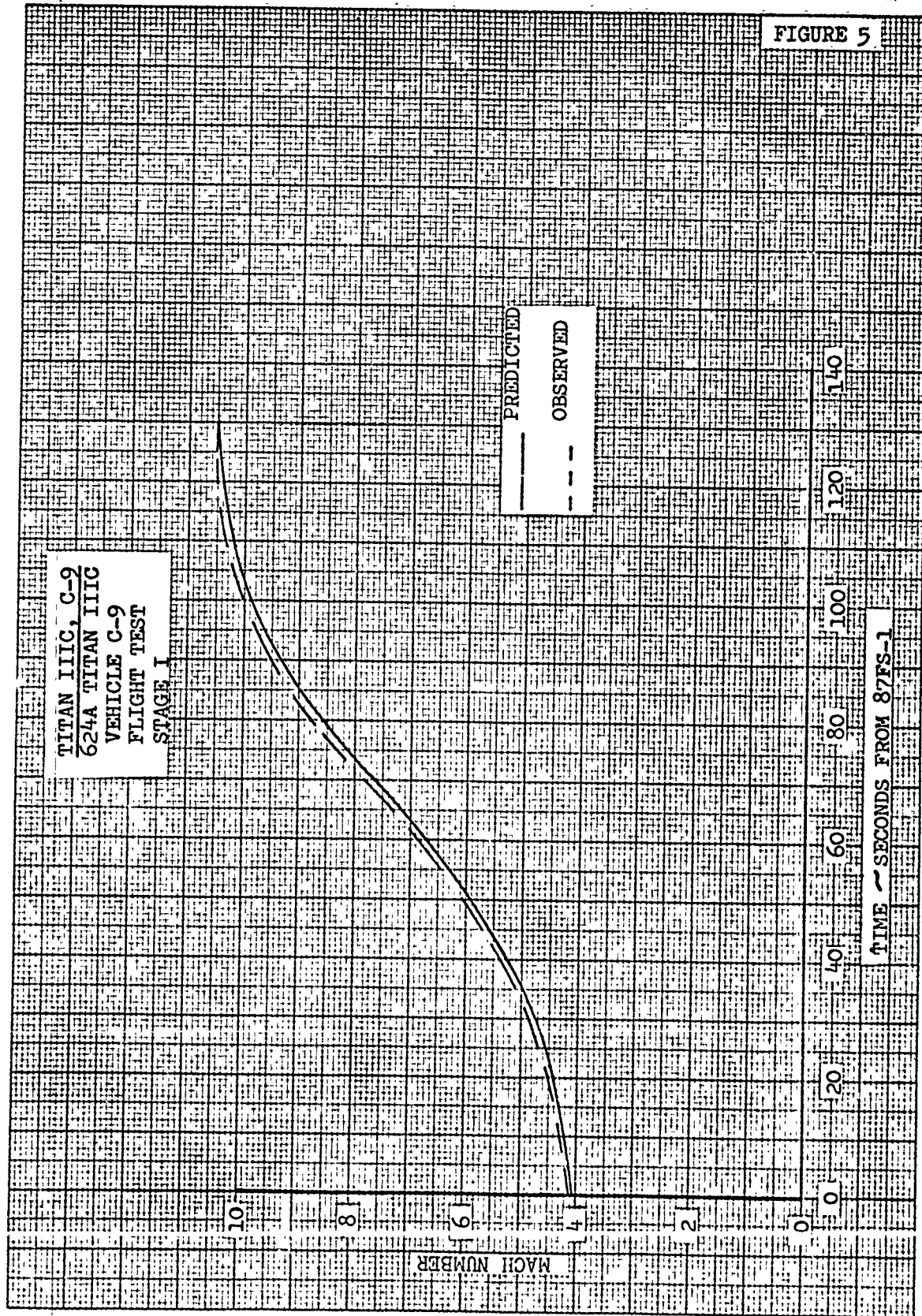
FIGURE 4

TITAN IIIC, C-9  
624A TITAN IIIC  
VEHICLE C-9  
FLIGHT TEST  
STAGE 0



CLEARPRINT CHARTS

FIGURE 5



### 3.1.3.2.2.3 Dynamic Pressure

The observed dynamic pressure history is presented in Figure 6 compared to the pre-flight predicted history. The two histories are quite similar although the observed is slightly low during the time of maximum dynamic pressure. The observed maximum dynamic pressure occurred at 58 seconds with a value of approximately  $789 \text{ lb/ft}^2$  corresponding to predicted values of 57 seconds and  $806 \text{ lb/ft}^2$  respectively.

### 3.1.3.2.2.4 Total Angle of Attack

The total angle of attack, presented in Figure 7, was calculated by resolving the wind speed of Figure 1 into components of relative wind velocity along the vehicle body axis by using the wind direction profile shown on Figure 2 and the body axis orientation from the guidance system gimbal angles. No predicted angle of attack history is presented, since a wind profile was not assumed in the reference trajectory. The figure shows a completely normal angle of attack history.

### 3.1.3.2.2.5 Dynamic Pressure - Angle of Attack Product

The airloads indicator, the product of dynamic pressure and total angle of attack, is presented in Figure 8. Analysis of the graph shows that the maximum value encountered throughout Stage 0 operation was approximately  $3,200 \text{ lb-deg/ft}^2$  which is considerably less than the Gemini imposed constraint of  $4,500 \text{ lb-deg/ft}^2$ .

## 3.1.3.3 Stage 0

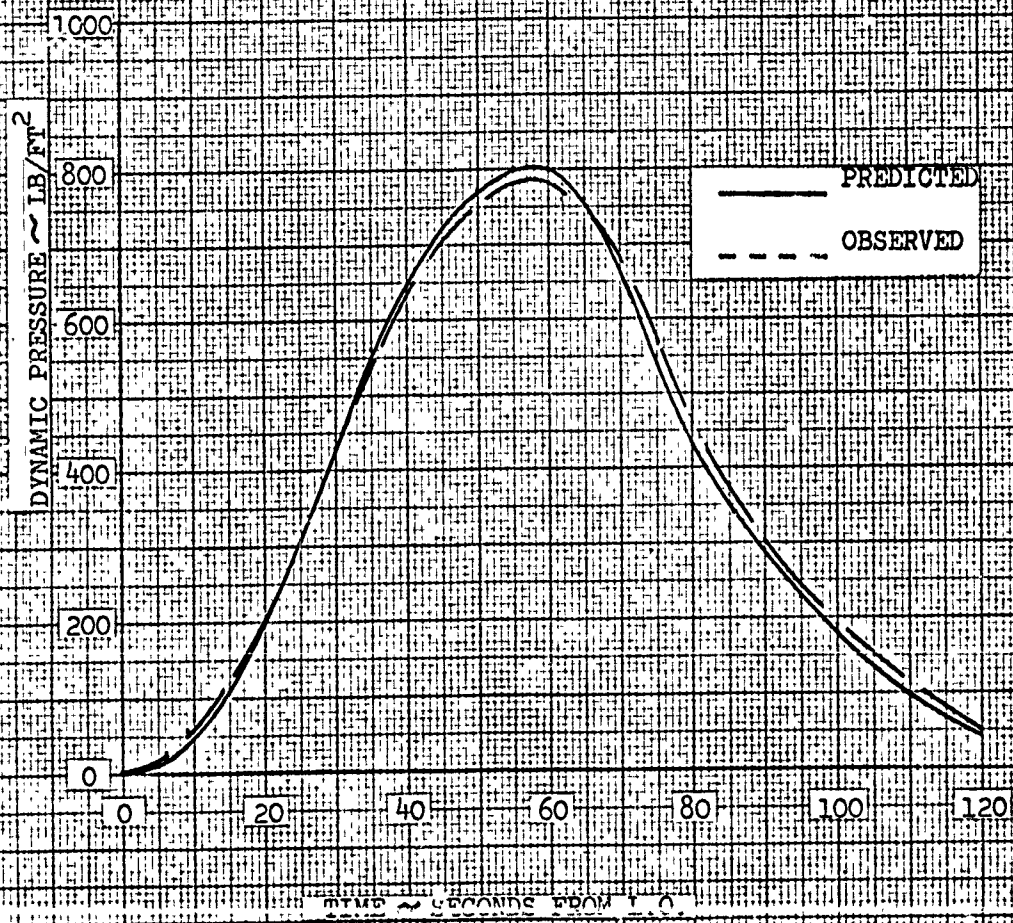
### 3.1.3.3.1 Trajectory Characteristics

The Titan III C Vehicle 9 flight started from Pad 40 of the AFETR on 3 November 1966 at 13:50:42.2 GMT and 0.370 seconds after ignition of the Solid Rocket Motors. The axial acceleration at liftoff was  $1.526 \text{ g's}$  which was only  $0.08 \text{ g's}$  lower than planned. The roll program was executed satisfactorily resulting in a pitchout azimuth of  $107.62$  degrees, or only  $0.12$  degrees more than expected. All discretes from the guidance system occurred as scheduled.

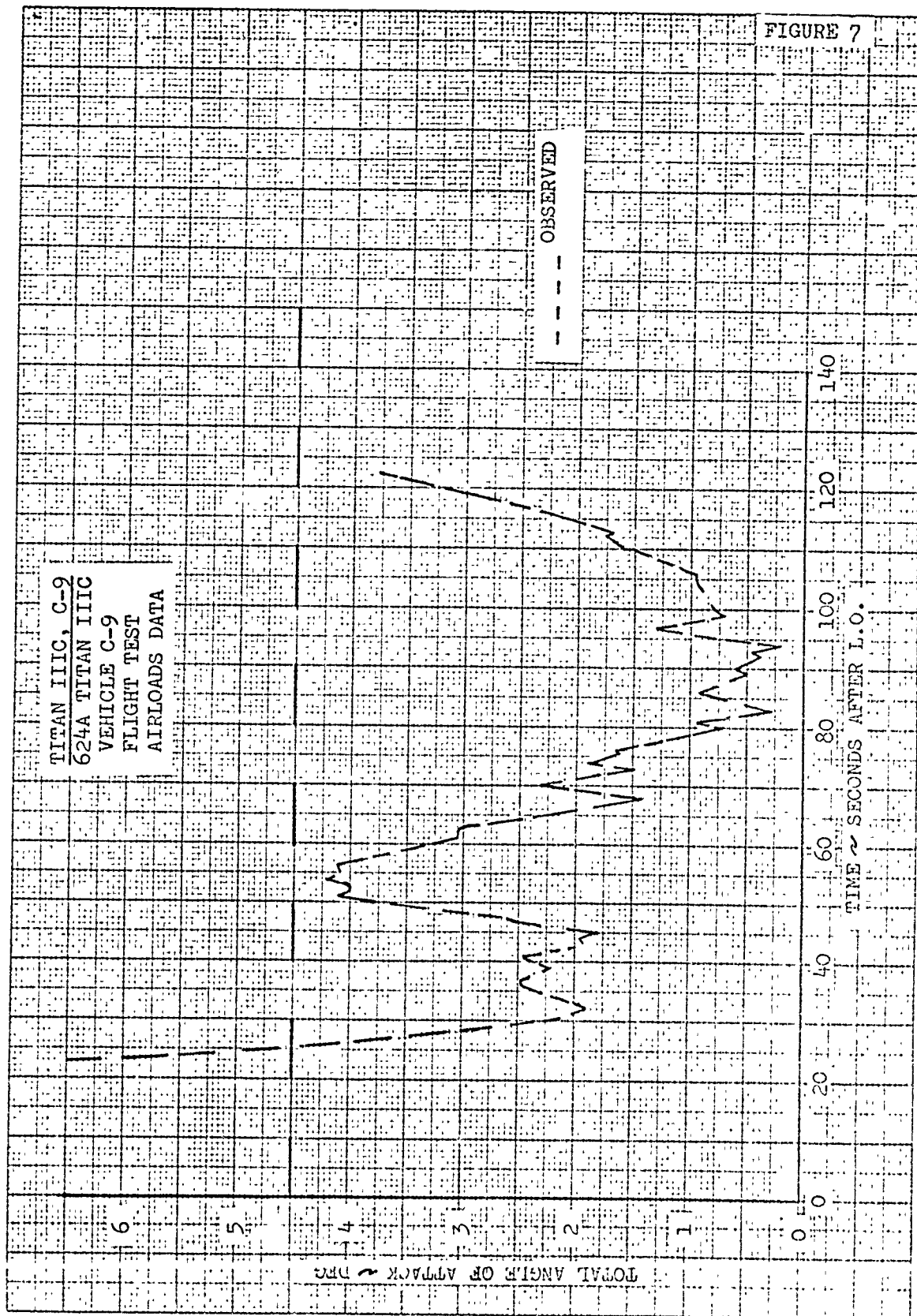


FIGURE 6

TITAN IIIC, C-9  
624A TITAN IIIC  
VEHICLE C-9  
FLIGHT TEST  
STAGE 0



CLEARPRINT QUARTZ



CONFIDENTIAL

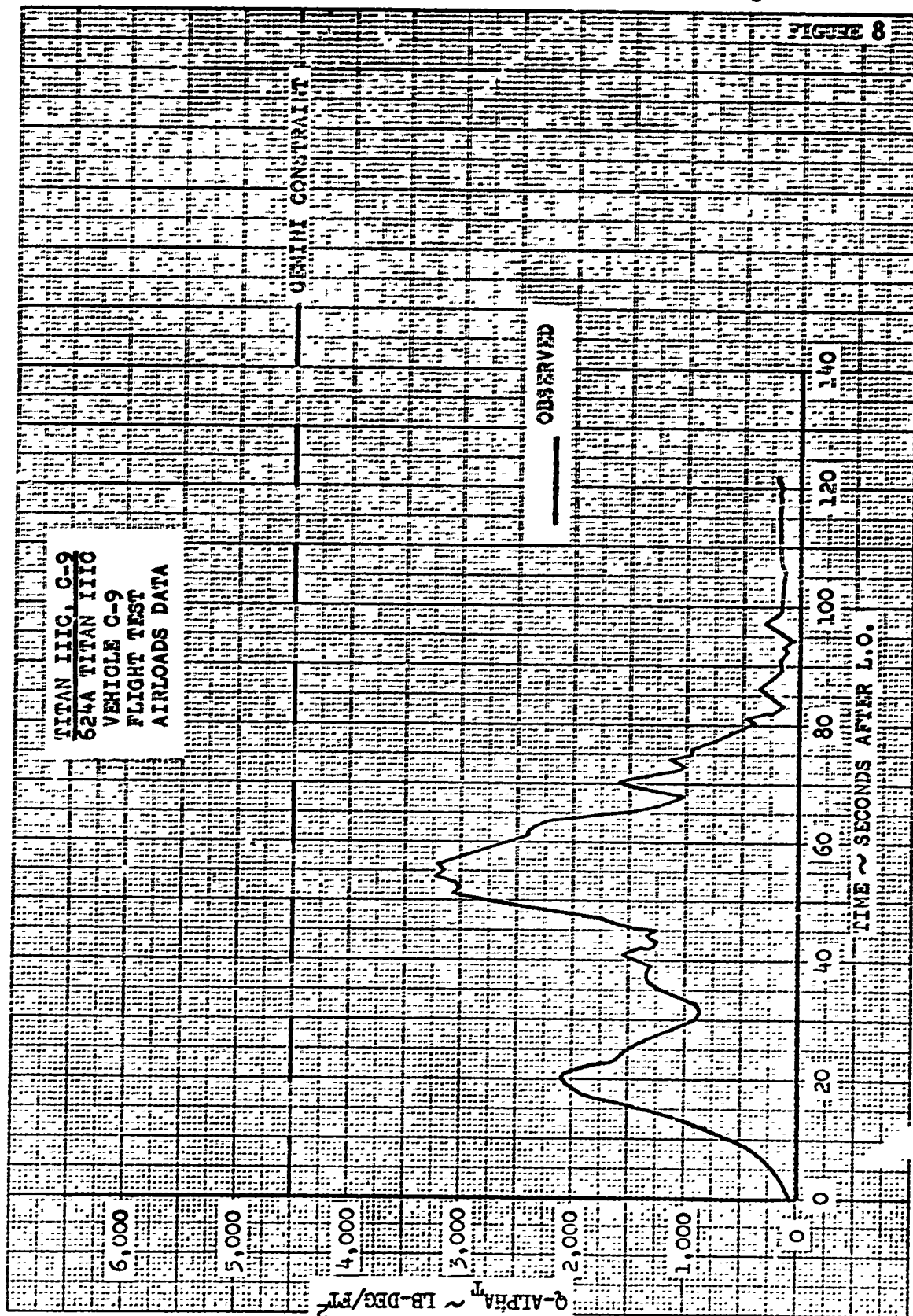
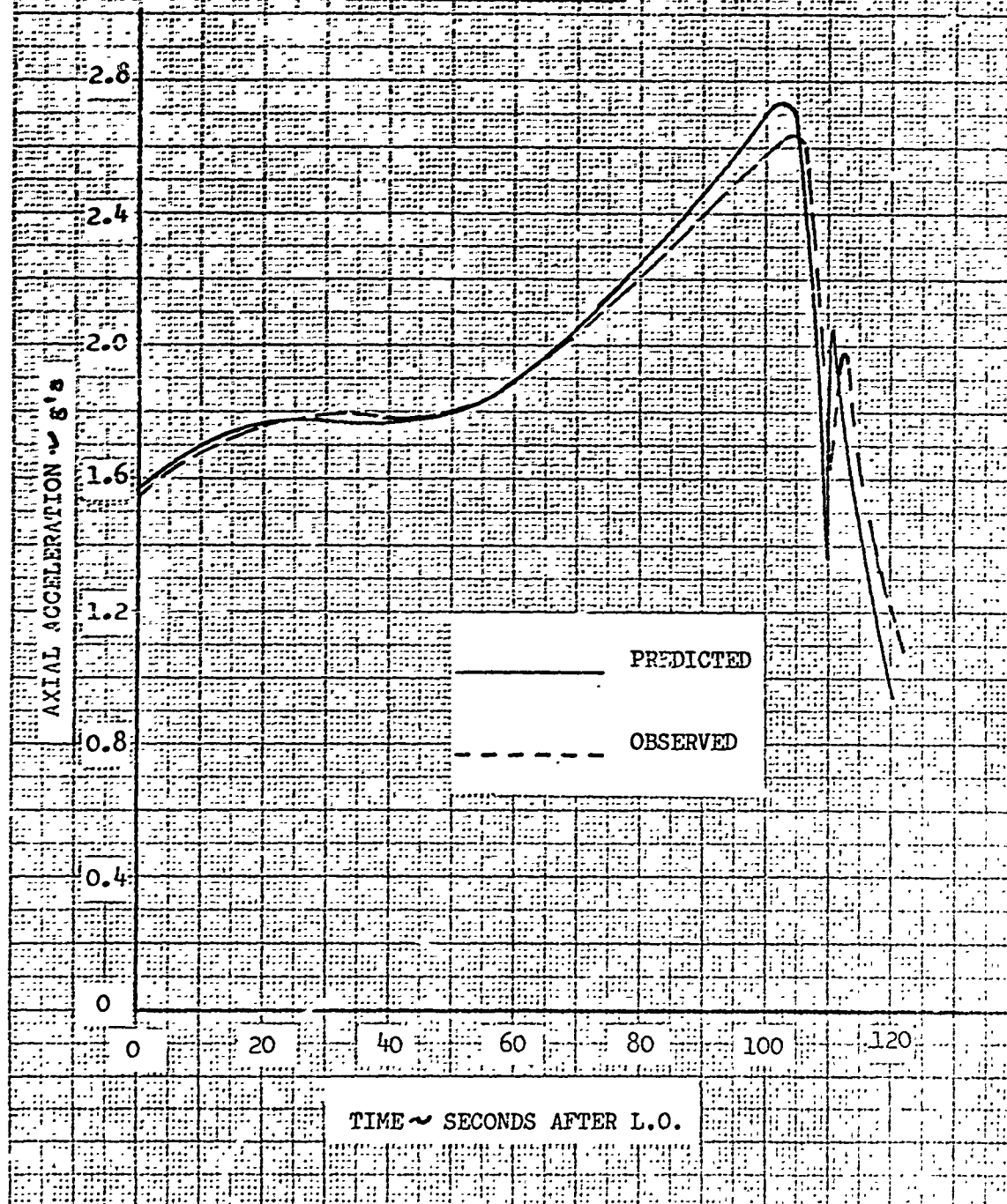


FIGURE 9

TITAN IIIC, C-9  
624A TITAN IIIC  
VEHICLE C-9  
FLIGHT TEST  
STAGE 0





#### 3.1.3.3.1 Trajectory Characteristics - (Cont.)

A comparison of Stage 0 predicted and observed longitudinal acceleration histories is presented in Figure 9. The comparison shows the observed to be low from liftoff to 20 seconds, above the predicted from 20 seconds to 50 seconds, and then dropping below from 50 seconds to web action time. Vehicle 9 also experienced significantly higher than planned acceleration levels during tailoff of the SRMs.

Figure 10 presents a comparison of Stage 0 inertial velocity histories, and shows the observed higher than expected and diverging due to the high acceleration level from 20 to 50 seconds. With the observed acceleration running below predicted from 50 seconds through web-action time, the velocity comparison of Figure 10 shows the observed, although still high, converging to predicted levels during this time interval. With the actual 87FS-1 signal being issued approximately 0.6 seconds later than planned, the observed velocity at 87FS-1 was approximately 55 ft/sec higher than expected. An additional 34 ft/sec gain over predicted was realized between 87FS-1 and SRM staging, due to the high SRM tailoff impulse, to make the observed velocity at SRM jettison 89 ft/sec higher than expected.

The observed altitude profile is compared with the nominal in Figure 11 and shows that due primarily to the tailwind experienced during flight, Vehicle 9 failed to maintain the predicted altitude history.

#### 3.1.3.3.2 Performance

Vehicle 9 lifted off with a gross weight of 1,420,671 pounds which is only 2.0 pounds heavier than predicted. This small difference in liftoff weight together with the fact that the SRM propellant grain temperature at liftoff was measured to be 70.7 degrees (the pre-test trajectory was generated assuming a propellant grain temperature of 70 degrees) would suggest that the SRMs performed very close to predicted.

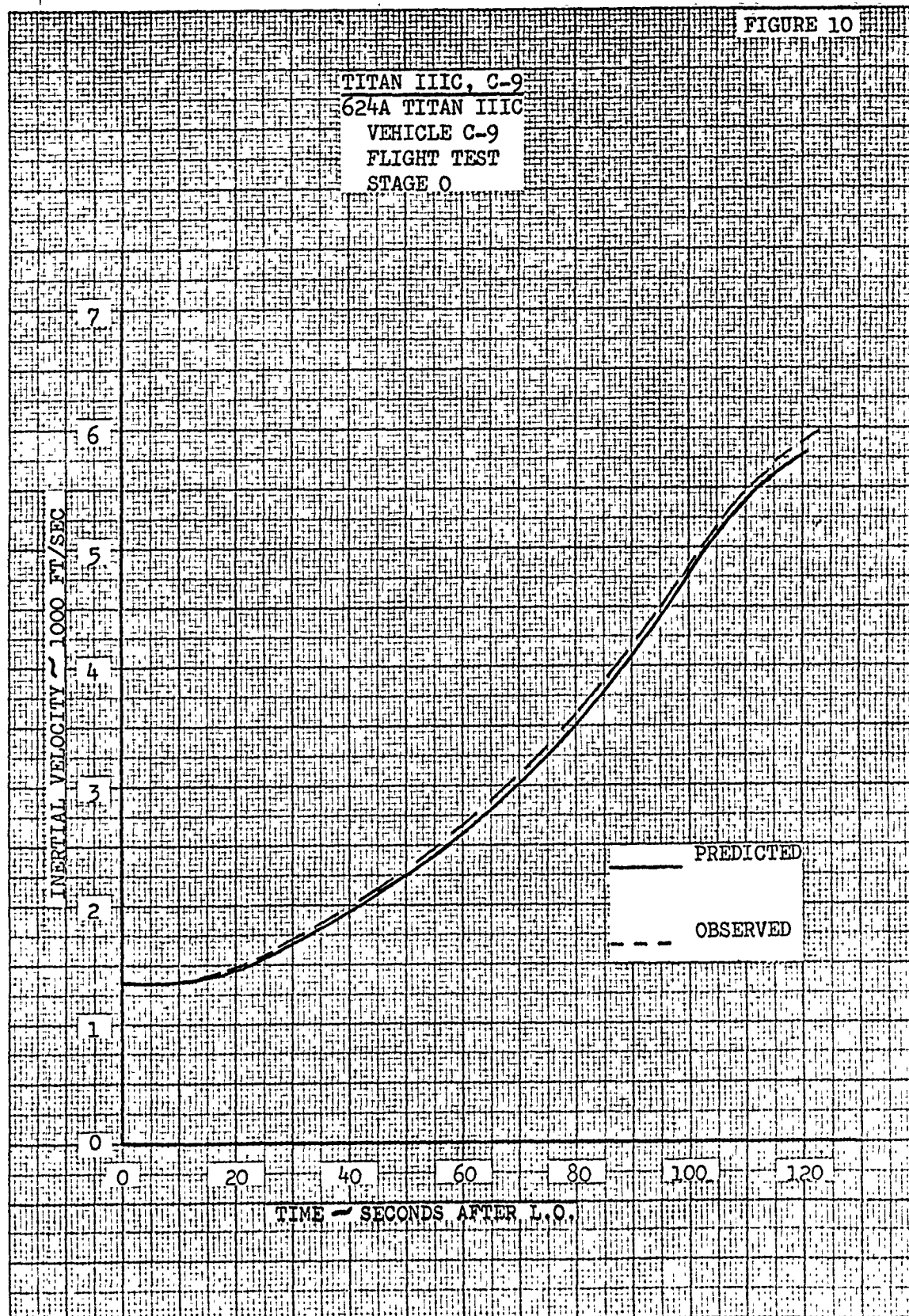
#### 3.1.3.4 Stage I

##### 3.1.3.4.1 Trajectory Characteristics

The axial acceleration histories presented in Figure 12 show the observed acceleration level significantly higher than predicted throughout Stage I operation.

FIGURE 10

TITAN IIIC, C-9  
624A TITAN IIIC  
VEHICLE C-9  
FLIGHT TEST  
STAGE 0



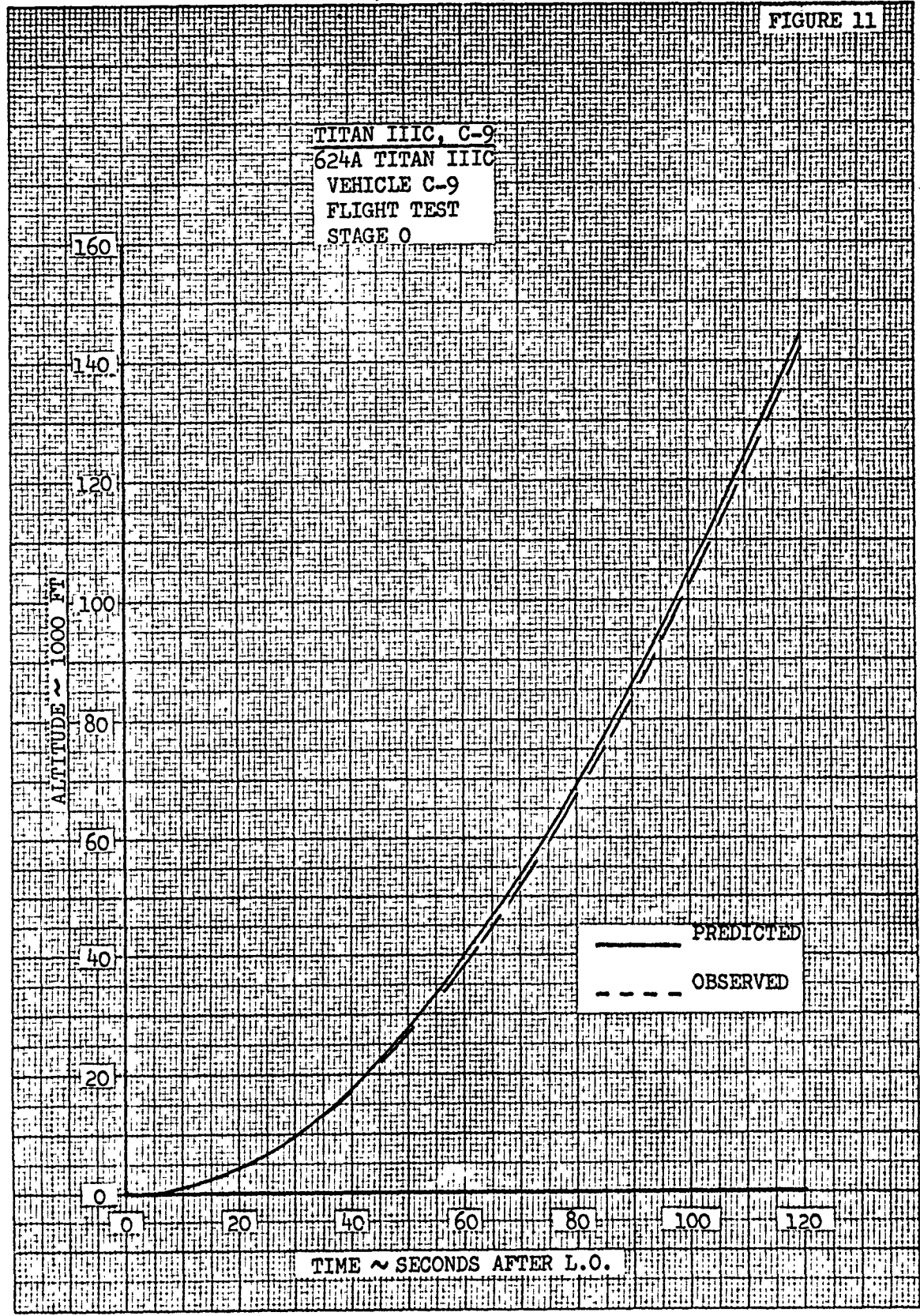
PRINTED IN U.S.A. ON CLEARPRINT TECHNICAL PAPER NO. 1018

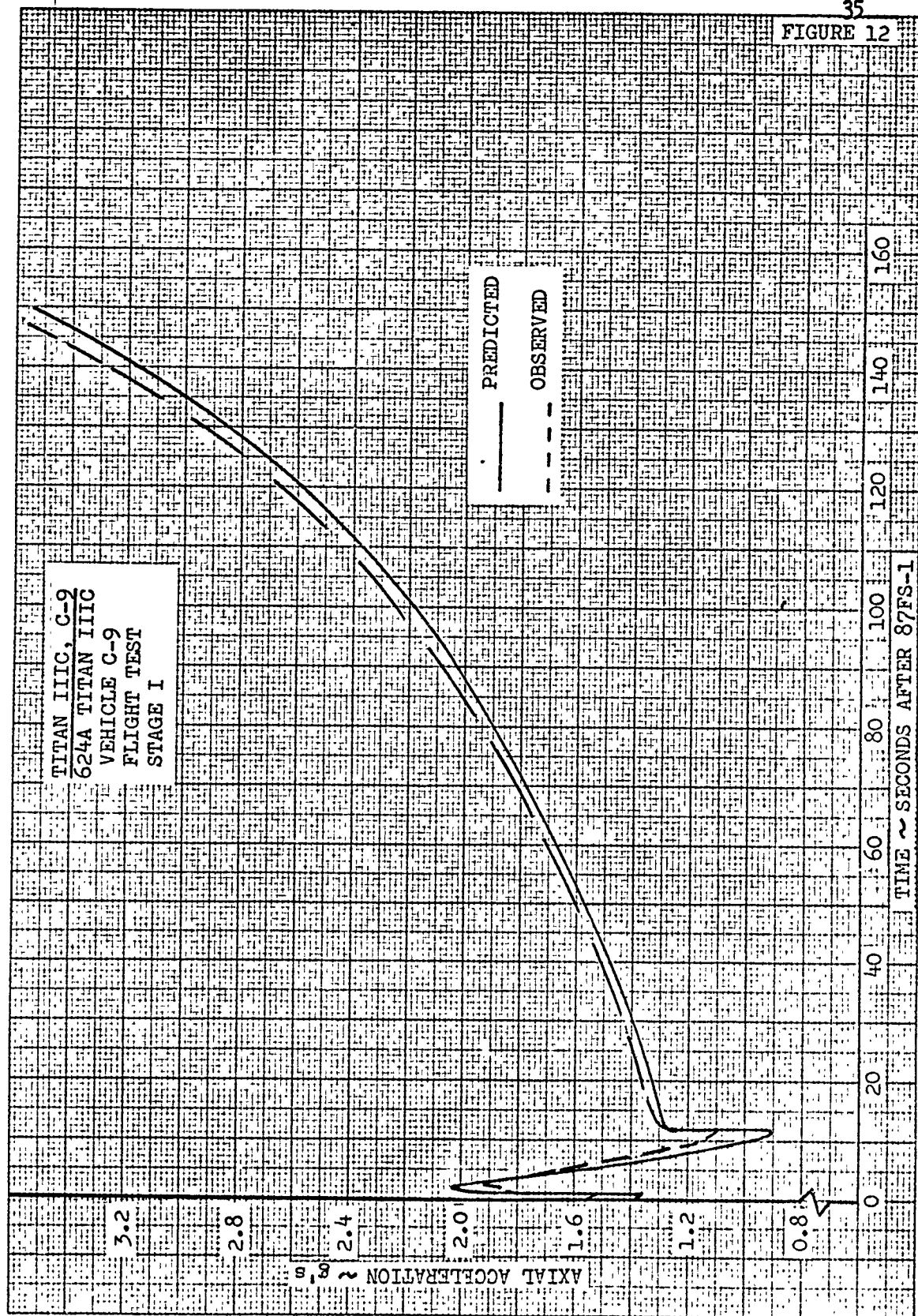
NO. C39. MILLIMETERS BOTH WAYS 160 X 220 DIVISIONS:

CLEARPRINT PAPER CO

CLEARPRINT CHARTS

FIGURE 11





CONFIDENTIAL

36

3.1.3.4.1 Trajectory Characteristics -(Cont.)

- (U) Figure 13 presents a comparison of predicted and observed inertial velocities and shows that, due to the high acceleration levels throughout Stage I operation, Vehicle 9 maintained a higher than predicted velocity profile. Stage I acquired approximately 7,960 ft/sec in velocity which is 42.0 ft/sec more than expected. With the 89.0 ft/sec velocity excess at SRM staging and the additional Stage I gain, the actual vehicle velocity at 87FS-2 was 13,878 ft/sec or 131 ft/sec higher than planned.
- (U) Observed and nominal altitude profiles are presented in Figure 14 for Stage I flight and shows that the observed was initially low although after the guidance loop was closed after SRM jettison the observed rose above the nominal late in stage operation.

3.1.3.4.2 Performance

- (C) The observed effective thrust time history is compared with the nominal in Figure 15 and shows the observed higher than expected throughout Stage I operation. Detailed analysis indicates that the actual thrust and effective specific impulse averaged out to be higher than predicted. The actual thrust had an average value of 489,557 pounds, approximately 9,670 pounds high and the effective specific impulse 0.96 seconds high at an average value of 288.21 seconds.
- (U) Analysis of Stage I burn time shows that the stage burned 2.28 seconds less than predicted and experienced an oxidizer depletion shutdown with approximately 538 pounds of fuel outage.

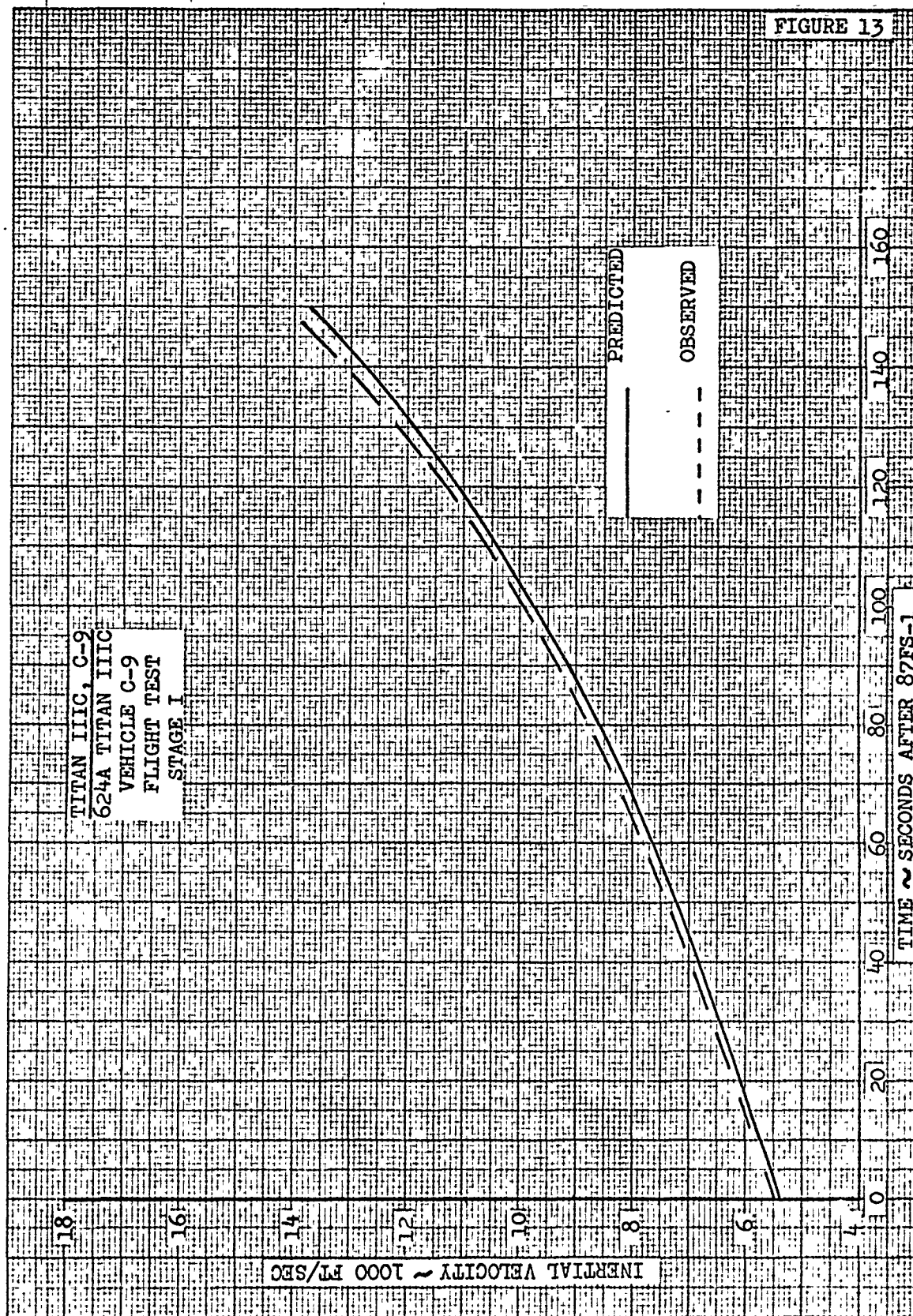
3.1.3.4.3 Staging Camera Impact

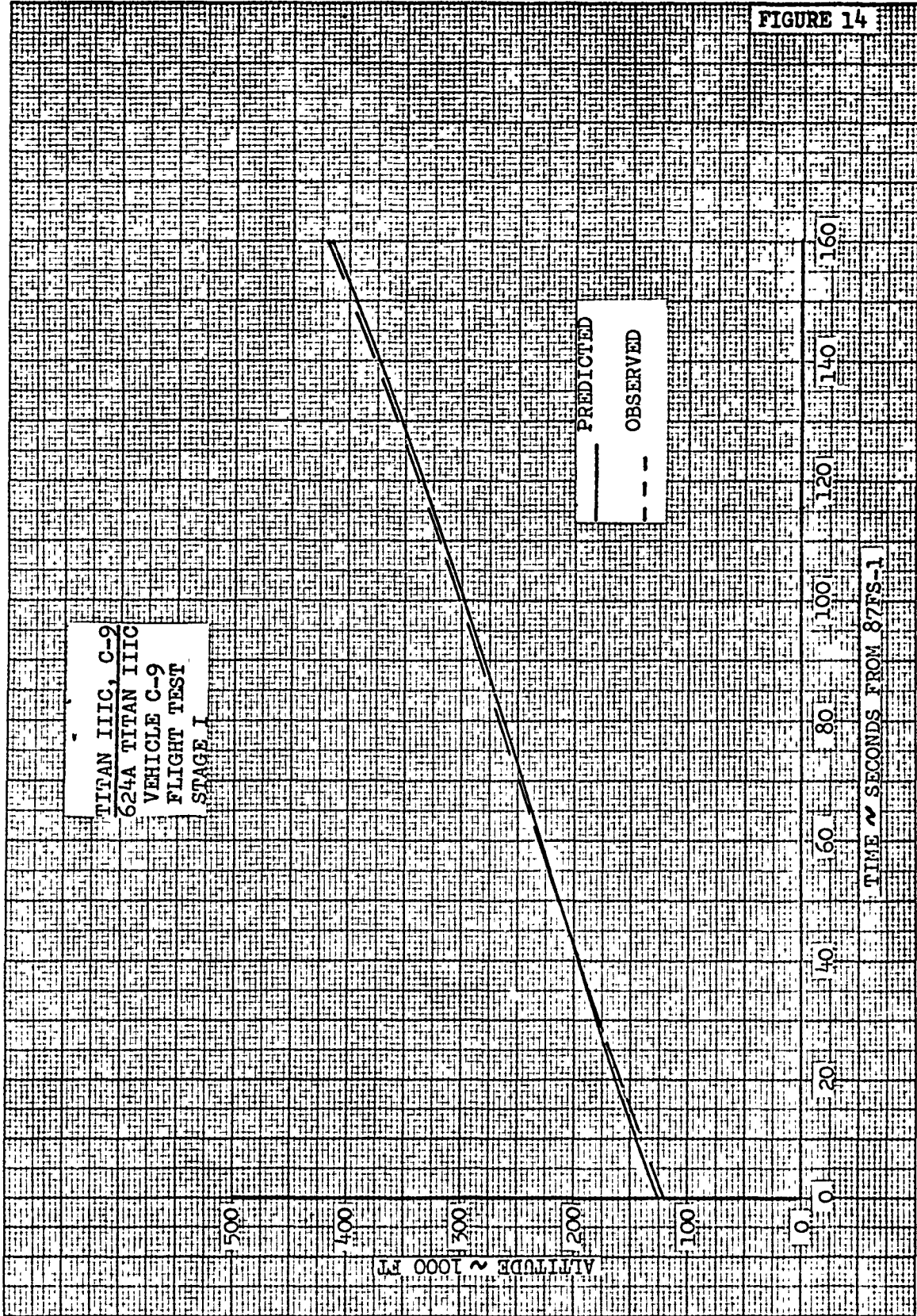
- (U) Figure 16 illustrates the location of staging camera impact point and includes the nominal impact point with its associated dispersion ellipse, an impact prediction determined from post-flight separation conditions, and the actual recovery location.

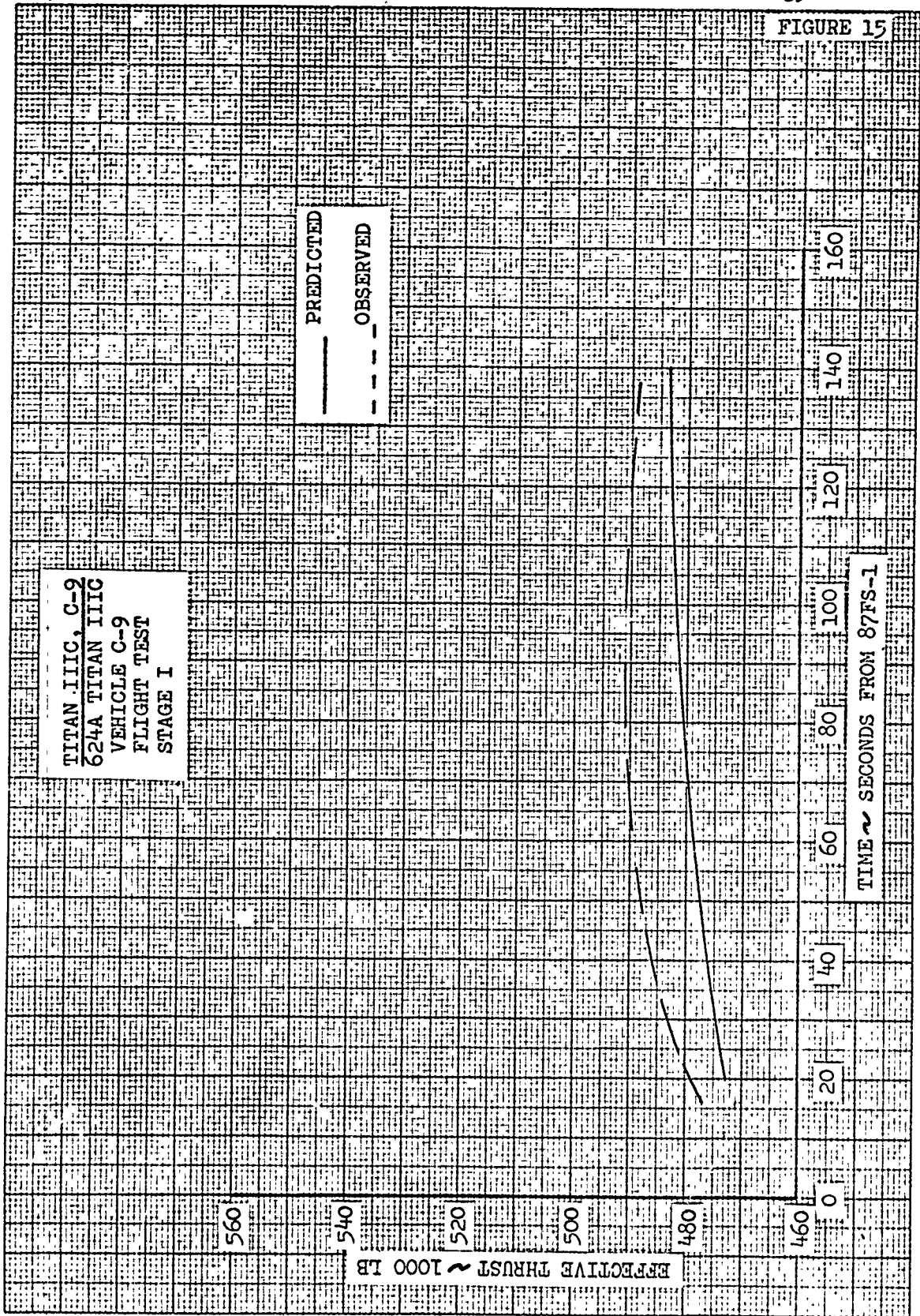
CONFIDENTIAL



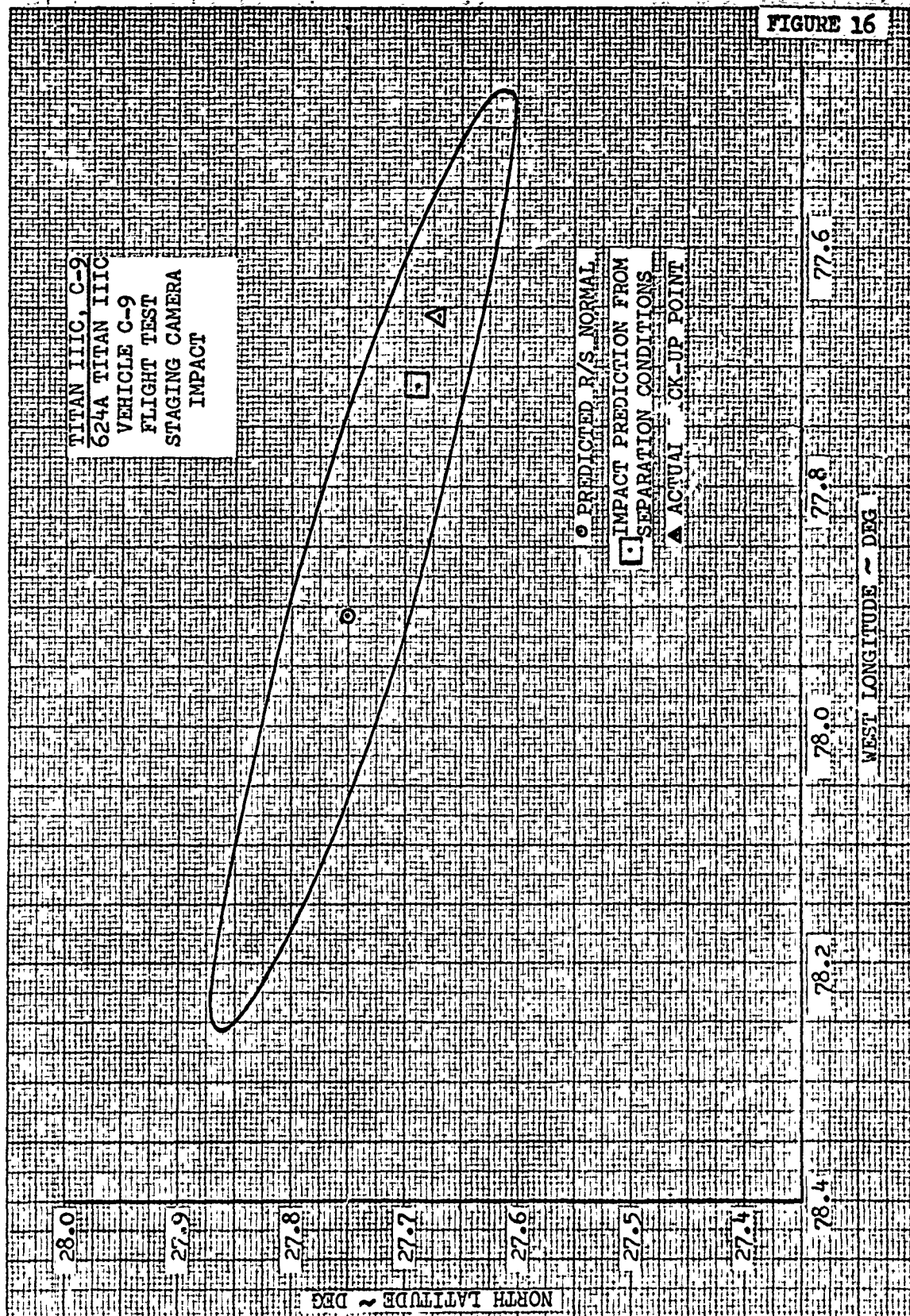
CLEARPRINT QUALITY











### 3.1.3.4.3 Staging Camera Impact - (Cont.)

The nominal impact location was determined from the pre-flight trajectory and the dispersions about this point include wind effects. The actual recovery point is approximately 16 n. mi. downrange from the nominal prediction, but on the ground track of the trajectory and well within the dispersion ellipse.

The actual recovery point would be expected to be downrange since the trajectory flown was hotter than predicted. For comparison an impact prediction was made using the separation conditions from the post-flight trajectory. This predicted point is approximately 12 n. mi. downrange of the nominal, however, wind effects were not included in the prediction.

### 3.1.3.5 Stage II

#### 3.1.3.5.1 Trajectory Characteristics

Stage II experienced slightly low acceleration levels throughout its operational period. A comparison of predicted and observed Stage II axial acceleration histories is presented in Figure 17 and shows the actual initially low, approaching nominal values for a short interval, and then diverging below nominal as burn time increased.

Velocity comparisons at Figure 18 show that with the slightly low acceleration level throughout its operational period, Stage II lost some of the velocity excess that existed at 91FS-1 (denoted by the converging velocity histories). The actual Stage II burn time was approximately 1.7 seconds longer than anticipated which accounts for the net velocity gain for the stage being 7,428 ft/sec or only 19 ft/sec less than predicted. Velocity comparison at 91FS-2 indicate that the observed was 112 ft/sec greater than nominal with a value of 21,306 ft/sec.

Stage II maintained a near-nominal altitude profile as shown in Figure 19, throughout its operational period. The actual altitude profile ran slightly higher than predicted throughout the Stage II burn period and was approximately 2,318 feet high at 91FS-2.

CONTRACT NO. 1015

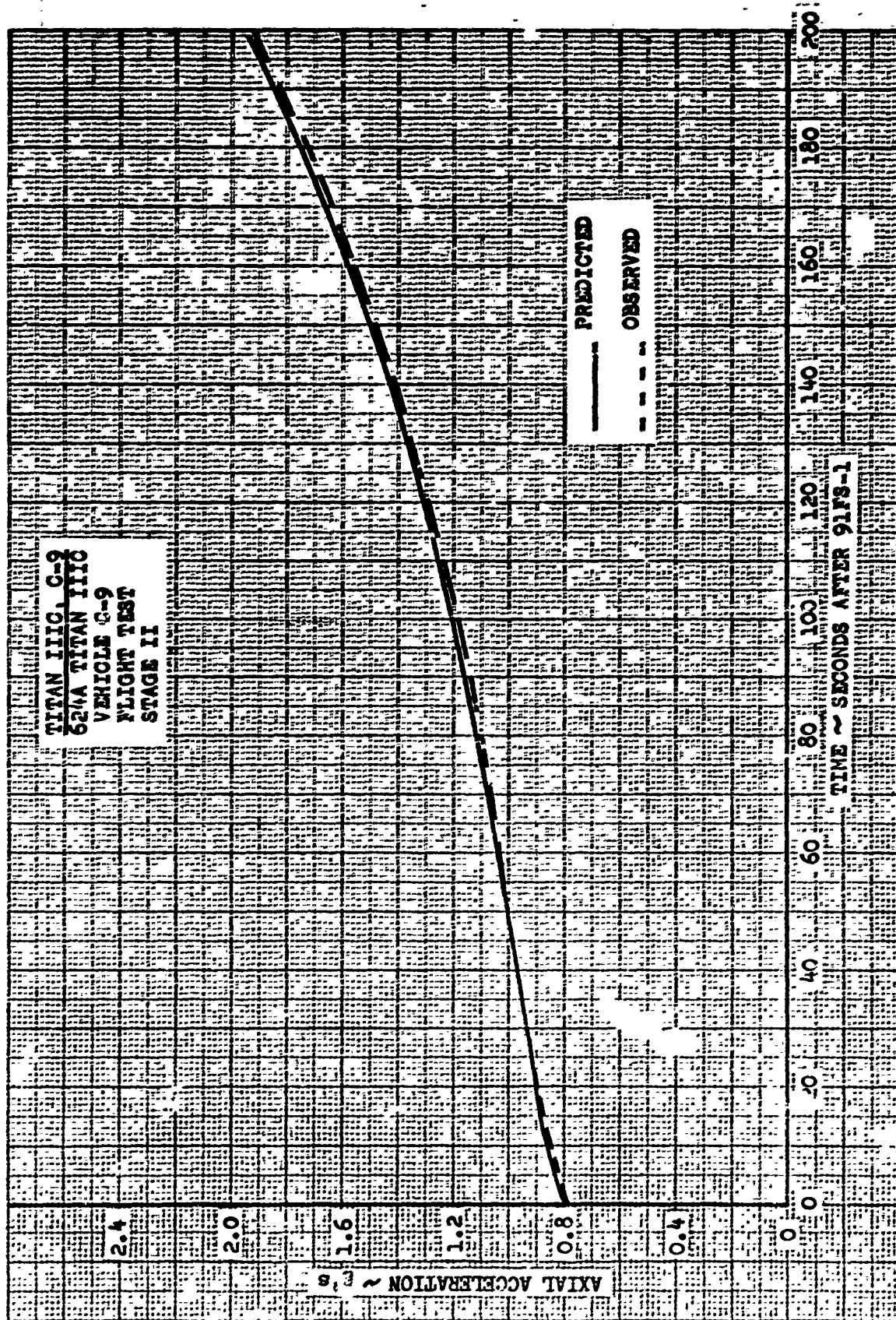


FIGURE 17

CLAMPINT PAPER CO.

PRINTED IN U.S.A. ON CLAMPINT TECHNICAL PAPER NO. 10'S

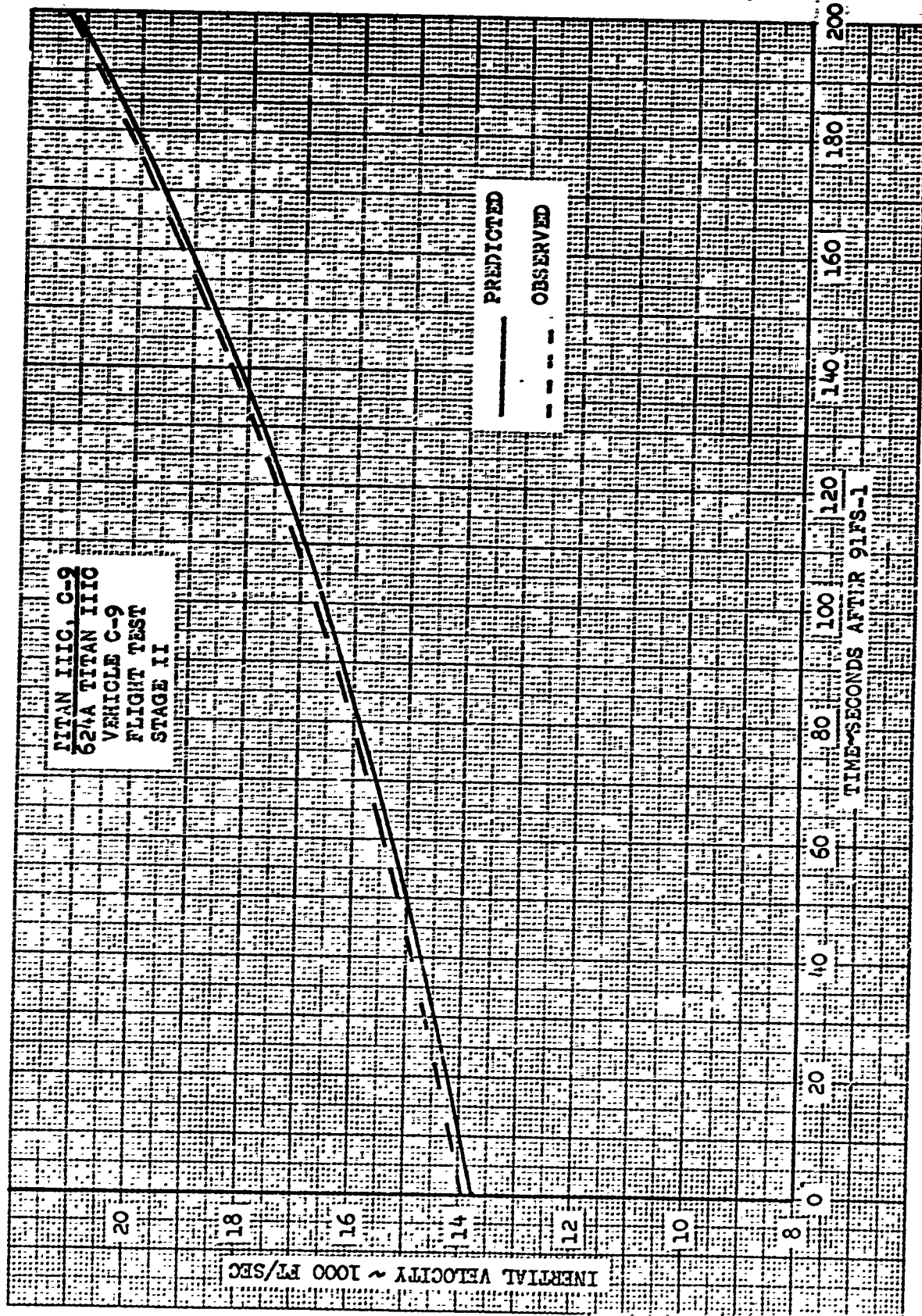
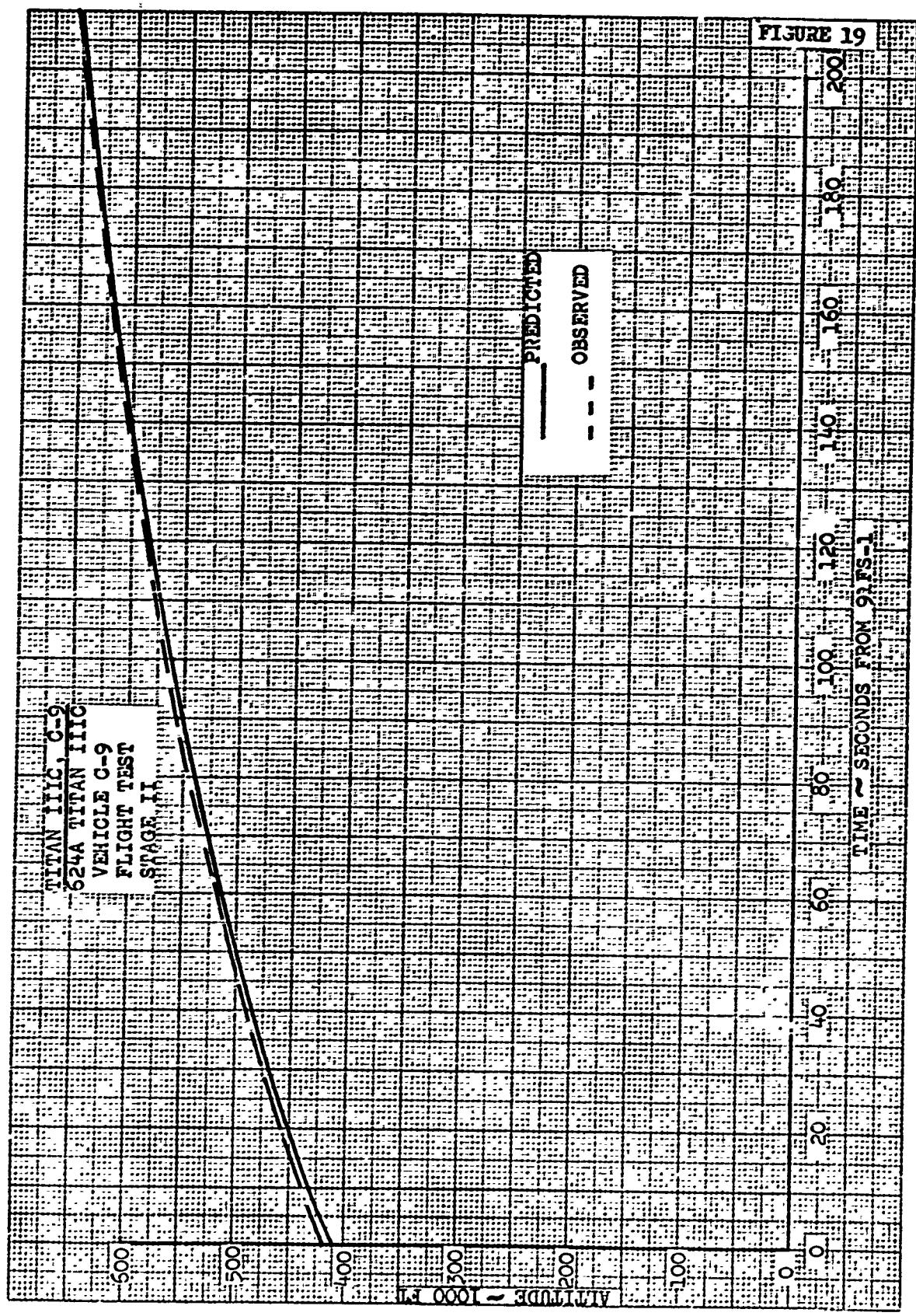


FIGURE 18





CONFIDENTIAL

45

3.1.3.5.2 Performance

- (C) The low Stage II accelerations and long burn time might indicate low Stage II performance. The detailed performance analysis shows that although the thrust was slightly low, the effective specific impulse was considerably higher than predicted. The actual effective thrust had an average value of 103,758 pounds compared to the predicted average of 103,876 pounds with the actual effective specific impulse 4.07 seconds high at an average value of 315.87 seconds. Figure 20 presents a comparison of the total effective thrust histories for Stage II and shows the actual to be considerably below nominal for the major portion of the burn time although rising above near 91FS-2.
- (U) Stage II experienced an oxidizer depletion shutdown with 403 pounds of fuel outage after burning 200.996 seconds, or 1.676 seconds longer than anticipated.

3.1.3.6 Stage III, First Burn

3.1.3.6.1 Trajectory Characteristics

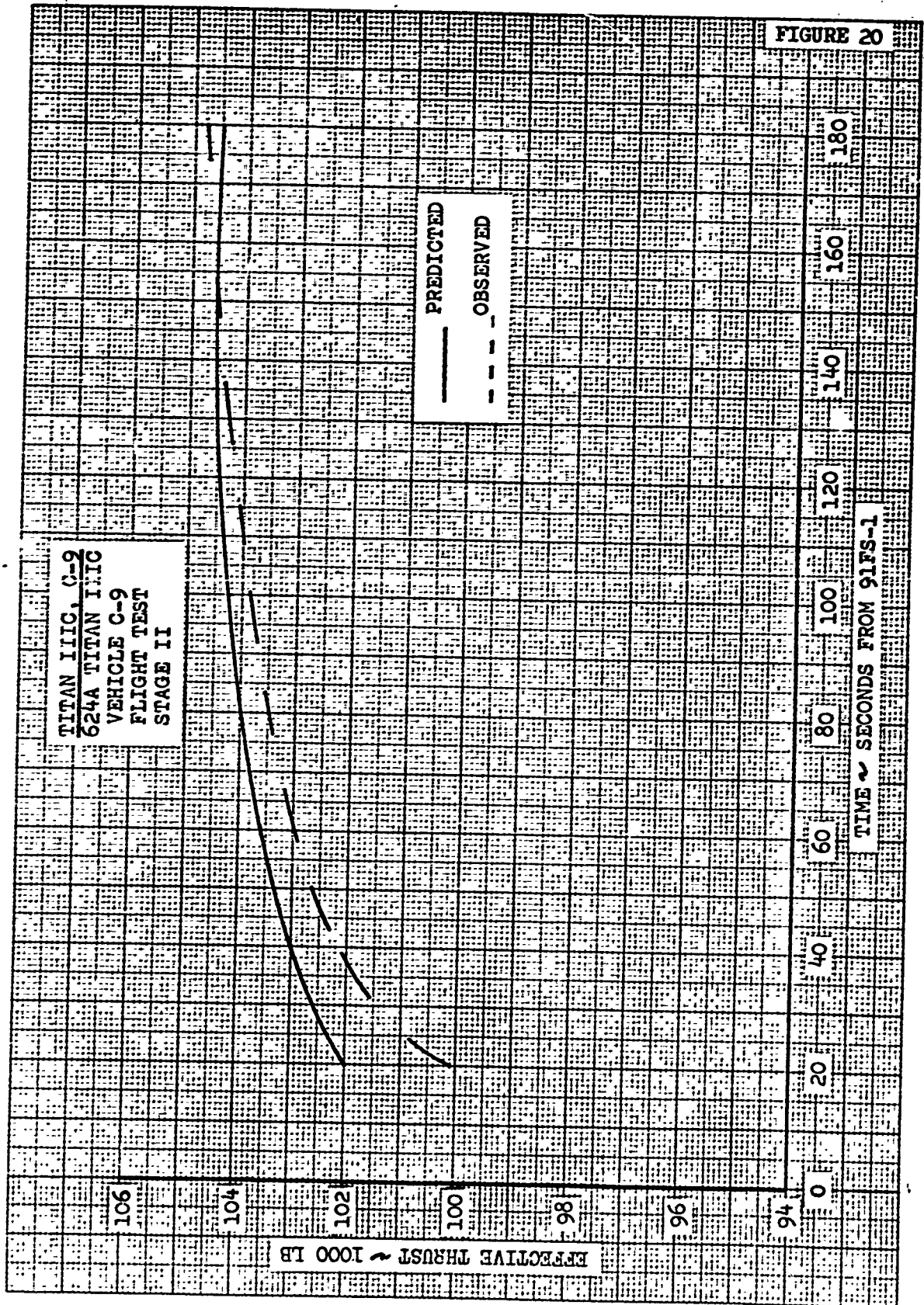
- (U) A comparison of the observed and nominal acceleration levels for the first burn period of Stage III is presented in Figure 21. As the figure shows, Stage III experienced above nominal acceleration levels throughout the first burn interval.
- (U) Figure 22 presents a comparison of the actual and nominal inertial velocity time histories for the first burn period and shows the actual higher than expected and diverging velocity as burn time increased with Stage III programmed to terminate the first burn on an inertial velocity of 25,693, ft/sec. Analysis indicates that the actual velocity at 138FS-2(1) was 25,691 ft/sec or only 2.0 ft/sec less than expected. The actual first burn altitude profile is shown with the nominal in Figure 23.

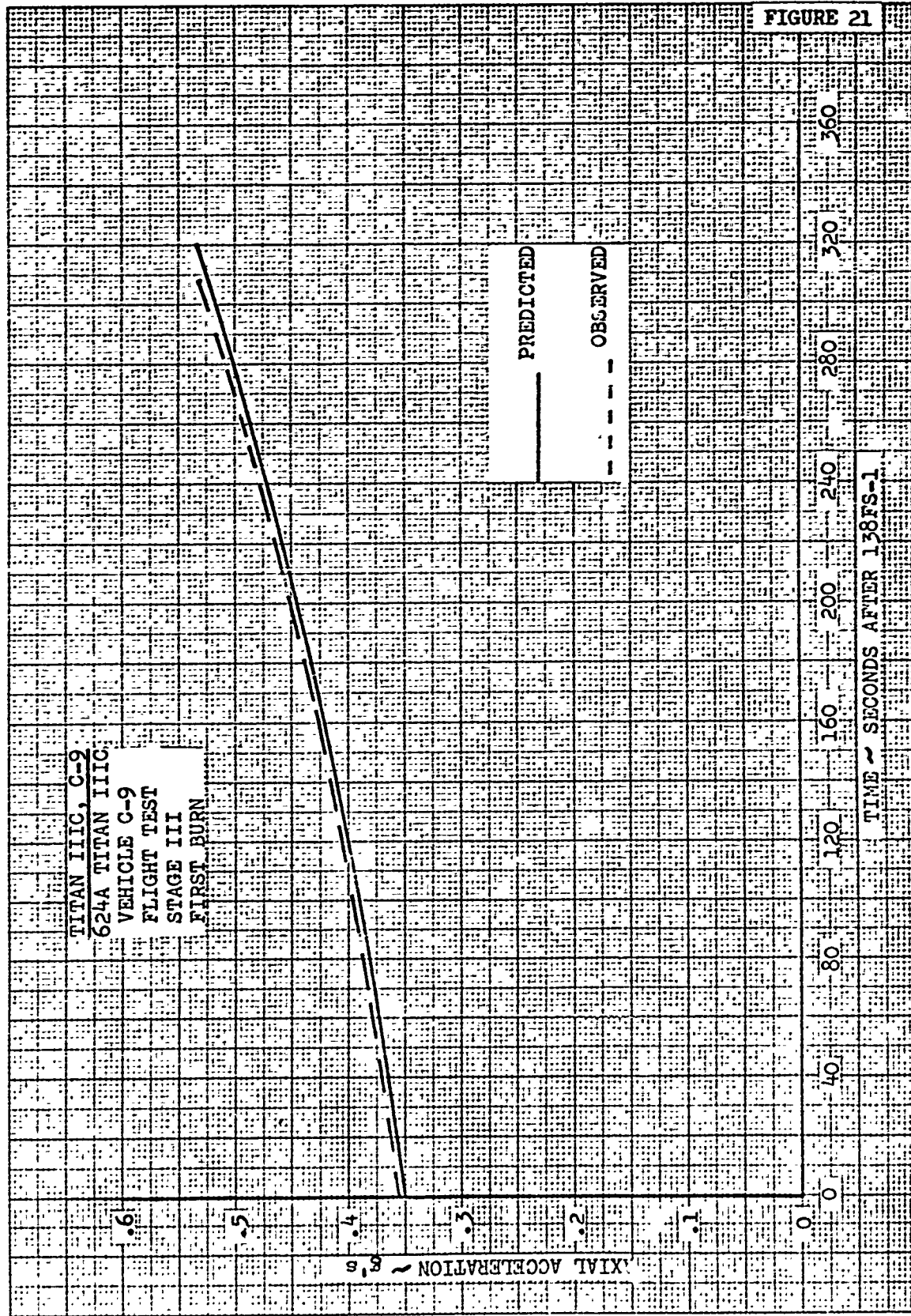
3.1.3.6.2 Performance

- (U) Analysis of the actual burning time indicates that Stage III, with the first burn, satisfied the shutdown criteria approximately 12.81 seconds earlier than expected. Of this 12.81 seconds, 7 seconds can be attributed to the 112 ft/sec velocity excess that existed at 138FS-1(1), the remaining 5 seconds must be attributable to high performance.

CONFIDENTIAL

CLEARPRINT CHART







CLEARPRINT PAPER CO.

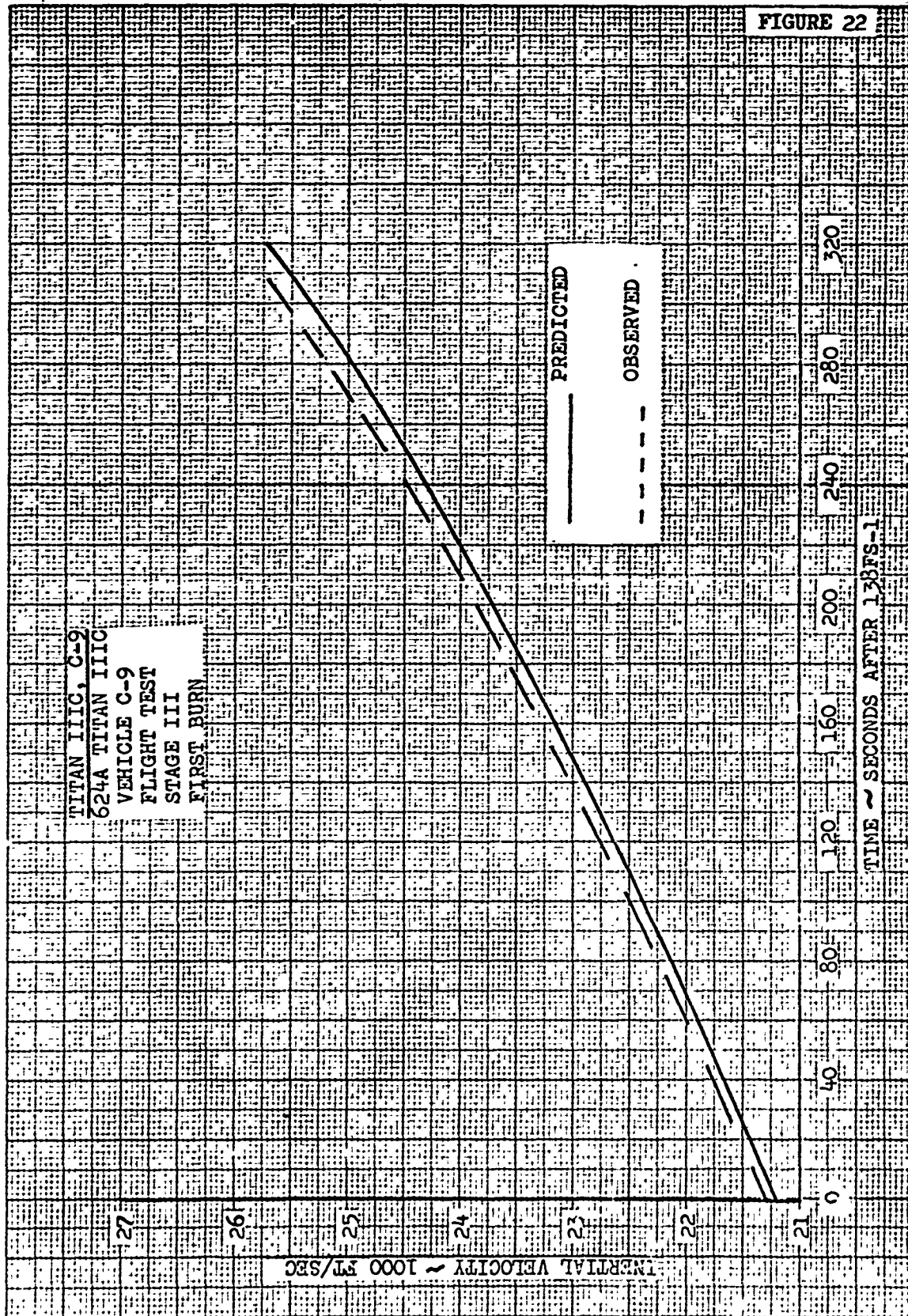
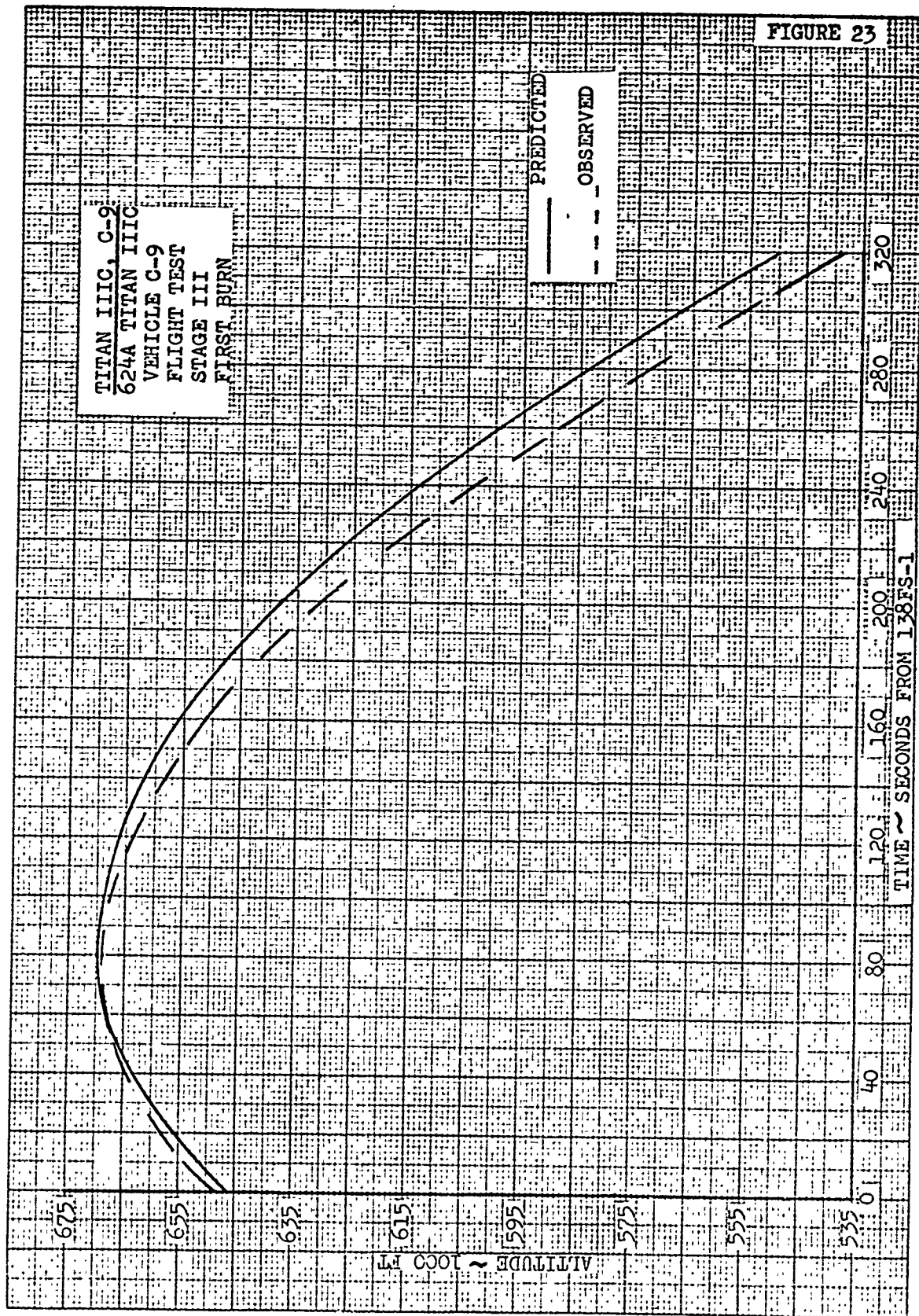


FIGURE 22



### 3.1.3.6.2 Performance - (Cont.)

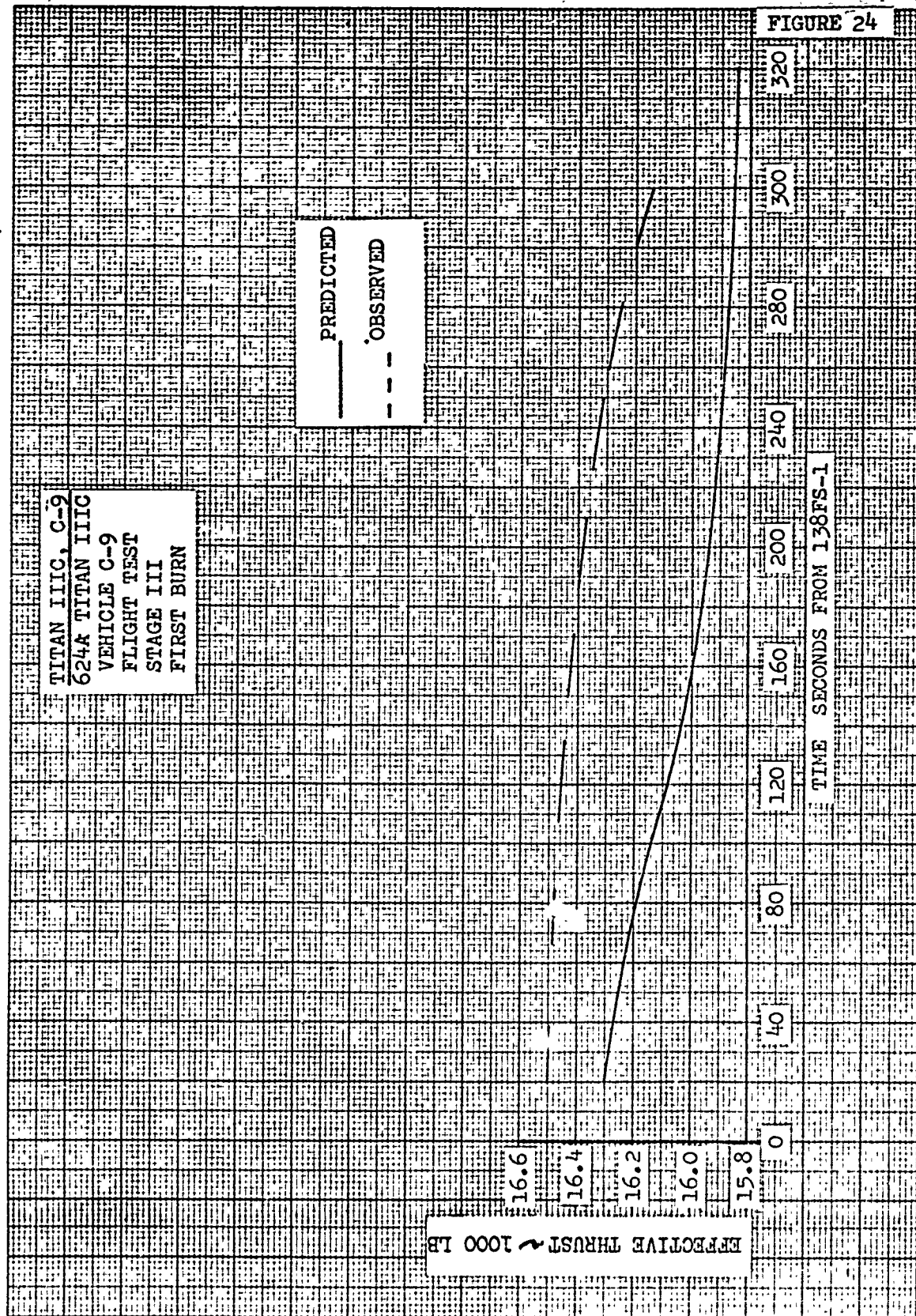
The high actual acceleration levels throughout the first burn period together with the shorter than anticipated burn time indicate high Stage III performance for the first burn period. The performance analysis agrees with this and demonstrates that both the thrust and effective specific impulse were considerably higher than predicted. The actual thrust was approximately 362 pounds high with an average value of 16,430 pounds and the specific impulse 3.64 seconds higher than predicted with an average value of 305.22 seconds. Stage III first burn thrust histories are presented in Figure 24.

### 3.1.3.7 Gemini Separation

The Gemini separation maneuver involved decelerating the transtage - MOL - Adapter (TMA) away from Gemini by the use of 5 retro-rockets, and pitching the TMA nose up by use of the asymmetric arrangement of the retro-rockets and pitch-roll mixing of the ACS rockets. The proper separation rates were achieved, but the TMA pitched nose-down during retro-rocket firing instead of nose-up. Figure 25 compares the predicted with the observed attitude changes after Gemini separation. The desired attitude was eventually achieved by virtue of an extended ACS action time. Quality verification and liftoff films confirmed that the retro-rockets were properly located on the vehicle, thus ruling out the remote possibility that the three rocket cluster had been placed on the side intended for the two-rocket cluster, and vice versa.

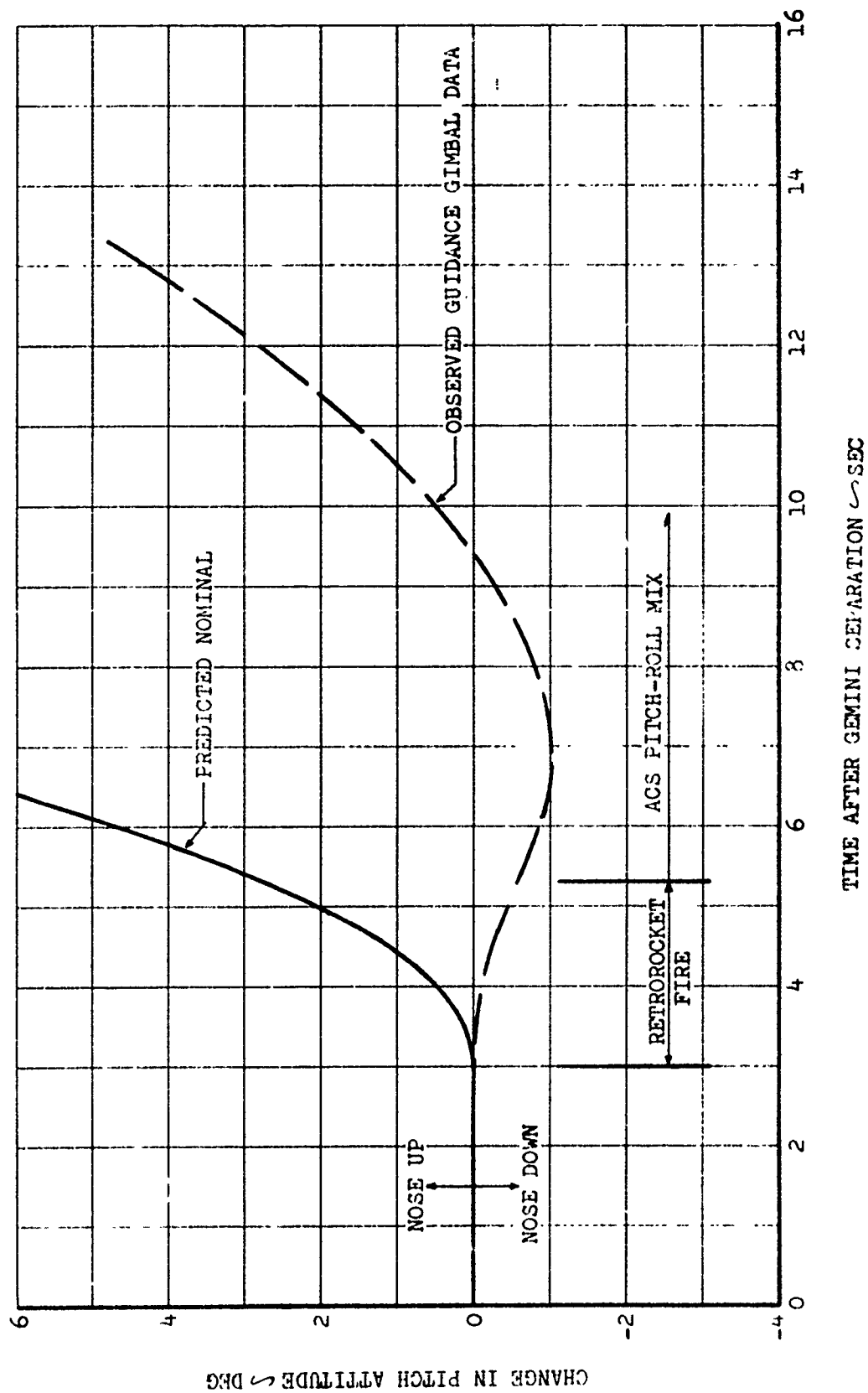
The initial longitudinal acceleration (before the transtage propellants have started to be accelerated) predicted during retro-rocket firing was  $3.9 \text{ ft/sec}^2$ . Guidance data indicated  $3.9 \text{ ft/sec}^2$ , and the  $\pm 2.5 \text{ g}$  accelerometer indicated  $3.5 \text{ ft/sec}^2$ . The predicted velocity increment during the period of retro-rocket firing was  $7.65 \text{ ft/sec}$ . This increment includes the effects of the propellants translating. Integration of the observed accelerations resulted in  $8.0 \text{ ft/sec}$  and  $7.5 \text{ ft/sec}$  from the guidance and the  $\pm 2.5 \text{ g}$  accelerometers respectively. From this data it is concluded that all five retro-rockets fired.

CLEARPRINT



624A TITAN IIIC VEHICLE C-9

ATTITUDE HISTORY AFTER GEMINI SEPARATION



### 3.1.3.7 Gemini Separation - (Cont.)

An analysis (documented in the Fluid Dynamics Section) indicates that the exhaust plume of one retro-rocket could exert a force of 177 pounds on the TMA skin 14 inches ahead of the nozzle exit plane. It was also indicated that the ACS pitch rocket plume could exert 8 pounds of force on the skin 20 inches ahead of the nozzle. These forces were calculated from a method accurate to within  $\pm 20$  percent. Since the plume impingement force of one of the retro-rockets is not counterbalanced by another force diametrically opposite, a net nose-down torque of 3700 ft-lb about the TMA center of gravity was produced by the retro-rocket plume impingement. Similarly, the pitch ACS rocket plume impingement force produces an additional nose-down torque of 130 ft-lb. Neither of these torques were considered in calculating the predicted TMR attitude history in Figure 25. Among those that were considered were the net torque from the retro-rocket longitudinal forces, 2740 ft-lb, and that from the ACS pitch-roll rockets, 930 lb. Both of these are nose-up torques. Algebraically summing these calculated torques produces a net of 160 ft-lb nosedown torque about the TMA center of gravity. The observed attitude data indicates a nosedown torque of 610 ft-lb was present. The difference between the calculated and observed torques could be caused by either the  $\pm 20$  percent uncertainty in the plume impingement forces or by the transtage propellants being located near the sides of their respective tanks. Other factors that could contribute a portion of the difference are uncertainties in predicted mass property characteristics and in thrust vector alignments and magnitudes. The torque values given in the preceding paragraph were obtained assuming the transtage propellants were in the aft end of the tanks.

The vehicle attitude history after retro-rocket firing was quite close to what would be expected with plume impingement forces considered. Maximum pitch-down rate also occurred at the end of retro-rocket burn. This indicates that the anomaly existed only during retro-rocket action which would further indicate the anomaly was caused by plume impingement.



### 3.1.3.7 Gemini Separation - (Cont.)

It is concluded that all five retro-rockets fired and that satisfactory separation rates were achieved. It is further concluded that rocket plume impingement on the TMA skin and possibly some motion of transtage propellant relative to the tanks caused a nosedown motion during retro-rocket action, instead of the desired noseup motion.

The Gemini spacecraft was separated at 810.237 seconds after liftoff with the following conditions:

Inertial Velocity	ft/sec	25,721.947
Altitude	feet	523,273.25
Flight Path Angle	deg	-1.8036

The pretest trajectory called for the Gemini spacecraft to be separated at 813.0 seconds with the following conditions:

Inertial Velocity	ft/sec	25,721.906
Altitude	feet	523,394.25
Flight Path Angle	deg	-1.8035

A comparison of the above numbers shows that the Gemini was separated with conditions that were very close to those desired.

### 3.1.3.8 Stage III Second Burn

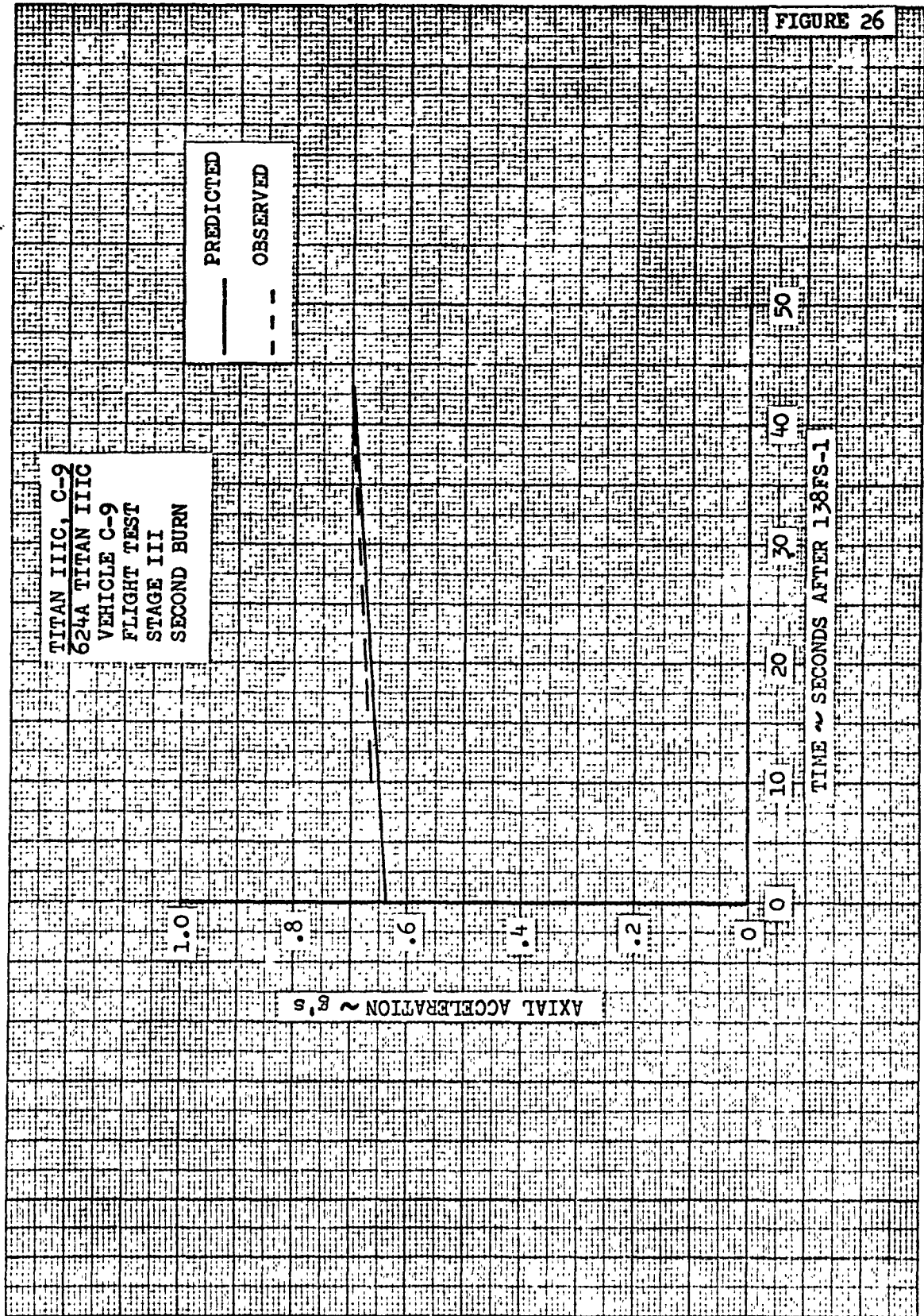
#### 3.1.3.8.1 Trajectory Characteristics

Figure 26 presents a comparison of nominal and actual acceleration levels for the second burn of Stage III and shows the actual acceleration level running slightly high although converging to nominal values by shutdown.

With the high acceleration level, Stage III maintained a high velocity profile throughout the second burn period as shown on the velocity comparisons of Figure 27. Analysis indicate that the second burn period was terminated on a velocity of 25,795 ft/sec which was only 2.0 ft/sec more than expected.

Stage III maintained an altitude profile lower than nominal throughout the second burn as shown in Figure 28, which resulted in an altitude 2,912 feet lower than predicted at 138 FS 2(2).

CLEARPRINT COMPANY





CLEARPRINT CHART

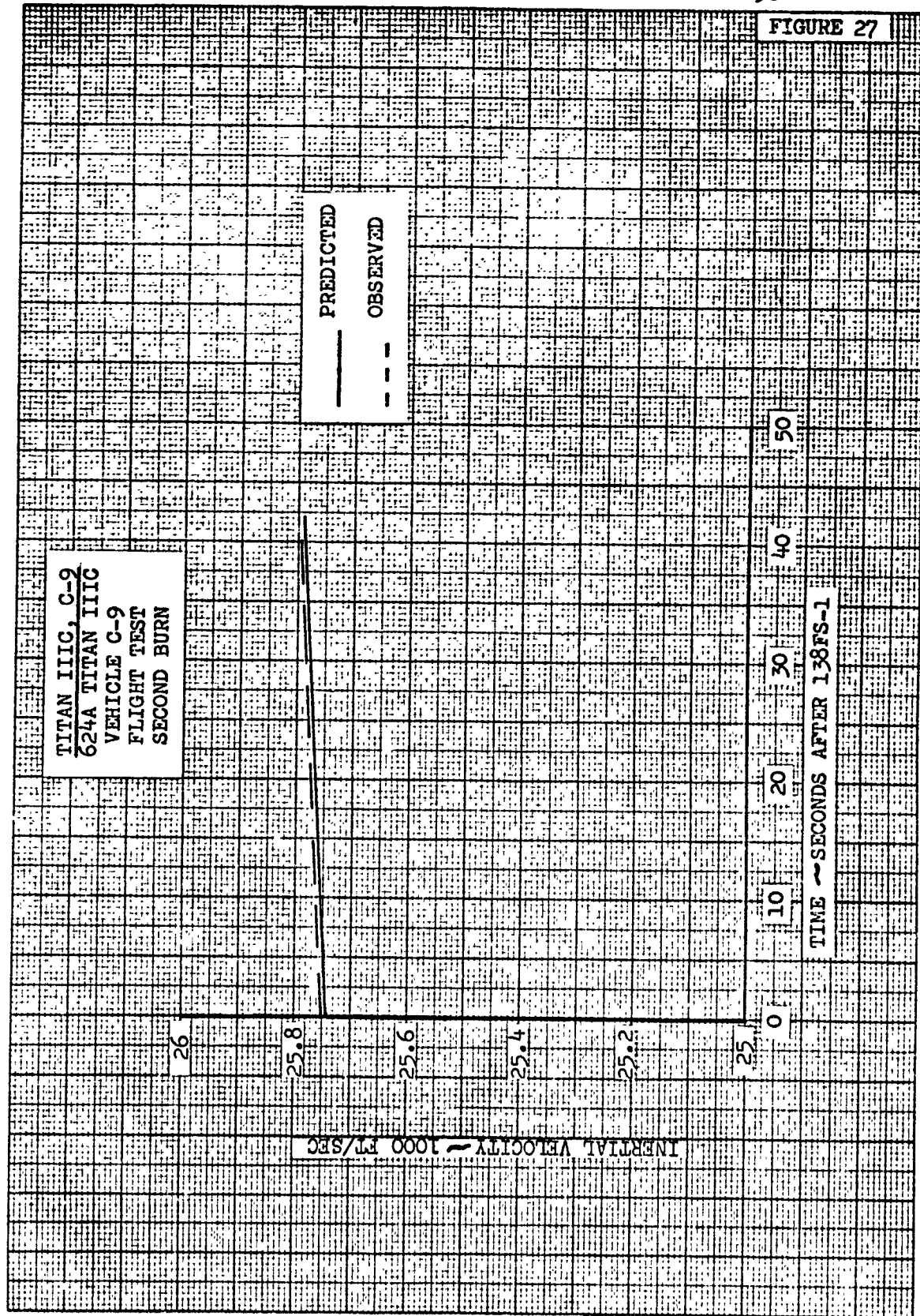
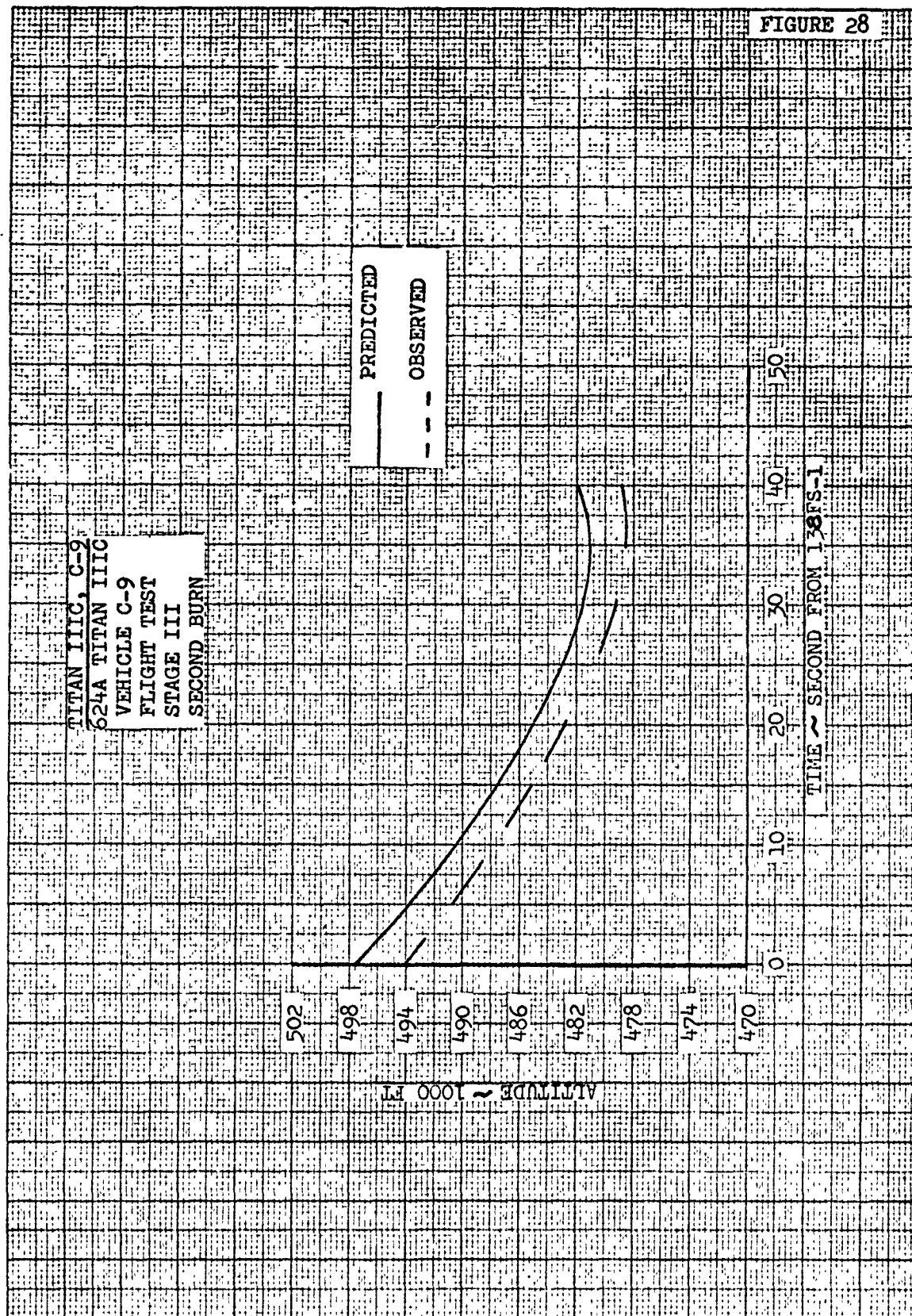


FIGURE 27



### 3.1.3.8.2 Performance

The orbital injection velocity requirement for termination of the second burn period of Stage II was satisfied 0.58 seconds earlier than expected. This fact, together with the slightly high acceleration level, would indicate high Stage III performance for the second burn period.

The performance analysis shows the actual thrust level averaging 16,420 pounds which is 617 pounds higher than predicted. Figure 29 presents a comparison of thrust histories for the second burn and shows the actual thrust high throughout the burn period. Further analysis of the specific impulse indicates that the actual effective specific impulse was also high with an average value of 305.04 seconds compared to the nominal of 300.96 seconds.

### 3.1.3.9 Transfer Orbit

The actual transfer orbit obtained with the second Stage III burn period is compared with the nominal in Table 3. The actual orbital data was derived from telemetered IGS data and shows that the second burn period established a transfer orbit that was very close to nominal.

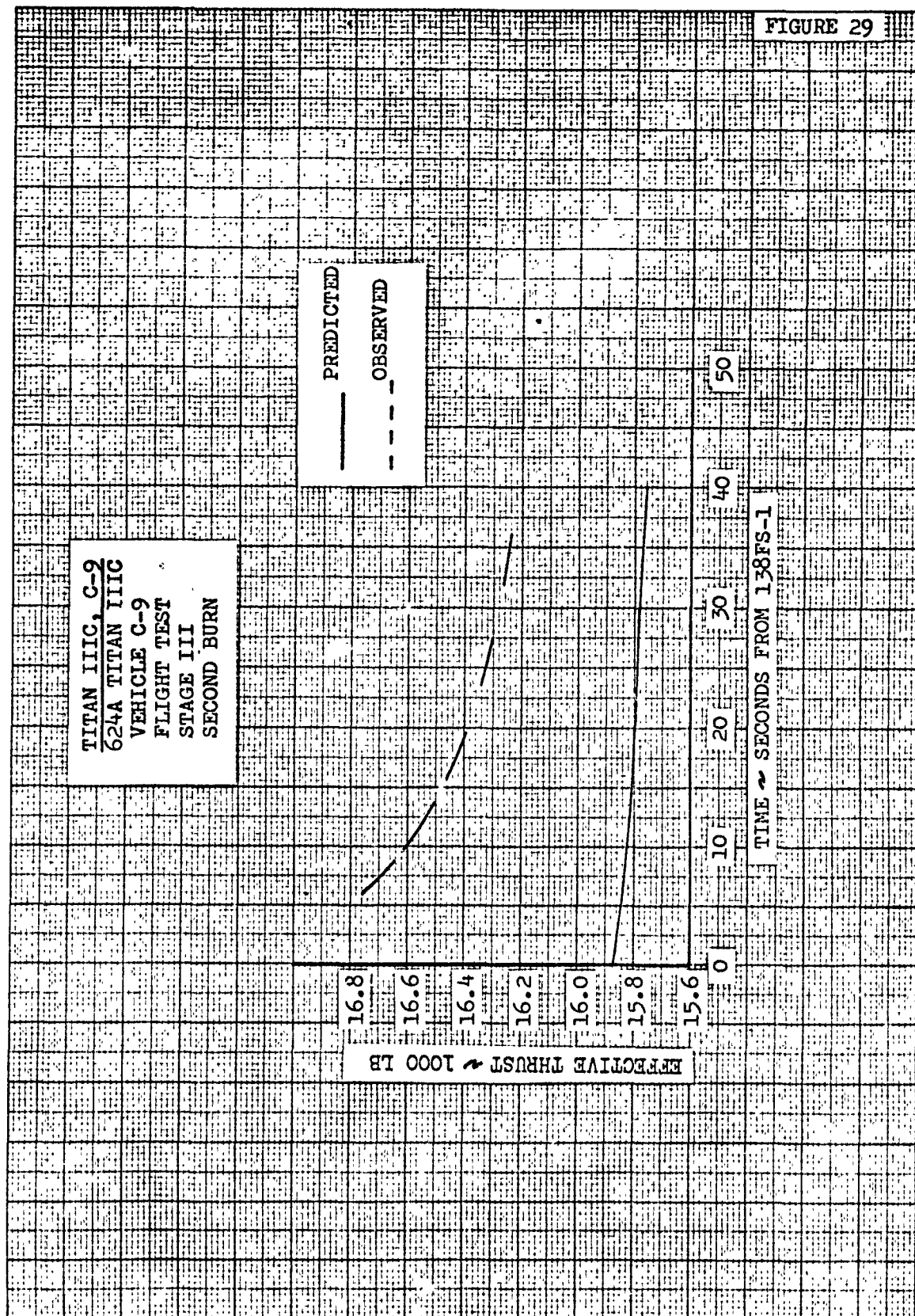
### 3.1.3.10 Stage III Third Burn

#### 3.1.3.10.1 Trajectory Characteristics

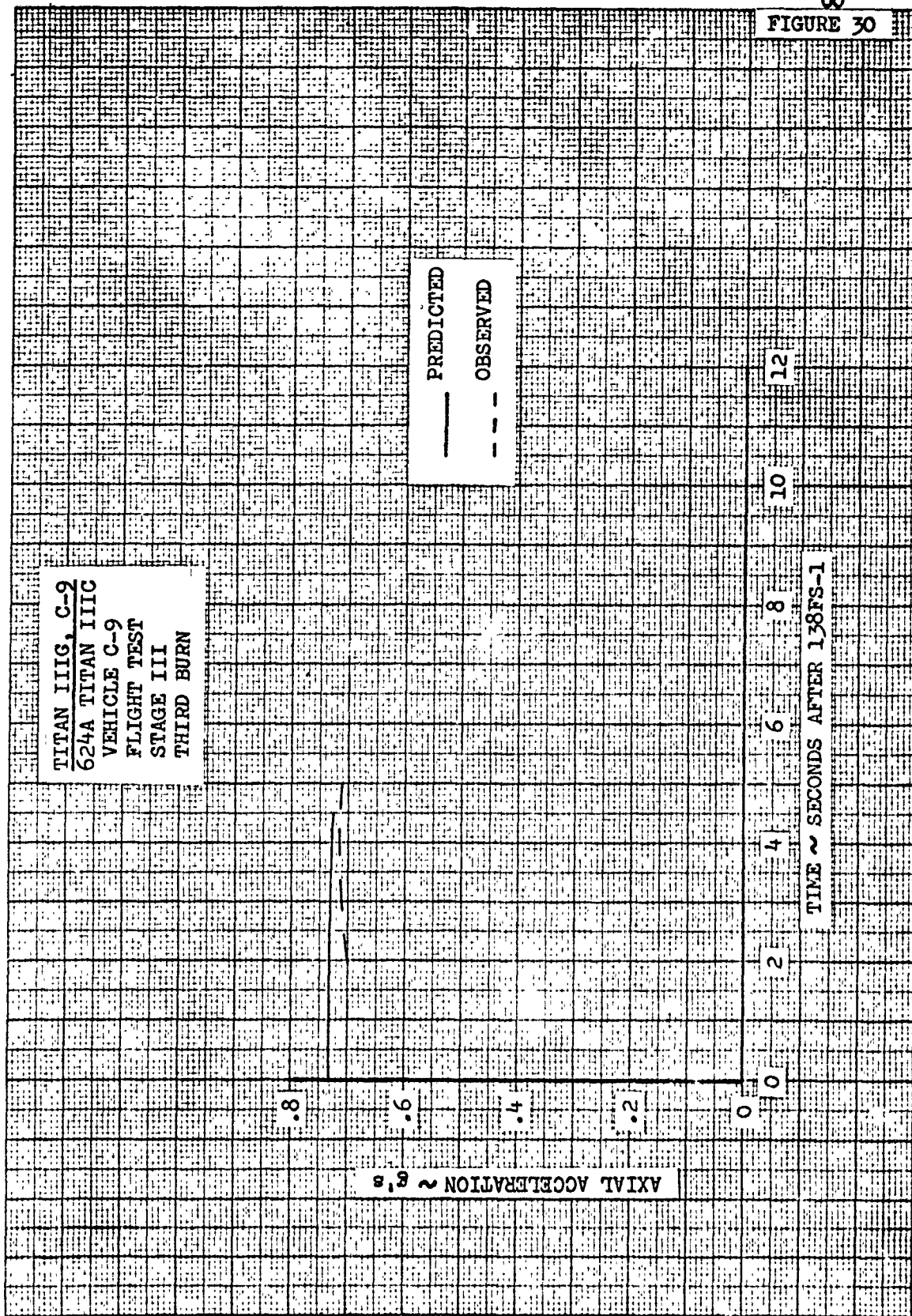
At 3,182.236 seconds after liftoff, Stage III ignited again for the third burn to inject the payload into the final circular orbit. The actual acceleration level was slightly low throughout the short burn period as shown in the acceleration comparisons of Figure 30.

Figure 31 presents a comparison of the actual and nominal inertial velocity histories for the third transtage burn and shows that Vehicle 9 failed to maintain the nominal velocity profile. Analysis indicates that with a burn time of 6.14 seconds, Stage III shut down on a velocity of 25,363 ft/sec to successfully inject the payload into the final circular orbit. The pretest trajectory called for Stage III to shutdown, after a burn of 5.81 seconds duration, with an inertial velocity of 25,365 ft/sec and an altitude of 971,390 feet. Therefore, the actual inject conditions

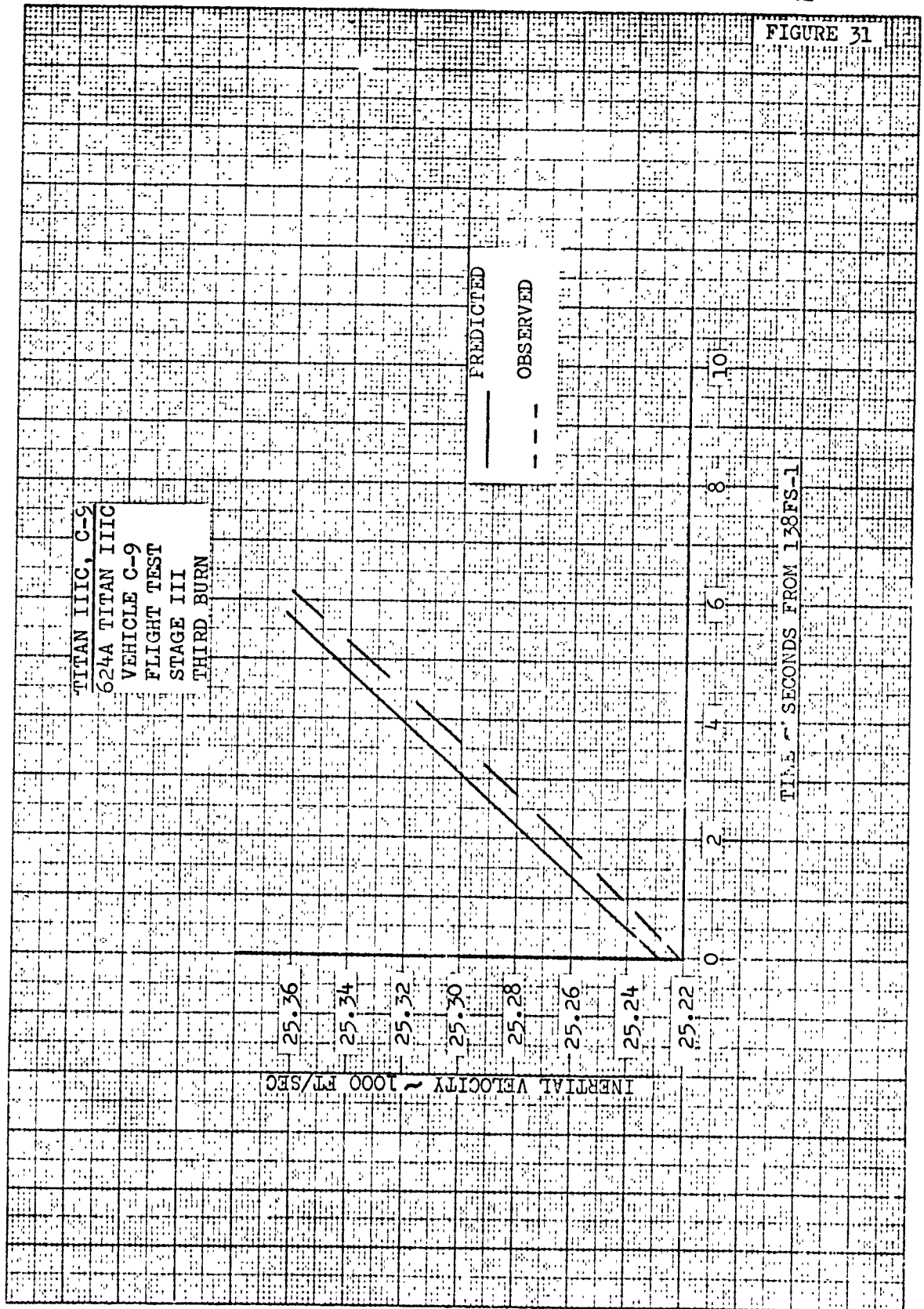
CLEARPRINT QUALITY



CLEARPRINT CHART







### 3.1.3.10.1 Trajectory Characteristics - (Cont.)

were only off 2.0 ft/sec and 493 feet in velocity and altitude respectively, and were sufficient to establish a final circular orbit that was close to nominal. Figure 32 presents the actual altitude profile for the third burn period.

### 3.1.3.10.2 Performance

A comparison of the actual and predicted thrust levels is presented in Figure 33 and shows that Stage III experienced low performance during the third burn period. Analysis shows the actual thrust to be 182 pounds low with an average value of 16,180 pounds coupled with a specific impulse averaging 300.58 seconds, slightly higher than predicted.

Stage III was required to burn an additional 0.33 seconds longer than expected to satisfy the orbital injection velocity requirement for termination of the third burn period and this further substantiates the low thrust conclusion drawn from the performance analysis. An oxidizer outage of 135 pounds together with a propellant margin of 1,787 pounds (33.2 seconds of burning time margin) existed at termination of the third burn. The pretest trajectory indicated that the Stage III propellant margin at termination of the third burn would be approximately 664 pounds or 12.34 seconds of burning time margin.

### 3.1.3.11 Final Orbit

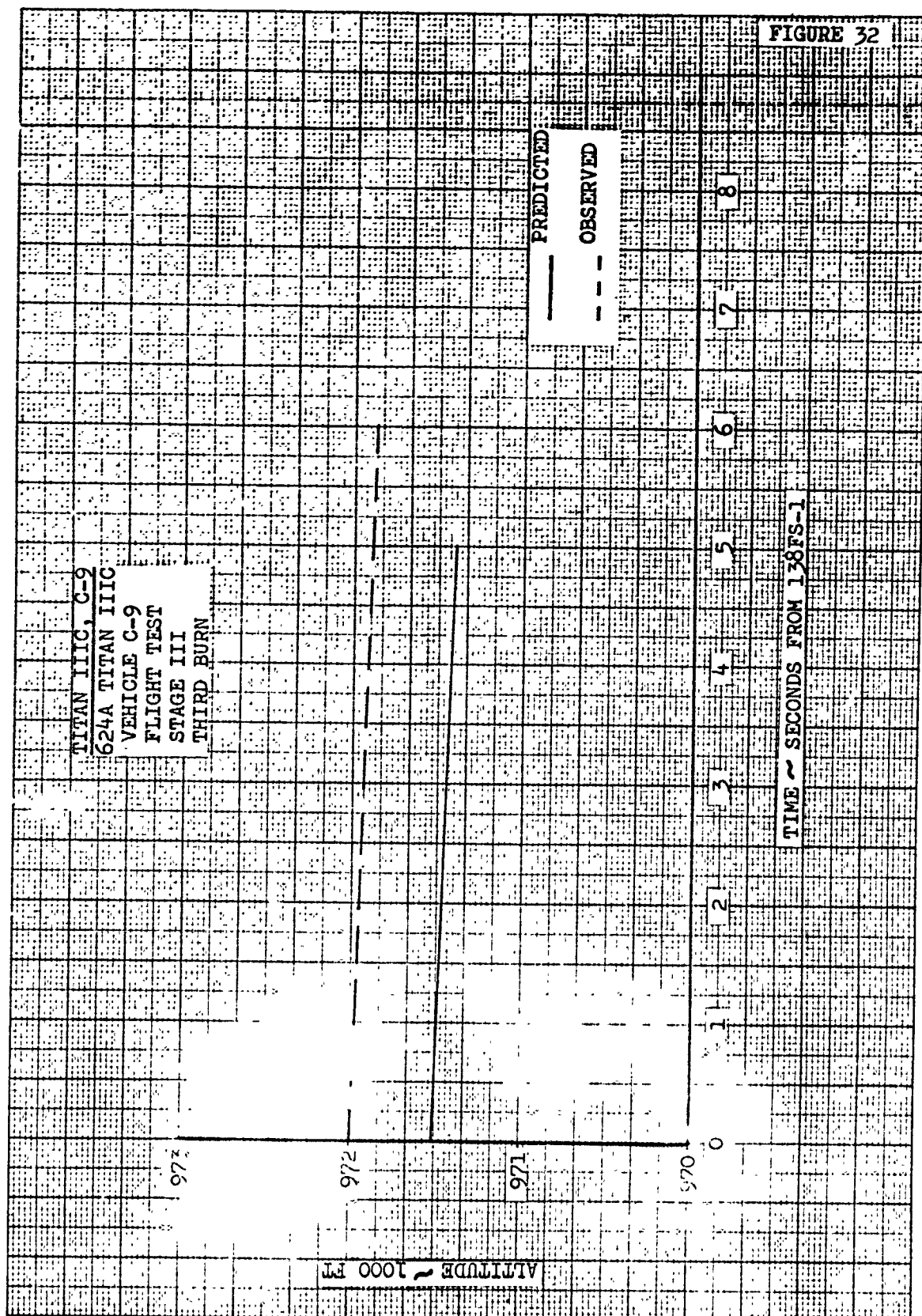
The MOL Simulated Laboratory and the three satellites (OV-1, OV4-1T, and OV4-1R) carried on Vehicle 9 were successfully injected into a circular orbit. Table 3 presents a comparison of the actual and nominal final circular orbit parameters. The actual orbit numbers were derived from telemetered IGS data and show that Stage III, with the third burn, established a final circular orbit very close to predicted.

### 3.1.3.12 Staging

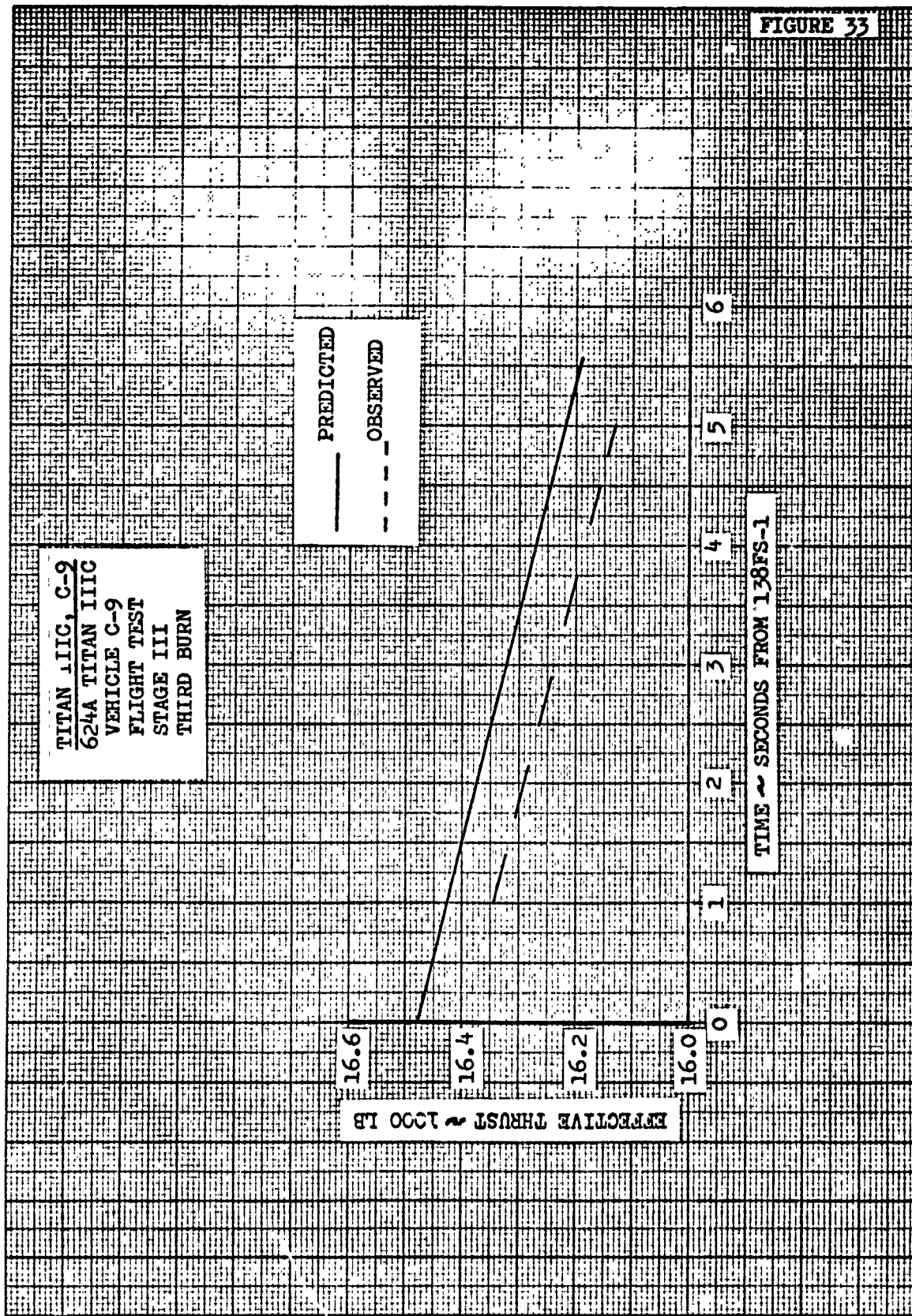
#### 3.1.3.12.1 Stage O/I Separation

Stage O/I Separation appeared to be normal with no anomalies noted. Figure 34 shows a comparison between telemetered and predicted reel data. The core roll transient was about the same magnitude as those run on Vehicles 4 and 7. All available data indicate a successful separation.

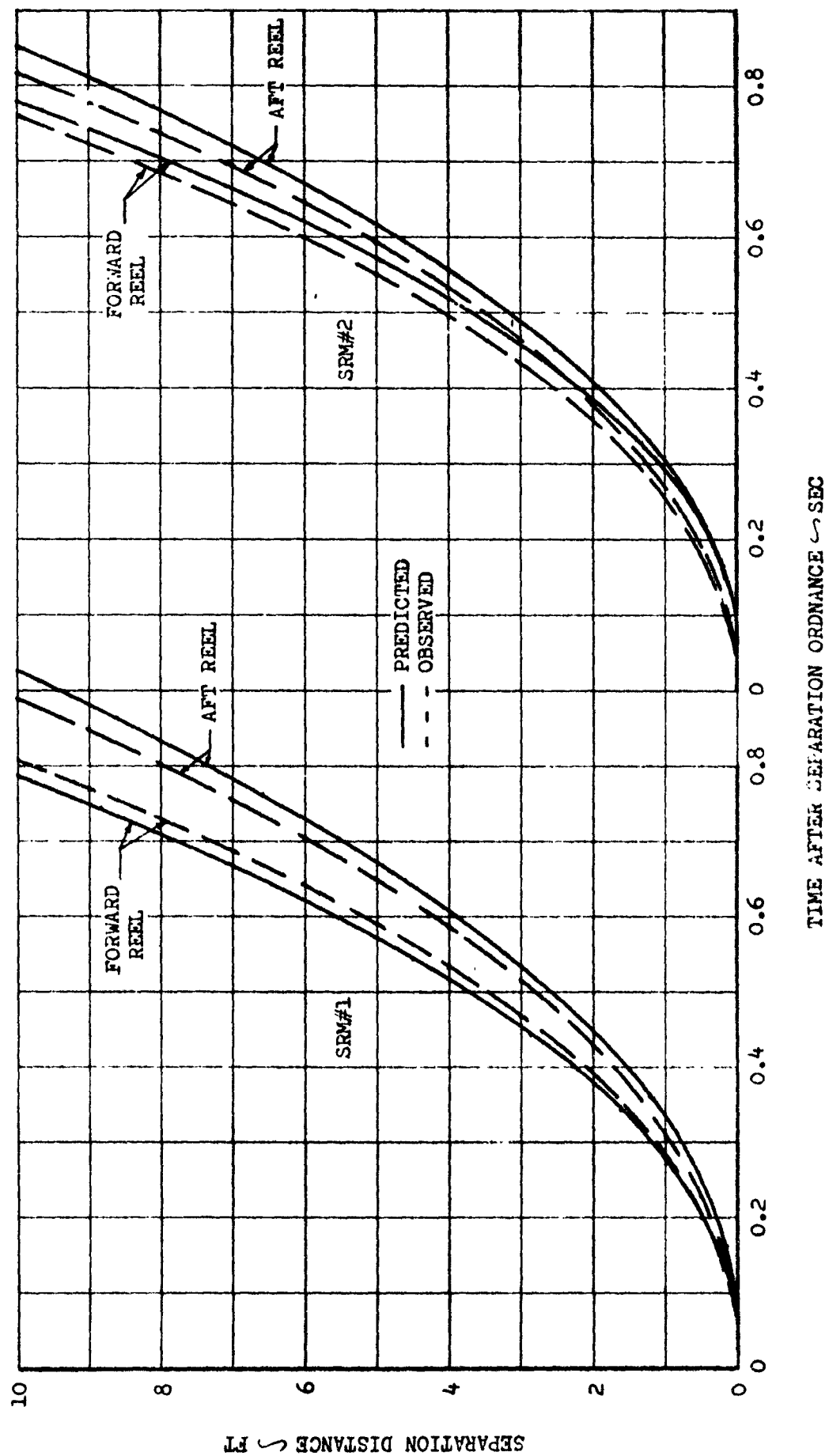
CHAPMAN & GUTH







624A TITAN IIIC VEHICLE C-9  
STAGE O/I SEPARATION HISTORY



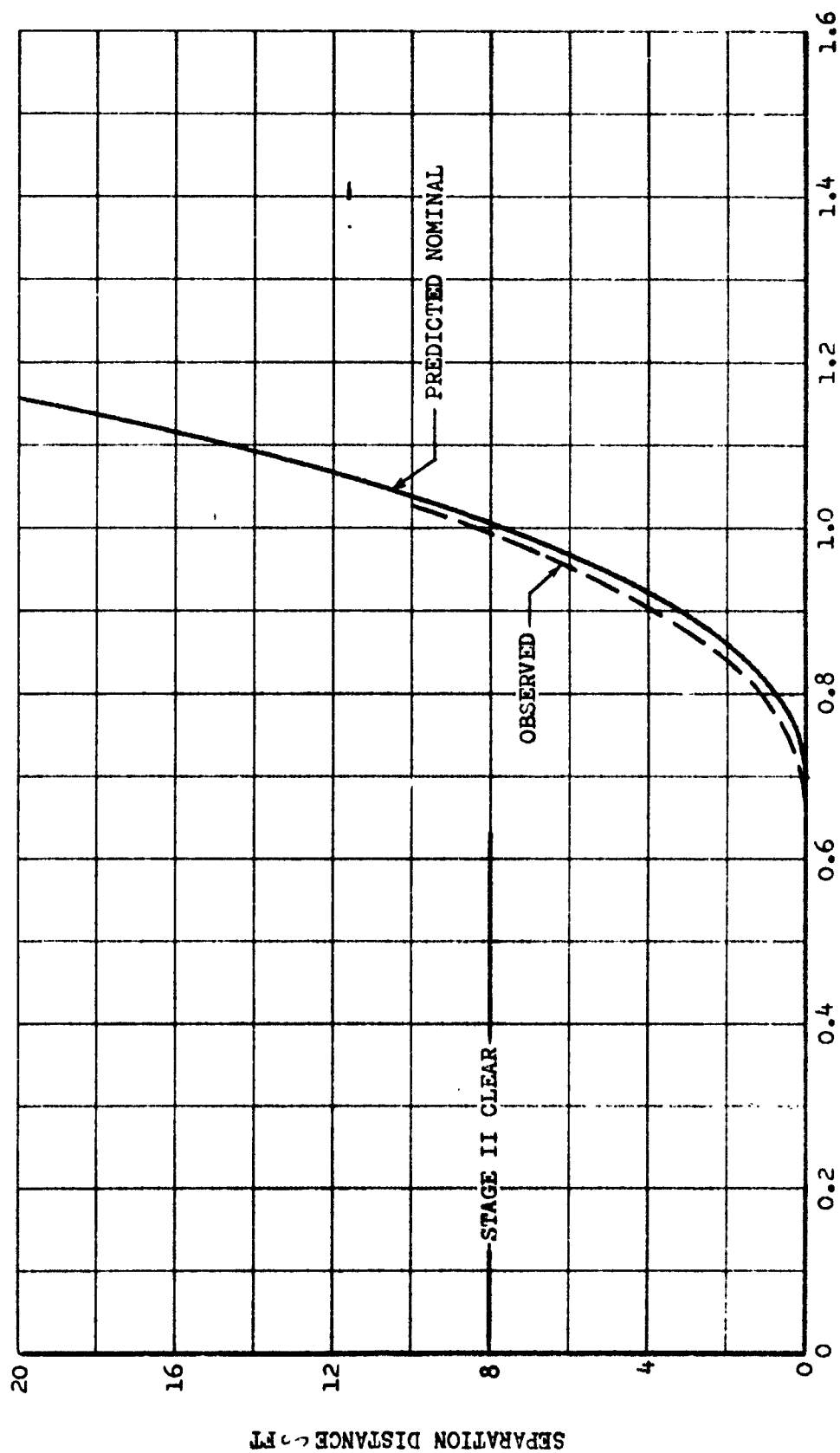
#### 3.1.3.12.2 Stage I/II Staging

The Stage I/II staging appears to have been successful. The separation reel data show initial motion occurred at 0.67 seconds after 87FS-2. Figure 35 presents the Stage I/II relative separation history and shows good comparison between the predicted and actual separation. No anomalies were noted during separation.

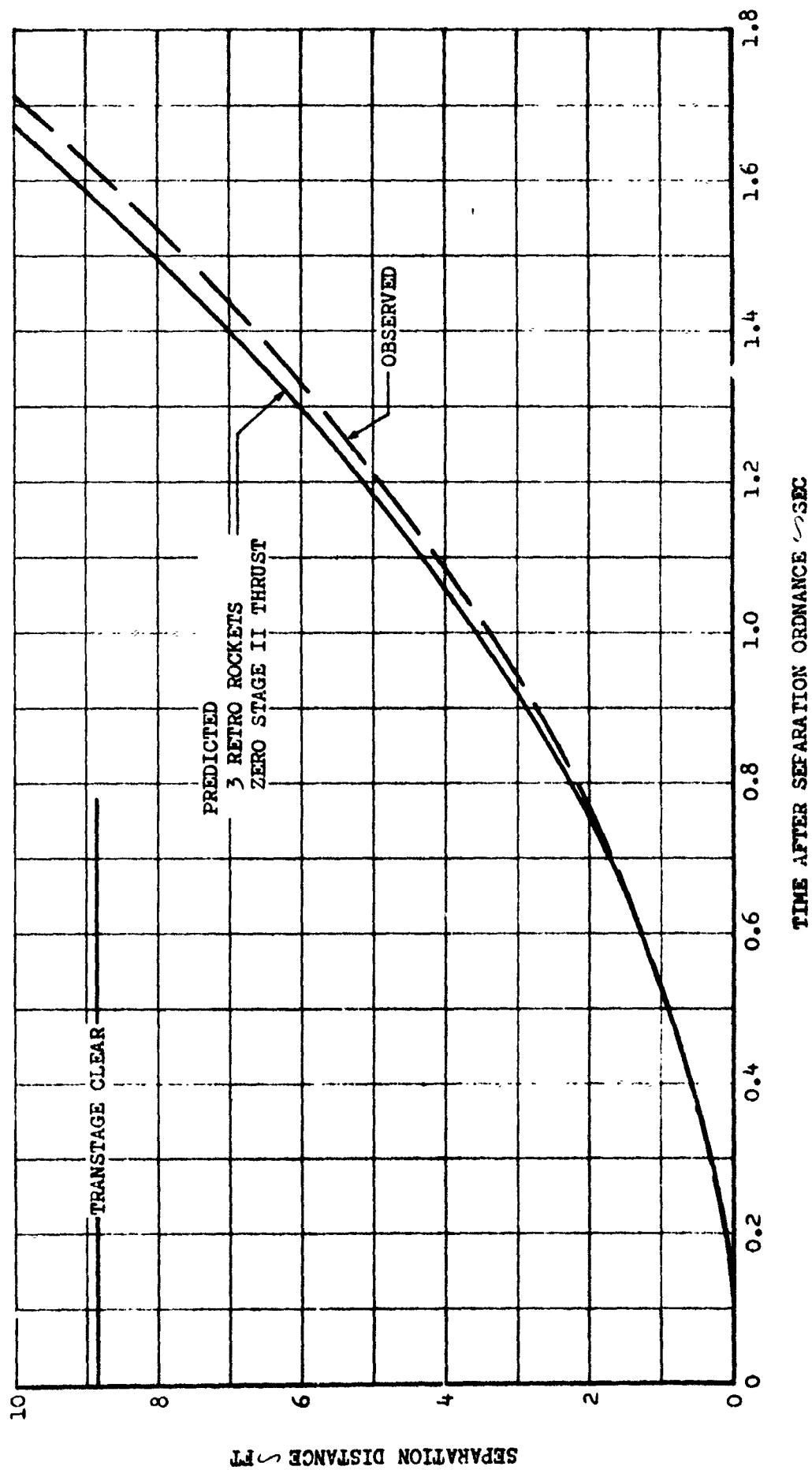
#### 3.1.3.12.3 Stage II/III Staging

The separation reel data shows that 10 feet of separation was achieved in 1.71 seconds. Figure 36 presents a comparison of measured data versus predicted with all the three retro-rockets firing and zero Stage II thrust at the time of separation ordnance. A good comparison is noted, indicating a successful separation.

624A TITAN IIIC VEHICLE C-9  
STAGE I/II SEPARATION HISTORY



624A TITAN IIIC VEHICLE C-9  
STAGE II/III SEPARATION HISTORY



68  
FIGURE 36

### 3.2 AIRBORNE SUBSYSTEM EVALUATION

#### 3.2.1 Propulsion

##### 3.2.1.1 Introduction

###### 3.2.1.1.1 Summary

All Article #C9 flight objectives were accomplished by the Propulsion systems except the final ACS maneuver. Due to depletion of ACS propellants and subsequent loss of attitude control, the final vehicle pitch and roll rates were not achieved.

###### 3.2.1.1.2 Configuration

The configuration of the Propulsion systems on Article #C9 was the same as Article #C11 and #C12 with the following Stage III exceptions:

- a. Redundant flight pressure switches were installed on #C9 as they will be on Article #C5 and #C10.
- b. The upper and lower mid-tank level sensors were not installed on Article #C9. The effectivity of this change is Article #C8, #C10 and up.
- c. Several changes were made to improve the thermal control of the Stage III engine and are covered in detail in that section.

Article #C9 was the second vehicle to fly a heavy ablative skirt on Stage II.

###### 3.2.1.1.3 Prelaunch

No holds were encountered in the countdown due to the Propulsion systems. The Stage II oxidizer tank decayed out-of-limits during a hold that was initiated for excessive high altitude winds.

Propellant tank temperatures were reduced by the cold front (44°F) that moved through the launch area. Due to the greater influence of the ground air-conditioning system on some tanks, all tanks were not affected the same. The effect of this cold front on propellant probe temperatures from completion of loading to lift-off was as follows:

3.2.1.1.3 Prelaunch - (Cont.)

	<u>Loaded</u>	<u>L/O</u>	<u>Ave. In-Flight</u>
Stage I Fuel	62.5	57.8	62.5
Stage I Oxidizer	82.6	64.0	67.0
Stage II Fuel	82.0	64.5	65.0
Stage II Oxidizer	82.0	63.4	65.0

3.2.1.1.4 Stage 0

The SRM ballistic performance was satisfactory. Ignition delay, web action time and tail-off performance were all within specification. Thrust vector control performance was also satisfactory during the terminal countdown and flight.

Motor performance predictions, i.e., thrust, total impulse, and specific impulse could not be calculated for this flight since UTC did not supply detailed propellant characteristics. All data in this report have been compared with the UTC predictions, UTC model specification and IFS-TIII-14001, where applicable.

Several anomalies were noted by the DRS on the SRM igniter S&A circuits after SRM ignition. UTC has advised Martin that these are not cause for concern.

3.2.1.1.5 Stage I

The overall performance of Stage I was satisfactory. A slight thrust spike was observed on the start transient. Although acceptance data for this engine are within specification, a tendency toward a "hot-start" is noted. Some evidence of "POGO" was observed during steady state operation. Shutdown exhibited normal oxidizer exhaustion.

3.2.1.1.6 Stage II

The overall performance of Stage II was satisfactory. A thrust overshoot was observed on the start transient which is in excess of the existing specification. On subsequent vehicles (except Article #C13), the amount of overshoot noted on Article #C9 will be acceptable due to a specification change. Stage II fuel tank gas pressure showed some deviation from predicted, however, flow box points are well within specification. Shutdown was caused by oxidizer exhaustion with several chamber pressure spikes noted before the thrust chamber valves were closed.



### 3.2.1.1.7 Stage III

Actual flight data showed tank gas pressures to be in general disagreement with preflight predictions. This occurred as a result of the following:

- a. The tank top pressurization system check valves were replaced prior to vehicle shipment. This information was not included in the Art. #C9 predictions.
- b. Agitation of the propellants at solid retro motor firing after Gemini separation caused an increase in tank gas pressures that was not predicted.

The error in the tank gas pressure predictions caused a corresponding error in the predicted mixture ratio.

Engine throat temperatures were higher than have been seen on previous flights indicating ineffectiveness of the radiation shields.

A slight thrust overshoot was experienced on the third burn start transient.

### 3.2.1.1.8 ACS

Attitude control was maintained for approximately 90% of the Article #C9 mission. Propellants were expended prior to the final pitch and roll maneuver due to the excessive duty imposed on the Attitude Control System. Exhaust plume impingement from the 45-lb. thrust engine modules reduced control effectiveness to approximately 50% of intended control authority. Additional ACS usage was also encountered at retro motor firing after Gemini separation. Due to plume impingement of the retro motors, an improper pitch rate was imparted to the vehicle. These excessive usages caused high heat soak-back and some loss of performance.

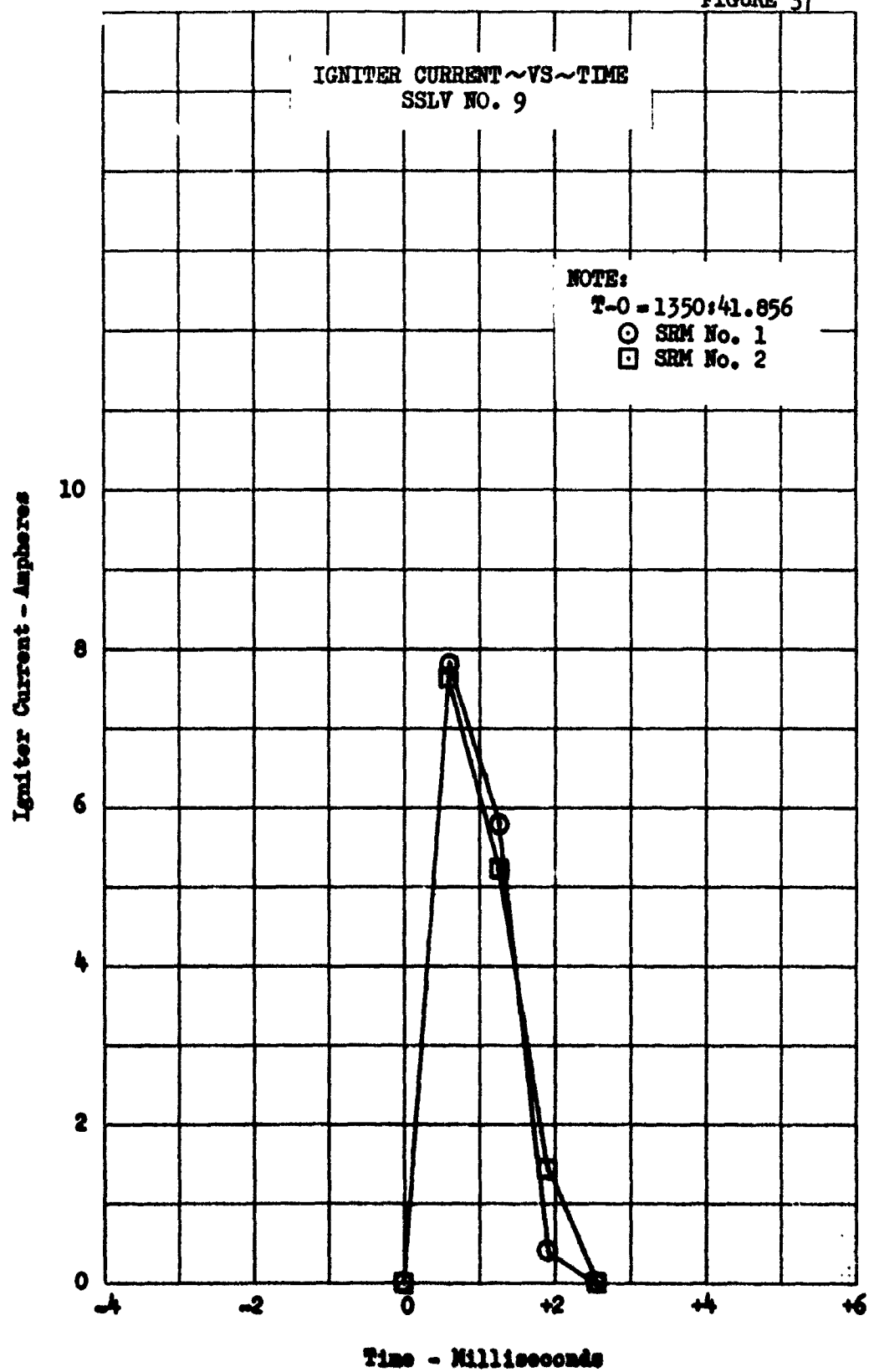
### 3.2.1.2 Solid Rocket Motors

#### 3.2.1.2.1 Ignition

Motor ignition delays were within limits and are presented in Table 4.

The ignition current history of both motors is shown in Figure 37. Analysis of the 1600 sps ignition current history showed igniter current starting to rise at 1350:41.856 GMT for SRM 1 and SRM 2.

FIGURE 37



#### 3.2.1.2.1 Ignition (Cont'd)

Igniter case pressure rise during ignition was normal, as indicated by Figures 38 and 39.

Several anomalies were noted on the DRS after SRM ignition. At SRM ignition command +00:00.040, DRS channels 43 and 44 indicated SRM-1 and 2 igniter S & A safe. To achieve these indications open contacts have to close. This phenomenon has been observed on previous flights and is attributed to contamination from the igniters shorting the open contacts in the igniter S & A's.

At this same time DRS channel 052 indicated SRM-1 ignitor S & A safe. To achieve this indication a closed S & A contact has to open. This condition could have been caused by the high vibration level associated with SRM operation.

At SRM ignition command +00:00.150, DRS channel 522 indicated SRM 1 and 2 igniter S & A arm command. This command was removed at SRM ignition command -00:00.5 and associated DRS channels indicate that the command did not originate from the AGE. DRS channel 522 pulsed several times prior to LBIE drop indicating an intermittent short within the igniter S & A.

UTC states that any electrical anomalies noted in the igniter S & A circuitry after SRM ignition are not cause for concern and they will not take any further action.

#### 3.2.1.2.2 Web Action Time Performance

The UTC predicted and actual head end pressure histories for the motors are shown in Figures 40 and 41. The actual conditions show excellent agreement with the predicted conditions during web action time. Examination of the data for both motors showed that the maximum initial head end pressure was within the limits as presented in Table 4.

#### 3.2.1.2.3 Tailoff

Analysis of the data for both motors indicates that the tail-off performance was normal. See Figure 42. A maximum thrust differential of approximately 70,000 pounds between the motors existed during tailoff. The thrust differential between the motors did not constitute a control problem during tailoff.

FIGURE 38

## Igniter Case Pressure &amp; Motor Head Pressure VS Time

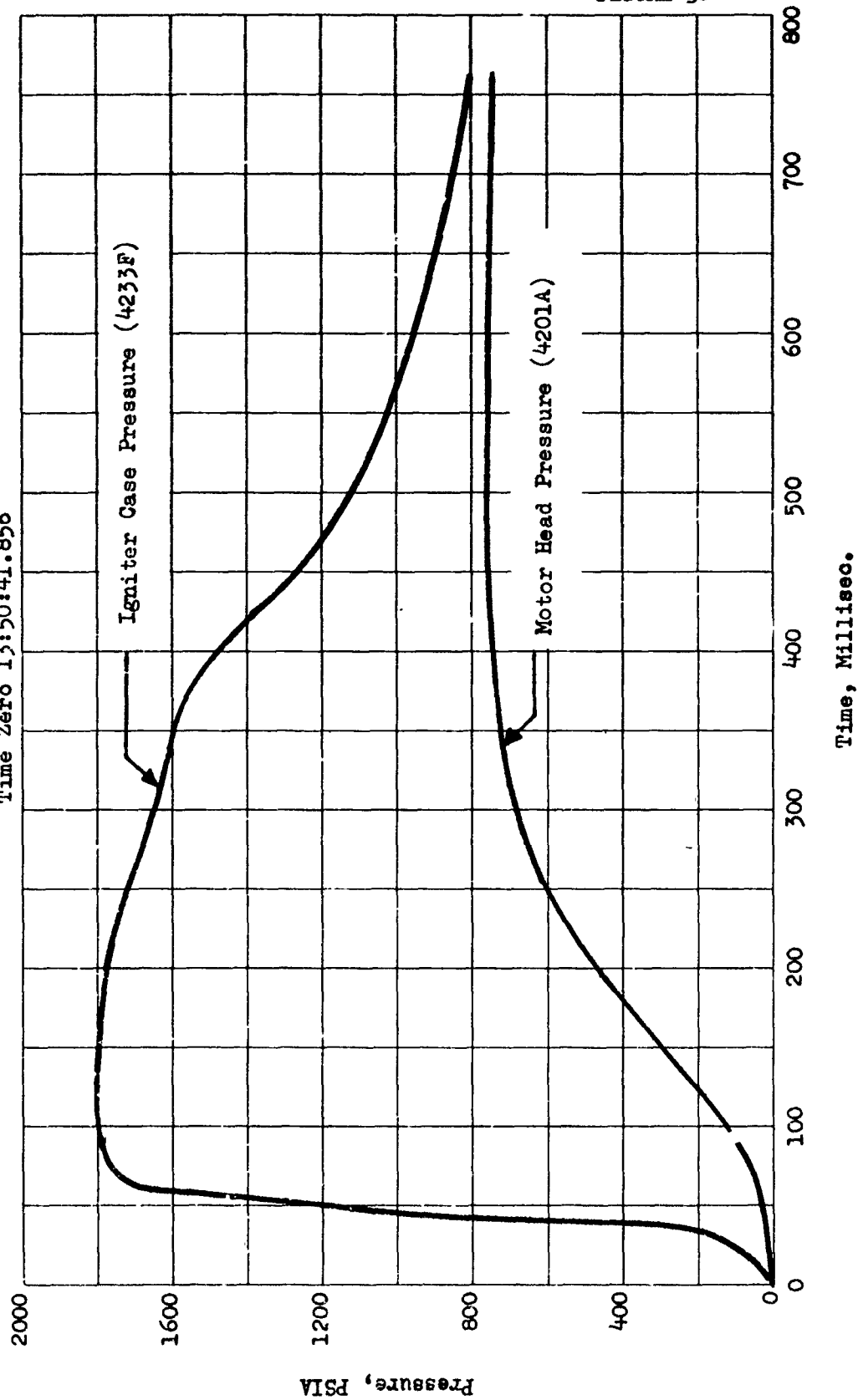
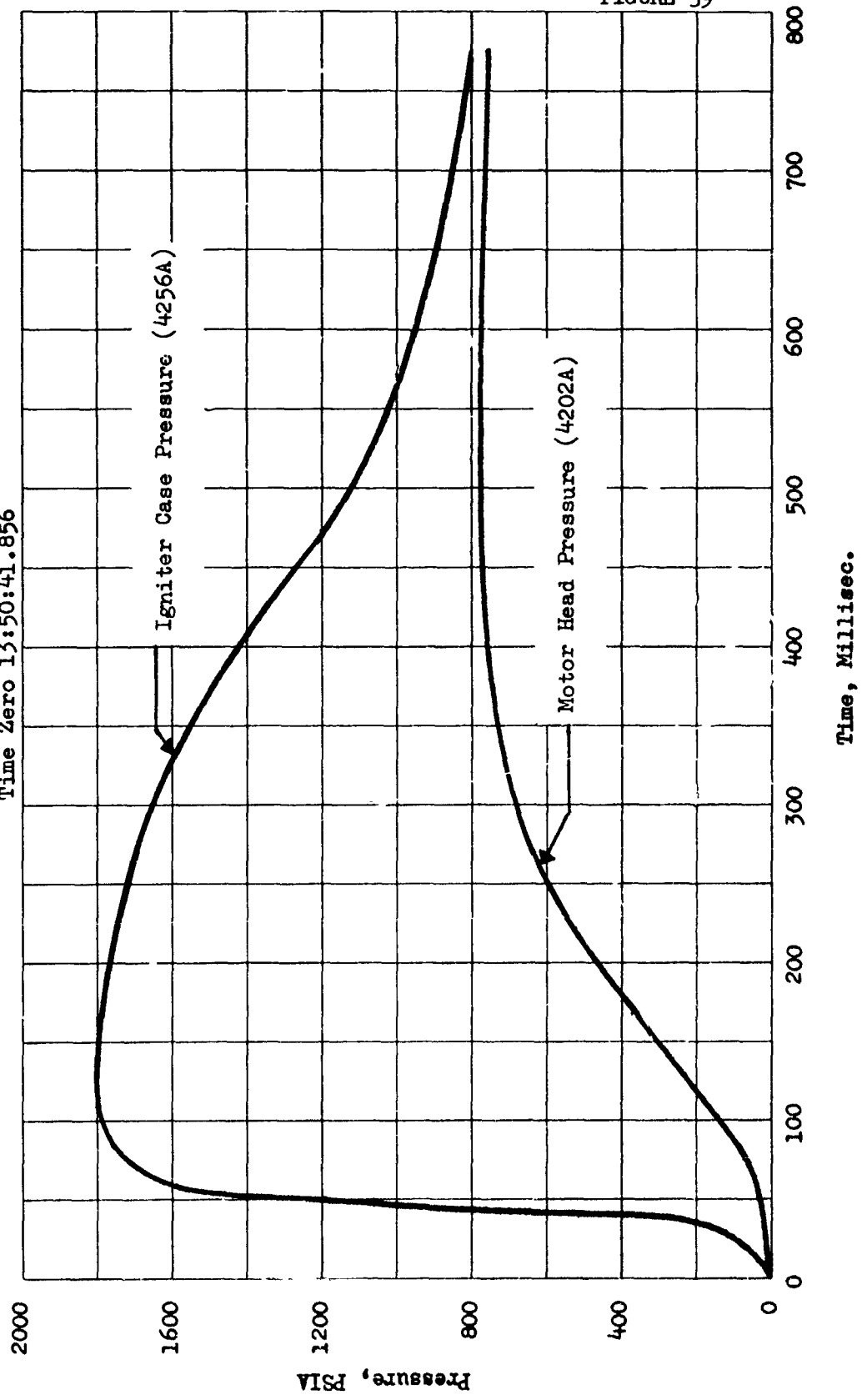
SRM NO. 1  
Time Zero 13:50:41.856

FIGURE 39

Igniter Case Pressure & Motor Head Pressure VS Time

SEM NO. 2  
Time Zero 13:50:41.856



HEAD END CHAMBER PRESSURE ~ PSIA

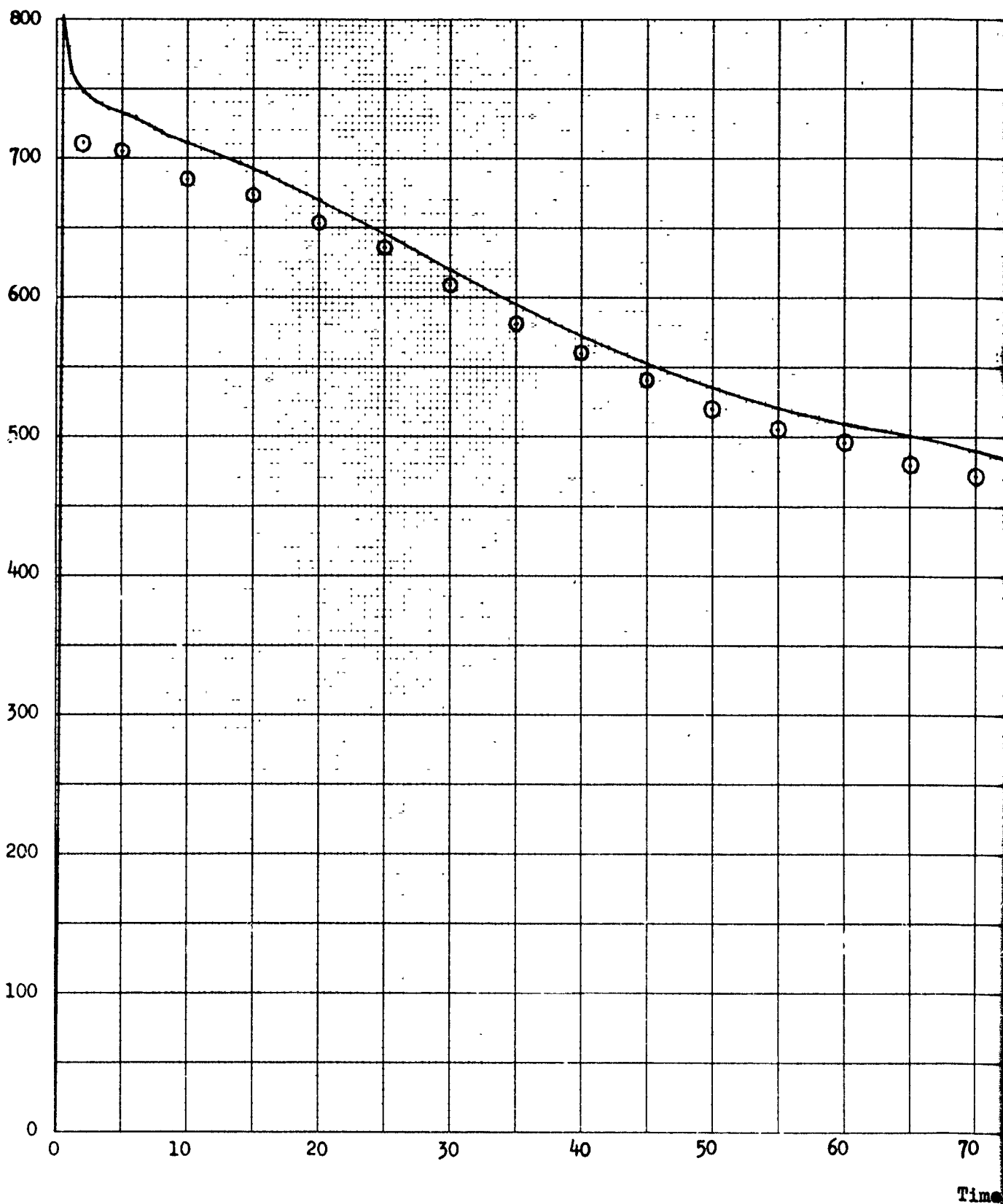


FIGURE 40

SSLV NO. 9  
HEAD END CHAMBER PRESSURE  
SRM NO. 1

## NOTE:

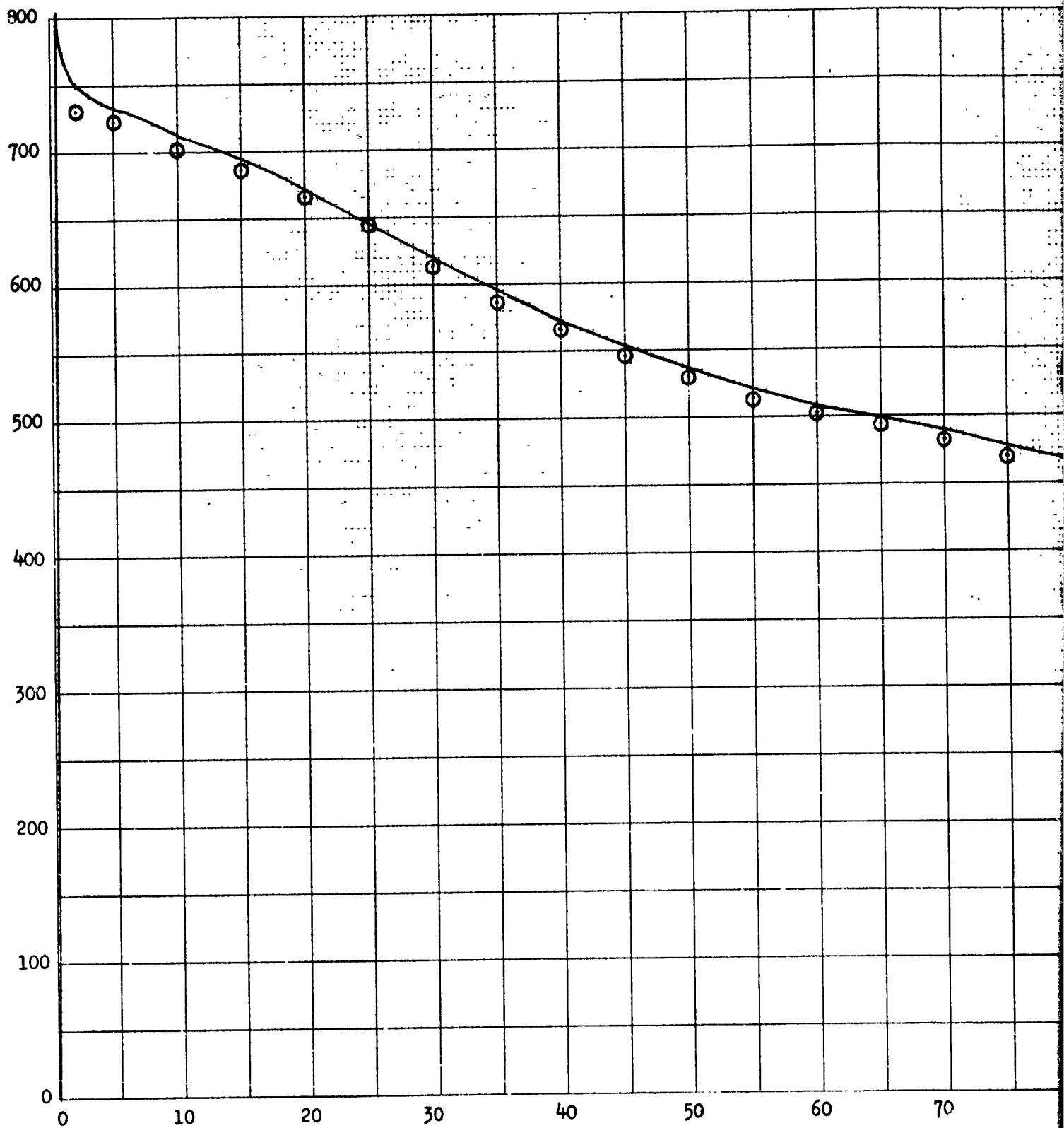
— UTC PREDICTION AT 80°F  
○ SRM NO. 1 FLIGHT DATA  
AT 70.2°F  
T-0 = 1350:41.856

70 80 90 100 110 120  
Time ~ Seconds

2



HEAD END CHAMBER PRESSURE ~PSIA



Time

FIGURE 41

SSLV NO. 9  
HEAD END CHAMBER PRESSURE  
SRM NO. 2

NOTE:  
— UTC PREDICTION AT 80°F  
○ SRM NO. 2 FLIGHT DATA  
AT 70.2°F  
T-0 = 1350:41.856

70 80 90 100 110 120

Time ~ Seconds

2

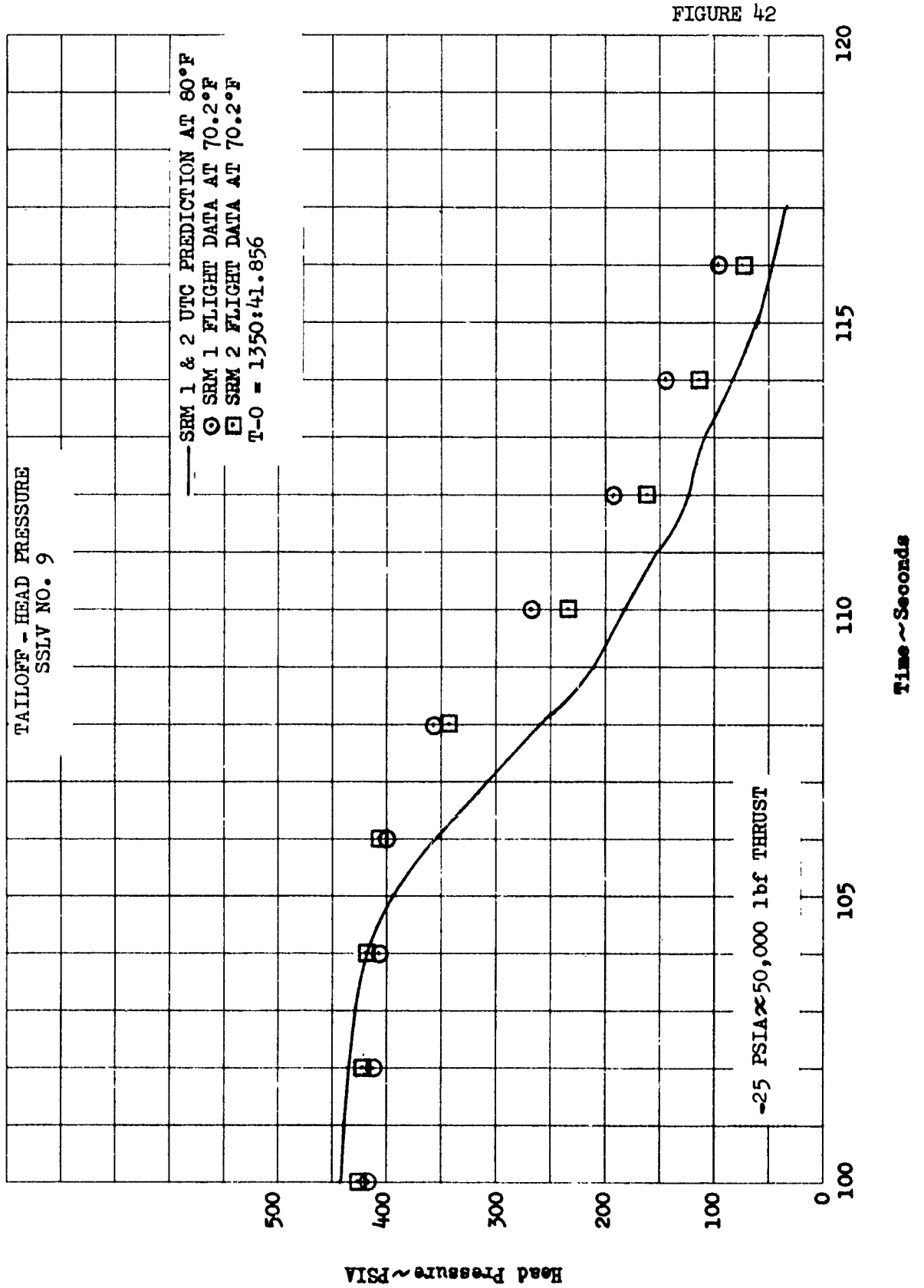


FIGURE 42

#### 3.2.1.2.4 Propellant Consumption

The UTC model specification states that the total SRM nominal propellant weight shall be 421,480 pounds. Actual propellant loaded was 421,970 pounds for SRM 1 and 422,390 pounds for SRM 2.

#### 3.2.1.3 Thrust Vector Control

##### 3.2.1.3.1 Tank Pressurization Control System

The thrust vector control (TVC) tank pressurization control system (TPCS) performed satisfactorily during the terminal countdown and flight. The TVC nitrogen and  $N_2O_4$  tank pressure histories are shown in Figures 43 and 44.

At T-00:30, the TVC  $GN_2$  tank pressures were 3146 and 3174 psia for SRM-1 and SRM-2, respectively. These values were measured by both landline and airborne telemetry. The loading tolerance on the tanks is  $3300 \pm 100$  psia. This decrease in tank pressure is attributed to the rapid drop in ambient temperature that occurred prior to launch.

The opening of the pre valve created a water hammer in the injectant manifold on both motors, (refer to Figure 45). The maximum injectant manifold pressure was 997 psia for SRM 1 and 785 psia for SRM 2. The injectant manifold is hydrostaticated to 1600 psia during acceptance.

##### 3.2.1.3.2 Hydraulic Power Supply

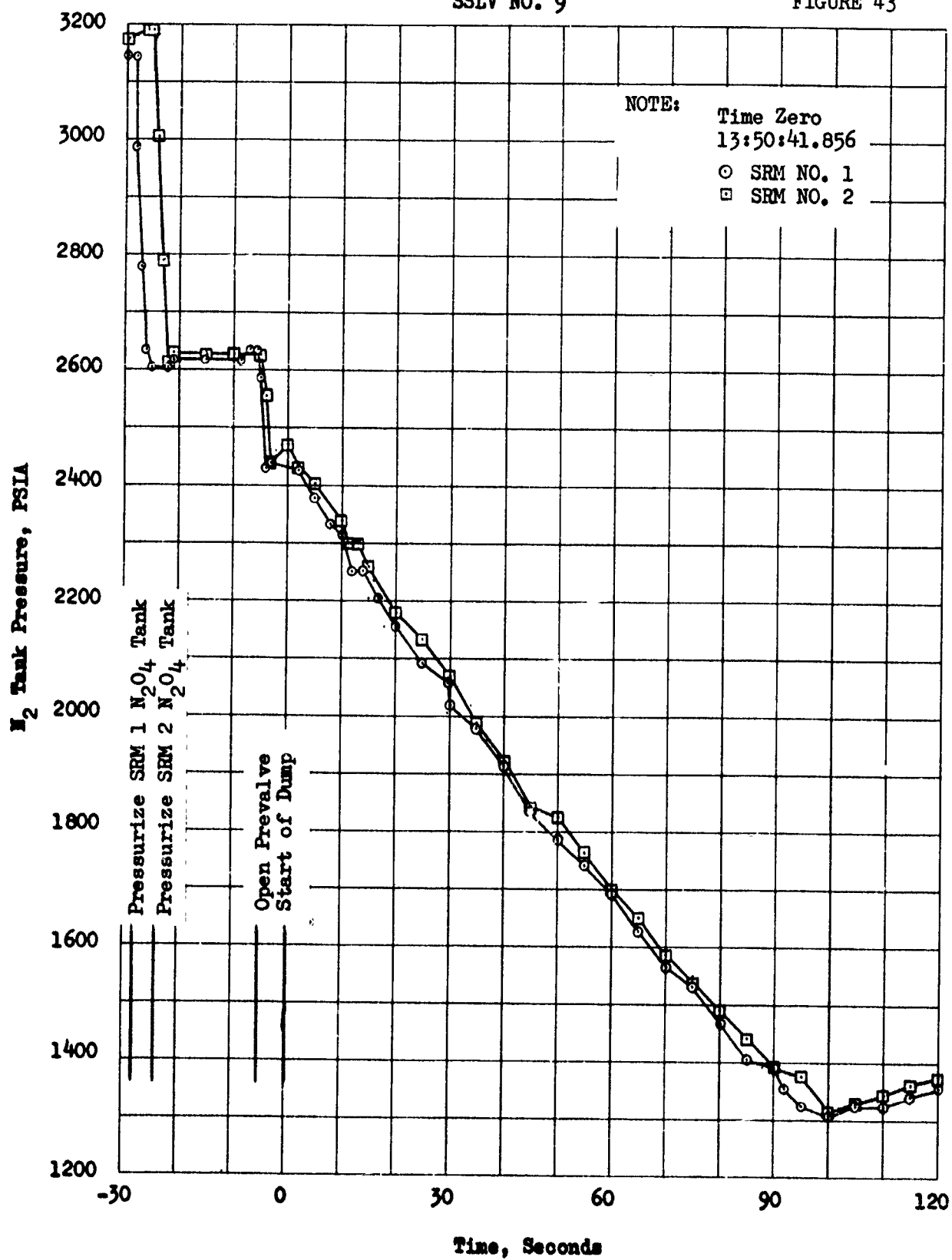
The hydraulic power supply operated within specification limits throughout the terminal countdown and SRM flight. Hydraulic supply pressures remained above 3,000 psia for both motors during the flight and the hydraulic reservoir level varied between 55 and 65 percent.

##### 3.2.1.3.3 TVC Injectant Valves

The TVC injectant valves responded to all autopilot commands issued during the flight.

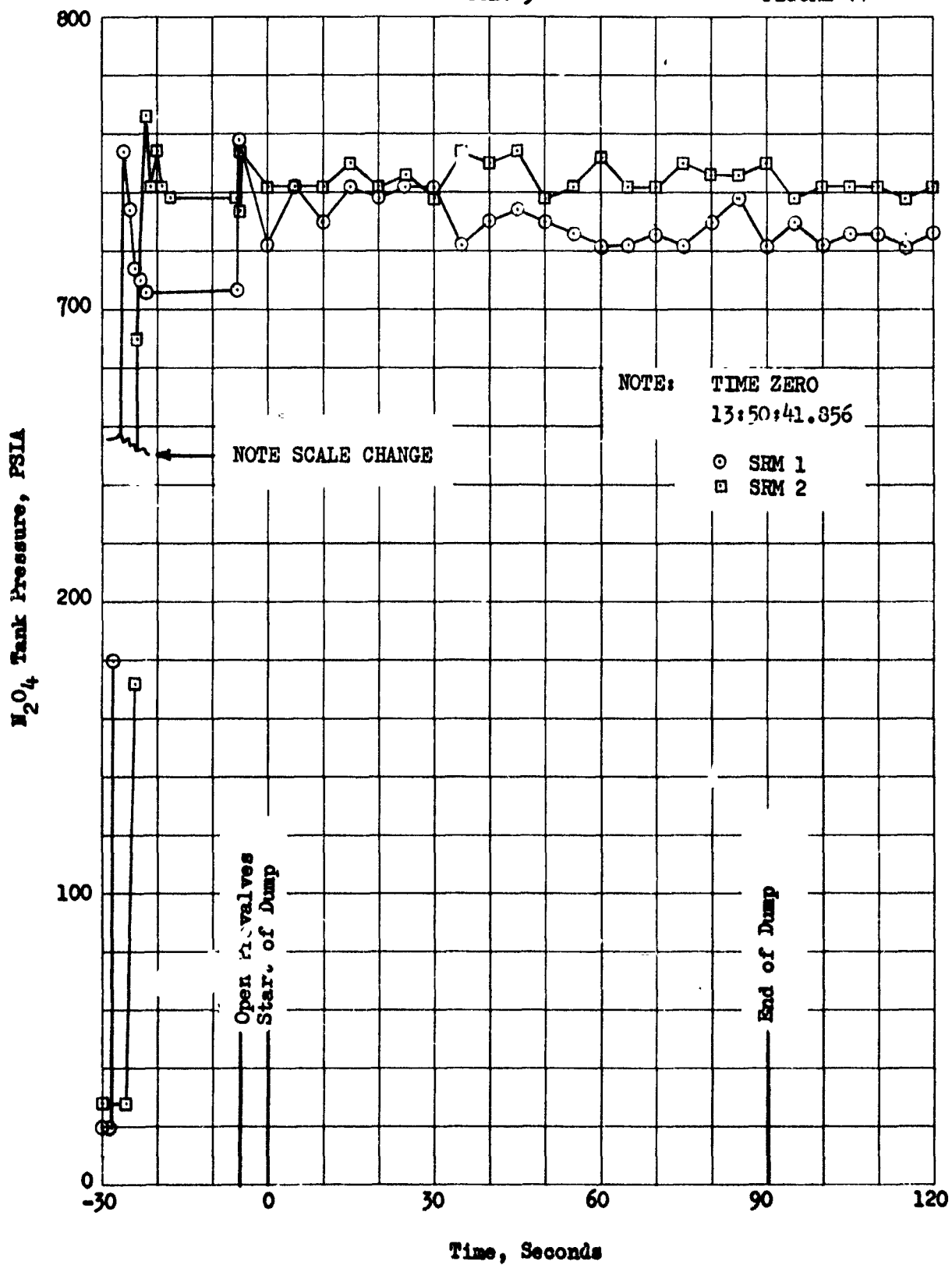
TVC N<sub>2</sub> TANK PRESSURE HISTORY  
SSLV NO. 9

FIGURE 43



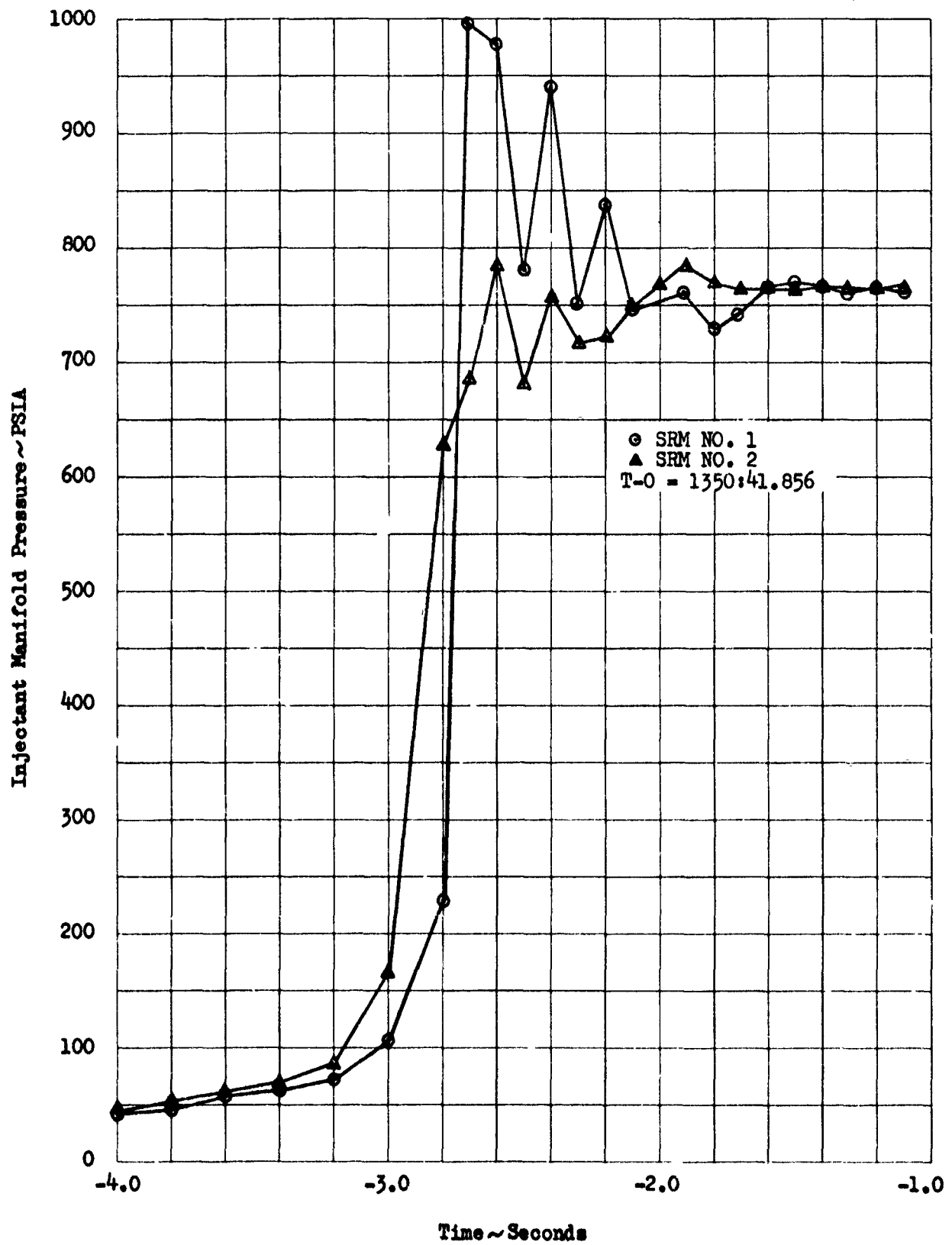
TVC  $N_2O_4$  TANK PRESSURE HISTORY  
SSLV 9

FIGURE 44



TVC INJECTANT MANIFOLD  
PRESSURE HISTORY  
SSLV NO. 9

FIGURE 45





#### 3.2.1.3.4 Pitch and Yaw Control

The performance of the TVC injectant dump programmer which is an integral part of the pitch and yaw control was satisfactory during Stage 0 flight. The dump command history was as follows:

		<u>SRM No. 1</u>	<u>SRM No. 2</u>
Igniter Current			
First Rise	GMT	1350:41.856	1350:41.856
Dump Start	GMT	1350:42.0	1350:42.0
Dump Off	GMT	1352:22.2	1352:22.6

#### 3.2.1.3.5 TVC Injectant Consumption

TVC injectant consumption was determined from injectant valve potentiometer voltages and autopilot pitch and yaw command voltages.

##### SRM No. 1

Total (Pitch and Yaw) Command Injectant Consumption	3,357 lbs.
Dump Command Injectant Consumption	6,562 lbs.
Total Injectant Consumption	9,919 lbs.

##### SRM No. 2

Total (Pitch and Yaw) Command Injectant Consumption	3,681 lbs.
Dump Command Injectant Consumption	6,432 lbs.
Total Injectant Consumption	10,113 lbs.

Total TVC Injectant Loaded was 13,680 lbs. for each SRM.

#### 3.2.1.4 Ordinance

##### 3.2.1.4.1 Inadvertant Separation Destruct System

The inadvertent separation destruct system (ISDS) was not required to function during the flight. The ISDS disable command was received at T+110.6 seconds.

#### 3.2.1.4.2 Thrust Termination and Destruct Systems

There were no thrust termination or destruct commands issued or received during the flight.

#### 3.2.1.4.3 SRM Staging Motors

Tracking cameras, airborne staging films, and staging reel data verified that proper staging of both motors from the core occurred.

The serial numbers of the SRM staging motors and their igniters installed on this vehicle are presented in Table 5.

#### 3.2.1.4.4 Stage II Retro Motors

Separation of Stage II from the transtage is accomplished by firing three retro motors located on Stage II. Staging reel data indicated a Stage II/Transtage separation of 10 feet in 1.6 seconds. All three motors must fire to achieve this separation rate. The specified minimum separation rate is 20 feet in 10 seconds.

#### 3.2.1.4.5 MOL Sim Lab Retro Motors

The MOL Sim Lab was to be separated from the Gemini capsule by firing five retro rocket motors identical to those used for Stage II/Transtage separation. Analysis of acceleration data indicates that all five motors fired at the predicted thrust level and burn time.

TABLE 4

## SRM PERFORMANCE

Events or Functions	Units	Interface Specification IFS TIII-14001 Minimum Nominal Maximum	SRM 1 (S/N 0000026) Predicted UTC	SRM 1 (S/N 0000026) Actual Flight	SRM 2 (S/N0000027) Predicted UTC	SRM 2 (S/N0000027) Actual Flight
Mean Bulk Temperature	°F	-	80	70.2	80	70.2
SRM Igniter Current Rise	GMT	-	-	1350:41.856	-	1350:41.856
Lift Off	GMT	-	-	1350:42.2	-	1350:42.2
Ignition Delay	Millisecond	150 244	300	230	-	238
Web Action Time (WAT)	Seconds	103.2	107.8	104.3	104.2	106.3
Action Time (ATO)(70°F)*	Seconds	110.96	118.8	113.8	113.7	115.9
Maximum Initial Head Pressure	PSIA	-	853	804	805	774

\*The limits are calculated values, no specification values exist at 70.2°F.

TABLE 5  
SRM STAGING MOTOR LOCATIONS

Location	SRM	Staging Motor S/N	Ingiter S/N
FWD Top	1	0001155	0001594
FWD 2	1	0001156	0001595
FWD 3	1	0001157	0001596
FWD Bottom	1	0001158	0001598
AFT Top	1	0001194	0001604
AFT 2	1	0001160	0001605
AFT 3	1	0001161	0001606
AFT Bottom	1	0001192	0001607
FWD Top	2	0001195	0001599
FWD 2	2	0001196	0001600
FWD 3	2	0001199	0001602
FWD Bottom	2	0001200	0001603
AFT Top	2	0001201	0001608
AFT 2	2	0001202	0001609
AFT 3	2	0001203	0001610
AFT Bottom	2	0001204	0001611

### 3.2.1.5 Stage I

#### 3.2.1.5.1 Engine (S/N 6241010)

##### Start Transient

The Stage I engine start transient exhibited a chamber pressure buildup spike which was out-of-tolerance with the specification stipulated in the Martin-Aerojet Interface requirements. No degradation was noted in engine performance as a result of the excessive buildup spike and at present Aerojet is analyzing the data in order to establish a possible cause for the anomaly. Subassembly chamber pressures during the start transient are shown on Figure 46. Summarized start transient data are presented in the following table:

<u>Parameter</u>	<u>Specification</u>	<u>S/A 1</u>	<u>S/A 2</u>
87 FS <sub>1</sub> to Ignition (sec) <sup>1</sup>	0.7 - 1.1	0.780	0.804
Thrust Spike (lbs)	177750 (max)	181837	176441
Thrust Spike %	75 (max)	76.7	74.4
Thrust Step (lbs)	142200 (max)	121246	126945
Thrust Overshoot (lbs)	300000 (max)	272016	263921

##### Steady State Operations

Stage I measured engine data are tabulated in Table 6. Level sensor data indicate that the average mixture ratio burned was approximately 0.46% less than that predicted utilizing the engine model program. This difference is within the three-sigma log-to-launch dispersion limits of  $\pm 1.60\%$  indicating normal engine operation.

The calculated engine thrust from flight data ( $F = P_c A_t C_F + F_{gg}$ ) at FS<sub>1</sub> + 90 seconds and accelerometer derived thrust were 1.31% and 2.22% greater than the preflight predicted thrust, respectively. With preflight data corrected to include post-flight inlet conditions, the difference in thrust are approximately 0.89% and 1.80% for  $P_c$  derived and accelerometer derived thrusts, respectively. This dispersion in thrust about the predicted thrust level is within the three-sigma log-to-launch limits of  $\pm 3.27\%$ . These data are shown in Figure 47.

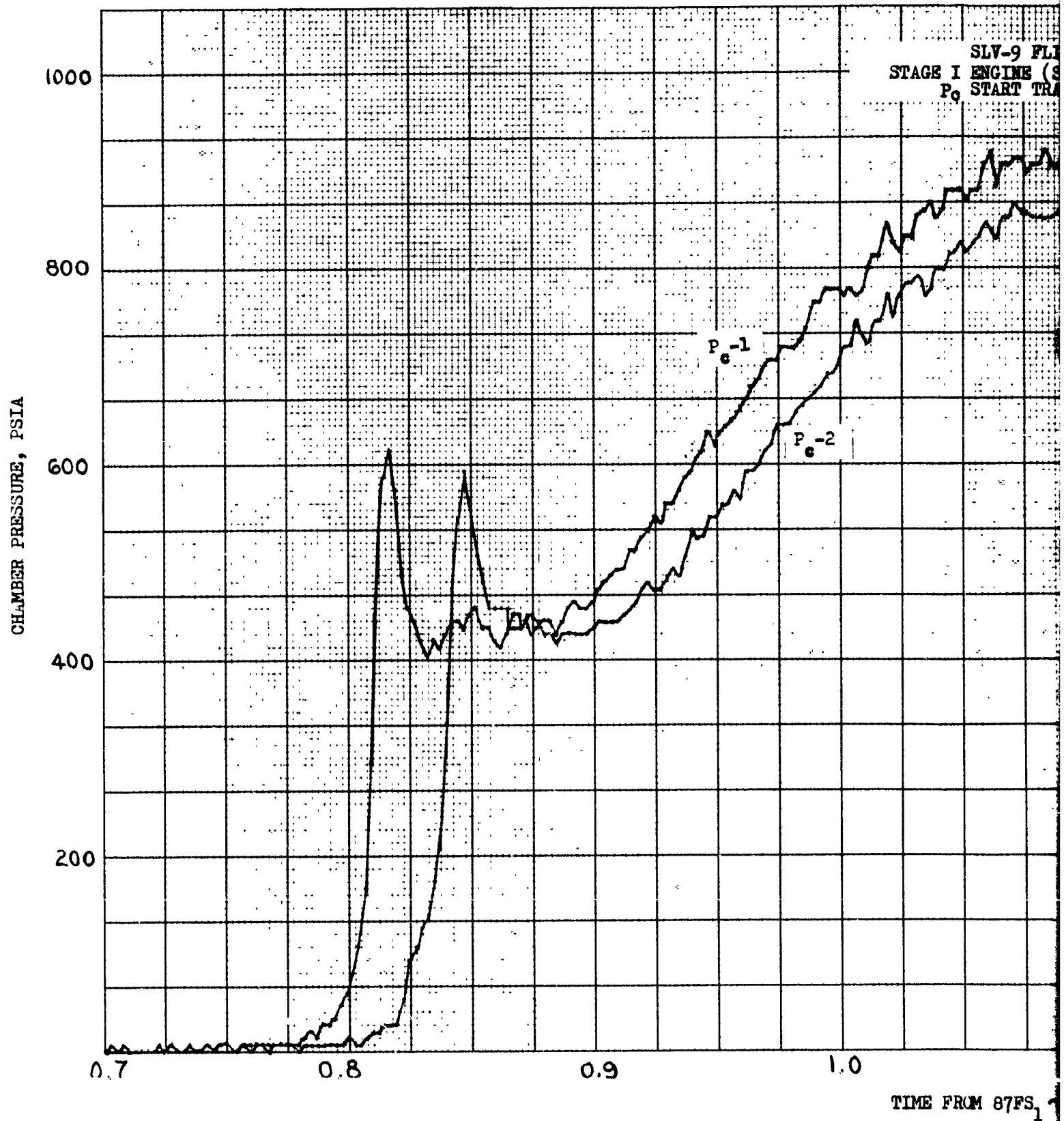
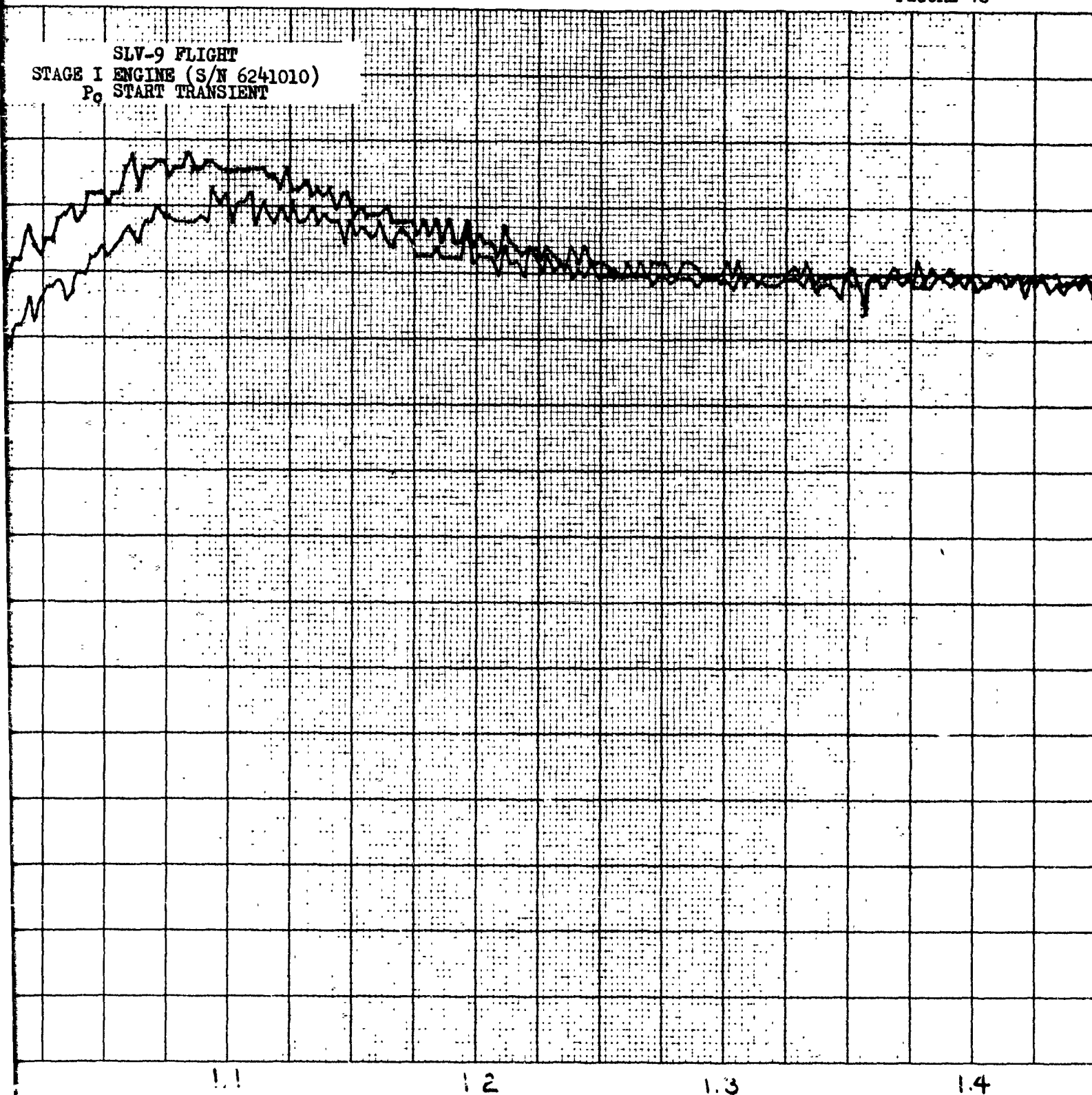


FIGURE 46

SLV-9 FLIGHT  
STAGE I ENGINE (S/N 6241010)  
P<sub>0</sub> START TRANSIENT

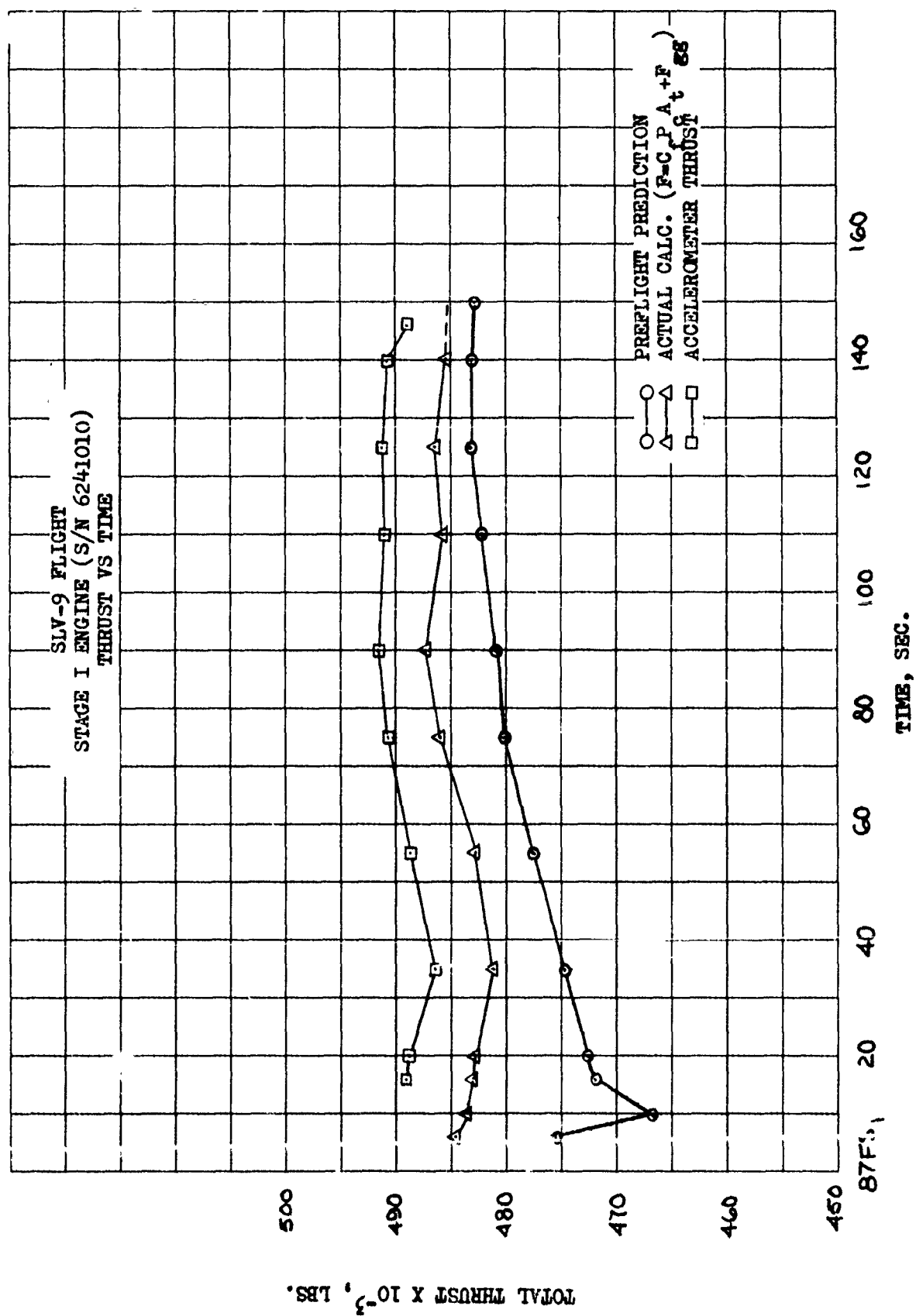


TIME FROM 87FS<sub>1</sub> ~ SEC.

2



FIGURE 47



CONFIDENTIAL

TABLE 6

90

STAGE I MEASURED ENGINE DATA

Data averaged over two second interval (100 sample/sec)

<u>Time from FS<sub>1</sub></u> <u>Sec.</u>	<u>P<sub>C1</sub></u> <u>psia</u>	<u>P<sub>C2</sub></u> <u>psia</u>	<u>P<sub>OS</sub></u> <u>psia</u>	<u>P<sub>FS</sub></u> <u>psia</u>	<u>T<sub>OS</sub></u> <u>°F</u>	<u>T<sub>FS</sub></u> <u>°F</u>
6	806	803	73.8	34.0	66.1	61.2
10	803	803	64.0	31.9	65.7	61.6
16	800	804	69.0	33.5	66.1	61.7
20	799	804	68.9	33.3	66.1	62.0
35	796	802	68.9	33.9	65.4	62.4
55	799	804	69.7	32.9	66.9	62.8
75	806	807	71.8	32.3	67.3	63.2
90	809	808	73.3	31.3	67.6	63.4
110	806	806	76.1	30.6	68.1	63.6
125	807	807	79.4	29.3	68.5	64.3
140	806	805	82.3	27.9	69.4	64.8
148	773	779	58.7	26.1	73.8	65.3

ENGINE PERFORMANCE AT 87 FS<sub>1</sub> + 90 SEC

<u>Parameter</u>	<u>Units</u>	<u>Predicted</u>	<u>Actual Flight</u>
F <sub>ENG</sub>	Lbs	4809 <sup>4</sup> 7	487269
W <sub>OT</sub>	Lbs/Sec	1115.31	1120.46*
W <sub>FT</sub>	Lbs/Sec	562.82	572.14*
W <sub>TOT</sub>	Lbs/Sec	1678.13	1692.60*
AVG.MR <sub>ENG</sub>	---	1.976	1.958*
ISP <sub>ENG</sub>	Sec	287.27	287.9*

\*Level sensor data.

CONFIDENTIAL

### Steady State Operations (Cont'd)

Inlet suction and pump discharge pressure variations indicate Stage I vehicle pogo. Details regarding the pogo analysis are given in the System Dynamics section of this report.

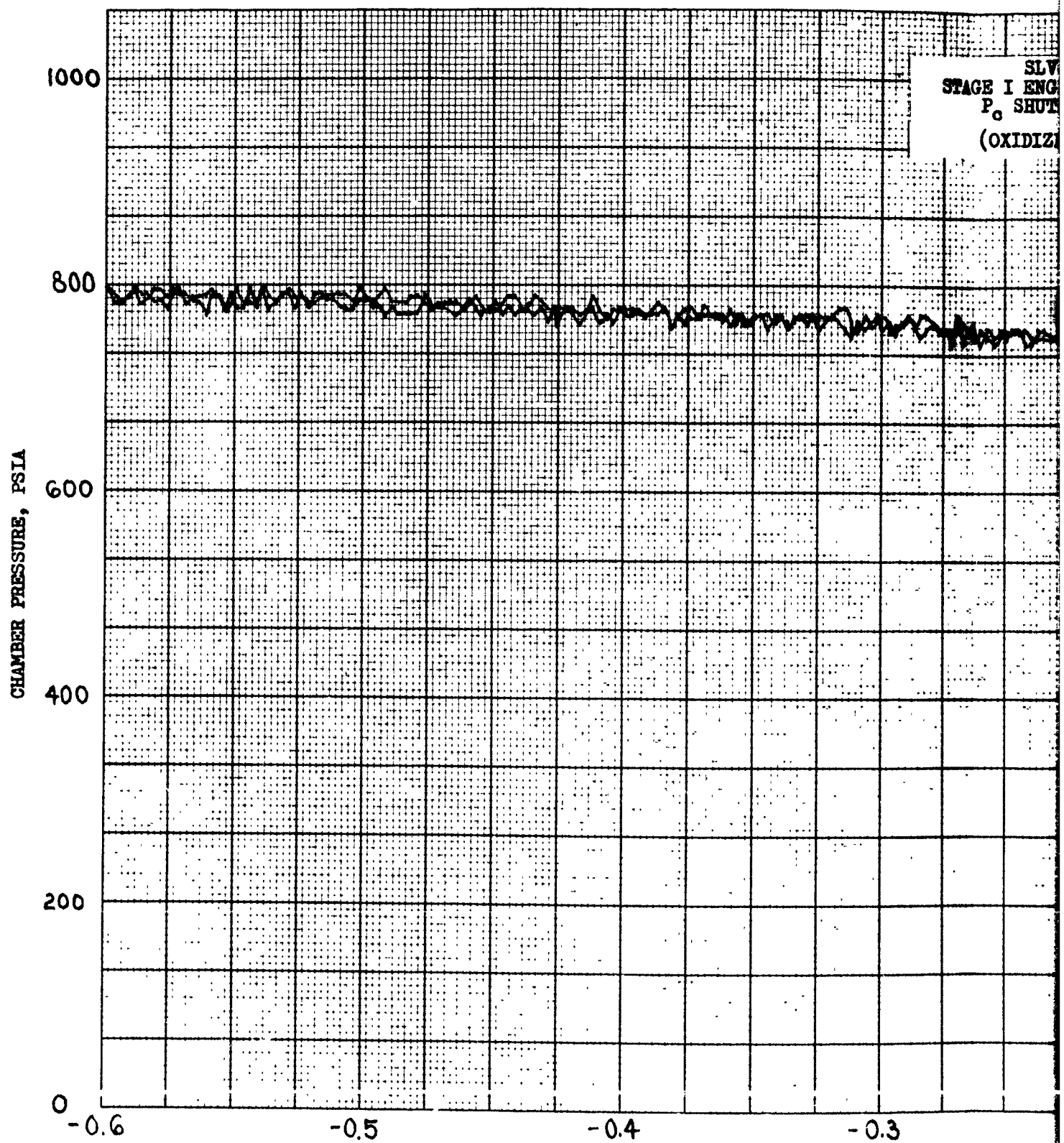
### Shutdown Transient

The Stage I engine exhibited a normal oxidizer exhaustion shutdown. The shutdown transient chamber pressures for both subassemblies are shown in Figure 48. Total Stage I engine burning time was recorded as 148.018 seconds. Ignition (87FS<sub>1</sub>) occurred at 13:52:32.382 and shutdown (87FS<sub>2</sub>) occurred at 13:55:00.377.

Flight controls data have indicated an actuator motion at 13:55:00.351 GMT during Stage I engine shutdown. Engine parameters were investigated at that time for a possible affect on the actuators. No significant variations from a normal oxidizer exhaustion shutdown were noted. Oxidizer shutdown transients such as seen on Vehicle B-1 and B-2 and C-7 were compared with C-9 for possible differences. No comparable actuator motions were seen in either B-1 or B-2; however, C-7 indicated actuator motions similar to those noted on C-9. Actuator motions for C-7 and C-9 coincided with P<sub>c</sub> spikes which are typical of Stage I engine oxidizer exhaustion shutdowns. Flight control system analysis indicates that the actuator motions were not internally induced and are probably a result of forces on the chamber. Refer to the Guidance and Controls section of this report for additional discussion of this phenomenon.

### Thrust Chamber Closures

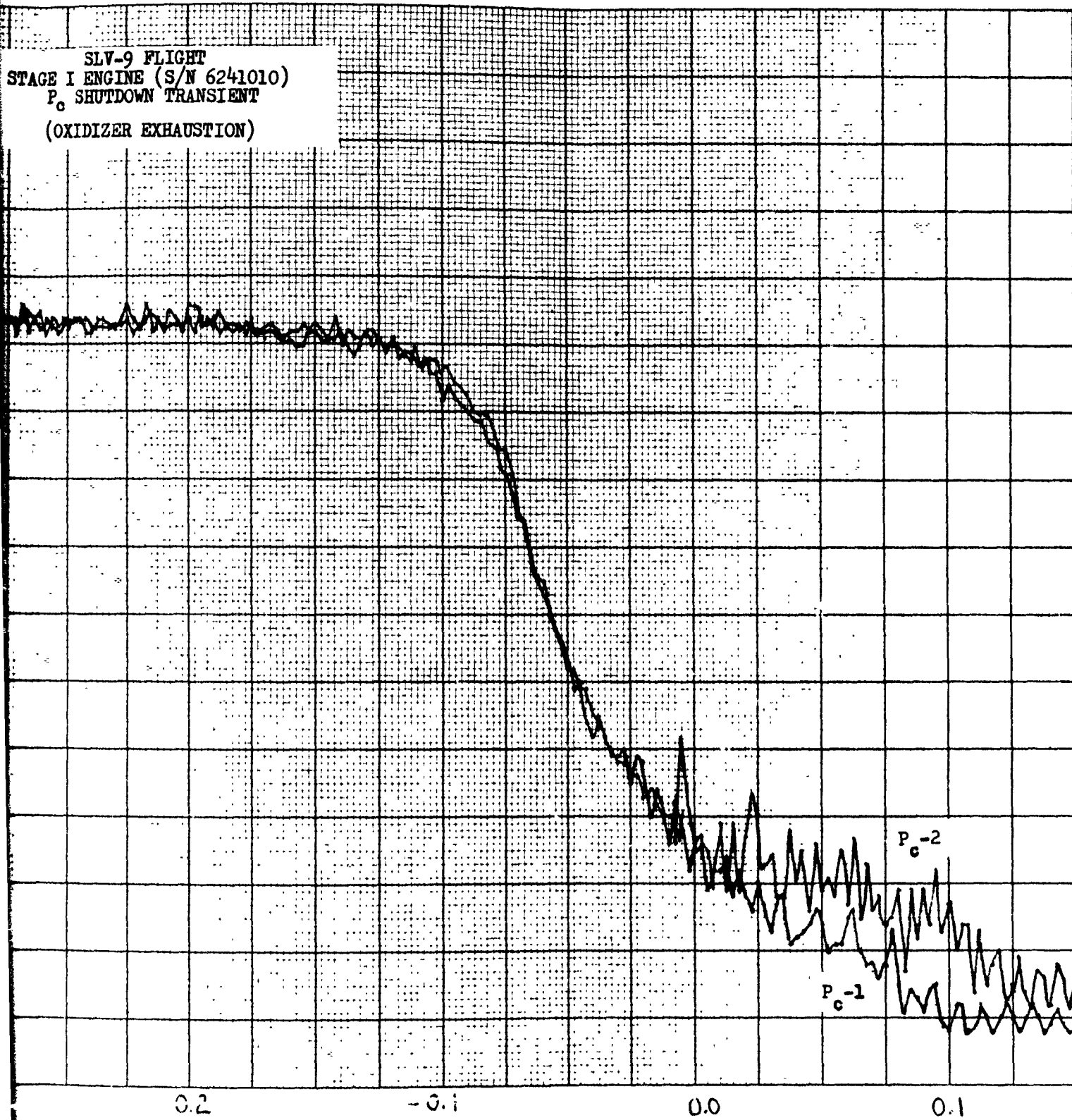
The recorded temperatures indicated no abnormal functioning of the Stage I thrust chamber closures throughout SRM thrusting. The measurements #3098 and #3099 are shown in Figure 49. These measurements are the skin temperatures of the fuel cross-over manifolds of subassemblies 1 and 2, respectively. Since these parameters are subjected to the Stage I engine flame, they can be disregarded beyond the time of Stage I engine ignition.



TIME FROM 87

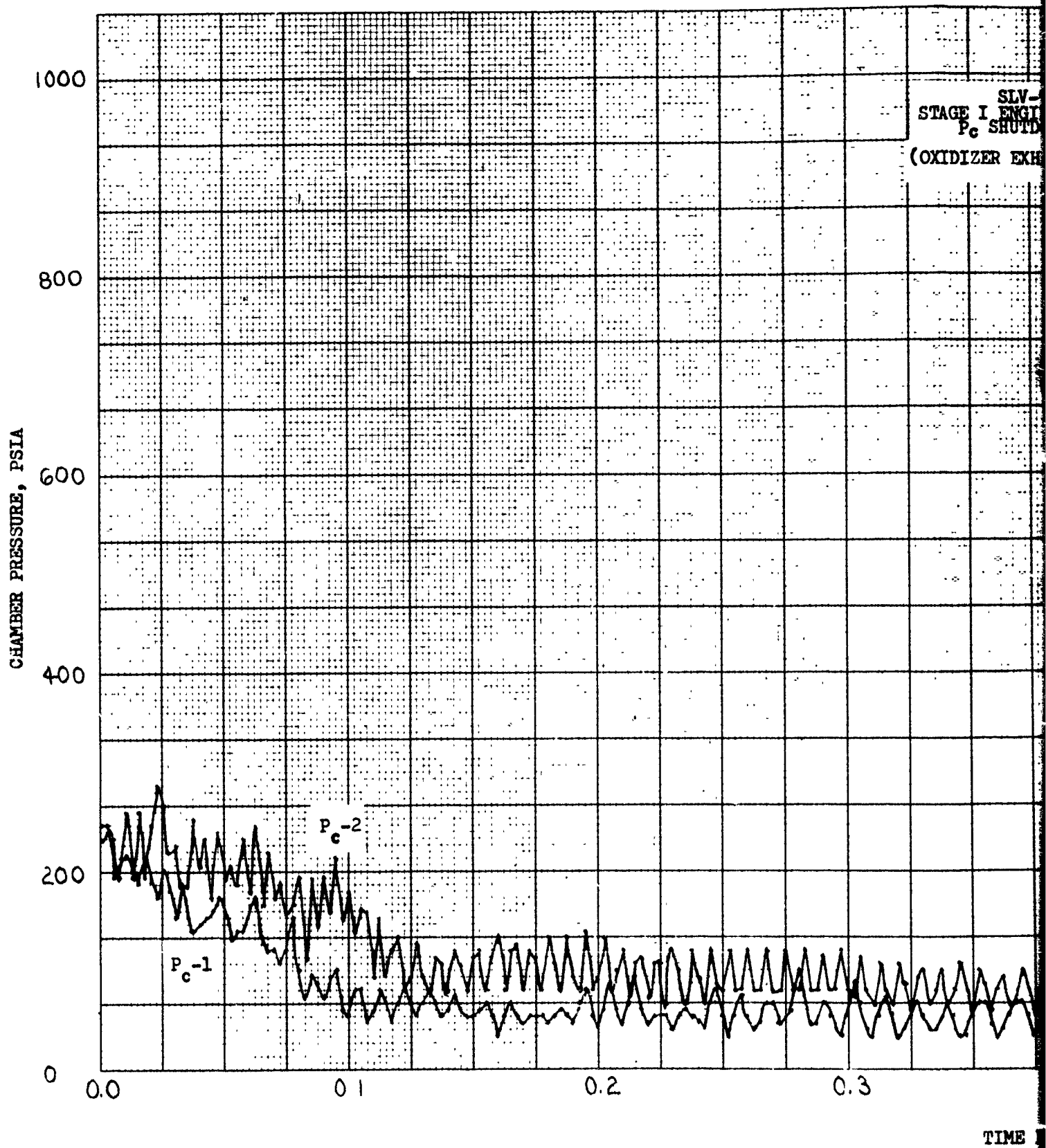
FIGURE 48

SLV-9 FLIGHT  
STAGE I ENGINE (S/N 6241010)  
 $P_c$  SHUTDOWN TRANSIENT  
(OXIDIZER EXHAUSTION)



ME FROM 87FS<sub>2</sub> ~ SEC.

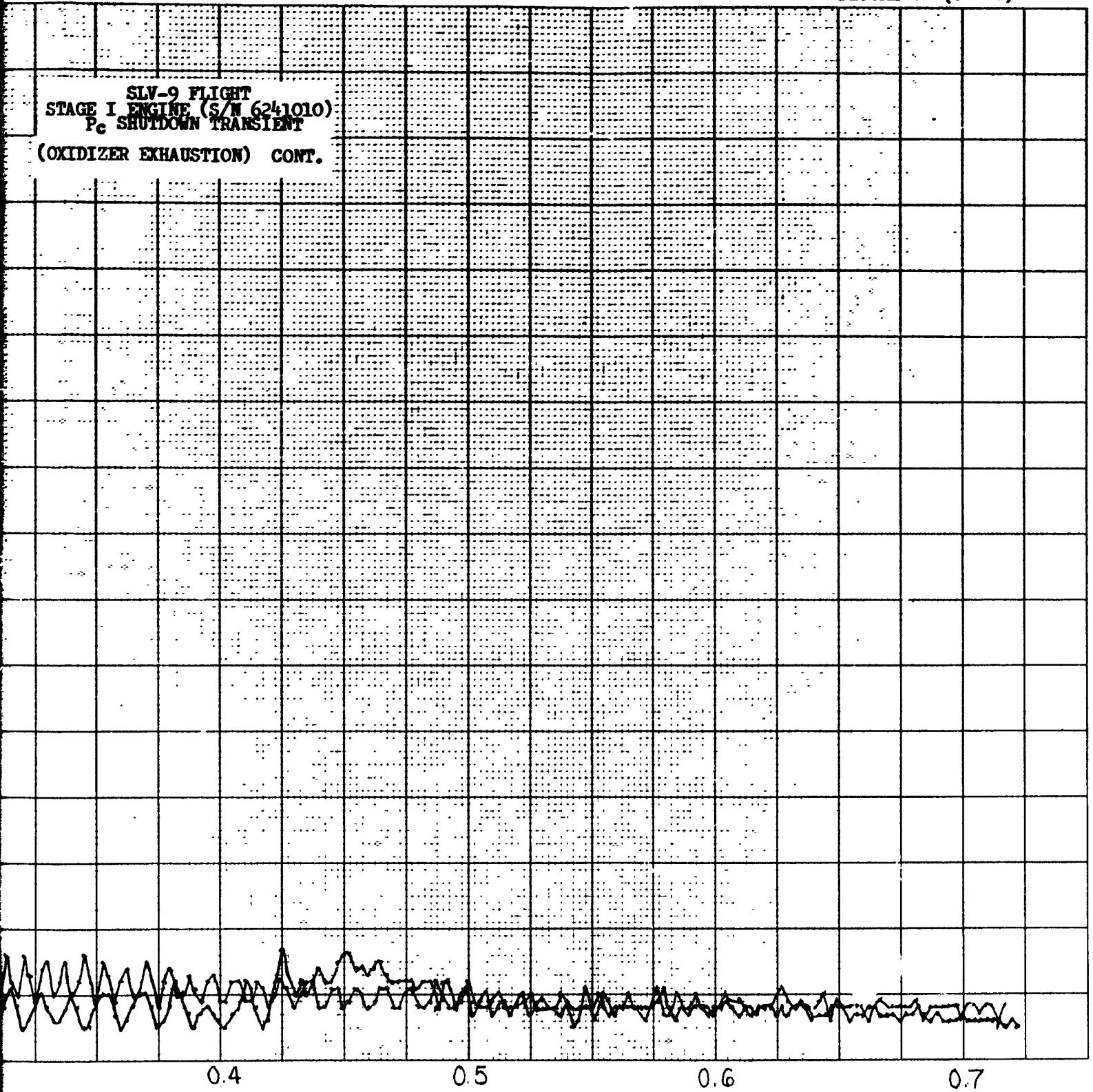
2



TIME

FIGURE 48 (Cont.)

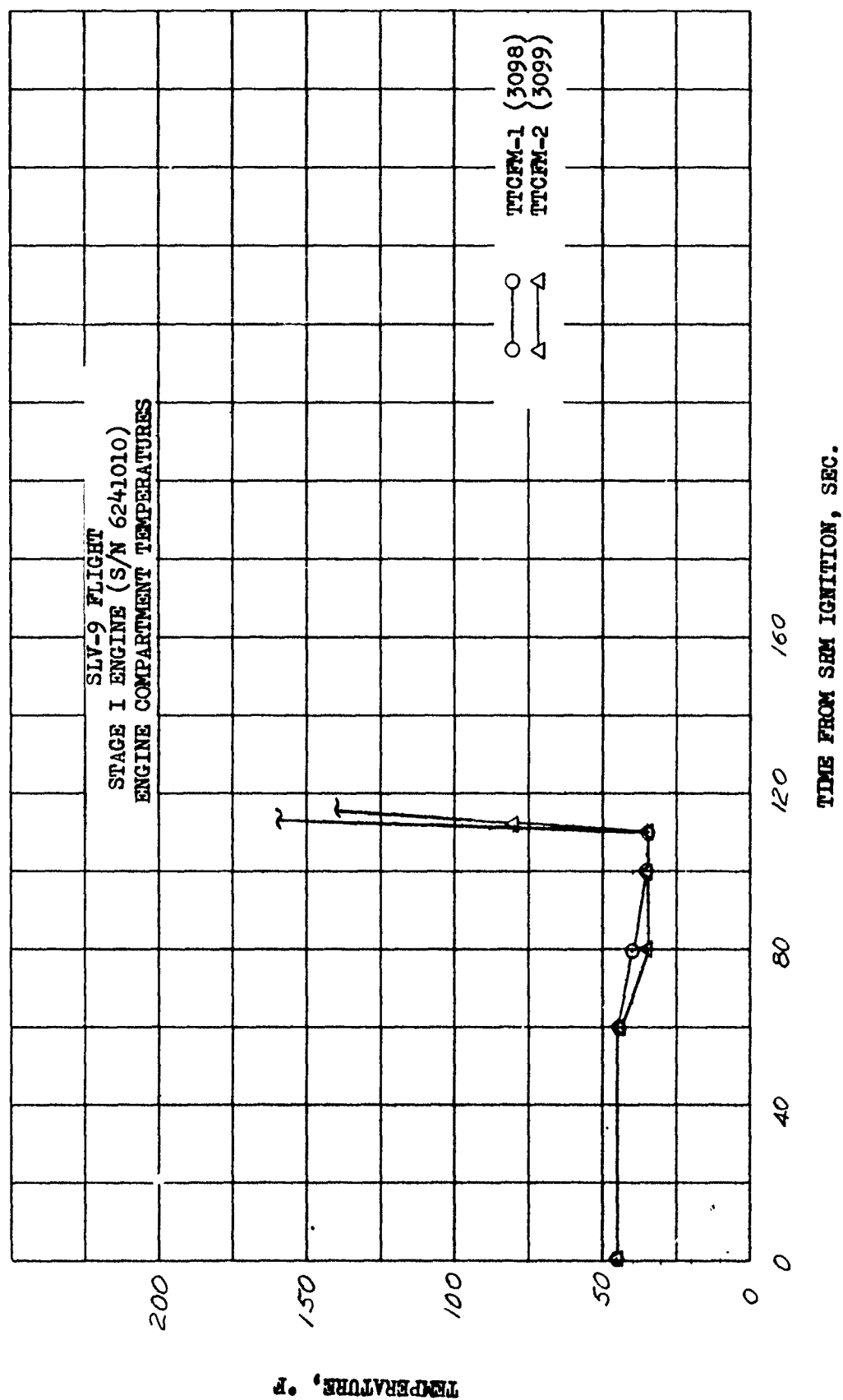
SLV-9 FLIGHT  
STAGE I ENGINE (S/N 6241010)  
P<sub>c</sub> SHUTDOWN TRANSIENT  
(OXIDIZER EXHAUSTION) CONT.



TIME FROM 87FS<sub>2</sub> ~ SEC.

2

FIGURE 49





### 3.2.1.5.2 Pressurization Subsystem

#### General

Stage I pressurization system operation was normal during the flight. Tank gas pressure curves and interface flow boxes are shown in Figures 50, 51, 52 and 53. Pressurization system parameters from acceptance test and flight test data are tabulated in Table 7 at 87 FS<sub>1</sub> plus 6, 20 and 110 seconds.

#### Fuel System

The tank gas pressure during flight deviated slightly (by a maximum of 1.1 psi) from the post flight prediction near the end of the Stage I burn. During the start transient and the first half of the burn, the maximum deviation was less than 1 psi. The flight data tracked the pre-flight prediction fairly closely (maximum deviation of about 1 psi) during the start transient, while deviating a maximum of approximately 2.0 psi during the remainder of the burn. The deviation of the flight data from the preflight prediction is a result of a higher than predicted weight of condensable gas in the ullage. The deviations from the post flight predictions are within the flight instrumentation inaccuracies and the tolerances of the mathematical model.

The flight test flow box data were slightly lower than acceptance test data, but well within specifications. The tank gas pressure during Stage 0 operation showed normal decay due to tank stretch.

#### Oxidizer System

Flight test pressure data agreed very well with the preflight prediction with a maximum deviation of 1.3 psi during the start transient. The data tracked the postflight prediction in a similar manner because the preflight and postflight predictions were nearly identical. During the start transient the 1.3 psi deviation of the data from both pre and post flight predictions are well within instrumentation inaccuracies.

Tank gas pressure during Stage 0 operation showed normal response to tank stretch.

The flight test flow box data was well within specifications, and showed good agreement with acceptance test data.

FIGURE 50

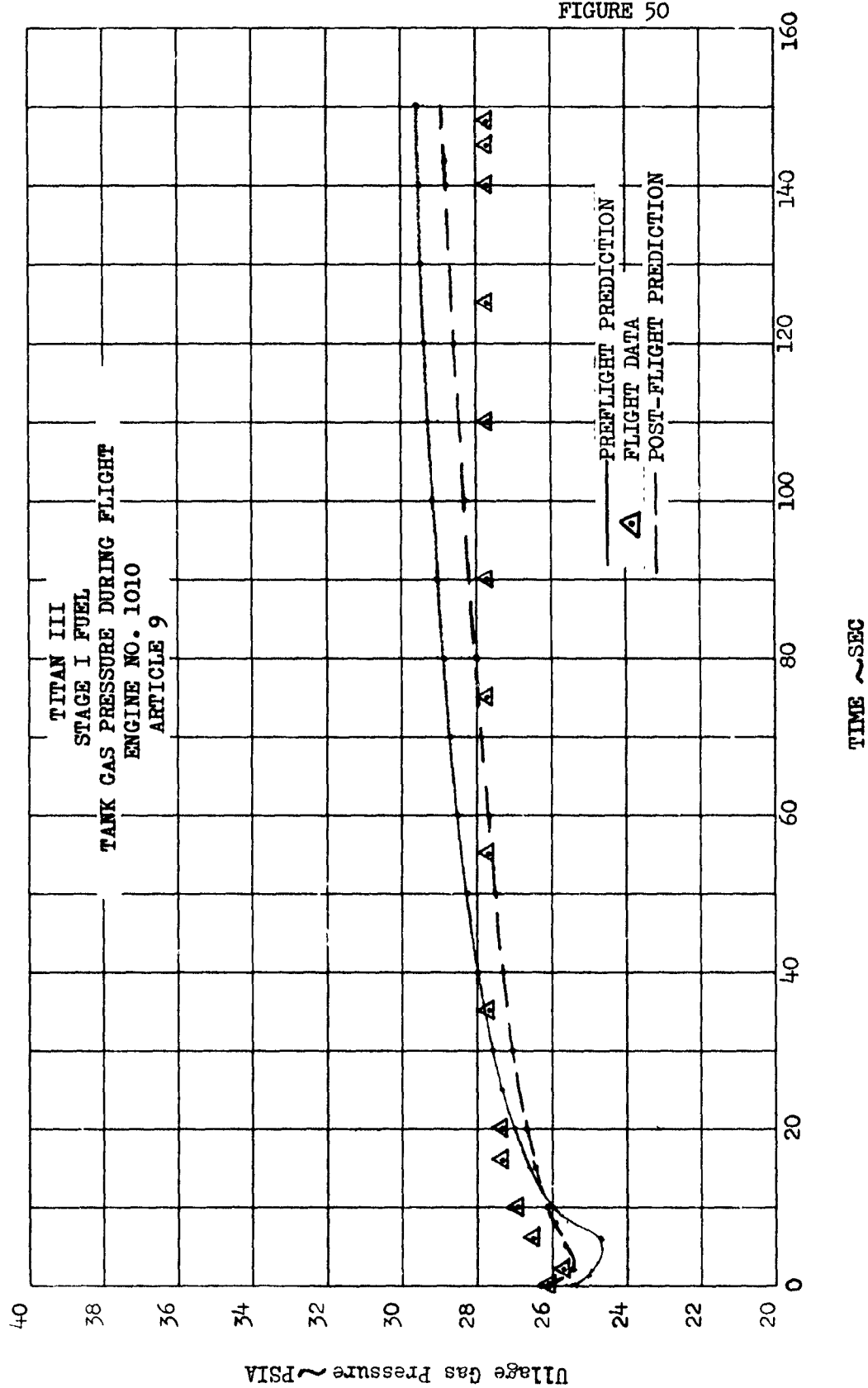


FIGURE 51

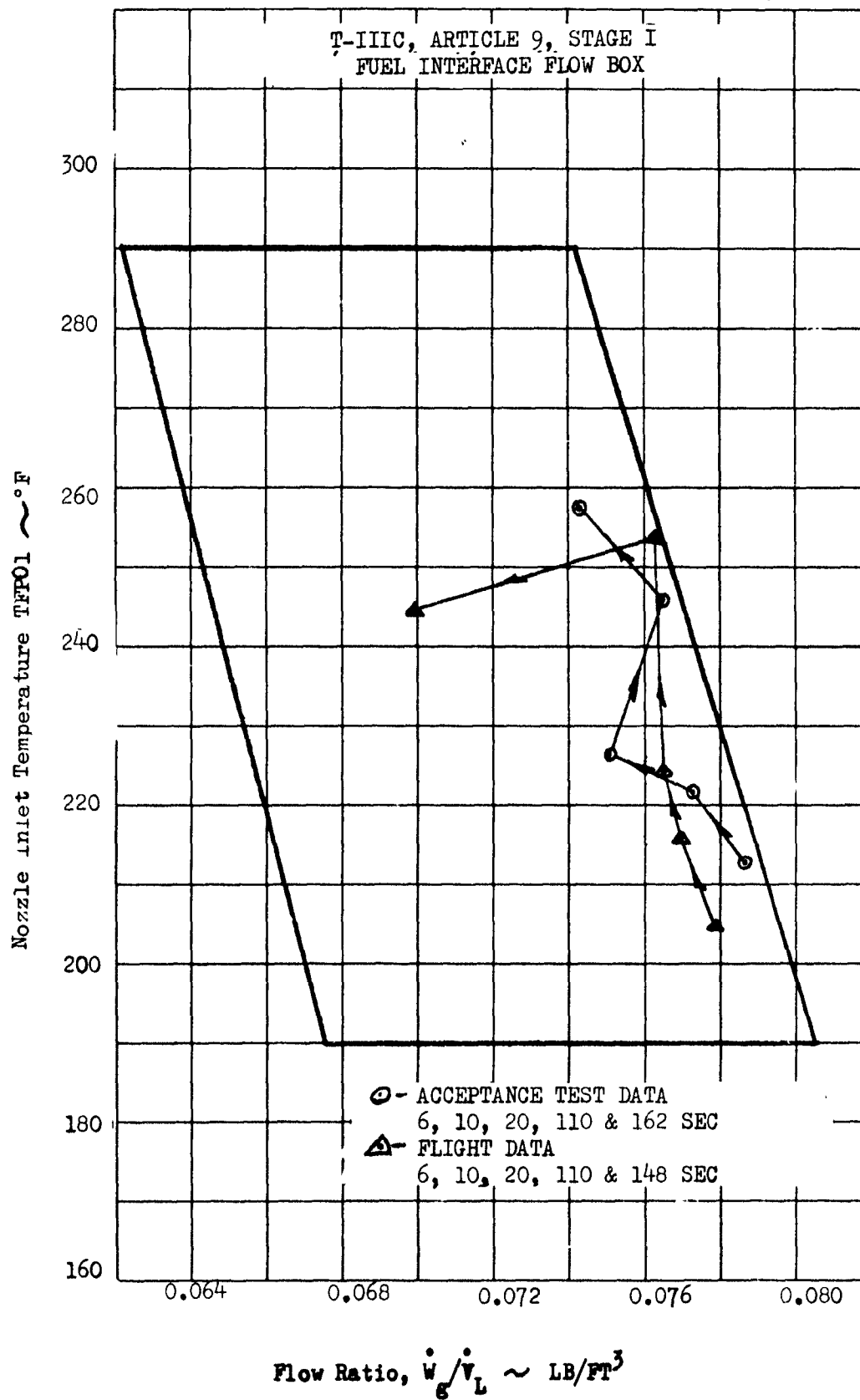
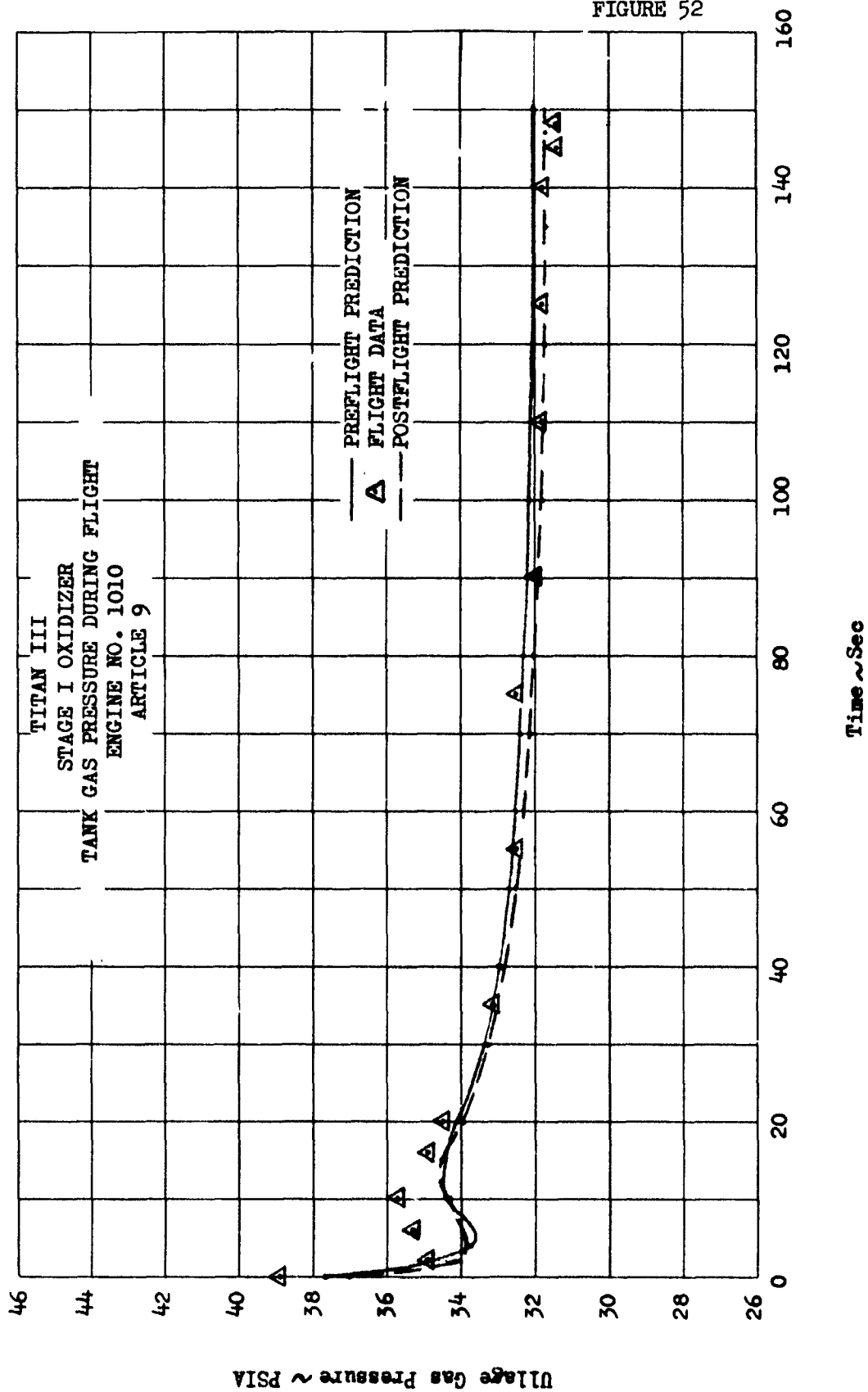


FIGURE 52



●



TABLE 7

## STAGE I PRESSURIZATION PARAMETERS

Parameter	6 Seconds		20 Seconds		110 Seconds	
	Accept Test	Flight	Accept Test	Flight	Accept Test	Flight
PGFT (psia)	---	26.5	---	27.3	---	27.7
PFPOI (psia)	344.3	345.1	331.5	342.0	345.3	350.8
TFPOI (°F)	212.8	204.7	226.0	224.4	245.8	253.9
WFP (lb/sec)	0.77839	0.7965	0.74432	0.7779	0.76232	0.7813
Flow Ratio (lb/ft <sup>3</sup> )	0.07863	0.07788	0.07540	0.07653	0.07645	0.07621
FFN (in.)	0.45	0.45	0.45	0.45	0.45	0.45
PGOT (psia)	---	35.3	---	34.5	---	31.8
POPOI (psia)	---	551.0	---	563.0	---	576.0
TOPOI (°F)	---	333.4	---	373.9	---	391.5
HOPOI (Btu/lb)	369.0	371.2	403.3	403.3	406.7	413.6
WOP (lb/sec)	3.1223	3.1898	3.1057	3.1609	3.1302	3.1795
Flow Ratio (lb/ft <sup>3</sup> )	0.25647	0.25905	0.25648	0.25811	0.25489	0.25402
OPV-K <sub>v</sub>	0.0817	0.0817	0.0817	0.0817	0.0817	0.0817

### 3.2.1.5.3 Propellants

#### Level Sensor Performance

Stage I level sensor histories are shown in Figure 54. The behavior of the Stage I sensors was similar to that of other TIIIC flights. There was some slosh indicated by the high level sensors, but the outage sensors uncovered cleanly. The fuel high level sensor uncovered three times over an interval of 2.4 seconds before remaining uncovered, and the oxidizer high level sensor uncovered twice during a 0.7 second interval.

#### Flight Sensor Analysis

Table 8 summarizes the metered propellant load, the indicated propellant load derived from level sensor data, mixture ratio predicted vs. that measured from the level sensors, calculated outage and a comparison of requested to metered propellant loads.

The propellant loads based on flight level sensor performance were lower than indicated by the propellant loading flowmeters, -0.47% for oxidizer and -0.34% for fuel. This agreement is within the tolerance limit of the level sensor data.

Level sensor checks made during propellant loading fell within the specified maximum and minimum limits. The oxidizer average meter readings were within 16 gallons of the midpoint between the maximum and minimum limits; the fuel readings were within 46 gallons of mid-range.

The shutdown characteristics of the system indicated oxidizer exhaustion with an outage of 514 lbs. of fuel.

The final published propellant inventory predicted a mixture ratio of 1.992. However, this was predicated on loading blocks of 60-75°F for both tanks. Prior to fuel loading, a cold front moved through the Cape area and the loading block for fuel was changed to 55-70°F. This combination of 55-70°F fuel block and 60-75°F oxidizer block resulted in a predicted mixture ratio of 1.954. The average steady state mixture ratio as measured by the level sensors during the flight was 1.959. This is in good agreement with the final predicted mixture ratio.





TABLE 8

STAGE I  
VEHICLE NO. 9

PROPELLANT LOADS

	REQUESTED		FLOW METER, GALLONS				LEVEL SENSOR POST FLIGHT			
			60° GALLONS	NO. 1	NO. 2	AVERAGE		ERROR		% OF FLOWMETER LOAD
	lbs					GAL	LB	LB	LB	
Oxidizer	165,896	13,664	13,654	13,665		13,660	165,848	-48	-0.03	-782
Fuel	85,388	11,276	11,275	11,277		11,276	85,387	-01	-0.01	-291

LEVEL SENSOR FLOW METER CHECK, PREFLIGHT

	MAXIMUM ALLOWABLE GAL	NO. 1 METER READING GAL	NO. 2 METER READING GAL	MINIMUM ALLOWABLE GAL
Oxidizer	12,822	12,698	12,712	12,620
Fuel	10,685	10,561	10,563	10,532

OUTAGE

	Tank	LB	% Of Usable
Maximum Allowable	-	2513	1% Max
Measured, Level Sensors	Fuel	514	0.21%

MIXTURED RATIO BURNED

Predicted Steady State	1.954
Measured, Level Sensors	1.959

### 3.2.1.5.3 Propellants - (Cont.)

Average propellant flowrates between high level and outage sensors were as follows:

Oxidizer	1120 lb/sec
Fuel	572 lb/sec

### Propellant Pressures and Temperatures

Propellant pressures and temperatures are plotted in Figure 55. The plots are as expected and similar to previous TIIIC flights. However, on previous flights the fuel suction temperature remained above the oxidizer suction temperature for the entire flight. On this flight, the reverse was true. This can be explained by the fact that the fuel bulk temperature was lowered by pre-cooling during the loading operation to ensure adequate thrust chamber jacket cooling during engine operation. It can also be noted that both oxidizer and fuel temperatures were lower than on other flights because of the presence of a cold front just prior to liftoff.

### 3.2.1.6 Stage II

#### 3.2.1.6.1 Engine (S/N 6242015)

#### Start Transient

Summarized start transient data are presented in the following table:

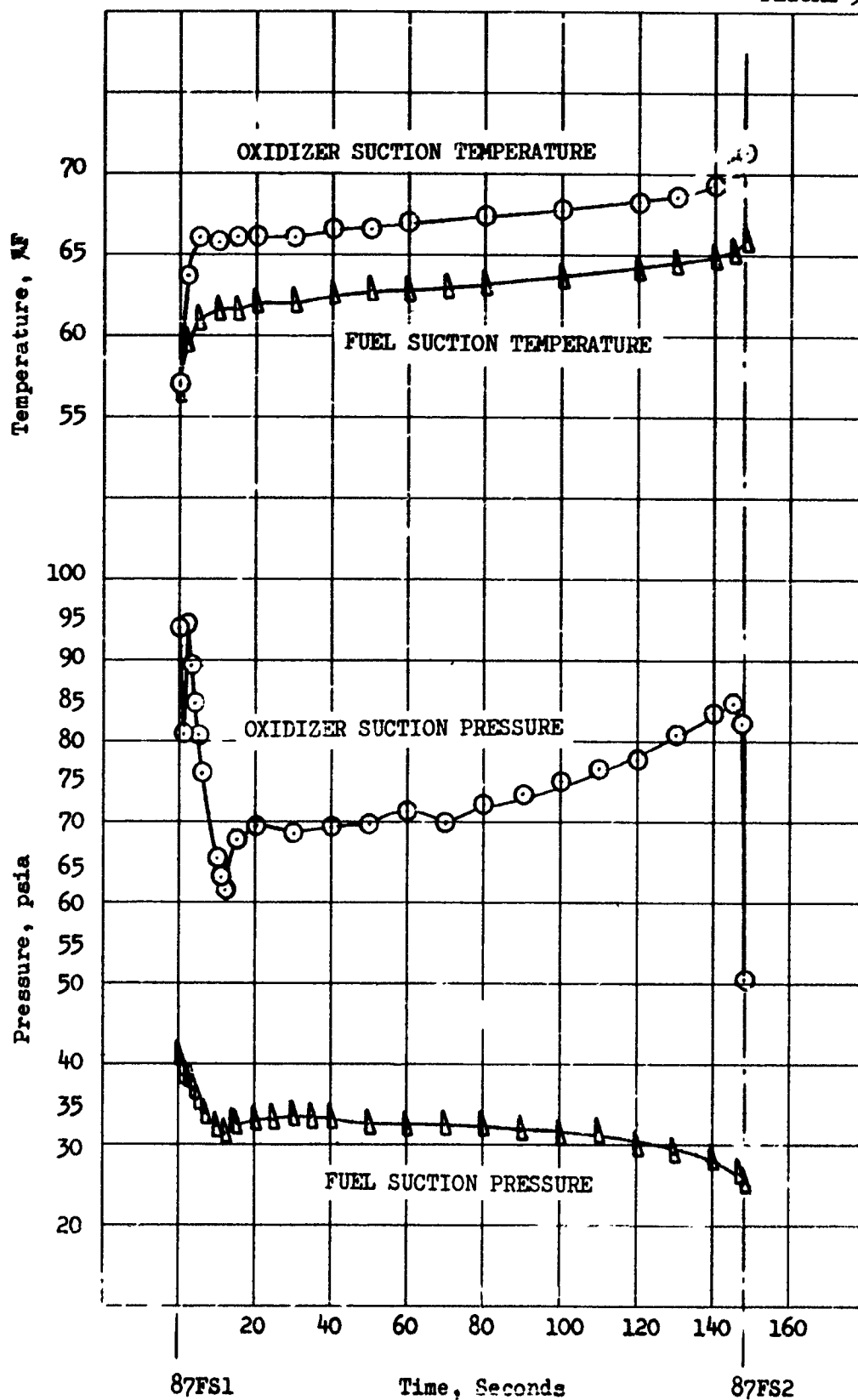
	<u>Specification</u>	<u>Flight</u>
FS <sub>1</sub> to Ignition (sec)	0.5 to 0.9	0.646
Thrust Spike (lbs)	95,000 (max)	72,498
Thrust Step (lbs)	70,000 (max)	54,978
Thrust during Overshoot (lbs)	114,160 (max)	115,272

Dwell time (that time during which the thrust level exceeds 103 percent of rated thrust) was 0.21 seconds. For this dwell time the interface specification for maximum thrust during overshoot is 114,160 pounds; thus Article C-9 had approximately 1,000 pounds of thrust in excess of the specified overshoot thrust. It will be noted here that for Articles C-5, C-10, C-14 and subsequent the interface specification for maximum thrust during overshoot is extended to 128,000 pounds for any dwell time not to exceed 0.5 sec. No degradation in performance was noted as a result of the excessive overshoot.

Article 9 - Stage I  
Suction Pressures and Temperatures History  
Figure

105

FIGURE 55



### 3.2.1.6.1 Engine (S/N 5242015) - (Cont.)

Figure 56 shows chamber pressure vs. time during the start transient. With the exception of excessive overshoot, the data indicate a normal start.

#### Steady State

	<u>Zulu Time</u>
91 FS <sub>1</sub>	13:55:00.377
91 FS <sub>2</sub>	13:58:21.396
Burn Time (sec)	201.019

Stage II engine measurements are presented in Table 9.

The thrust level calculated from flight engine data at 120 seconds ( $F = C_{F_t} P_c + F_{gg}$ ) was approximately 0.85% lower than the preflight predicted thrust level. No significant difference in thrust existed between predicted and accelerometer derived thrust at 120 seconds. When correction is made to include those inlet conditions of flight into the preflight prediction the difference between predicted and calculated thrust is approximately 0.32%. These data are compatible with the three-sigma log-to-launch dispersion of  $\pm 3.08\%$  and are shown on Figure 57. The data are indicative of normal engine operation.

Level sensor data indicate that the average mixture ratio was approximately 0.66% less than predicted by the engine model. This is indicative of normal engine operation when compared with the three-sigma log-to-launch dispersion limits of  $\pm 2.05\%$ .

#### Ablative Skirt

Article C-9 was the second successful C configuration to incorporate a heavy ablative skirt. Instrumentation consisted of eight thermocouples; their location and nomenclature are shown on Figure 58. Temperature-time curves are shown on Figure 59. Thermocouples 1-6 showed expected temperature rise rates and normal temperatures at shutdown. Thermocouples 7 and 8, located in the roll nozzle exhaust impingement area, yielded noisy data and erratic temperatures during the burn. A change to increase the size of AGC's lead wire has been recommended by MC instrumentation to improve the thermocouple data, but it has not been approved at this time. In general, temperature levels were as predicted.

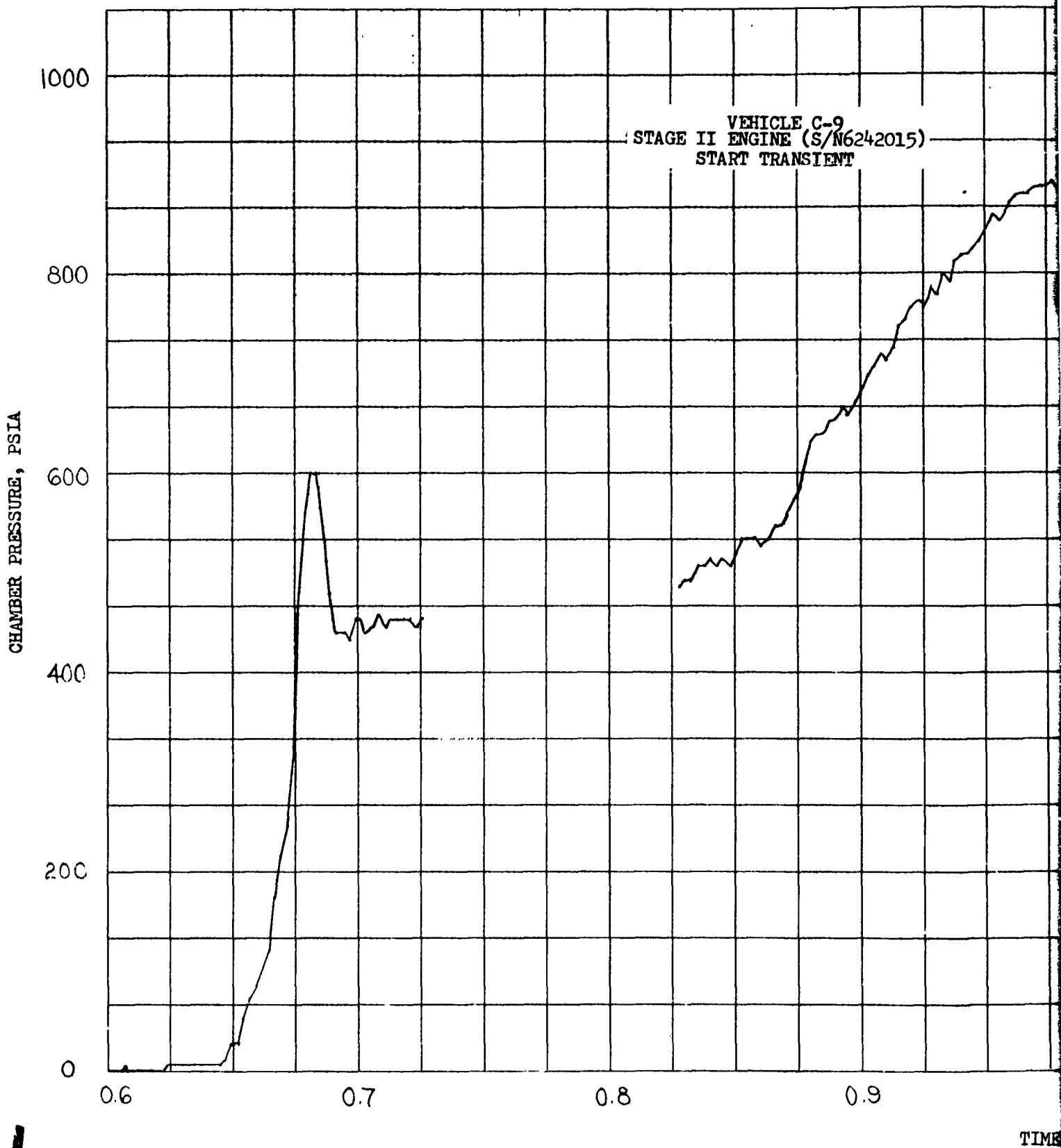
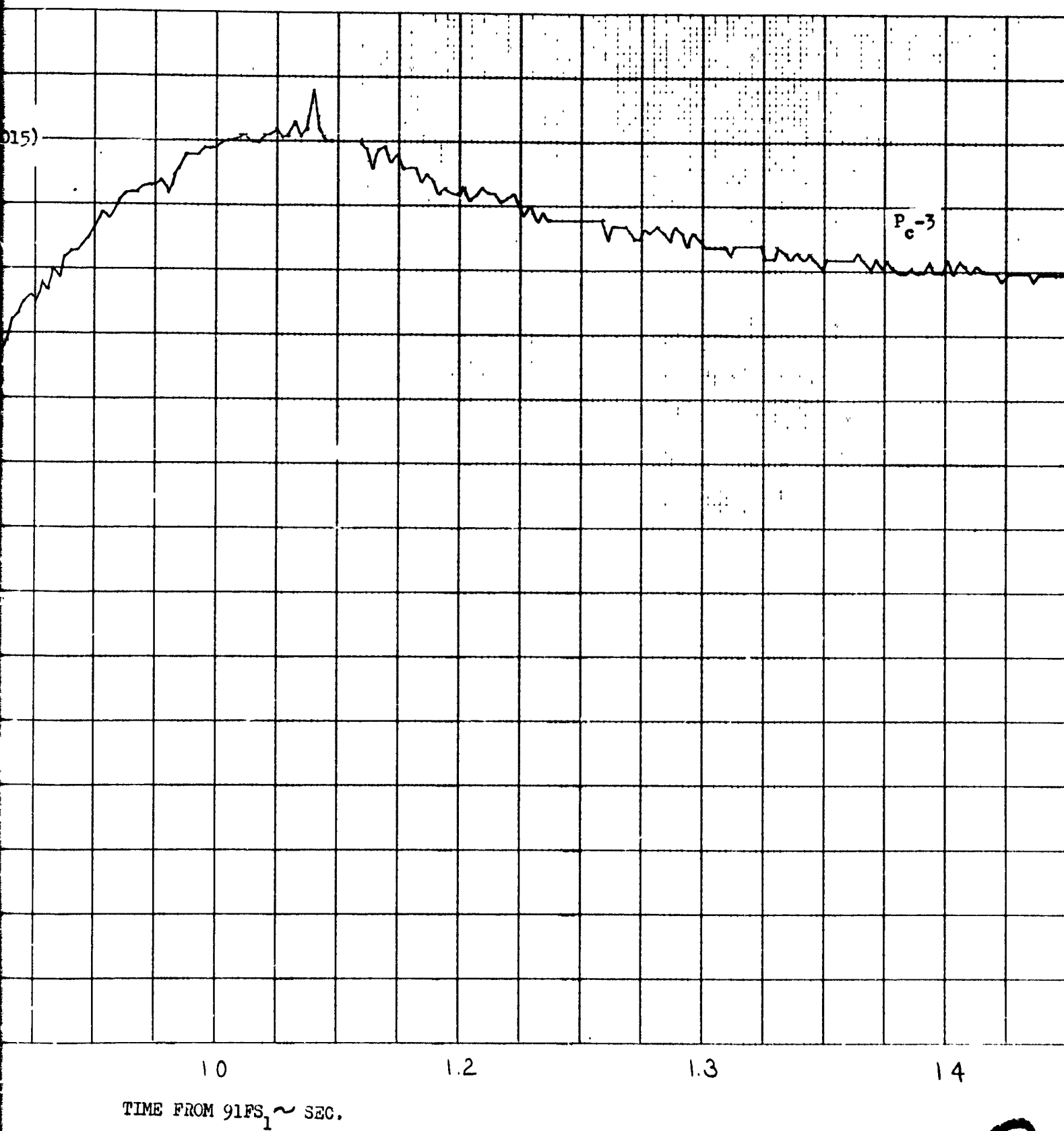
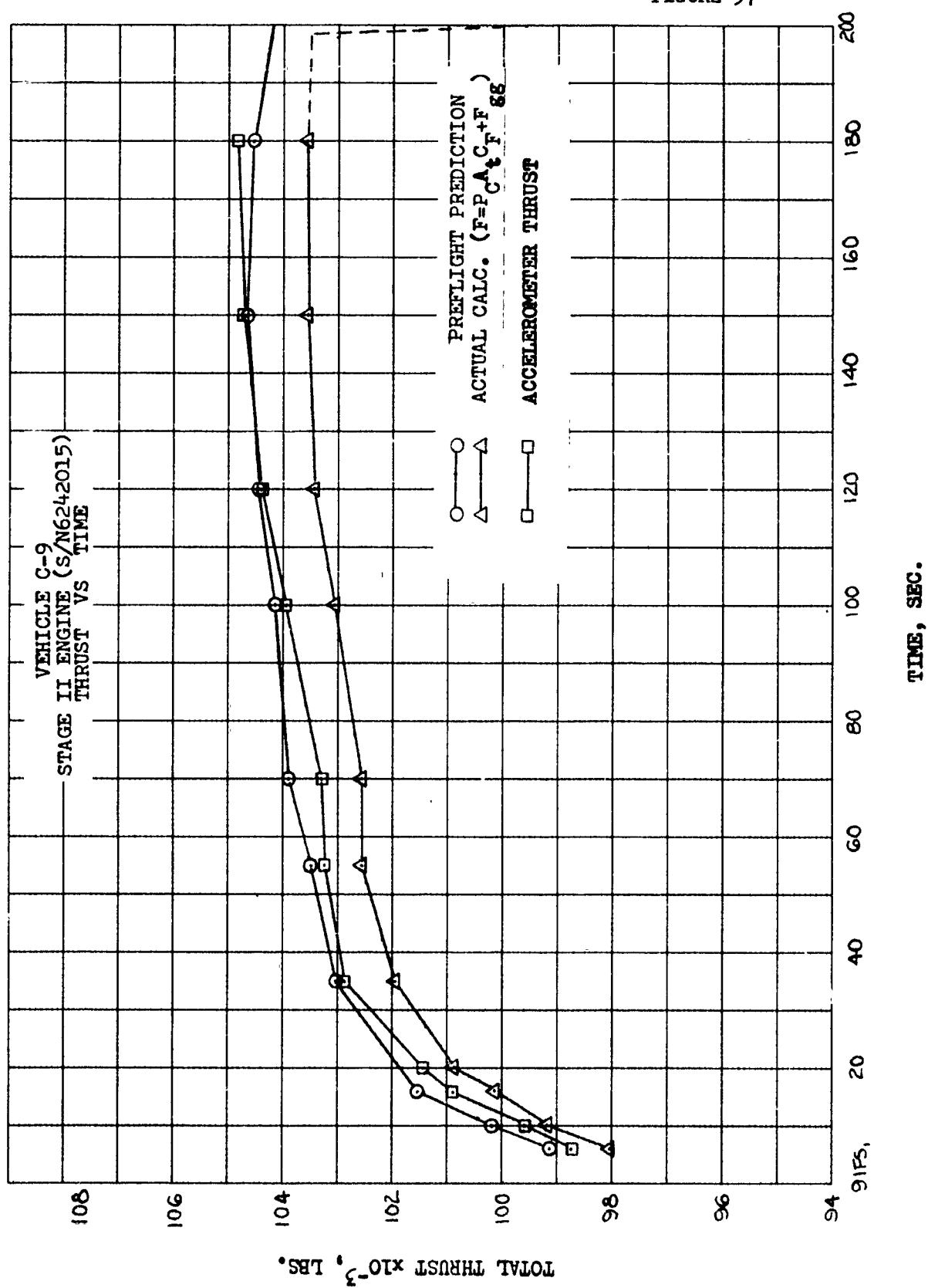


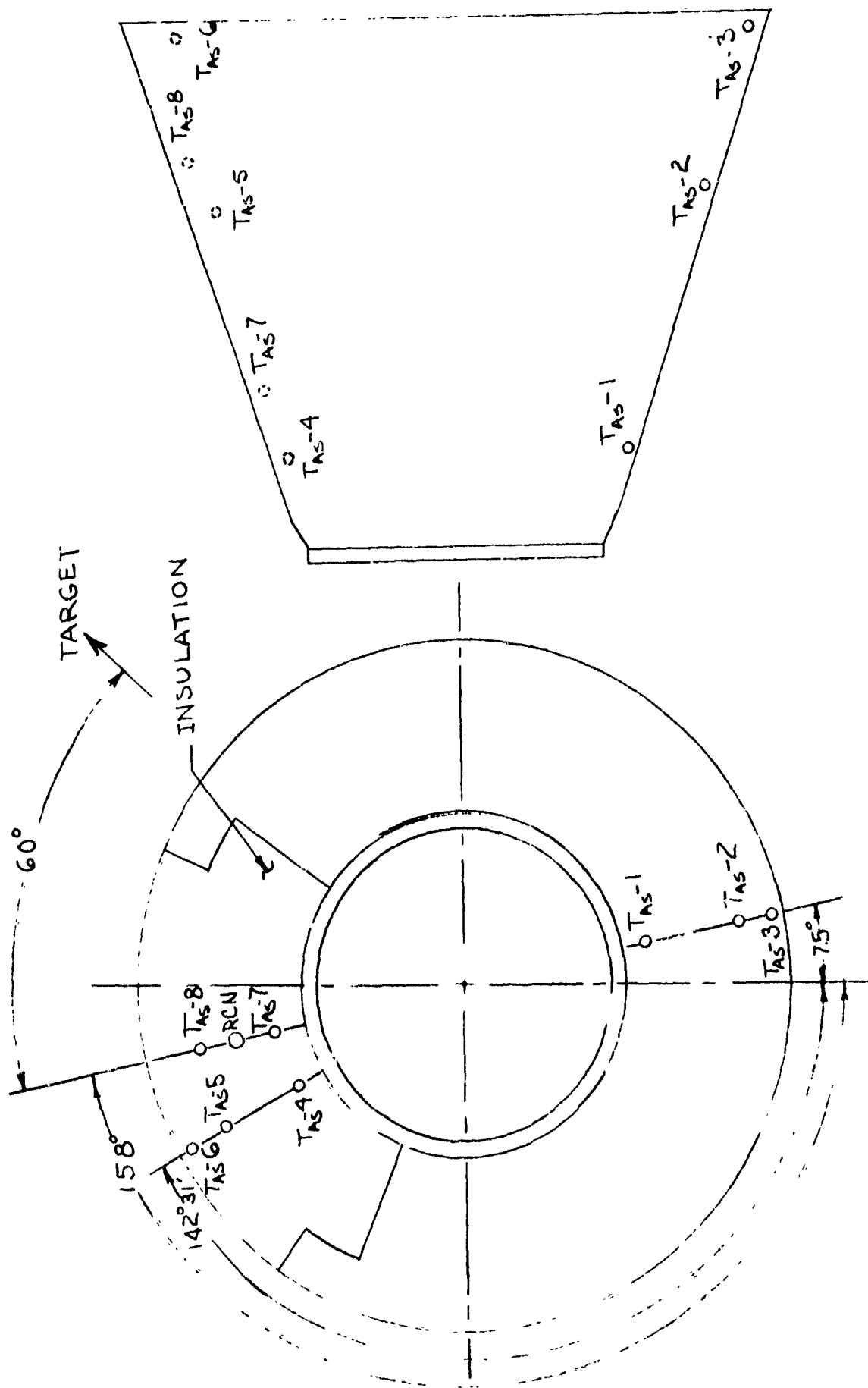
FIGURE 56



2

FIGURE 57



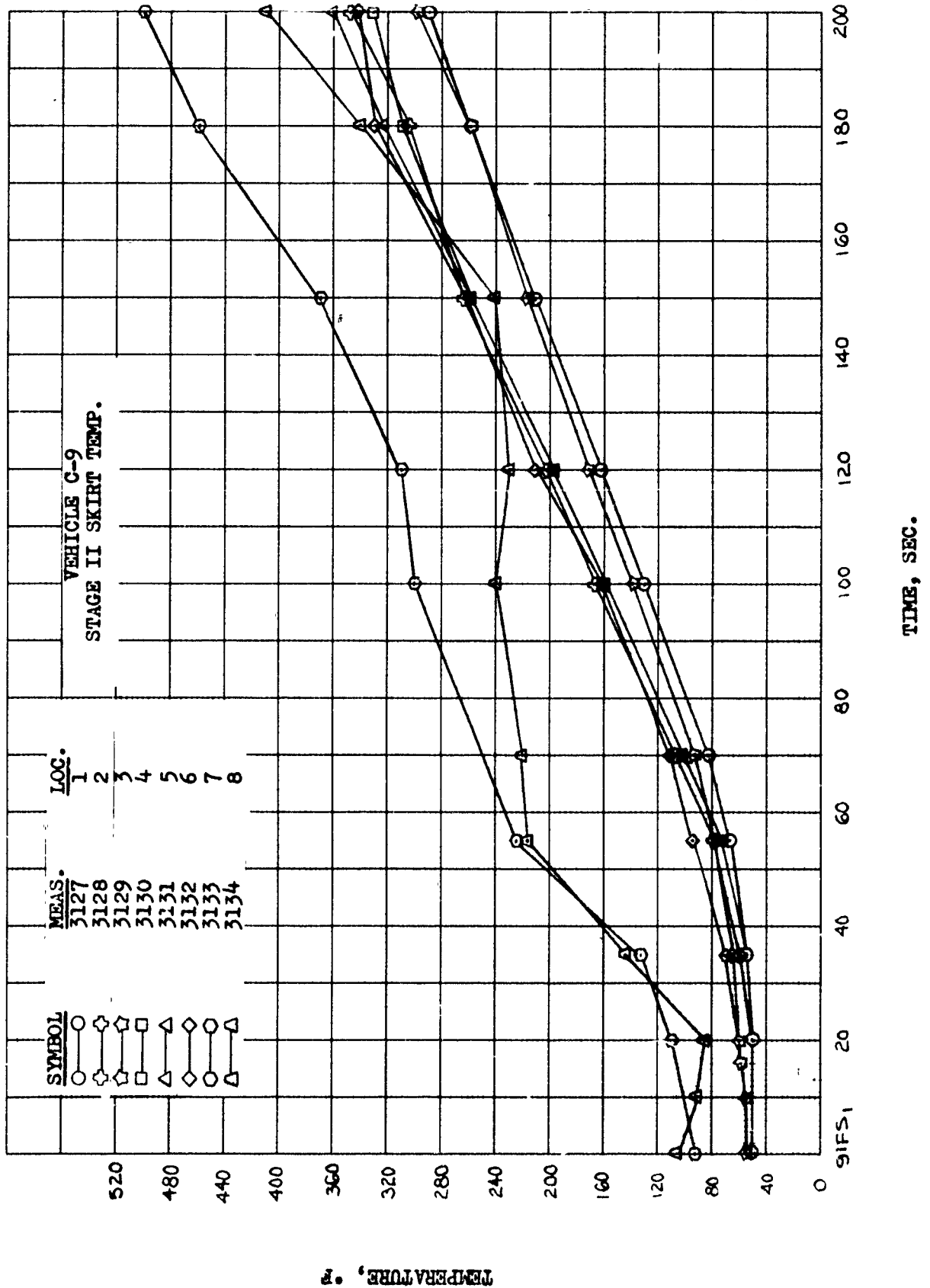


STAGE II ABLATIVE SKIRT TEMP.

FIGURE 98



FIGURE 57



During shutdown, at 91 FS<sub>2</sub> + 2.8 seconds, temperature transients appeared in all ablative skirt thermocouple data and lasted for a duration of approximately 4 seconds. The apparent cause of the temperature rise was a cracking of the ablative liner after shutdown allowing residual hot gas to penetrate to the back-side of the liner. No degradation of the mission resulted from this Post-SECO anomaly.

#### Shutdown Transient

The Stage II engine was shutdown as a result of oxidizer exhaustion. Transient data are presented in Figure 60. Chamber pressure perturbations appeared in the data at 91 FS<sub>2</sub> + 0.144 and 0.226 seconds and reached maximum pressures of approximately 165 and 790 psia respectively. These pressure spikes are assumed to be the result of residual oxidizer expulsion into a fuel rich chamber prior to the complete closure of the thrust chamber valves. A rise in the fuel discharge pressure reached its maximum at approximately 0.38 seconds after 91 FS<sub>2</sub> indicating the thrust chamber valves were partially open when perturbations were noted in chamber pressure. Disturbances in the oxidizer bootstrap venturi inlet pressure during the interim between FS<sub>2</sub> and complete valve closure also give supporting evidence to the conclusion that there was residual oxidizer in the system.

It is concluded that the engine functioned normally for an oxidizer exhaustion shutdown.

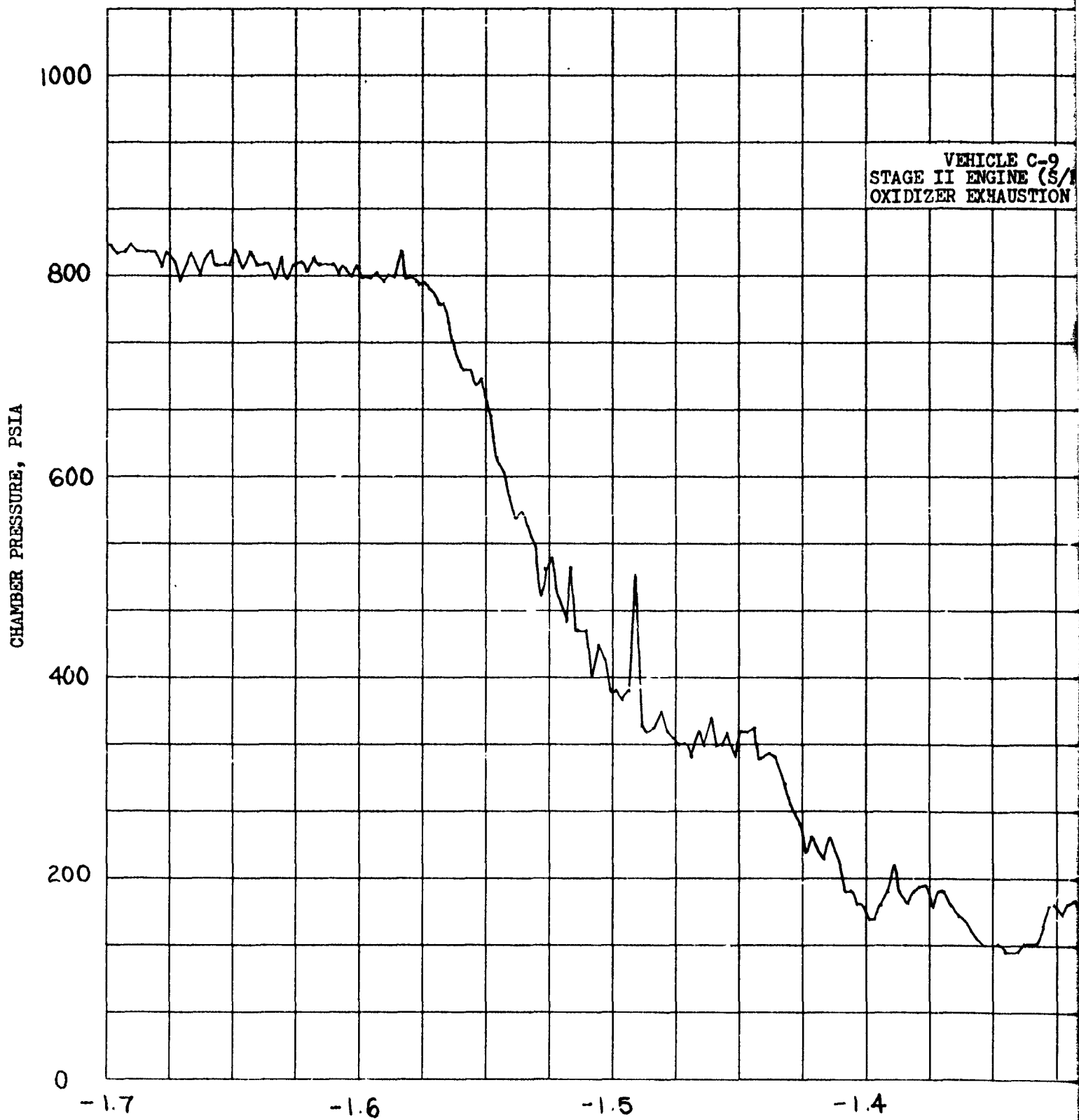
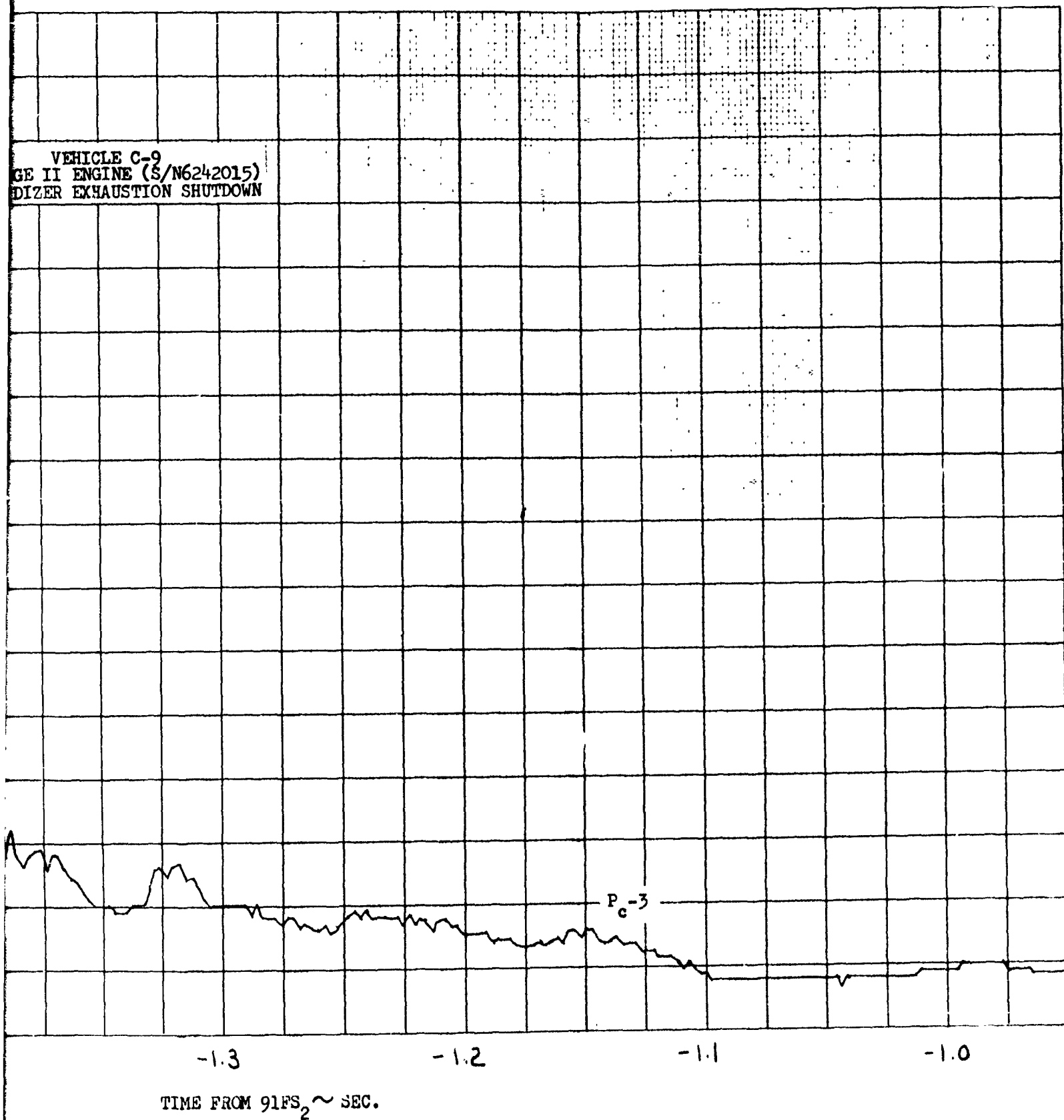


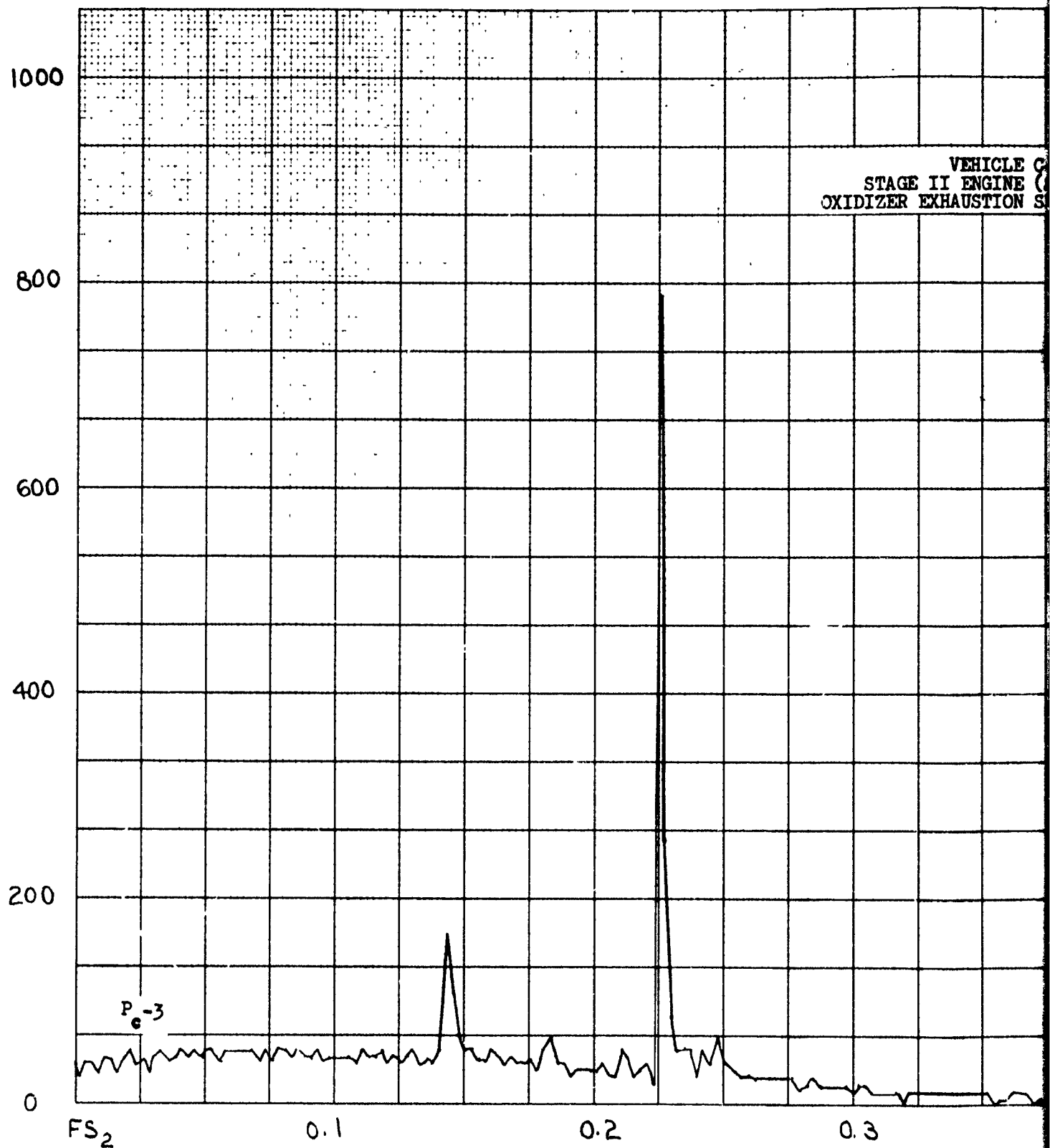
FIGURE 60

VEHICLE C-9  
GE II ENGINE (S/N6242015)  
DIZER EXHAUSTION SHUTDOWN



2

CHAMBER PRESSURE, PSIA



TI

FIGURE 60 (Cont.)

VEHICLE C-9  
STAGE II ENGINE (S/N6242015)  
ZER EXHAUSTION SHUTDOWN (CONT)

0.4 0.5 0.6 0.7  
TIME FROM 91FS<sub>2</sub> ~ SEC.

2

CONFIDENTIAL

114

TABLE 9

STAGE II ENGINE MEASURED DATA

Data averaged over two second interval (100 sample/sec)

<u>Time from FS<sub>1</sub></u> <u>Sec</u>	<u>P<sub>c</sub></u> <u>psia</u>	<u>P<sub>os</sub></u> <u>psia</u>	<u>P<sub>fs</sub></u> <u>psia</u>	<u>T<sub>os</sub></u> <u>°F</u>	<u>T<sub>FS</sub></u> <u>°F</u>
0	805	54.1	53.0	63.0	62.9
10	814	54.6	54.0	63.0	62.9
16	822	54.2	55.1	63.1	62.9
20	828	53.7	55.3	63.2	63.3
35	837	52.8	55.8	63.4	63.3
55	842	52.1	56.5	63.4	63.7
70	842	52.4	57.1	63.4	64.1
100	846	53.0	57.7	63.4	64.2
120	849	54.3	57.7	64.2	65.0
150	850	56.1	58.3	66.6	67.3
180	850	57.8	58.3	69.4	68.1
200	820	48.4	57.3	---	73.7

ENGINE PERFORMANCE AT FS<sub>1</sub> + 120 SEC

<u>Parameter</u>	<u>Units</u>	<u>Predicted</u>	<u>Actual</u>
F <sub>TOT</sub>	lbs	104452	103560 (F = P <sub>c</sub> A <sub>t</sub> C <sub>F</sub> + F <sub>gg</sub> )
W <sub>ot</sub>	lbs/sec	215.65	214.0*
W <sub>ft</sub>	lbs/sec	120.26	119.0*
AVG.MR <sub>E</sub>	---	1.810	1.798*
I <sub>sp</sub>	sec	309.56	310.99*

\*Based on level sensor data.

CONFIDENTIAL

### 3.2.1.6.2 Pressurization

#### General

Stage II pressurization system operation was normal during the flight. Tank gas pressure curves and interface flow boxes are shown in Figures 61, 62, 63 and 64. Pressurization system parameters from acceptance test and flight test data are tabulated in Table 10 at burn times 91 FS<sub>1</sub> plus 6, 20, and 120 seconds.

#### Fuel System

The preflight pressure prediction averaged 2.0 to 3.0 psia above the flight data. The post flight prediction shows much better agreement with the flight data. The maximum deviation of the postflight prediction from the data was less than 1 psi during steady state and about 1.5 psi during the start transient. This post flight prediction is considered to be good agreement with the flight data, well within the inaccuracies of the instrumentation system and the mathematical model.

The large deviation of the preflight prediction from flight data is due, in part, to the method of handling the percentage condensibles of the autogenous gas entering the tank. In the past, this percentage has been considered to be constant throughout the burn. A more detailed analysis indicates that this percentage is not constant, but varies with time. This revised analytical technique was applied in the post flight prediction and resulted in a significant improvement.

Also contributing to the deviation of the flight data was a slight shift in the flight position in the flow box from the acceptance test position. This shift would cause tank pressure to be lower than predicted.

The tank pressure during Stage 0 and Stage I operation displayed normal response to tank stretch.



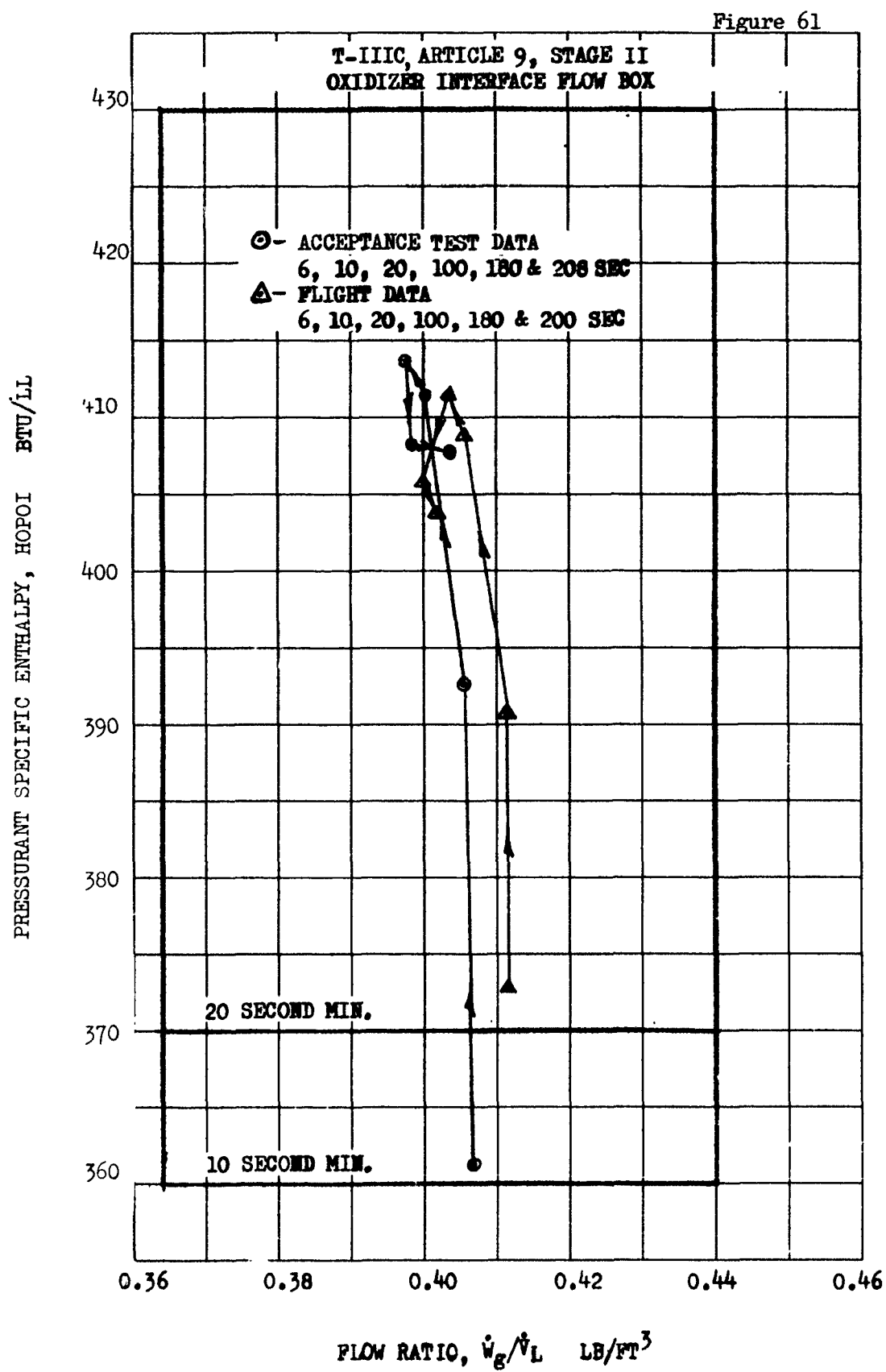
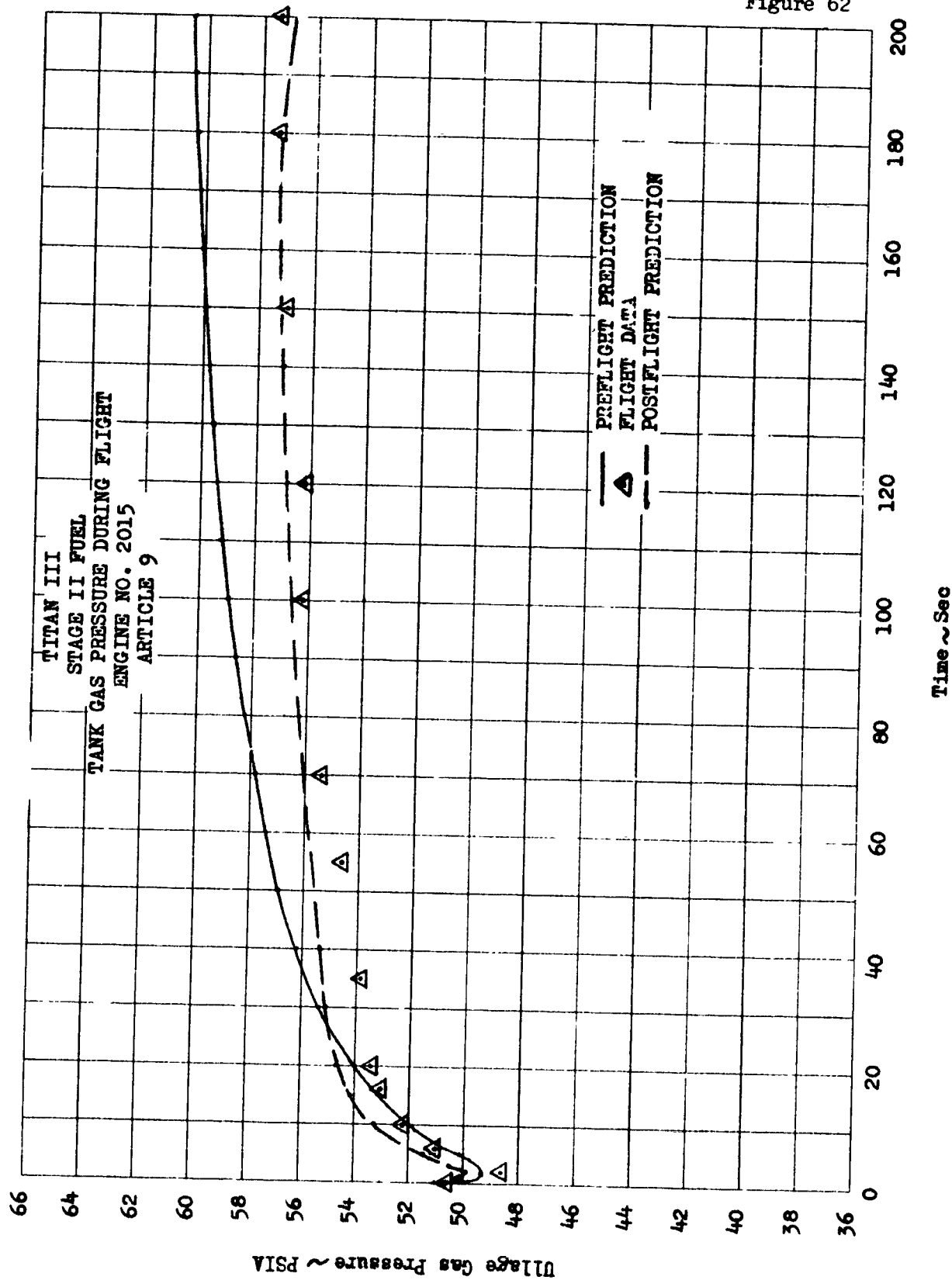


Figure 62





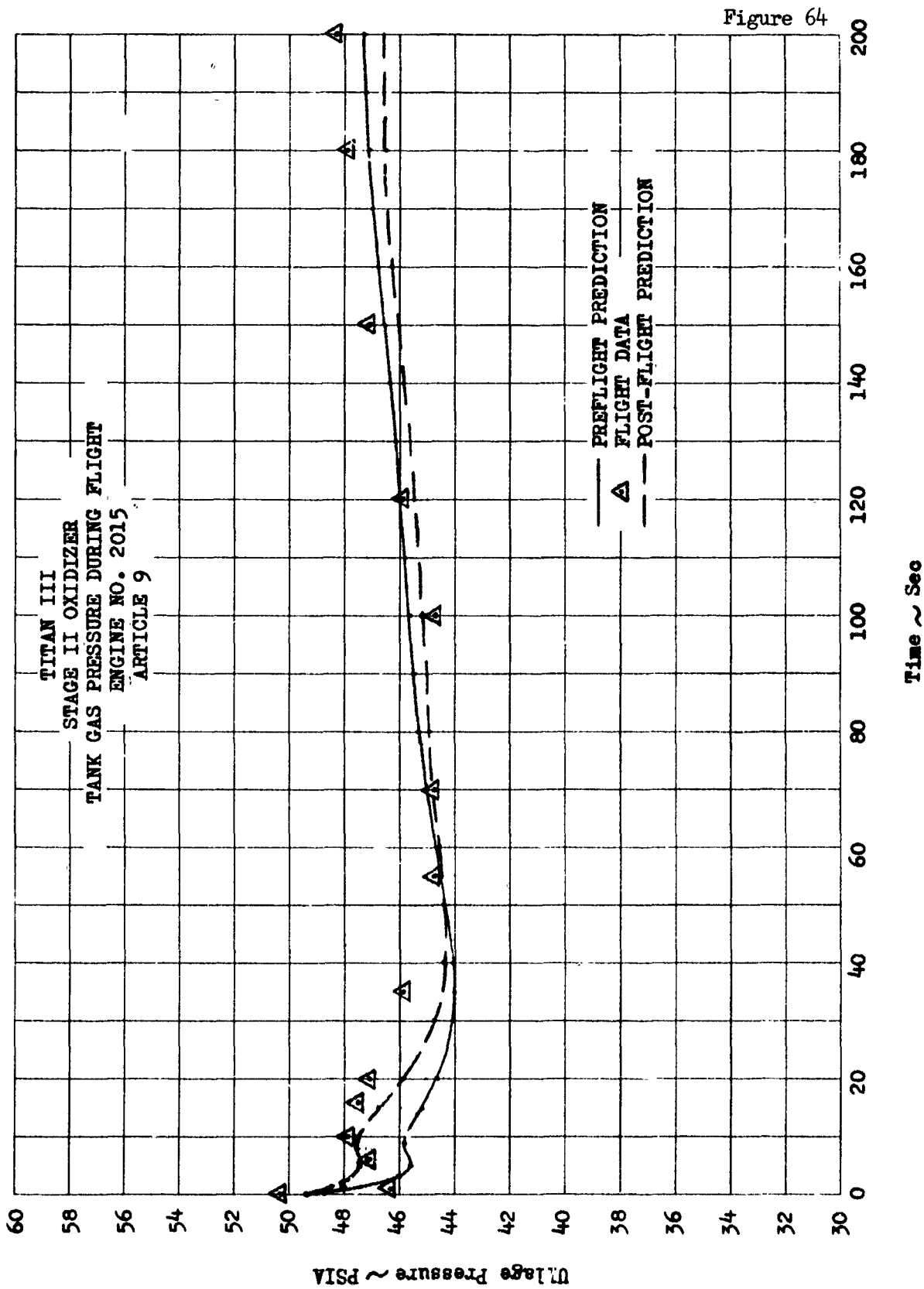


TABLE 10

## STAGE II PRESSURIZATION PARAMETERS

Parameter	6 Seconds		20 Seconds		120 Seconds	
	Accept Test	Flight	Accept Test	Flight	Accept Test	Flight
PGFT (psia)	---	51.0	---	53.4	---	56.2
PFPOI (psia)	360.1	355.7	376.2	375.8	402.3	397.8
TFPOI (°F)	205.8	198.5	217.5	218.4	228.3	224.1
WFP (lb/sec)	0.31652	0.3163	0.32765	0.3293	0.34770	0.3471
Flow Ratio (lb/ft <sup>3</sup> )	0.15813	0.15375	0.15998	0.15387	0.16521	0.15964
FPW (in.)	0.28	0.28	0.28	0.28	0.28	0.28
PGOT (psia)	---	47.1	---	47.1	---	45.9
POPOI (psia)	---	582.0	---	629.0	---	661.0
TOPOI (°F)	---	337.3	---	386.9	---	391.9
HOPOI (Btu/lb.)	361.3	372.9	411.3	409.0	412.7	410.9
WOP (lb/sec)	0.91735	0.9497	0.93169	0.9723	0.94778	0.9858
Flow Ratio (lb/ft <sup>3</sup> )	0.40652	0.41481	0.40033	0.40575	0.39912	0.40305
OPV-K <sub>v</sub>	0.024	0.024	0.024	0.024	0.024	0.024

### 3.2.1.6.2 Pressurization - (Cont.)

#### Oxidizer System

The flight data showed slightly higher tank pressure than both the pre and post flight predictions except for a period from 91 FS<sub>1</sub> plus 60 seconds to 91 FS<sub>1</sub> plus 120 seconds. During the latter part of the burn, the preflight prediction was a better approximation of the data than the post flight, deviating a maximum of 1.0 psi by 91 FS<sub>2</sub>. During the start transient, the post flight prediction was much better than the preflight prediction, although both deviated by as much as 2.0 psi at times prior to 91 FS<sub>1</sub> plus 50 seconds.

This deviation was caused by the fact that the initial pressure for the predictions was about 1 psi below the data, and a slight shift in the flow box position caused the pressure to be higher than the preflight prediction.

Although there was a slight flow box shift, the data was well within specification.

The tank pressure prior to 91 FS<sub>1</sub> was normal.

### 3.2.1.6.3 Propellants

#### Level Sensor Performance

Stage II level sensor histories are shown in Figure 65. The sensors behavior was similar to that of other THIC flights; the fuel and oxidizer outage sensors uncovered cleanly, and the high level sensors exhibited slosh. The high level sensor interval of 0.9 seconds from first to last uncover for the fuel and 1.8 seconds for the oxidizer are within expected limits.

#### Flight Sensor Analysis

Table 11 summarizes the metered propellant load, the indicated propellant load derived from level sensor data, predicted mixture ratio vs. that measured from the level sensors, calculated outage and a comparison of requested to metered propellant loads.

The propellant loads based on flight level sensors were higher than indicated by the propellant loading flowmeters; +0.23% for the oxidizer and +0.05% for the fuel. Both of these values are well within allowable limits.

Level sensor checks during propellant loading fell within the specified maximum and minimum limits. The oxidizer average meter readings were within 18 gallons of the midpoint between the maximum and minimum limits; the fuel readings were within 13 gallons of mid-range.

The final published propellant inventory predicted a mixture ratio of 1.784, using loading blocks of 70-85°F for fuel and 60-75°F for oxidizer. Final preflight loading blocks were 65-80°F for both tanks, with a corresponding mixture ratio of 1.764 as the final preflight prediction. This is in good agreement with the average steady state mixture ratio of 1.797 indicated from level sensor data and is consistent with the oxidizer exhaustion.

The outage was calculated to be 445 lbs. of fuel.

The average propellant flowrates between the high level and outage sensors were as follows:

Oxidizer	214.0 lb/sec
Fuel	118.9 lb/sec

FIGURE 65

Article 9 - Stage II  
Level Sensors' History  
Figure

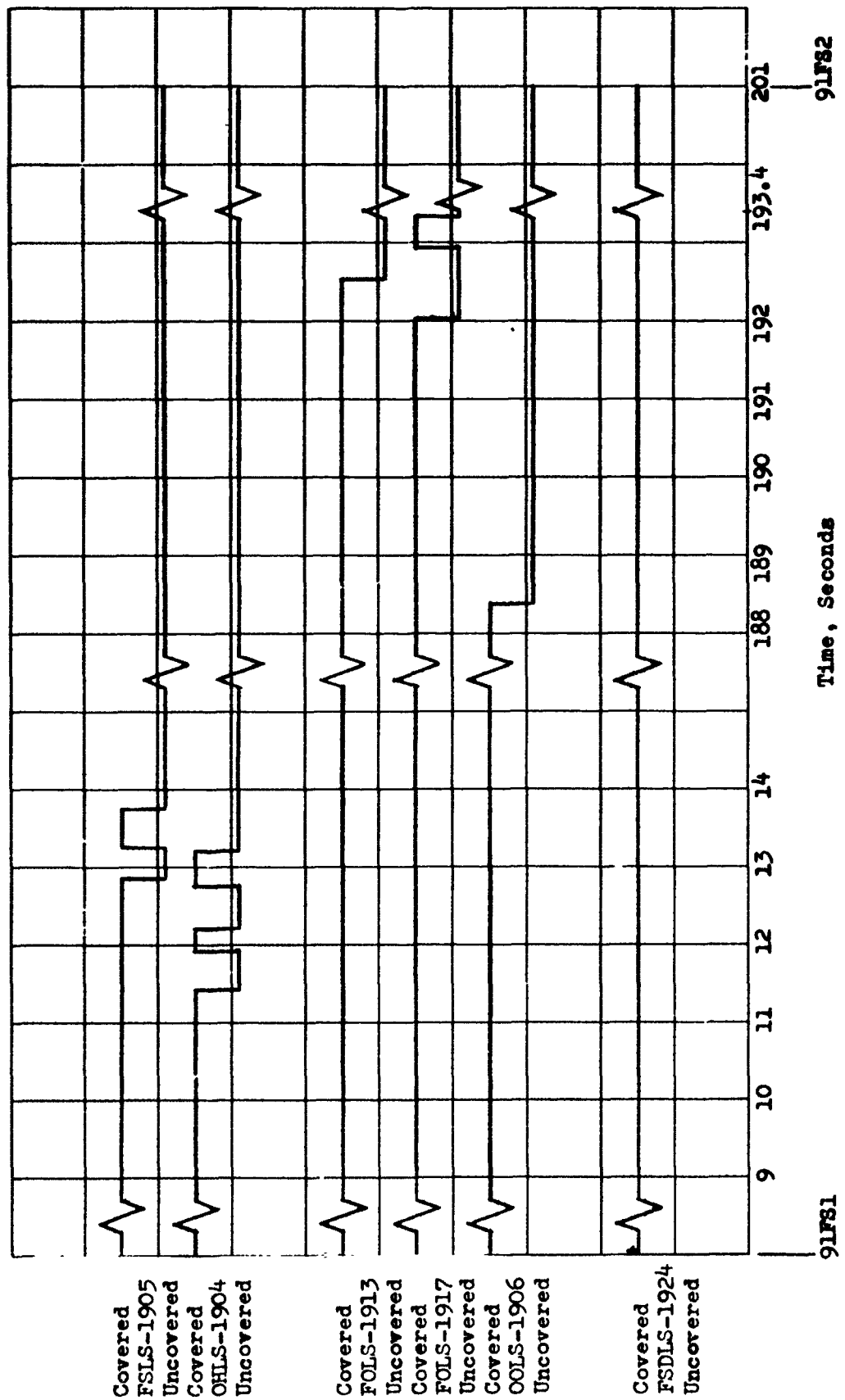




TABLE 11

STAGE II

VEHICLE NO. 9

PROPELLANT LOADS

	REQUESTED		FLOW METER, GALLONS		AVERAGE			ERROR			LEVEL SENSOR POST FLIGHT		
	LBS	60° GALLONS	NO. 1	NO. 2	GAL		LB	LB	% OF REQUESTED	LB	LB	LB	% OF FLOWMETER LOAD
Oxidizer	42,415	3,493	3494	3494	3494		42,422	+07	+0.02	42519	+97		+0.23
Fuel	24,202	3,196	3197	3197	3197		24,209	+07	+0.03	24220	+11		+0.05

LEVEL SENSOR FLOW METER CHECK, PREFLIGHT

	MAXIMUM ALLOWABLE GAL	NO. 1 METER READING GAL	NO. 2 METER READING GAL	MINIMUM ALLOWABLE GAL
Oxidizer	3290	3244	3245	3235
Fuel	3001	2969	2961	2954

OUTAGE

	Tank	LB	% Of Usable
Maximum Allowable	-	666	1% Max
Measured, Level Sensors	Fuel	445	0.67%

MIXTURED RATIO BURNED

Predicted Steady State	1.764
Measured, Level Sensors	1.797

### 3.2.1.6.3 Propellants - (Cont.)

#### Propellant Pressures and Temperatures

Propellant suction pressures and temperatures are plotted in Figure 66. The temperature history is typical of those for a comparatively cool day. There is no significant temperature rise in the oxidizer suction line over the interval of 91 FS<sub>1</sub> + 20 to +100 seconds. This would normally be attributed to stratification caused by the air conditioning system prior to flight. The conditioned air on this flight was approximately the same temperature as the propellant.

Oxidizer suction pressure dipped down and then recovered between 91 FS<sub>1</sub> +20 and +120 seconds. This dip, although present on previous flights was more pronounced on this flight.

In part, suction pressure is determined by acceleration head (the product of acceleration and propellant level). On this flight the acceleration rise rate was less than on previous flights and the acceleration head term decreased to a more pronounced level prior to recovery, than on previous flights.

### 3.2.1.7 Stage III

#### 3.2.1.7.1 Engines

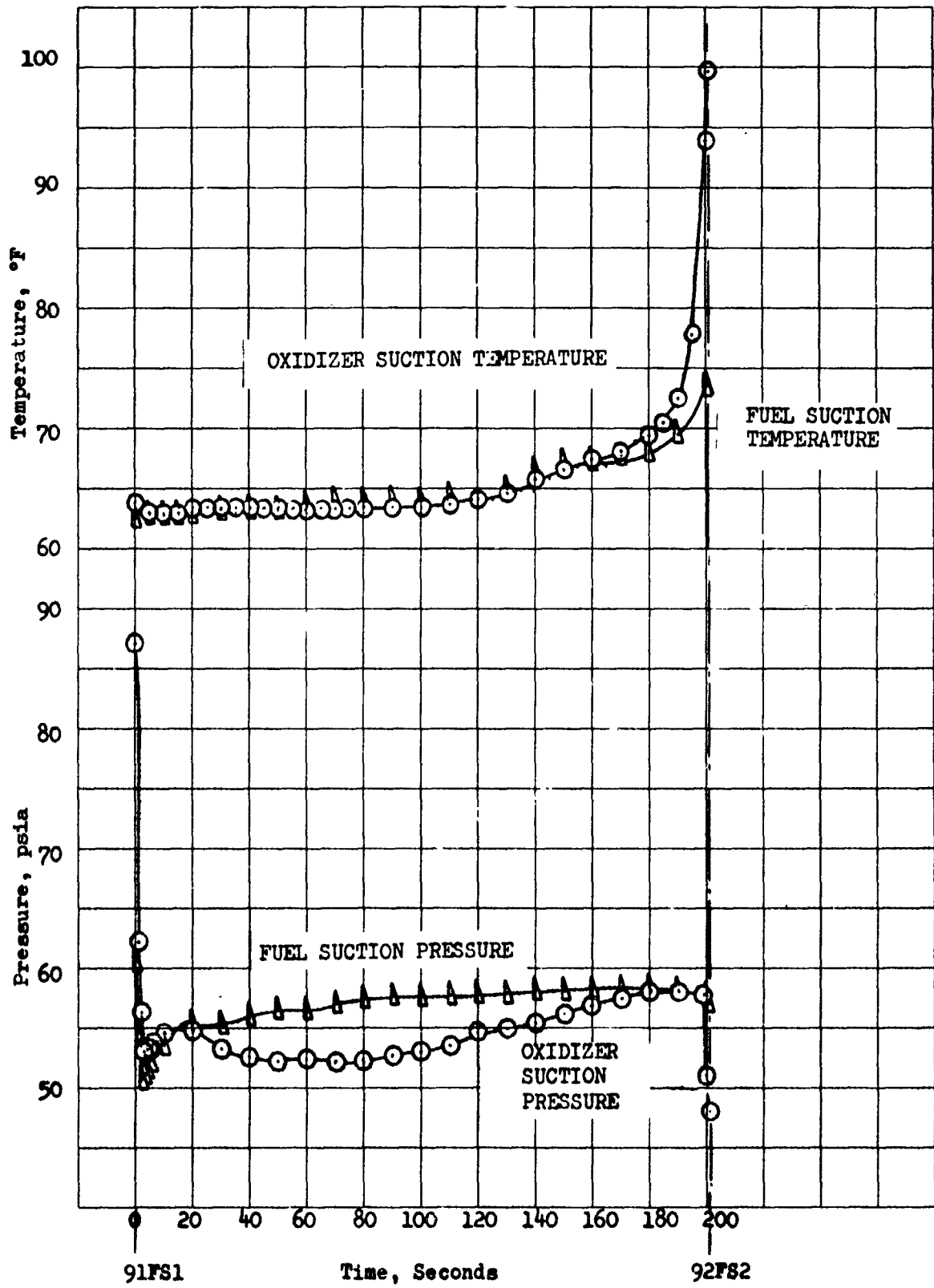
The Art. C9 Stage III engine subsystem was similar to that used on the Art. C11 vehicle. Gold plated stainless steel foil thermal insulation was added to the propellant feedlines. The outboard portion of the combustion chamber was painted white from the throat to the injector flange. The engine insulation cover was modified such that only the bi-propellant valve assembly was insulated.

There were minor additional configuration changes made to the Art. C9 engines. The bi-propellant valve insulation cover and the injector feedlines were also painted white for more effective solar heating thermal control. A Teflon-lined pilot valve vent tube was used to preclude the possibility of an engine restart during the orbital portion of the mission.

The vent tube heaters were wired in series with the 150 degree pilot valve thermostats to improve effectiveness of the heaters in case of a propellant leak. The heaters had been previously wired through the 60 degree thermostats.

Article 9 - Stage II  
Suction Pressures' and Temperatures' History  
Figure

FIGURE 66



### 3.2.1.7.1 Engines - (Cont.)

#### First Burn

##### Engine Start

The start signal was received by the engines at 13:58:34.41 GMT. All engine pressure parameters indicated a normal start transient. Both valves opened normally and there was no resulting thrust overshoot above the steady state level. The start transient profiles are depicted in Figure 67. The bi-propellant valve functioning times are listed in Table 12.

##### Steady State Operation

The engines performed satisfactorily during the 307.6 sec. firing sequence. Time-averaged instrumented parameters are listed in Table 14. Engine performance parameters were calculated by considering engine data from all three engine firings, level sensor data, weight data and vehicle thrust accelerations. The composite engine calculations for burns are presented in Table 13.

The engine temperatures were normal except for the throat temperatures which appeared to be abnormally high. The engine 4 external throat temperature saturated the sensor at 588°F after 260 sec of engine operation. The engine 5 external throat temperature was 505°F at 1-138FS2. Engine throat temperature profiles as depicted in Figures 68 and 69 are similar to those experienced during the Article A1 and A2 flights. Radiation shields were hung from the engine truss on Article A3 (and up) to block the thermal radiation from the adjacent nozzle extensions and thereby keep the throat temperature below 500°F. Accordingly, the Article C9 temperature data indicates that the throat radiation shields were ineffective during the engine firing sequence.

The SLV 9 flight vehicle had one significant configuration difference in comparison to previous flight articles and that difference was the MOL Sim Lab. The MOL Lab was vented to atmosphere through the Stage III engine compartment. Analysis is being conducted to determine whether or not venting could displace the radiation shields and thereby make them ineffective. It is also possible that environmental radiation effects are causing the high throat temperatures.

CHAMBER PRESSURE, PSIA

120

100

80

60

40

20

0

.05

.10

.15

.20

.25

.30

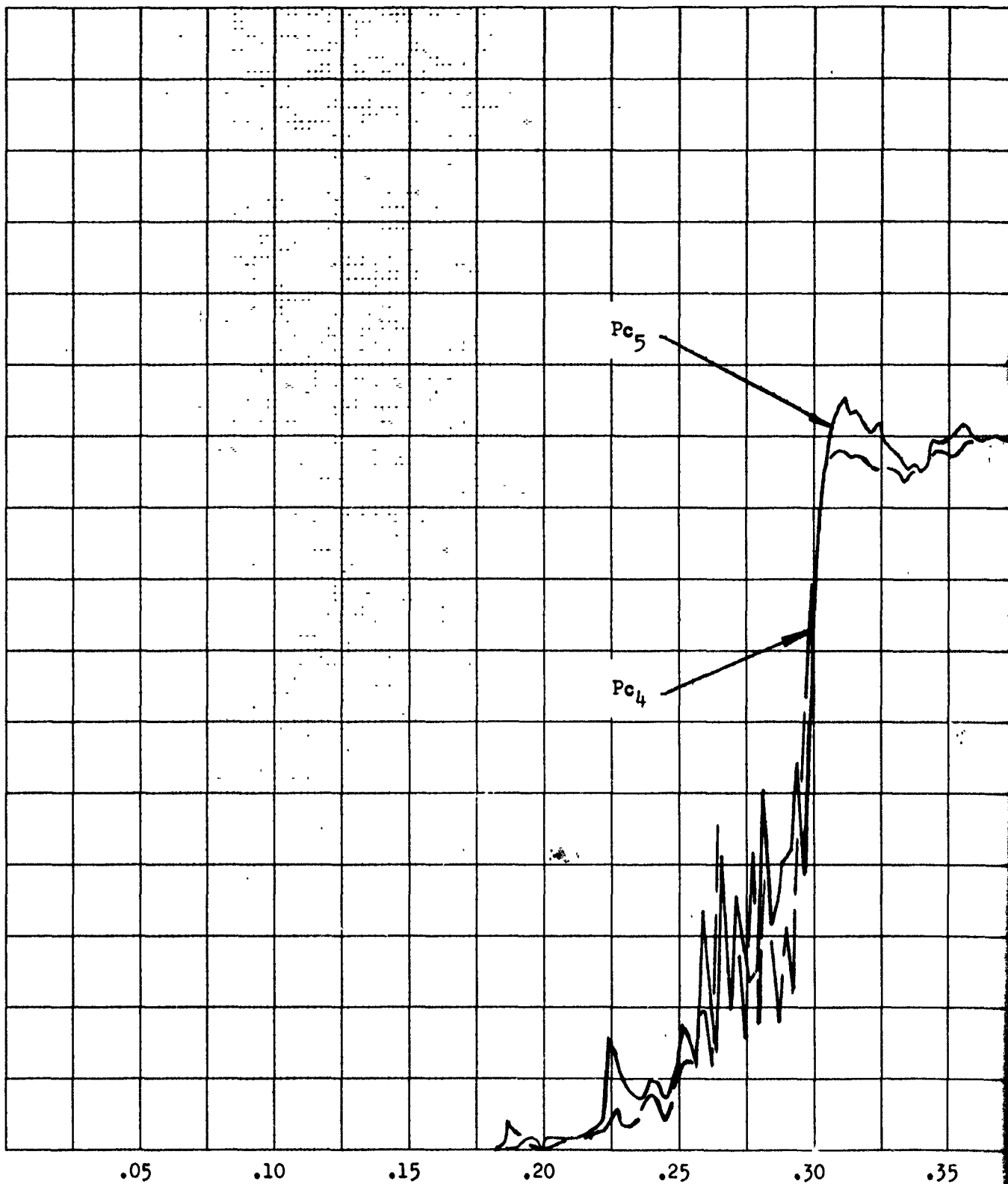
.35

$P_{c5}$

$P_{c4}$

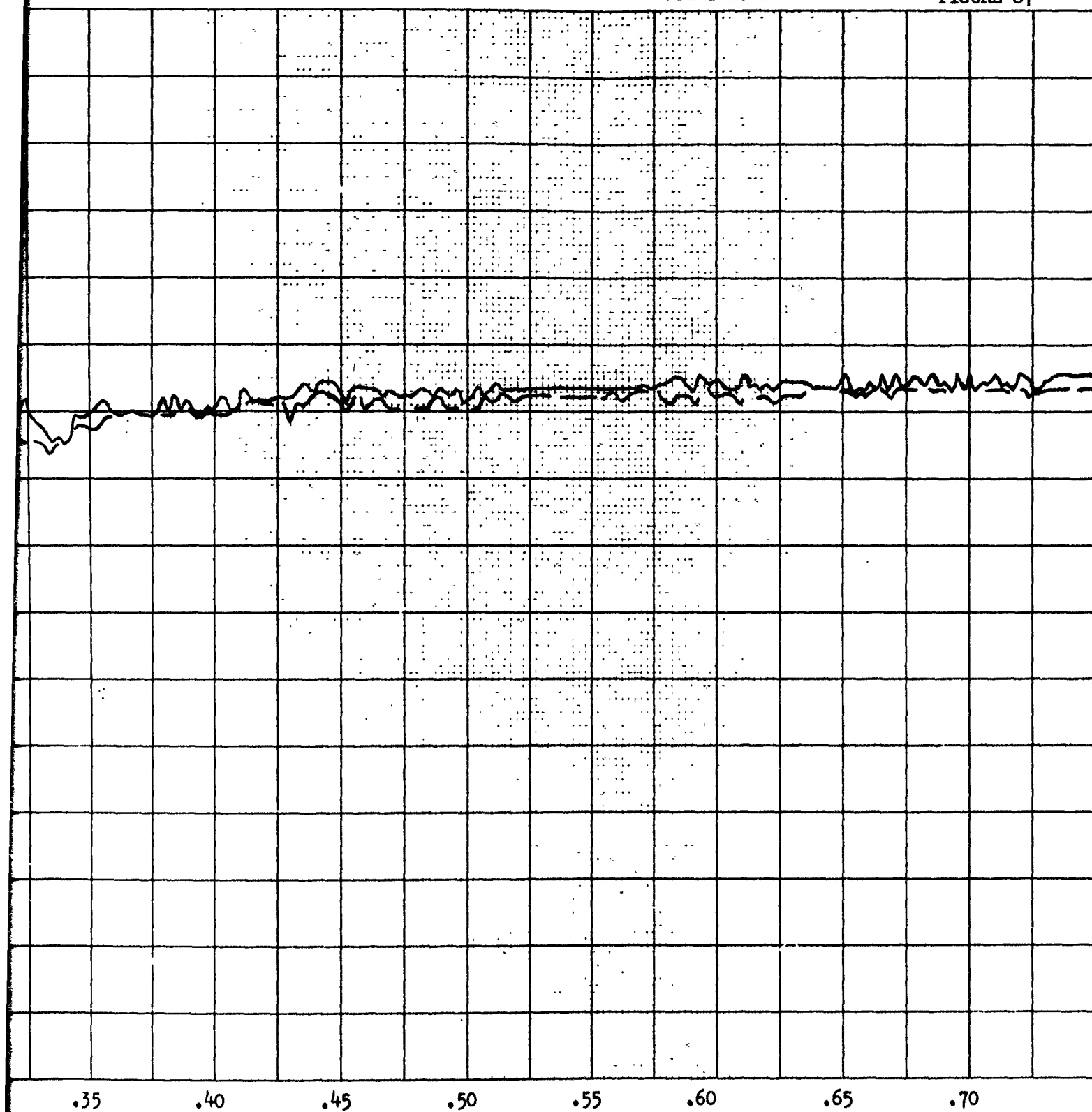
1-138FS1

Flight Time, S



SLV 4  
3 November 1966  
START TRANSIENTS  
FIRST BURN

FIGURE 67



Light Time, Seconds

2

TABLE 12  
STAGE III ENGINE VALVE TIMES

	<u>First Burn</u>	<u>Second Burn</u>	<u>Third Burn</u>
LTCV4 SO	.079	.065	.065
LTCV5 SO	.079	.071	.071
LTCV 4 OT	.348	.339	.327
LTCV 5 OT	.352	.339	.320
LTCV 4 SC	.111	.105	.092
LTCV 5 SC	.100	.091	.078
LTCV 4 CT	.150	.149	.170
LTCV 4 CT	.175	.160	.172





TABLE 14  
TRANSTAGE MEASURED PERFORMANCE PARAMETERS  
(AVERAGED DATA)

FIRST BURNING TIME SEC. *****	BURN POL PSIA *****	PFL PSIA *****	TOL DEG. F *****	TFL DEG. F *****	ACCEL. G *****	PC-4 PSIA *****	PC-5 PSIA *****
.0001	152.7	154.7	60.2	60.9	.358	104.9	106.2
5.03	152.4	157.5	63.9	65.8	.360	106.5	107.5
20.14	152.6	158.6	64.9	66.8	.364	106.7	107.6
40.27	152.7	158.3	64.9	66.9	.372	106.8	107.5
60.41	152.8	158.0	65.5	66.9	.380	107.0	107.5
80.55	152.6	157.4	65.5	66.9	.389	106.7	107.1
100.68	152.4	156.9	66.0	67.4	.398	106.6	106.9
120.82	152.5	156.7	66.1	67.5	.408	106.6	106.8
140.96	152.4	156.3	66.1	67.5	.419	106.6	106.8
161.09	152.6	156.1	66.1	67.5	.430	106.7	106.9
181.23	152.6	155.8	66.1	67.9	.442	106.8	106.9
201.36	152.3	155.1	66.1	68.1	.453	106.6	106.7
221.50	152.6	155.2	66.1	68.1	.466	107.0	107.0
241.64	152.2	154.4	66.3	68.1	.480	105.7	106.8
261.77	151.5	153.6	66.5	68.1	.495	106.5	106.5
281.91	151.2	153.2	66.6	68.1	.512	106.4	106.2
302.25	152.1	153.8	66.6	68.3	.528	106.1	106.0
307.61	152.1	153.8	66.6	68.3	.534	106.1	106.0

SLV 9 FLT

3 NOV 1966

132

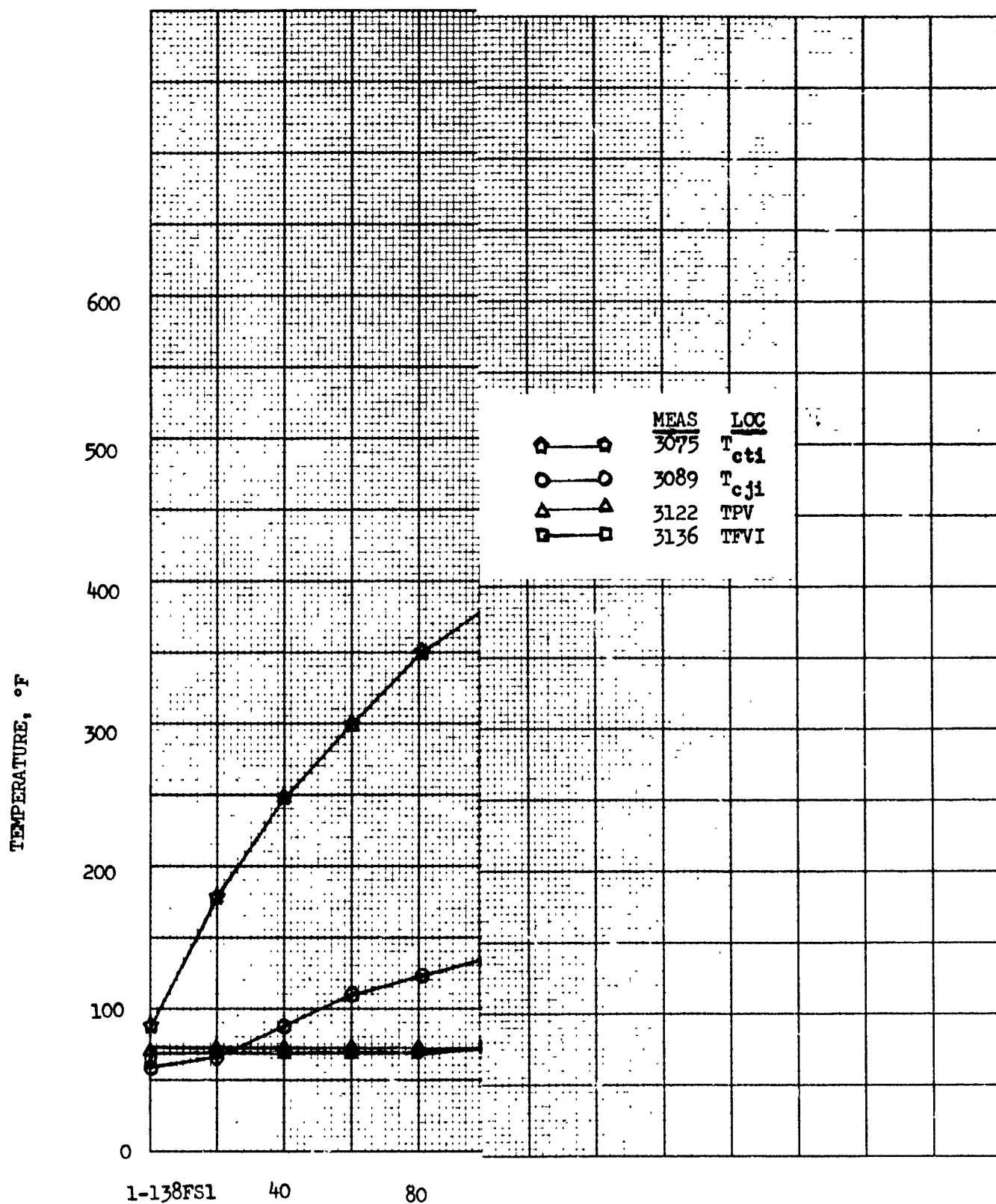
ENGINE

TEMPERATURES

ENG 4 S/N 3026

FIRST BURN

FIGURE 68



SLV 9 FLT 3 NOV 1966

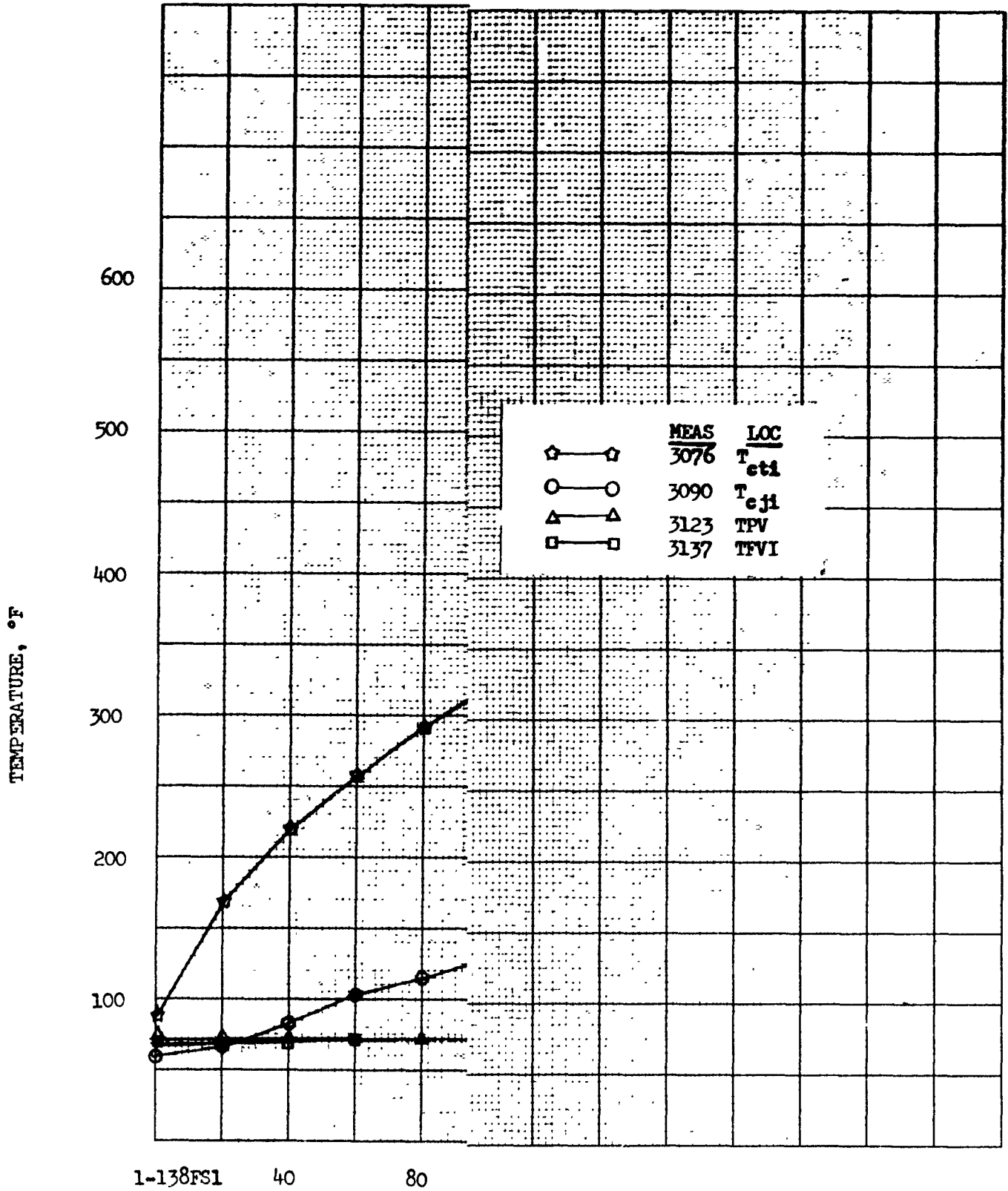
133

ENGINE TEMPERATURES

ENG 5 S/N 3027

FIRST BURN

FIGURE 69



### 3.2.1.7.1 Engines - (Cont.)

Two basic factors determine the thrust chamber external surface temperatures. The most influential is the internal heat generation or engine soak back heat. The other is the surrounding environment which could consist of adjacent radiating surfaces such as engine nozzles, fuel tanks, oxidizer tanks; direct solar on the external surface; direct solar on the internal surfaces; reflected solar on the external surface; reflected solar to the internal surface from nozzle skirt; albedo and earth radiation; reflected earth and albedo radiation from transtage; and outer space heat sink of  $-460^{\circ}\text{F}$ .

There are two engine subassemblies, one of which is mounted on the (#4) target side and the other on the side opposite target (#5). The engine subassembly on the side opposite target receives direct solar influence during the initial phase of the elliptical transfer orbit. The throat external temperature of  $590^{\circ}\text{F}$  indicates that this influence may be significant for such long duration daylight space firings. An influence of this nature could be detrimental to engine operation. The same duration of firing on the backside of the earth, night time, for the corresponding temperature measurement is  $175^{\circ}$  to  $225^{\circ}$  cooler. Investigations will continue to determine the influence of the solar energy on the transtage engine thrust chamber. Conclusions and recommendations on the high throat temperature phenomenon will be presented after the investigations have been completed.

#### Engine Shutdown

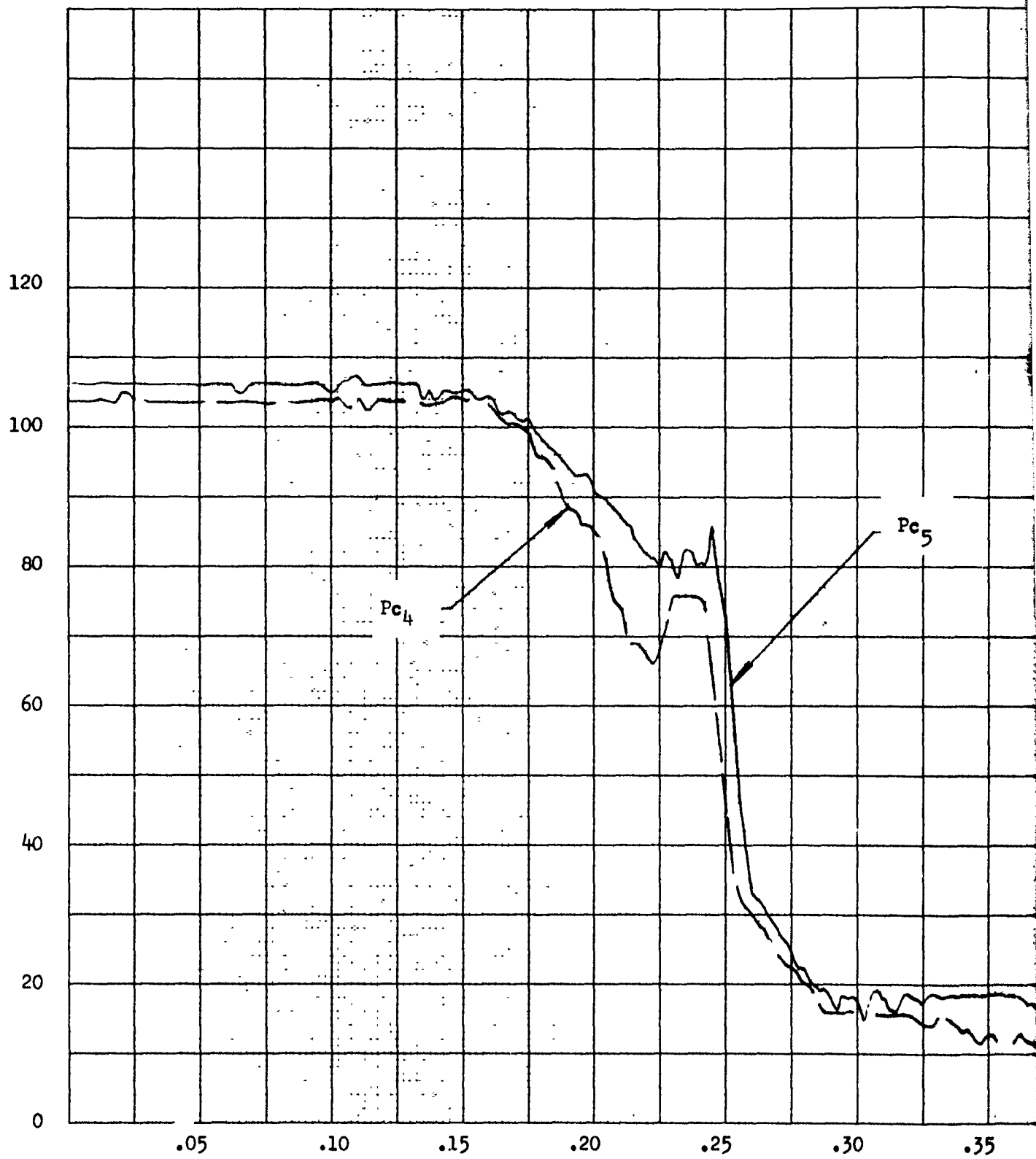
The engine underwent a normal decay transient after receipt of the shutdown signal. Both bi-propellant valves closed smoothly signifying normal operation. The engine 4 valve started to close at  $\text{FS}_2 + 0.111$  sec. and the engine 5 valve started to close at  $\text{FS}_2 + 0.100$  sec. The valve functional times are listed in Table 12. Chamber pressure shutdown transient profiles are depicted in Figure 70.

#### Second Burn

##### Engine Start

The second engine start signal was received after a 64.4 second coast period. All instrumented engine parameters indicated a normal start. There was no thrust overshoot above the steady state thrust level. Chamber pressure profiles as shown in Figure 71, indicated there was little start differential impulse. Valve operation times appeared

CHAMBER PRESSURE, PSIA

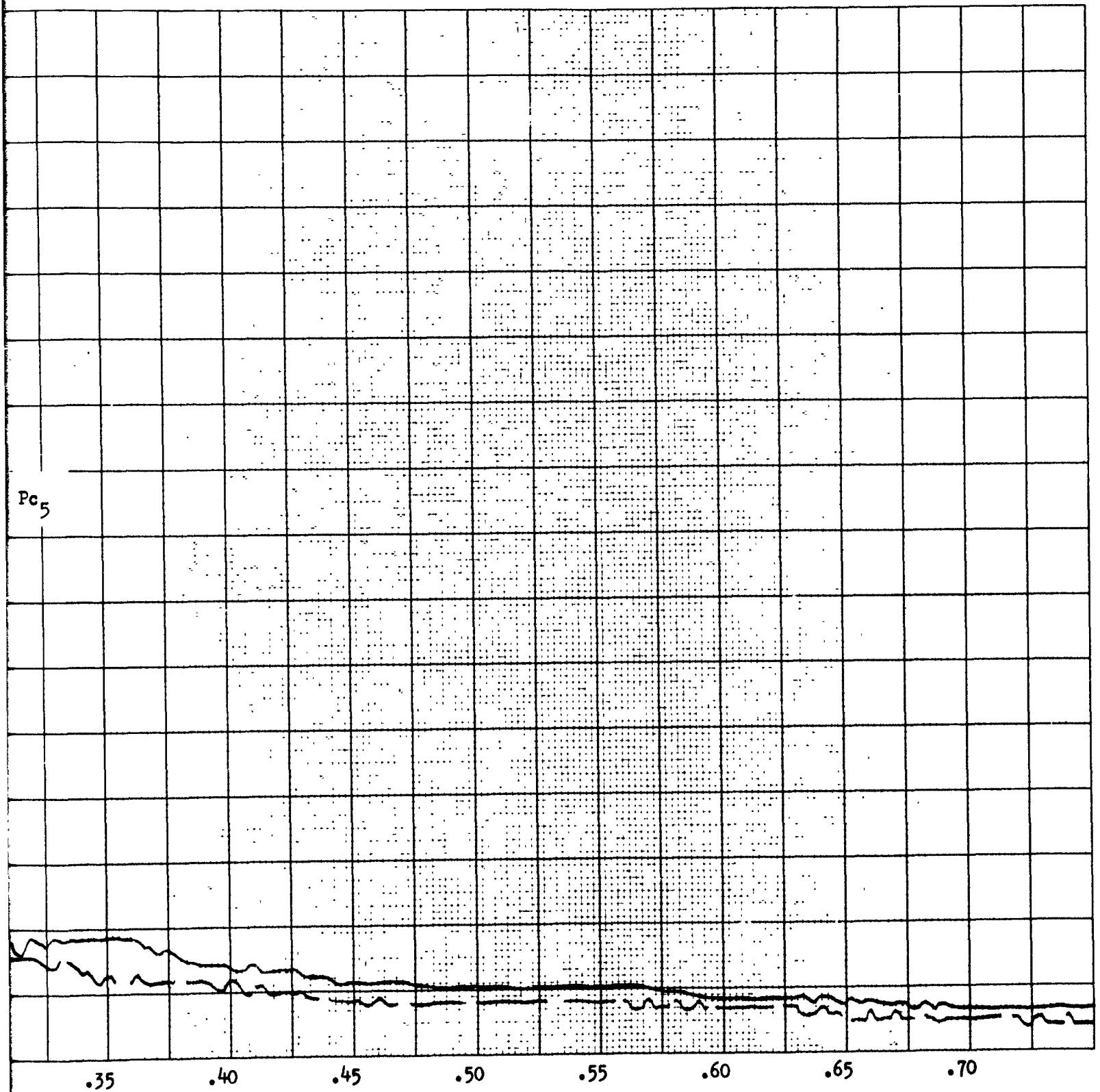


Flight Time, S

1-138FS2

SLV 4  
3 November 1966  
SHUTDOWN TRANSIENTS  
FIRST BURN

FIGURE 70



Flight Time, Seconds

2

CHAMBER PRESSURE, PSIA

120

100

80

60

40

20

0

.05

.10

.15

.20

.25

.30

.35

$P_{c4}$

$P_{c5}$

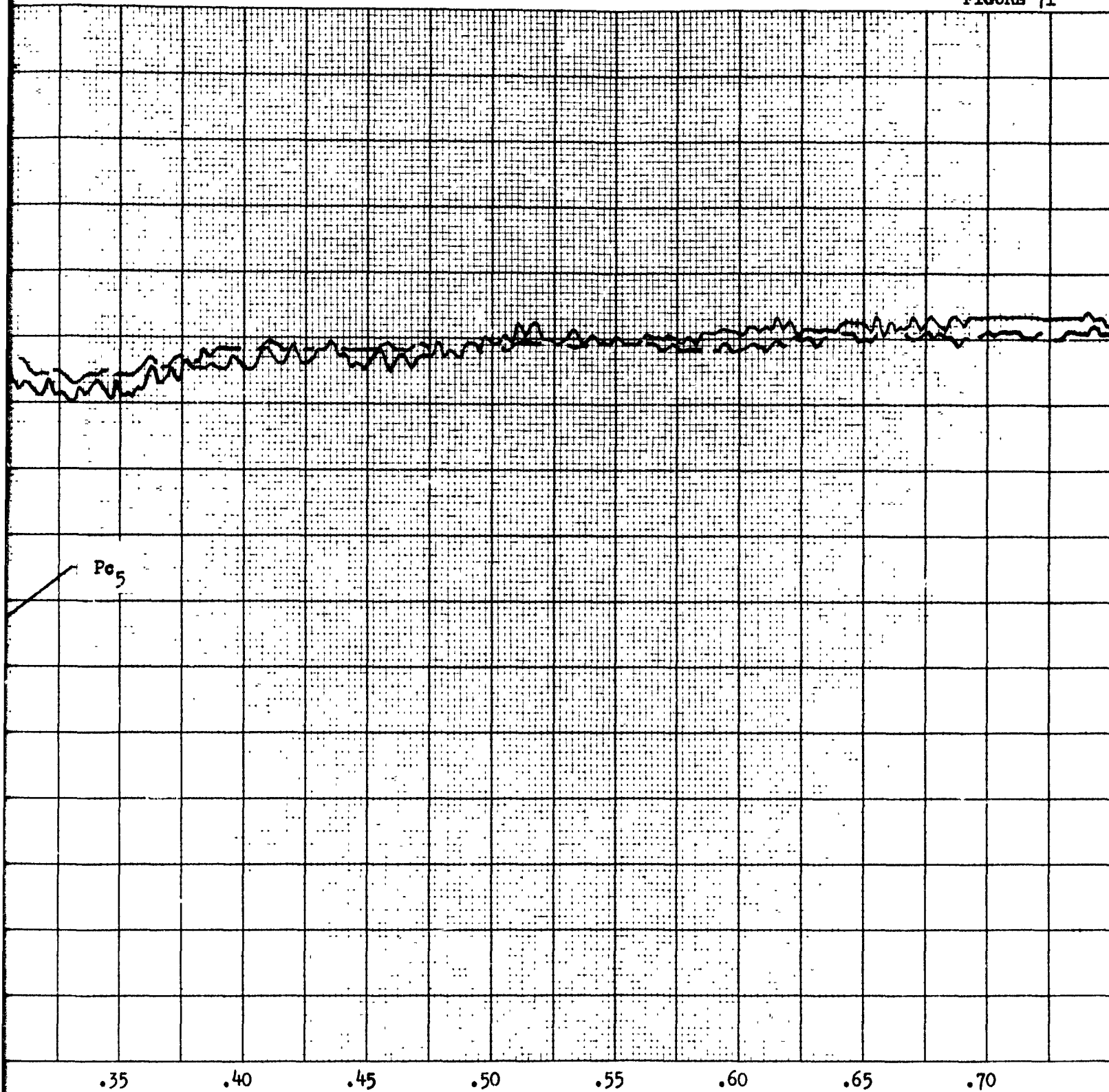
2-138FS1

Flight Time

SLV 4  
3 November 1966  
START TRANSIENTS  
SECOND BURN

136

FIGURE 71



Flight Time, Seconds

2



normal; they are listed in Table 12. Engine feedline pressures were 172 psia for oxidizer and 163.6 psia for fuel just prior to the start. The high feedline pressures were not expected to occur until the third engine firing. Vehicle maneuvers, as explained in the pressurization section, induced the high feedline pressures. The engines responded normally to the higher pressures.

#### Steady State Operation

Both engines operated normally throughout the 42.68 sec. time period as evidenced by the instrumented parameters. The averaged values for the instrumented parameters are listed in Table 15. Performance as calculated using data from the three engine firings are presented in Table 13.

The engine throat temperatures were also high for the second burn. The engine 4 temperature sensor was saturated at 588°F after 20 sec. of engine operation. Engine temperature profiles are depicted on Figures 72 and 73.

#### Engine Shutdown

The pressure profiles as depicted in Figure 74 were typical of a normal engine shutdown transient. The engine 4 valve was closed at  $FS_2 + 0.254$  sec and the engine 5 valve was closed at  $FS_2 + 0.251$  sec. Valve closing times are listed in Table 12.

#### Third Burn

##### Engine Start

The third burn was initiated after a 38 min, 21.45 sec. coast period. Both engines underwent a normal start transient as evidenced by the chamber pressure profiles shown on Figure 75. Valve functional times as listed in Table 12 are normal. Thrust overshoot above the steady state level was not excessive; both engines had approximately a 5% thrust overshoot.

TABLE 15  
TRANSTAGE MEASURED PERFORMANCE PARAMETERS  
(AVERAGED DATA)

BURNING TIME SEC. *****	SECOND BURN		PFL		TOL		TFL		ACCEL.		PC-4		PC-5	
	POL	PSIA	*****	PSIA	DEG. F	*****	DEG. F	*****	G	*****	PSIA	*****	PSIA	*****
307.611	165.2	157.4	157.4	71.2	74.5	.663	111.8	113.0						
312.61	162.6	155.2	155.2	65.6	69.3	.664	110.8	111.3						
317.61	160.1	152.5	152.5	64.8	68.7	.6645	109.0	109.6						
322.61	157.9	151.4	151.4	64.3	68.7	.667	107.9	108.1						
327.61	156.6	152.3	152.3	63.8	68.7	.672	107.5	107.8						
332.61	155.8	153.0	153.0	63.7	68.8	.678	107.1	107.5						
337.61	154.7	152.5	152.5	63.7	68.5	.684	106.6	106.9						
342.61	154.2	151.8	151.8	63.7	68.7	.690	106.0	106.3						
348.61	153.3	151.9	151.9	63.7	68.7	.697	105.6	105.7						
350.29	153.3	151.9	151.9	63.7	68.7	.699	105.6	105.7						*

SLV 9 FLT 3 NOV 1966

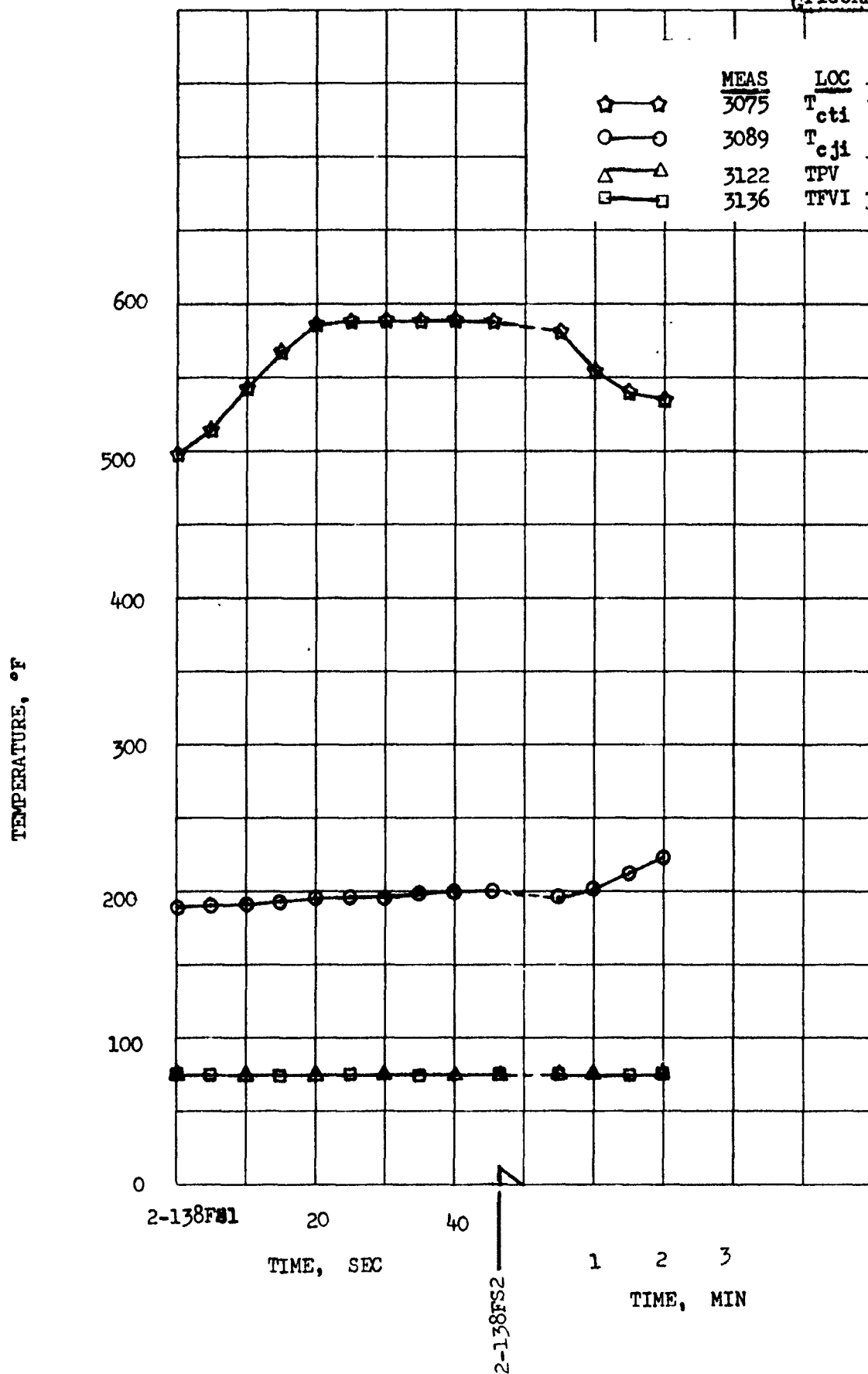
# ENGINE TEMPERATURES

ENG 4 S/N 3026

SECOND BURN

139

FIGURE 72



SLV 9 FLT 3 NOV 1966

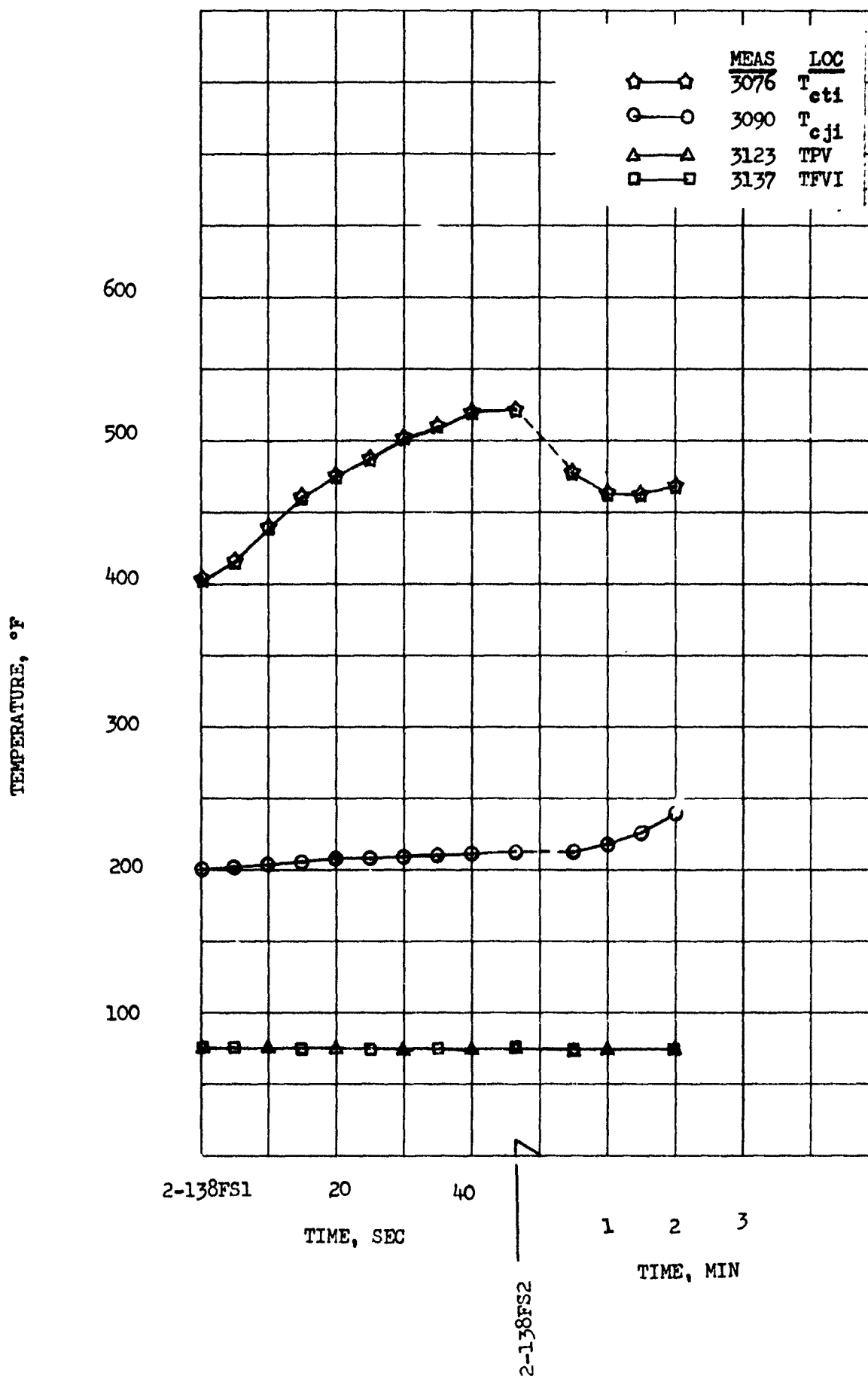
ENGINE TEMPERATURES

ENG. 5 S/N 3027

SECOND BURN

140

FIGURE 73



CHAMBER PRESSURE, PSIA

120

100

80

60

40

20

0

.05

.10

.15

.20

.25

.30

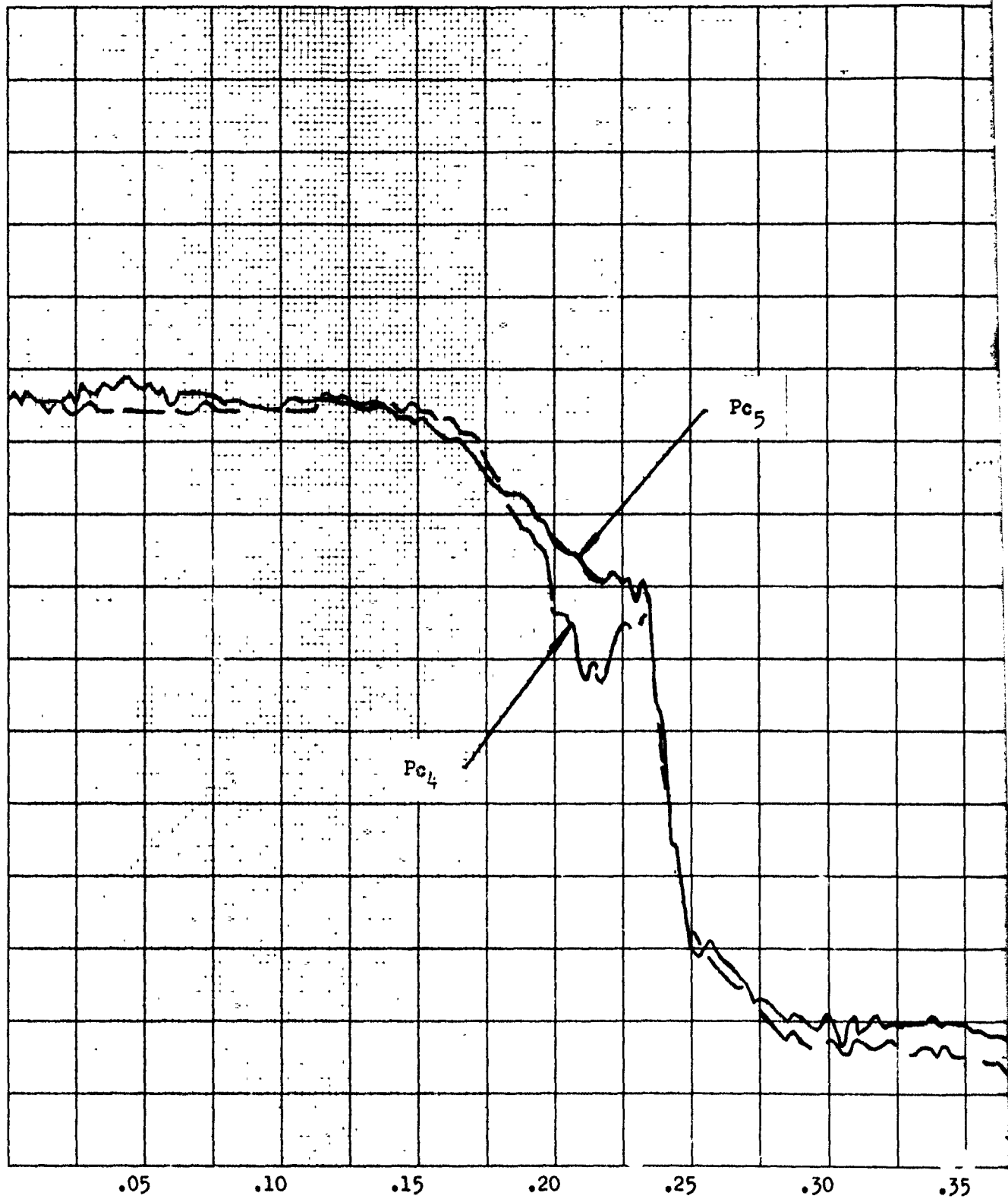
.35

Pc<sub>4</sub>

Pc<sub>5</sub>

2-138FS2

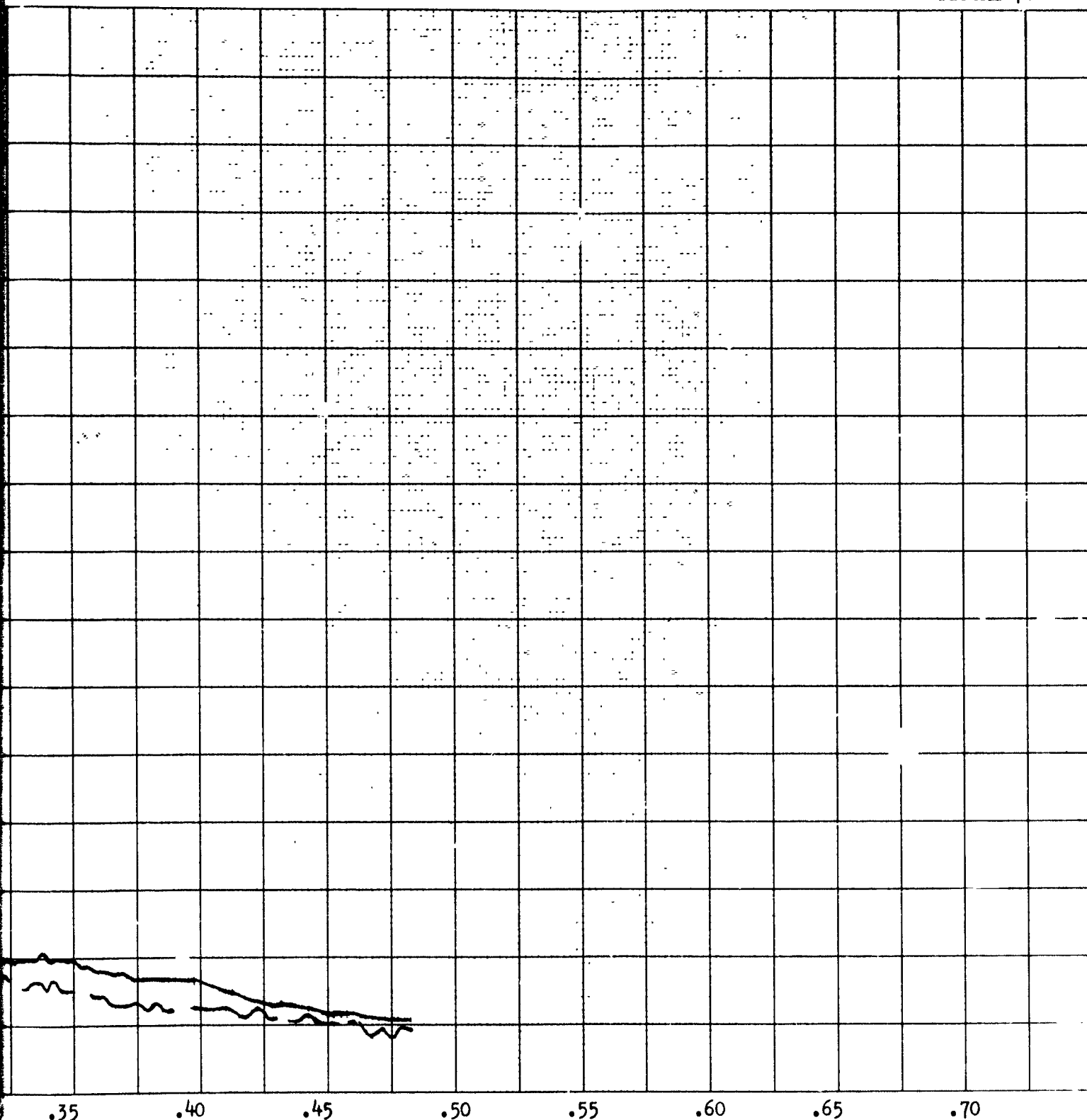
Flight Time, S



SLV 4  
3 November 1966  
SHUTDOWN TRANSIENTS  
SECOND BURN

141

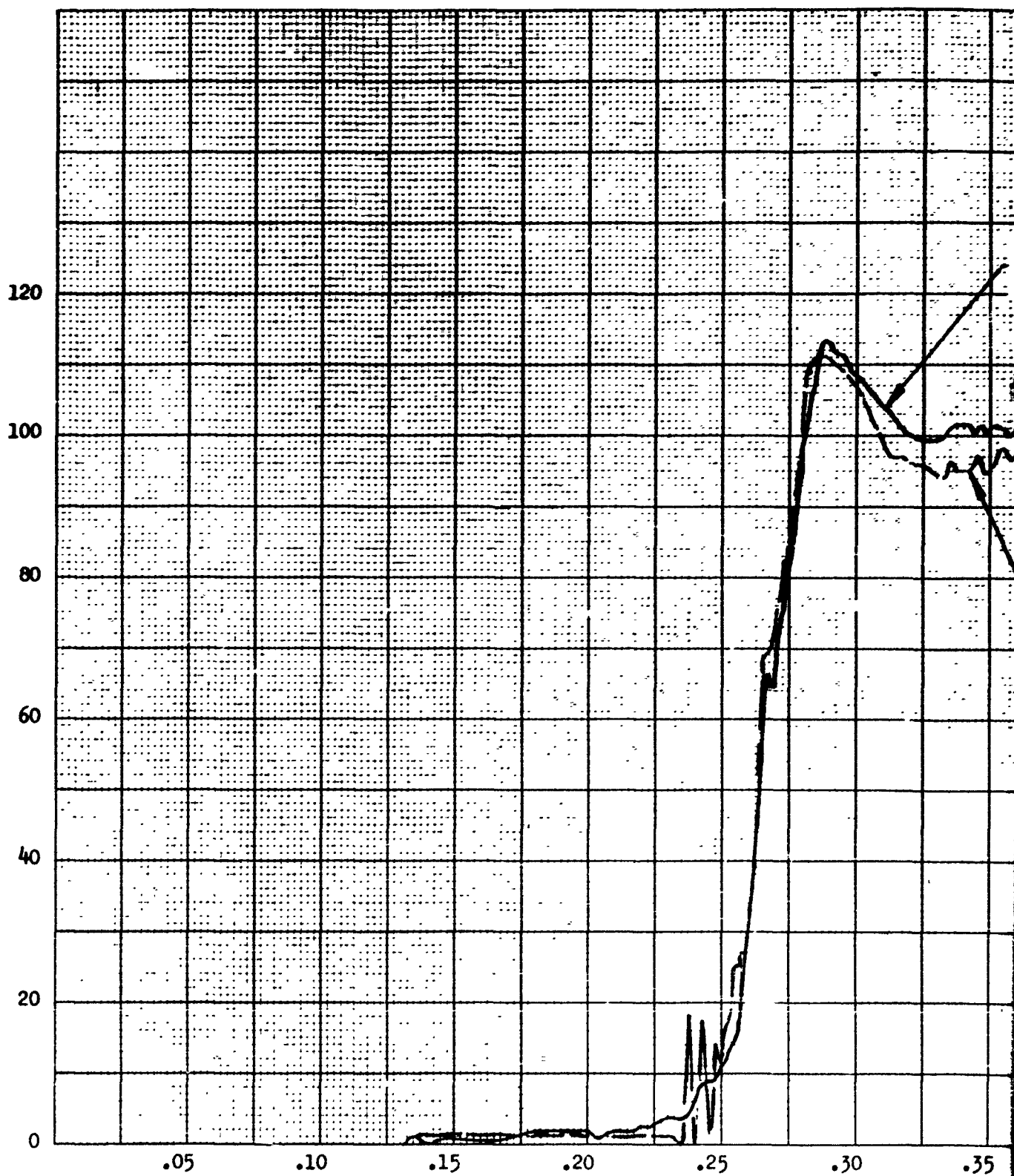
FIGURE 74



ight Time, Seconds

2

CHAMBER PRESSURE, PSIA



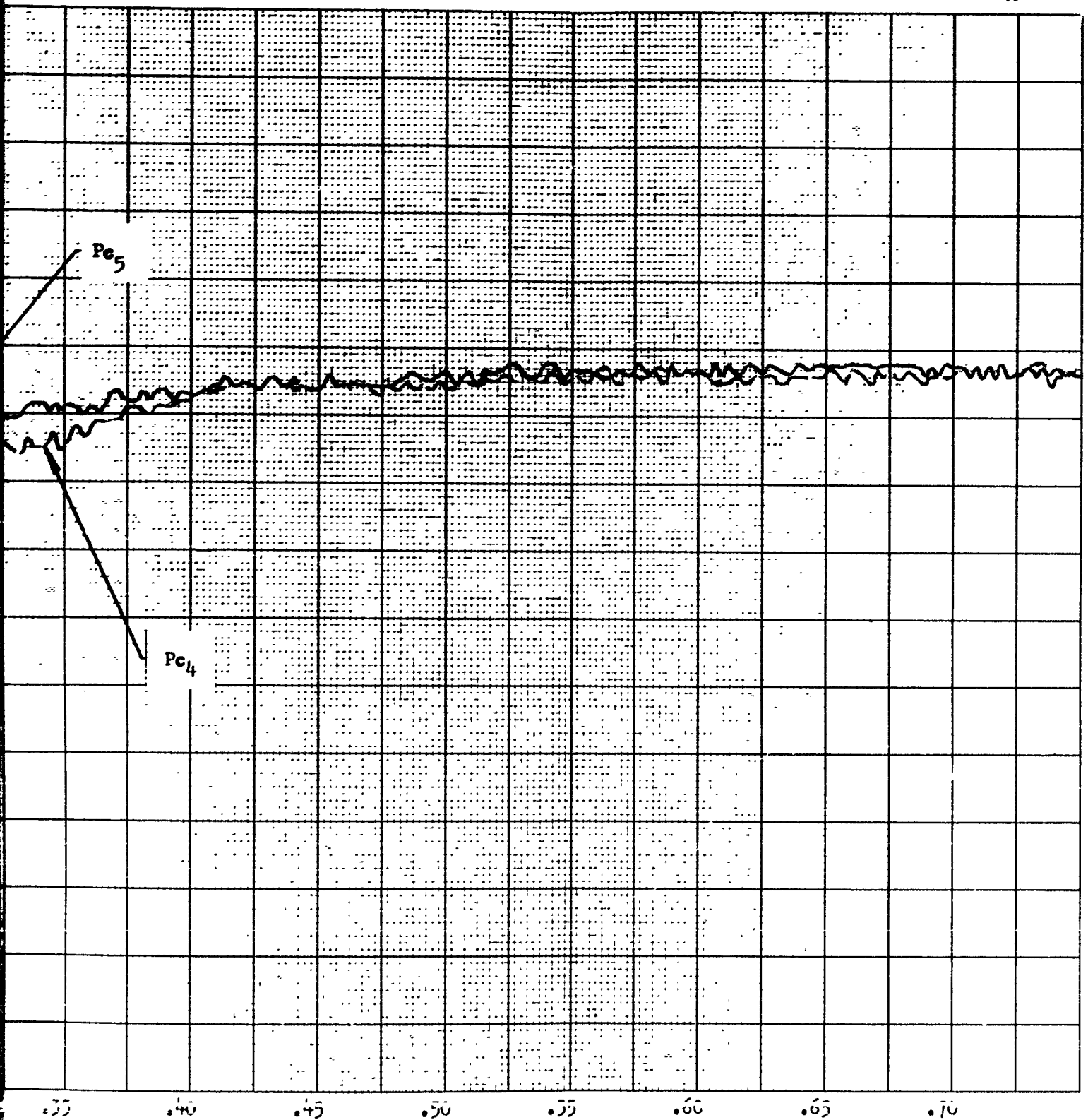
3-138FS1

Flight Time,

SLV 4  
3 November 1966  
START TRANSIENTS  
THIRD BURN

142

FIGURE 75



Time, Seconds

2



### 3.2.1.7.1 Engines - (Cont.)

#### Steady State

The engines operated normally throughout the 6.14 sec. burn period. The averaged data for the instrumented parameters are listed in Table 16. Engine performance is summarized in Table 13.

The engine temperatures for the third burn are shown in Figures 76 and 77. Both throat surface temperature sensors were saturated at 588°F throughout the engine firing cycle.

#### Engine Shutdown

The engine underwent a normal decay transient after receipt of the shutdown signal. Both engine valves closed normally. The engine combustion chamber pressure decays are depicted on Figure 78. Valve closing times are listed in Table 12.

#### Engine Performance Calculations

Propellant flow rates and engine performance were calculated from the following data: vehicle weight, outage sensor uncover times, guidance thrust acceleration, propellant temperatures, calibrated tank volumes and engine pressure parameters.

Thrust was calculated from the relationships  $F = ma$ , where  $m$  was determined by subtracting the integrated flow rate data from the initial vehicle weight. Specific impulse was calculated by dividing thrust by total engine flow rate. The initial (Table 13) values for the averaged integrated specific impulse, AISP, appear high during the first burn. The reason for the high AISP values is because of the sensitivity of the thrust calculation to changes in thrust acceleration. The value which is the most representative of the in-flight specific impulse is the last value tabulated under AISP since all of the thrust acceleration data are used.

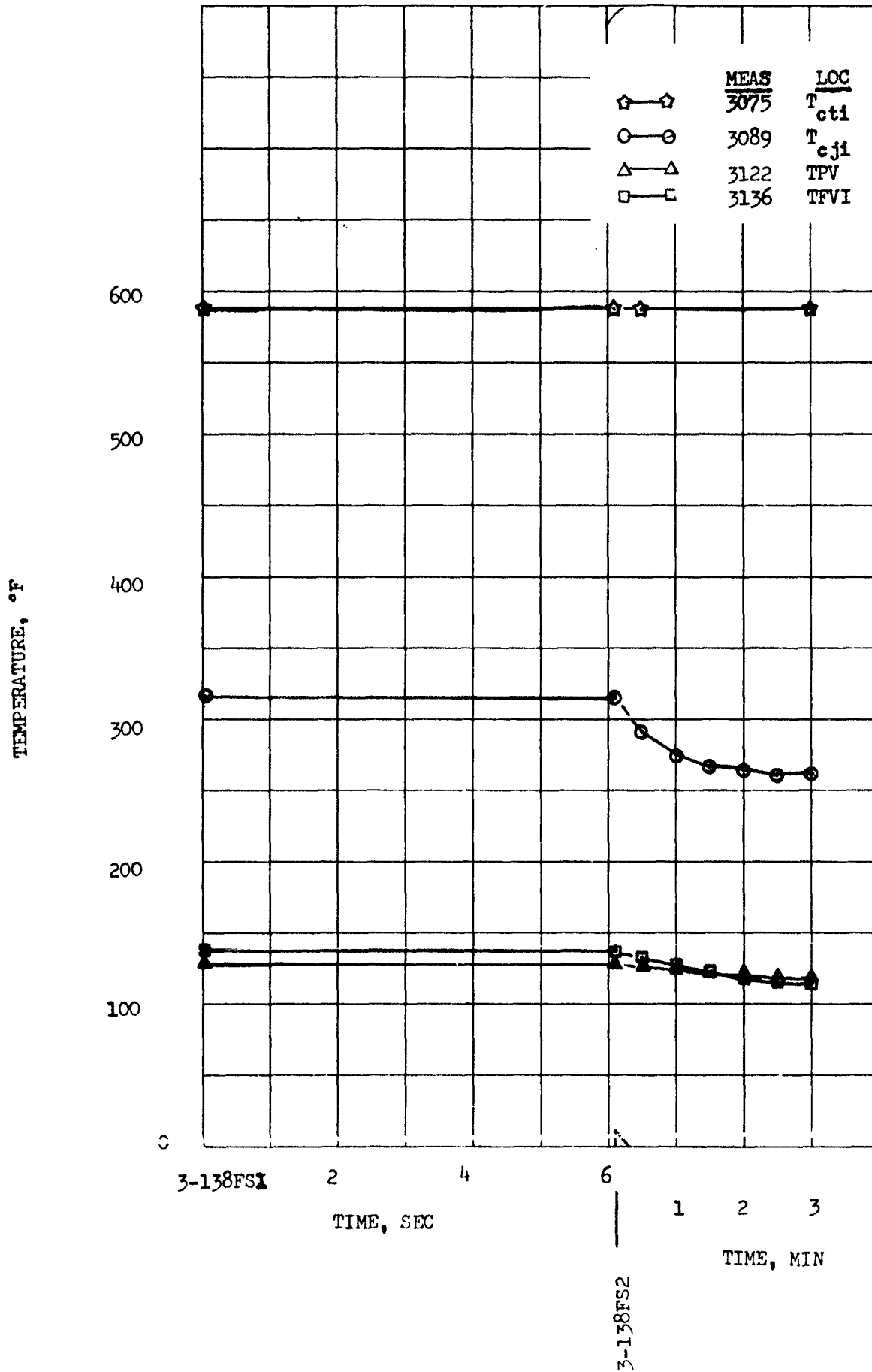
TABLE 16  
TRANSISTOR MEASURED PERFORMANCE PARAMETERS  
(AVERAGED DATA)

THIRD BURNING TIME SEC. *****	THIRD TURN	TRANSISTOR MEASURED PERFORMANCE PARAMETERS (AVERAGED DATA)									
		PUL	PFL	TOL	TFL	ACCEL.	PC-4	PC-5	PSIA	PSIA	
		PSIA *****	PSIA *****	DEG. F *****	DEG. F *****	G *****	PSIA *****	PSIA *****			
350.291		53.8	156.2	72.2	78.9	.6991	109.7	108.9			
351.29		53.8	156.2	72.2	78.9	.701	109.7	108.9			
352.29		53.3	155.6	67.7	75.6	.702	111.1	110.6			
353.29		53.0	155.2	66.2	72.9	.704	110.3	110.1			
354.29		52.4	154.6	65.5	72.3	.706	109.4	108.8			
355.29		52.1	154.0	64.9	71.9	.7075	109.0	108.2			
355.44		51.8	153.5	64.9	71.7	.708	108.3	108.0			
356.43		51.8	153.5	64.9	71.7	.709	108.3	108.0		*	

SLV 9 FLT 3 NOV 1966  
 ENGINE TEMPERATURES  
 ENG 4 S/N 3026  
 THIRD BURN

145

FIGURE 76



SLV 9 FLT

3 NOV 1966

ENGINE

TEMPERATURES

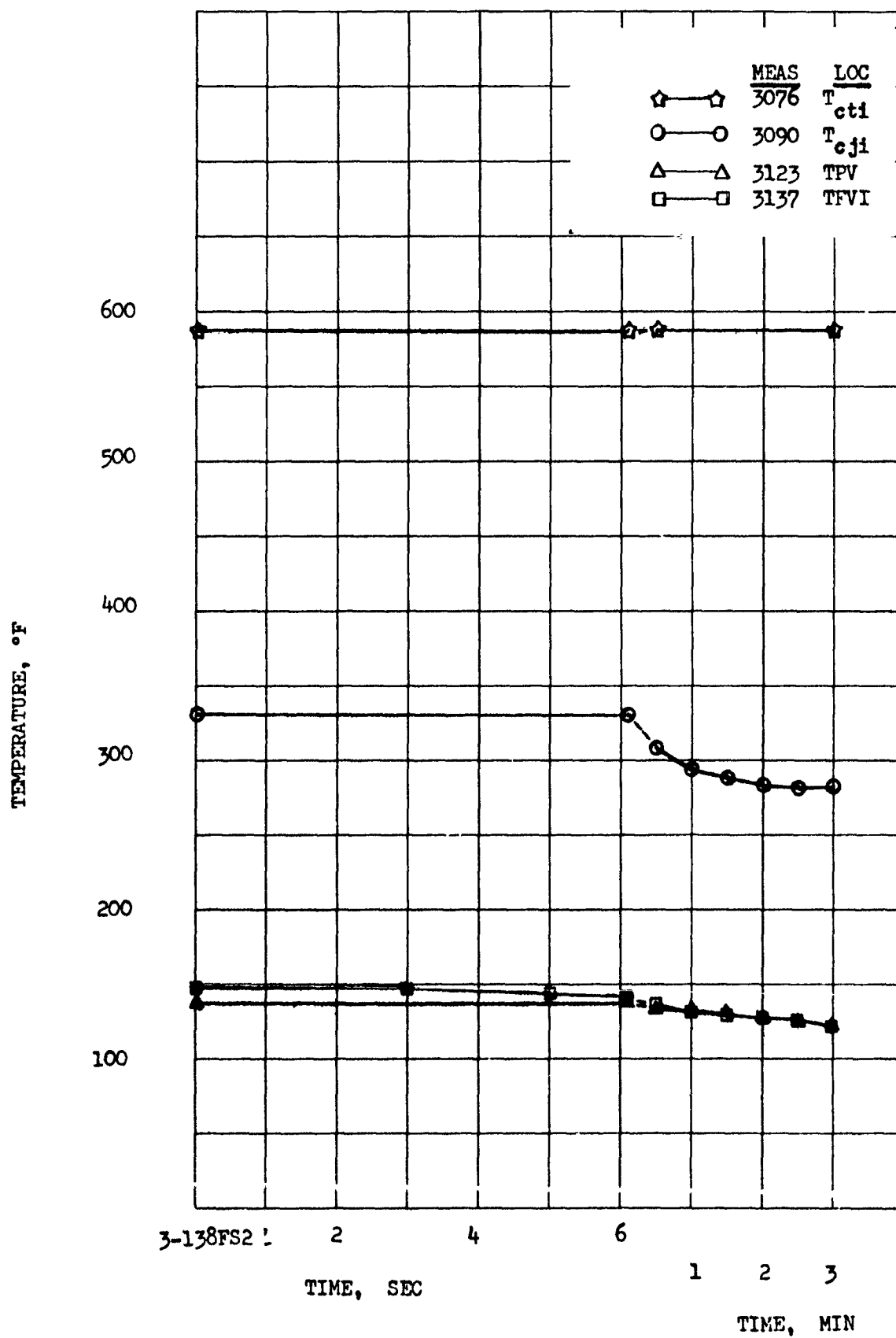
146

ENG 5

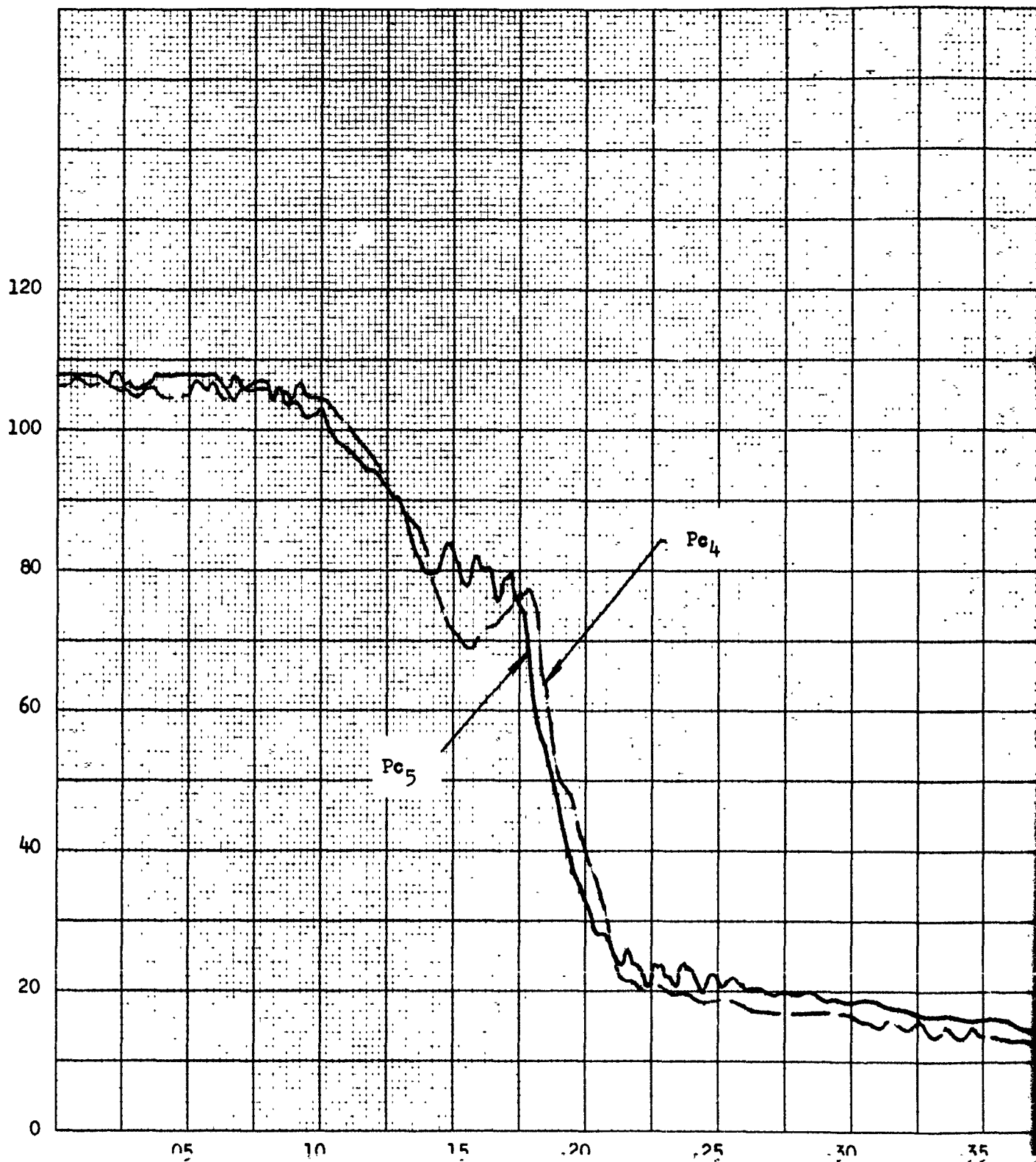
S/N 3027

THIRD BURN

FIGURE 77



CHAMBER PRESSURE, PSIA



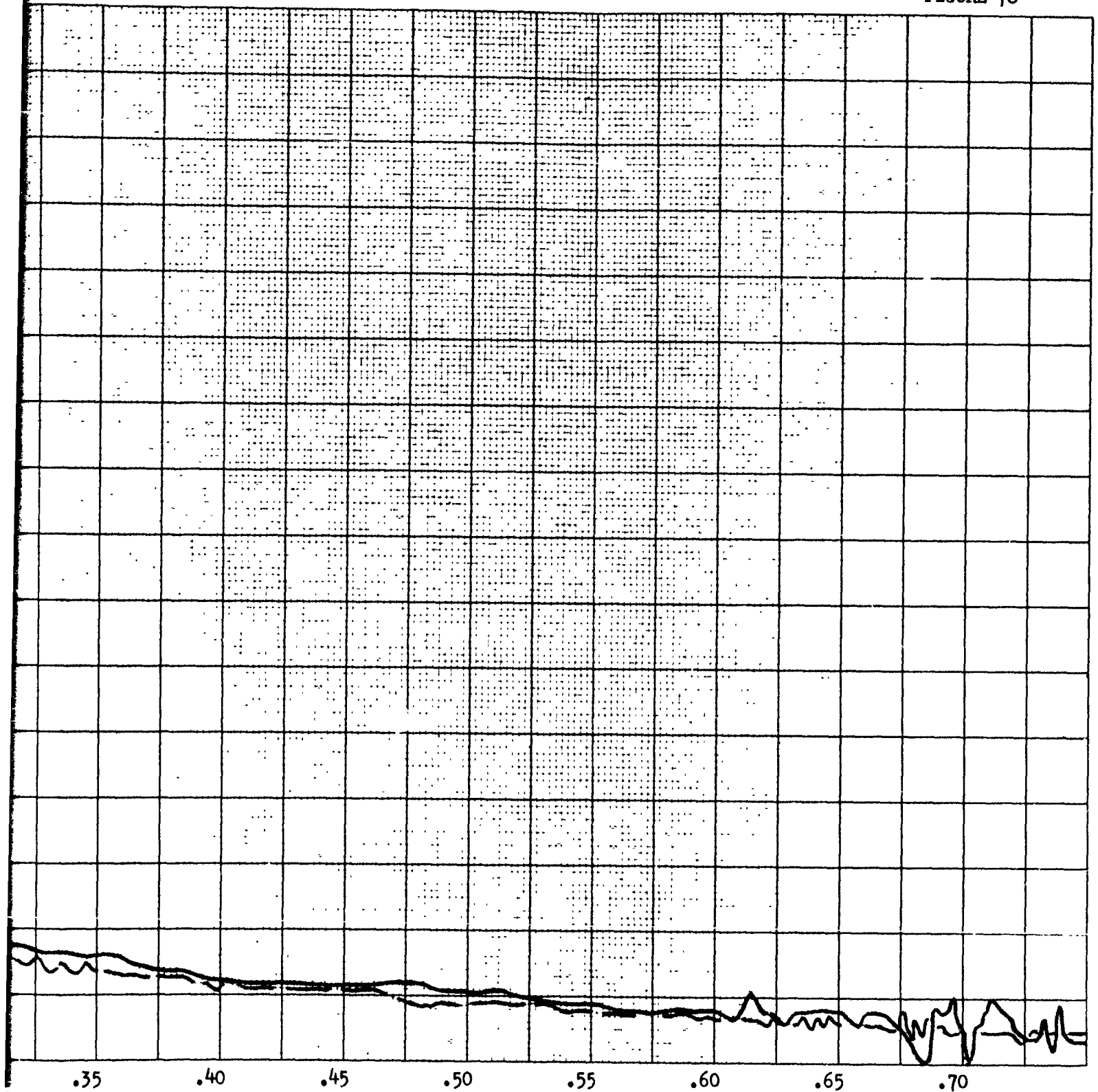
3-138FS2

Flight Time

SLV 4  
3 November 1966  
SHUTDOWN TRANSIENTS  
THIRD BURN

147

FIGURE 78



Flight Time, Seconds

2

### 3.2.1.7.1 Engines - (Cont.)

The average calculated specific impulse was 303.4 sec as compared to the predicted specific impulse of 302 sec over the same time period. The average calculated thrust over the three engine firings was 16,322 lbs as compared to a predicted thrust of 16,084 over a comensurate time period.

Mixture ratio was calculated by using the outage level sensor data. The outage sensor uncover times were considered to be the average of the first and last uncover indications. The resulting in-flight mixture ratio for the three burns was 1.94 which was lower than the predicted value. The reason for the lower than predicted mixture ratio has been attributed to the preflight pressurization system prediction as explained in detail under the Pressurization section of this report.

Propellant outage and burning time margin were calculated by projecting the engine performance past the third burn. Burning time margin was calculated to be 33.7 sec. in conjunction with an oxidizer outage of 34 lbs.

### 3.2.1.7.2 Pressurization

#### System Configuration

The pressurization system configuration was identical to that flown on Articles 8, 11 and 12. The pressure balance orifice was located in the oxidizer tank pressurant line so that fuel tank pressure would be maintained above the oxidizer tank pressure.

#### Preflight Operation

Pressurization system functional tests were run at both the Denver Y-lot facility and at ETR. The functional tests consisted of pre-pressurizing the tanks to a pressure 2 to 4 psi below check-out pressure and activating the system through the check-out pressure switch, thereby allowing the system to bring the tanks to check-out pressure (90+4 psia). The Y-lot functional tests were performed satisfactorily with the check-out pressure switch controlling the tanks at 90.3 to 90.8 psia. During the functional test at ETR, solenoid valve currents and accumulator pressures were monitored. The data showed that system operation was normal. Three of the four transtage pressurization system check valves were rejected. Two of the four check valves were rejected on MARS B4152 during Y-lot tests due to suspected contamination. Of the remaining two original valves, one was rejected at the Cape due to excessive internal leakage during the back flow leakage checks.

As on Articles 11 and 12, Stage III tank pressure histories were monitored during countdown and compared to specified allowable decay rates to determine if leaks were present. All decay rate data showed rates within the allowable range, indicating no leakage.

The indicated tank pressures at lift-off were 85.3 psia and 89.5 psia for the oxidizer and fuel tanks, respectively.

#### Flight Operations

The pressurization system performed satisfactorily during all portions of the flight.



### 3.2.1.7.2 Pressurization - (Cont.)

#### L/O to 91 FS<sub>1</sub>

Tank pressures experienced a normal decay during Stage 0 and I operation. The reason for pressure decay is due to an increase in the ullage volume caused by tank stretch as vehicle acceleration builds up. At 91FS<sub>1</sub> the pressures were 85.3 psia and 88.5 psia for oxidizer and fuel, respectively. This pressure decay was less than that seen on Article 8 and 11, due to the larger ullage on this flight. The tank stretch produced a smaller percentage change in ullage which resulted in a smaller decay in tank gas pressure.

#### 91 FS<sub>1</sub> to 138 FS<sub>1</sub> (1)

Tank pressure histories are shown in Figure 79. The oxidizer and fuel tanks were brought to flight pressures of 158.2 and 161.3 psia in 19.0 and 18.6 seconds, respectively. This is nearly twice the time that was required on Articles 8 and 11. The reason for this increase was the greater ullage volume on this flight. The predicted pressurization time was 15 seconds. This resulted in the slightly increased helium usage reflected in the sphere pressure history presented in Figure 79. The slight increase in both pressures during the remainder of the Stage II burn was the result of the bleed orifice flow periodically bringing the accumulator pressure down to the pressure switch make point. The pressure increase at 91FS<sub>2</sub> was the result of the sudden loss of acceleration from 1.9 g's to near zero g causing the propellant tanks to contract and the ullage to decrease.

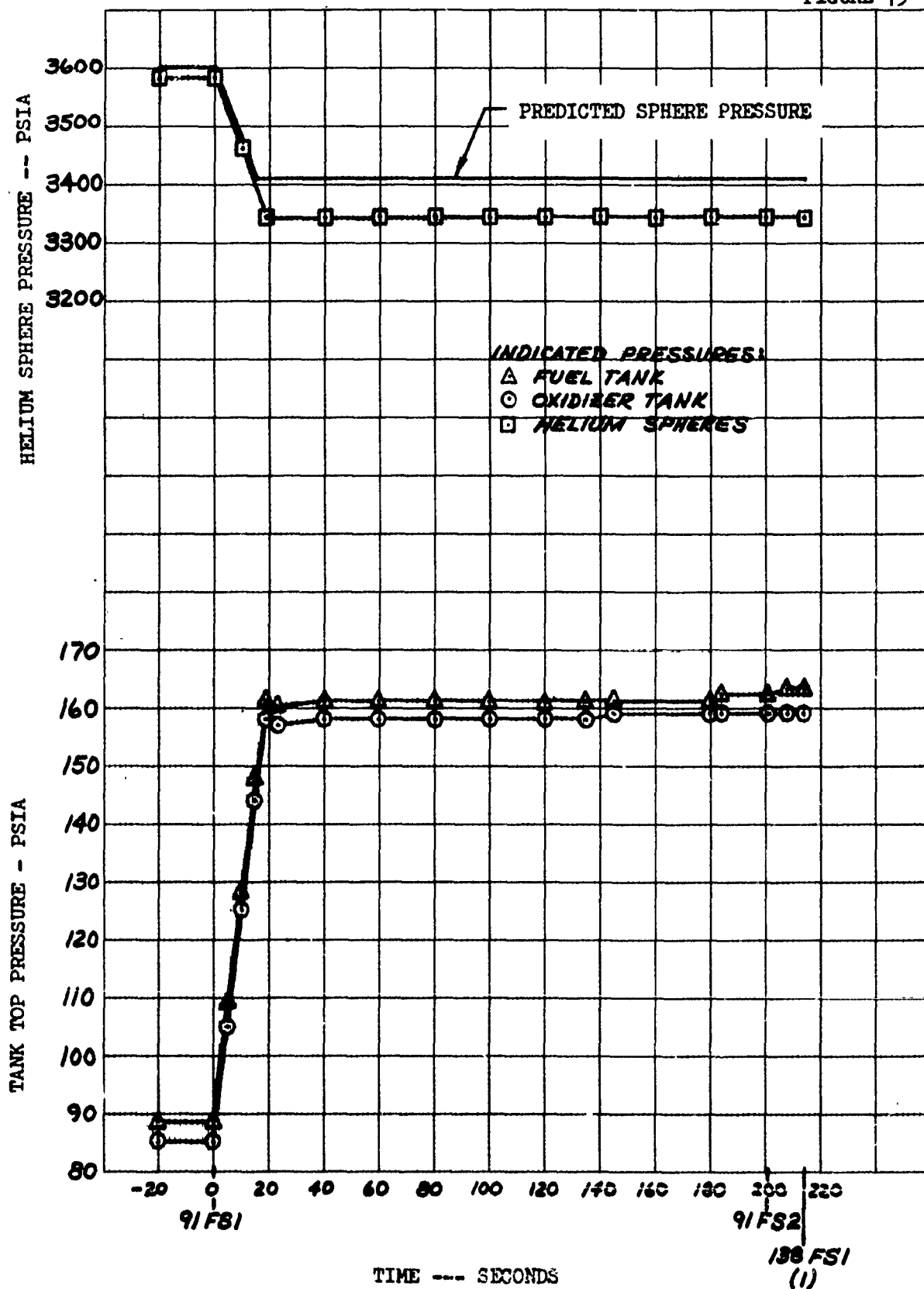
#### First Burn

Propellant tank pressure histories during all Stage III burns and coast periods are shown in Figure 80. Actual and predicted oxidizer tank gas pressure agree quite well during the first burn; whereas, indicated and predicted fuel tank gas pressure do not agree. This indicated difference varies from about 2.5 to 1.5 psi at first burn shutdown and is a result of the following factors: (1) fuel tank gas pressure is indicating approximately one psi high; (2) check valves were replaced in the pressurization system; and (3) inaccuracy in predicting fuel tank pressure.

ARTICLE 9 STAGE III  
TANK GAS PRESSURE HISTORY

151

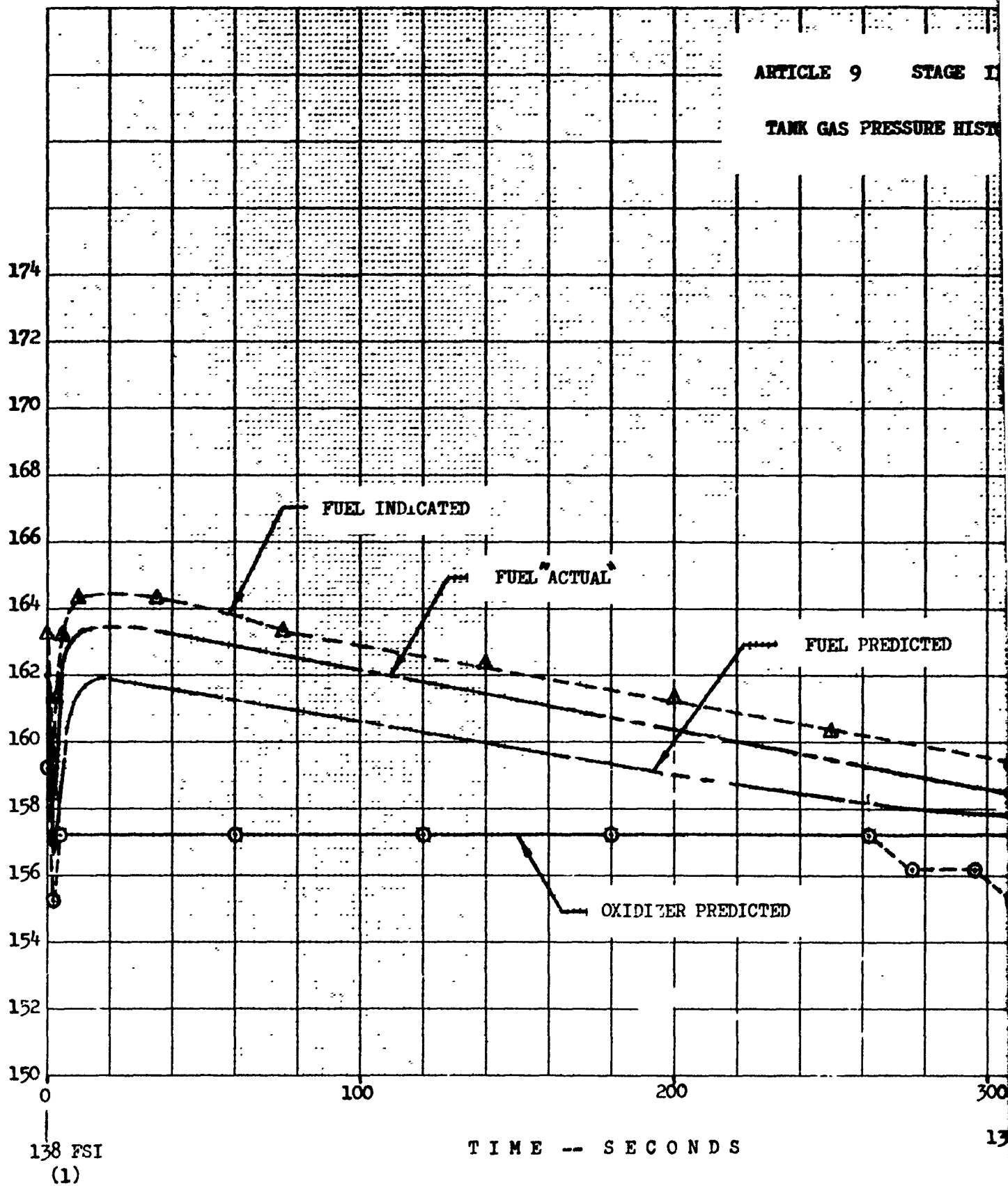
FIGURE 79



ARTICLE 9 STAGE I

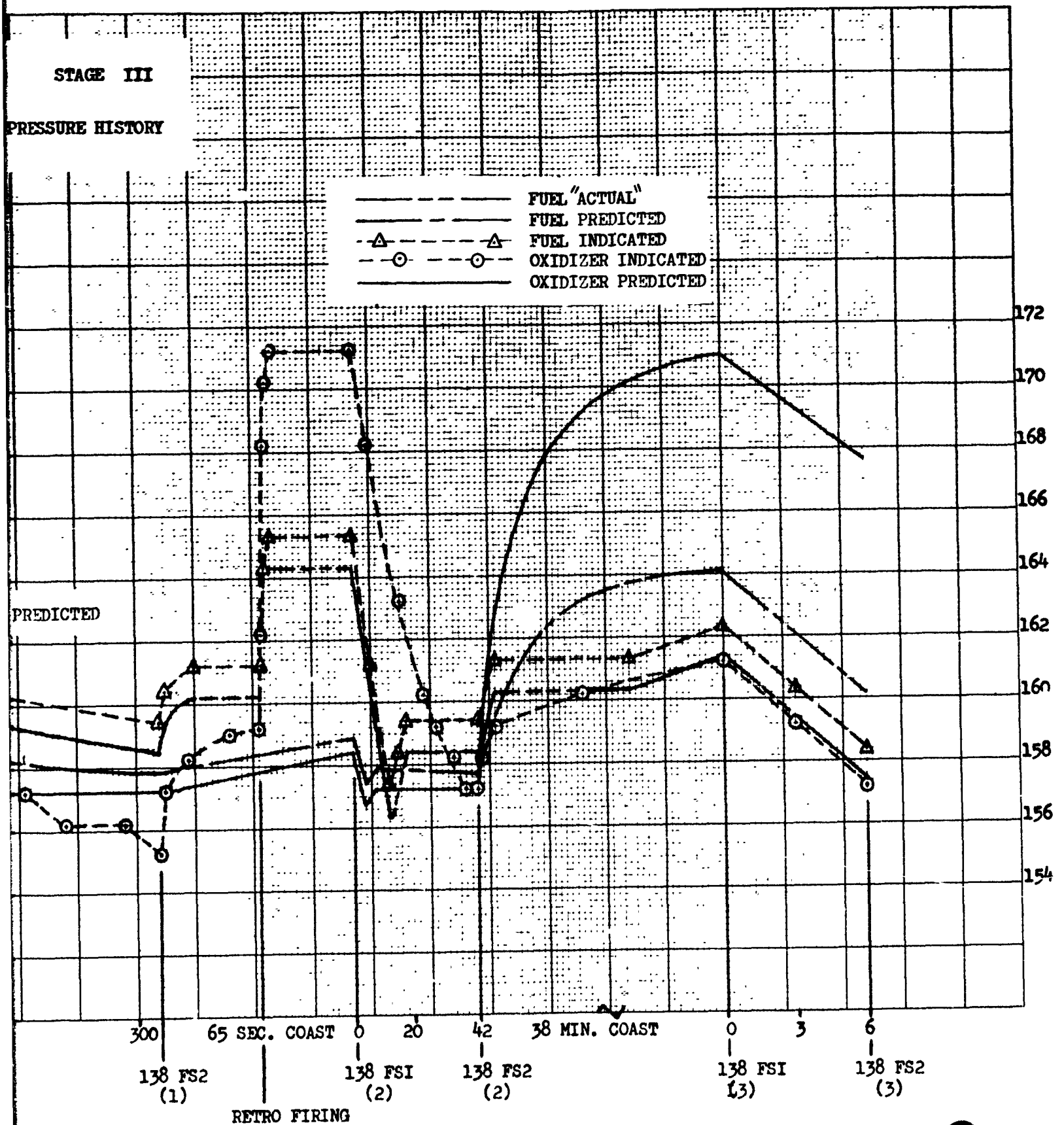
TANK GAS PRESSURE HIST

PRESSURE -- PSIA



TIME -- SECONDS

FIGURE 80



2

3.2.1.7.2 Pressurization - (Cont.)

It was concluded from the following data that the fuel tank gas pressure transducer was indicating 1 psi high:

- (1) During the first burn when the oxidizer tank was controlling the system, oxidizer tank gas pressure ran below pressure switch make pressure by an amount equal to check valve cracking pressure. During the second burn when the fuel tank was controlling the system, fuel tank pressure was 1 psi higher than cracking pressure indicated it should have been.
- (2) A comparison of fuel suction and tank pressure during the coast just before second burn indicates that fuel tank gas pressure was indicating one psi high.
- (3) A reconstructed fuel tank gas pressure from fuel suction pressure during the second burn indicated again the fuel pressure was reading one psi high.
- (4) The calculated mixture ratio shift indicates that actual fuel tank gas pressure is approximately 1.6 psi above predicted and not 2.5 psi (See mixture ratio discussion in the Propellents section).
- (5) Fuel tank gas pressure at 300 seconds is 1 psi higher than any data seen to date, including all flight and Cold Flow Lab battleship test data.

Consequently, it appears from the above discussion, that the fuel tank gas pressure transducer was indeed indicating approximately 1 psi higher than actual. When considering the high reading transducer, it appears that actual fuel tank pressure varied 1.6 to 1 psi above the preflight prediction. Approximately  $\frac{1}{2}$  psi of this difference can be attributed to the fact that two of the pressurization system check valves were repaired without input to the prediction. If a revised prediction had been made with the new check valves, the error would have been nearer 1 psi which is within the accuracy of the prediction method.

### 3.2.1.7.2 Pressurization - (Cont.)

#### First Coast

Actual and predicted tank gas pressures during the first coast do not agree. This large difference is a result of the propellant tank ullage reaching complete saturation and near thermal equilibrium in approximately five seconds; whereas, in the past, this phenomenon has required 45 to 60 minutes. This very rapid equilibrium process was caused by the solid retro rockets, which backed the transtage away from the Gemini spacecraft. This agitation of the propellant was not considered in the predictions and as a result, the actual and predicted values differ.

#### Second Burn

Because of the incorrectly predicted tank pressures during the first coast, propellant tank gas pressures during the second burn do not agree with predicted operation. However, performance during the second burn appears normal considering the high pressures obtained during the first coast.

#### Second Coast

As seen in Figure 80, the large pressure rise was expected to occur during the second coast, rather than the first. Consequently, the small pressure rise expected during first coast occurred during the second coast. The data obtained looks normal and as expected considering the effects of the first coast period.

#### Third Burn

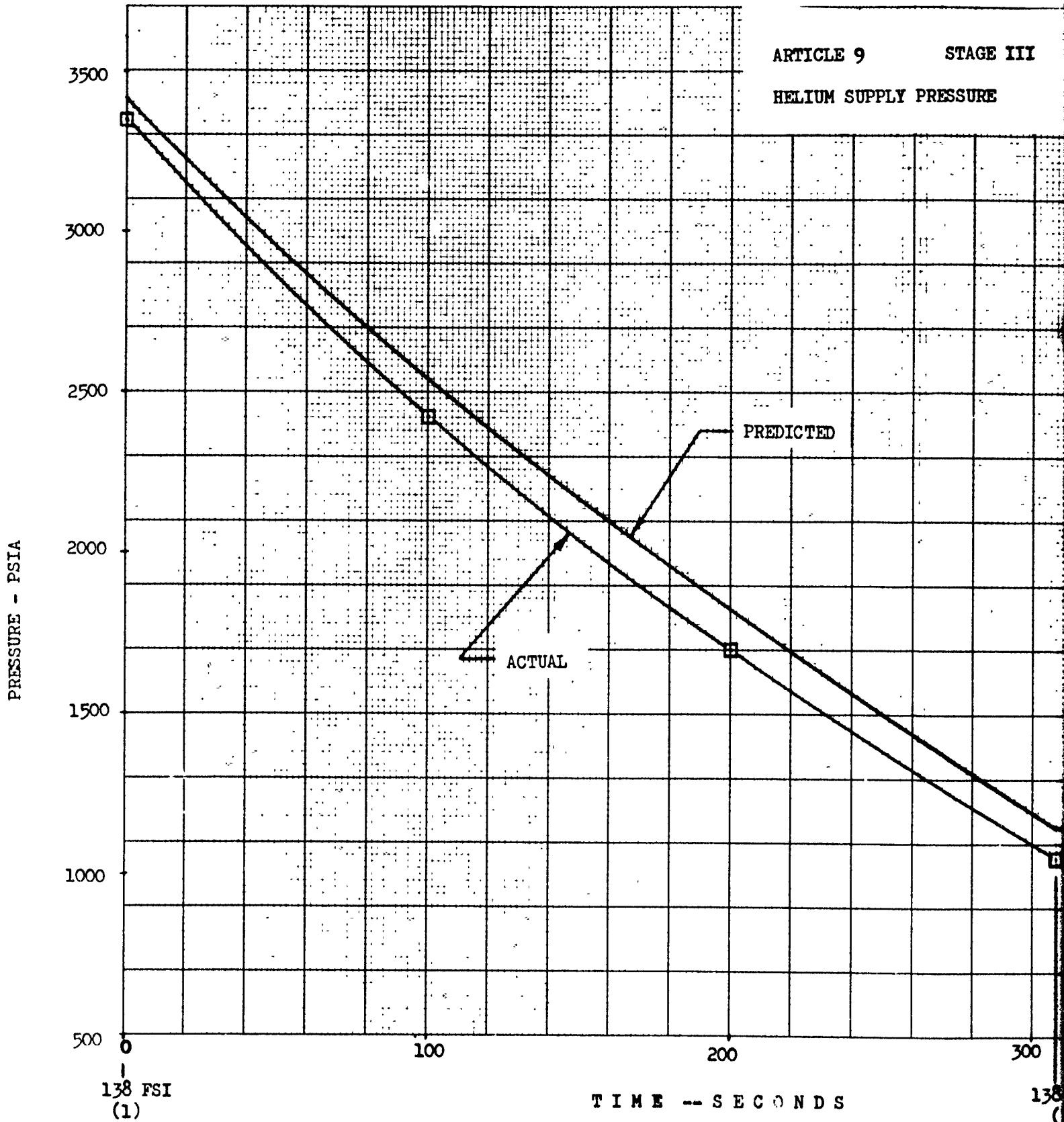
The propellant tank pressure decay after ignition match predicted rates quite closely. However, the start pressures are in error because of the large pressure rise during the first coast period.

### 3.2.1.7.3 Propellants

#### Configuration

Article C9 was the last vehicle which did not incorporate the tank midpoint sensors. Two outage sensors were installed in the lower portion of each tank. These sensors were predicted to uncover during the second burn.

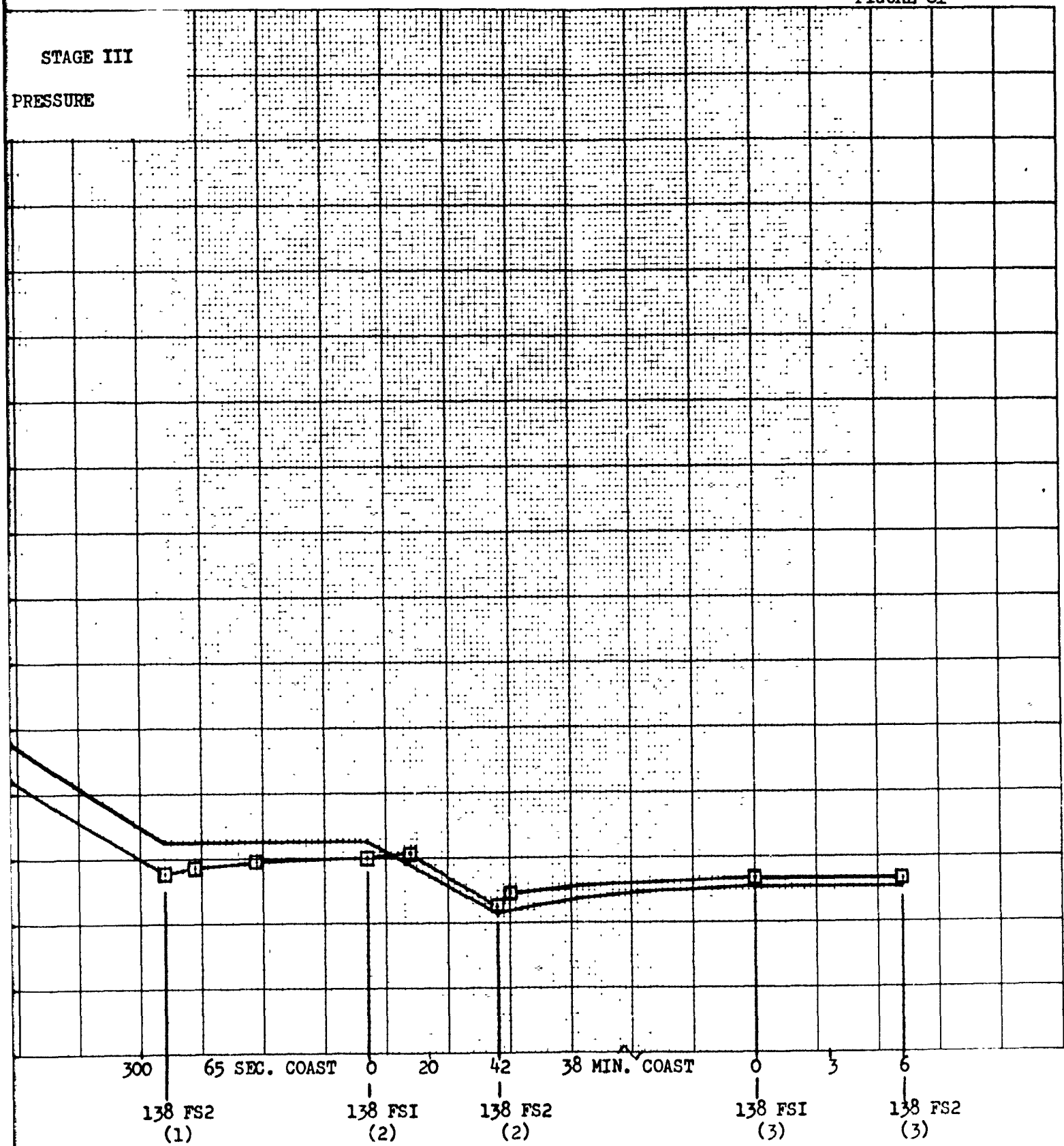
ARTICLE 9      STAGE III  
HELIUM SUPPLY PRESSURE



138 FSI  
(1)

138  
(1)

FIGURE 81



2



### 3.2.1.7.3 Propellants - (Cont.)

#### Level Sensor Performance

The outage sensors uncovered with more slosh activity than has been noted on previous flights (See Figure 82). The fuel sensors (measurement numbers 1901 and 1919) uncovered approximately 10 seconds into the second burn with no additional activity during the third burn (except for a one data bit cover on sensor 1901 during the third burn start transient). The slosh activity existed for a 16.5 sec. duration which is approximately twice as long as has been recorded on recent flights. The excessive slosh activity was apparently caused by the lower acceleration and greater control activity resulting from the MOL Sim/Lab payload.

The oxidizer sensors (measurement numbers 1903 and 1918) indicated uncovering near the end of second burn and the start of third burn. Evaluation of the slosh activity indicated apparent uncover to have occurred approximately 41 seconds into the second burn. The slosh activity existed for approximately 9.5 seconds during the second burn and 5 seconds during the third burn. This cumulative slosh activity of approximately 14.5 seconds is four times longer than noted on previous flights. The MOL Sim/Lab. effects, plus the third burn start transient, are the apparent reasons for the excessive slosh.

Investigation into the erratic uncover on each sensor indicates that slosh, not sensor malfunction, caused the lengthy uncover duration. Examination of the data indicates a slosh period of approximately 0.75 sec/cycle in the fuel tank and 1.4 sec/cycle in the oxidizer tank. The resulting mean uncover time for the fuel tank was determined to occur approximately 11.7 sec into the second burn. However, determination of the mean uncover time for the oxidizer tank was complicated by the fact that sensor uncover was in the regime of 2-138 FS<sub>2</sub> and 3-138FS<sub>1</sub>. Consequently, resolution of the data indicates mean uncover time to occur approximately 41.1 seconds into the second burn.

#### Flight Load Analysis

Table 17 summarizes the propellant loading data for Stage III. The actual flow meter loads compared favorably with the requested loads, less than 0.1% for each tank.

FIGURE 82

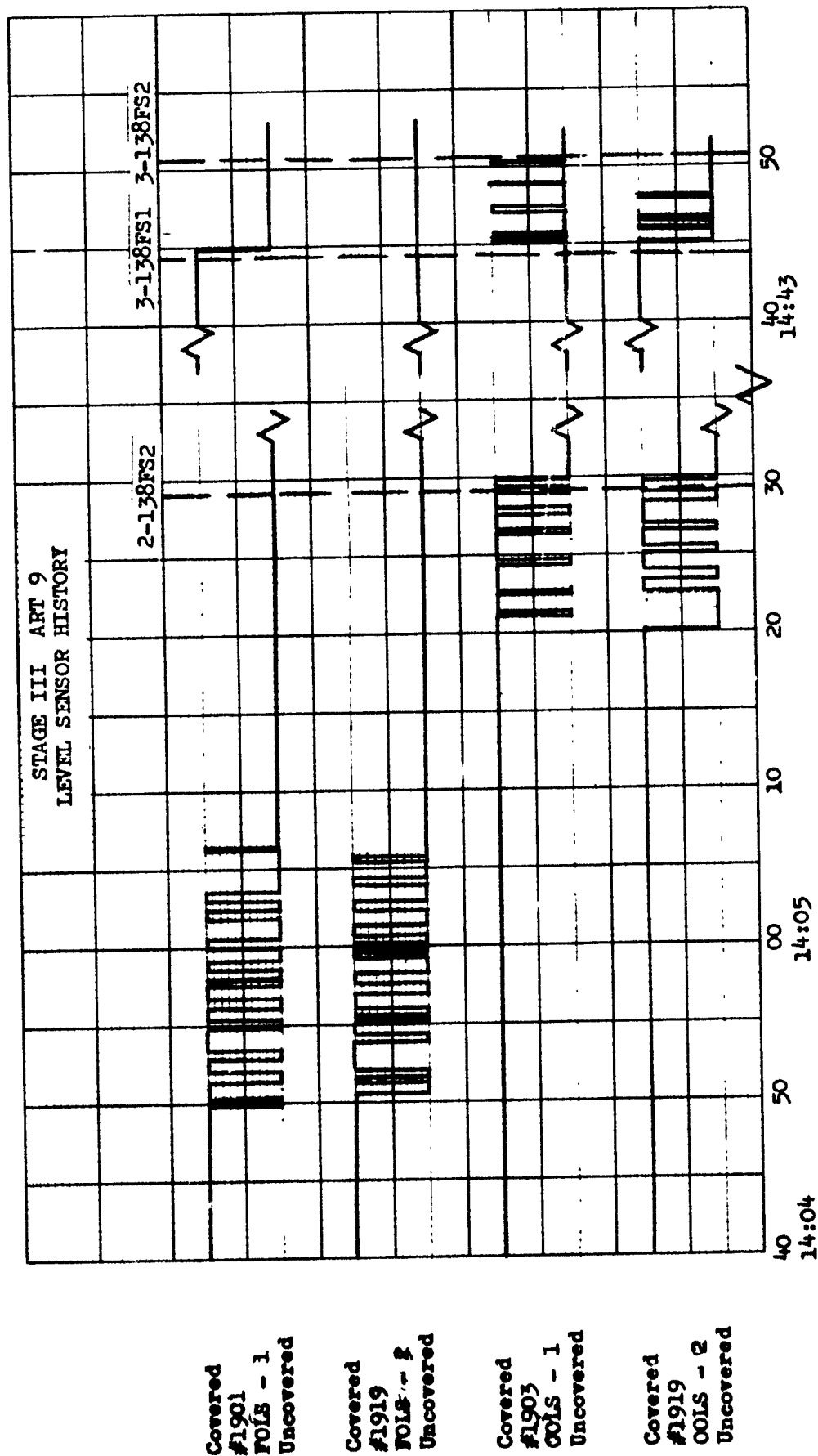


TABLE 17  
 STAGE III  
 VEHICLE NO. C-9

PROPELLANT LOADS

	REQUESTED		FLOW METER, GALLONS				LEVEL SENSOR POST FLIGHT			
	LBS	60° GALLONS	NO. 1	NO. 2	AVERAGE		ERROR		LB	% OF FLOWMETER LOAD
					GAL	LB	LB	% OF REQUESTED		
Oxidizer	13957	1149.5	1150.66	1150.37	1150.52	13969	+12	0.086	NA	NA
Fuel	7113	939.3	940.10	940.55	940.32	7121	+ 8	0.085	NA	NA

LEVEL SENSOR FLOW METER CHECK, PREFLIGHT

	MAXIMUM ALLOWABLE GAL	NO. 1 METER READING GAL	NO. 2 METER READING GAL	MINIMUM ALLOWABLE GAL
Oxidizer	145.42	131	131	130.65
Fuel	176.80	170	170	166.45

OUTAGE

	Tank	LB	% Of Usable
Maximum Allowable		333	1.58
Measured, Level Sensors	Ox	135	.641

MIXTURED RATIO BURNED

Predicted Steady State	1.974
Measured, Level Sensors	1.941

### 3.2.1.7.3 Propellants - (Cont.)

#### Mixture Ratio and Outage Analysis

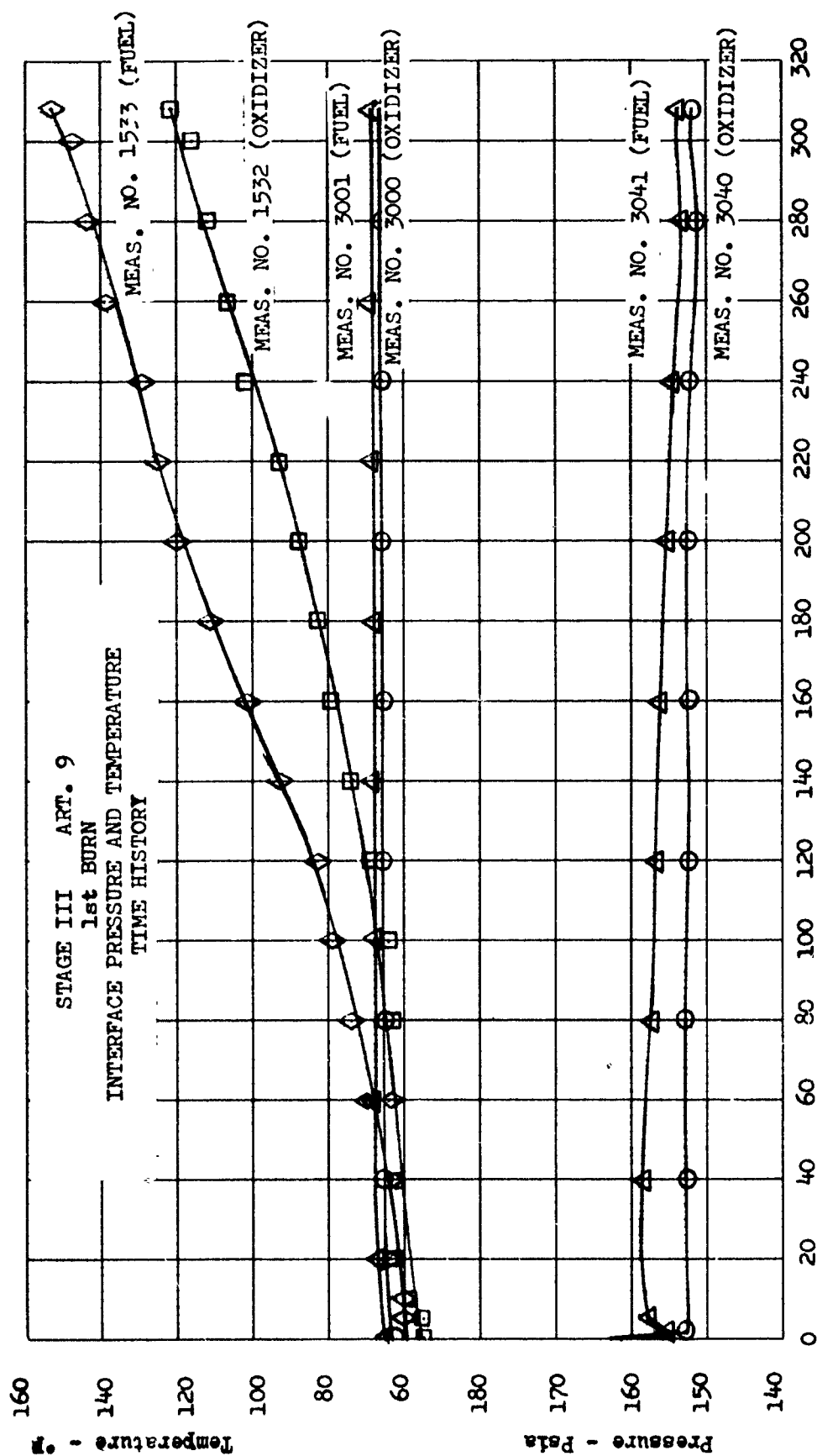
Because of the erratic sensor activity and the apparent error in predicted fuel tank pressures, a detailed analysis was conducted on outage and mixture ratio. The results of this analysis indicated that the in-flight mixture ratio was 1.941 with a resulting outage of 135 lb. of oxidizer. Comparison of the in-flight mixture ratio of 1.941 with the preflight predicted value of 1.974 results in an error of -1.67%, which is analytically consistent with the outage. Investigation into the individual tank flow rates indicates the oxidizer outflow rate to have been essentially as predicted (35.53 lb/sec actual vs. 35.26 lb/sec predicted) but a significant increase was noted in the fuel flow rate (18.30 lb/sec actual vs. 17.86 lb/sec predicted). These results support the suspected low fuel tank pressure prediction.

In order to quantitatively estimate the increase in fuel tank pressure suggested by the flight data, the predicted flows were evaluated only during the actual burn operation (original predictions are necessarily calculated to propellant exhaustion for outage optimization). The resulting modified predicted values were: MR = 1.974; oxidizer flow rate = 35.43 lb/sec; and fuel flow rate = 17.95 lb/sec. The mixture ratio variation can be seen to result primarily from the fuel flow rate variation. A fuel tank top pressure 1.6 to 1.7 psi greater than predicted would produce the noted fuel flow rate variation. This supports, within data accuracy, the corrected fuel tank top pressure error of +1.5 psi as outlined under the Stage III Pressurization section of this report.

It can be therefore concluded that the computed outage of 135 pounds of oxidizer is consistent with the computed mixture ratio and flow rates and occurs because of a 1.5 psi low fuel tank gas pressure prediction.

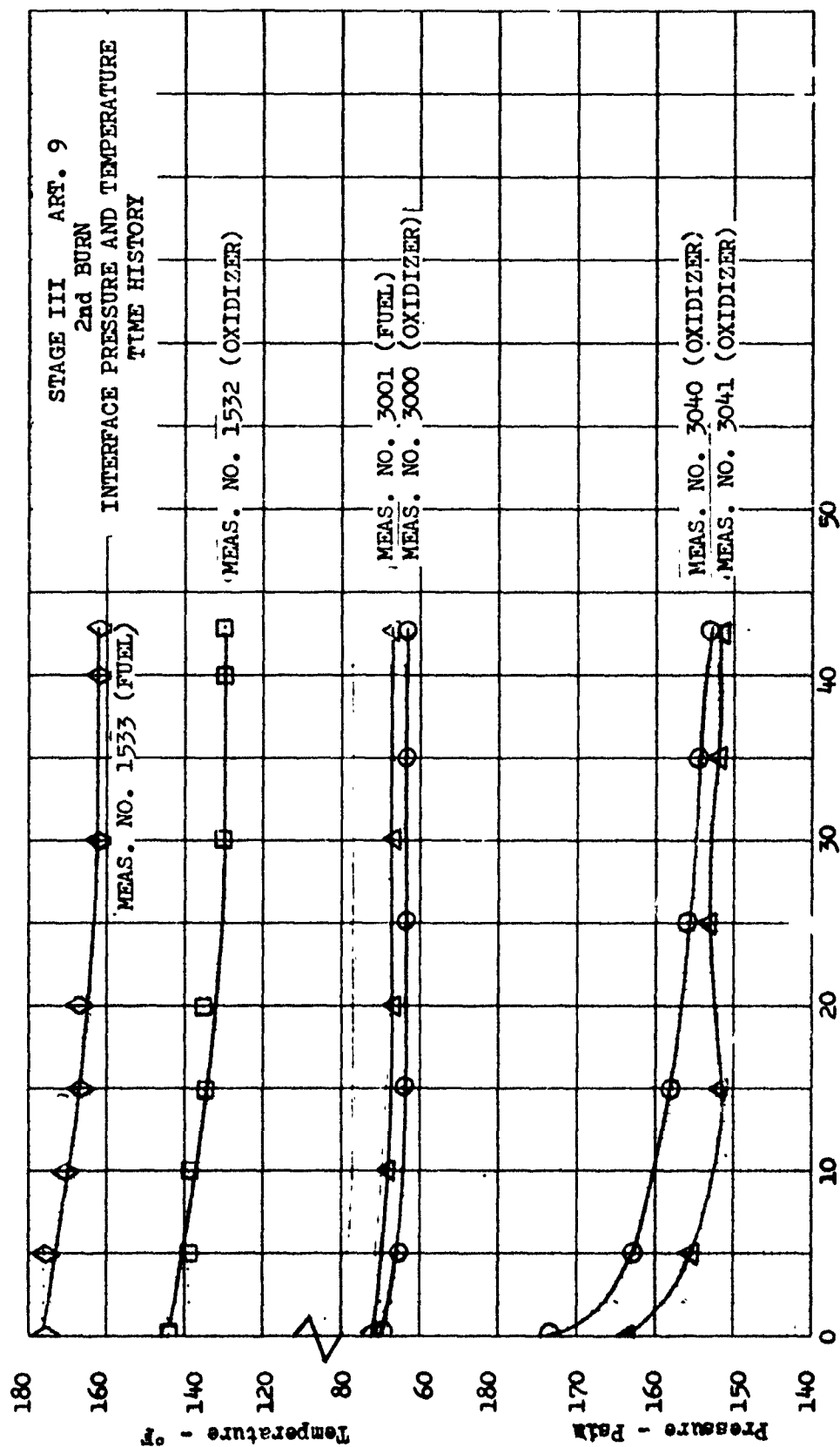
#### Propellant Pressures and Temperatures

Propellant pressures and temperatures are shown in Figures 83, 84 and 85, for the first, second and third burn, respectively and in Figure 86 during the coast periods of the first orbit. Propellant pressures measured at the interface are shown for oxidizer on S/A 4 (measurement No. 3040) and for fuel on S/A 5 (measurement No. 3041). Interface propellant temperatures are measured for the oxidizer on S/A 4 by measurement No. 3000 and for the fuel on S/A 5 by measurement No. 3001. The interface temperatures were measured on the opposite subassemblies (Meas. No. 3125 for S/A 5 oxidizer and meas. No. 3124 for S/A 4 fuel) but were omitted from the plots for clarity since the two subassemblies were identical.



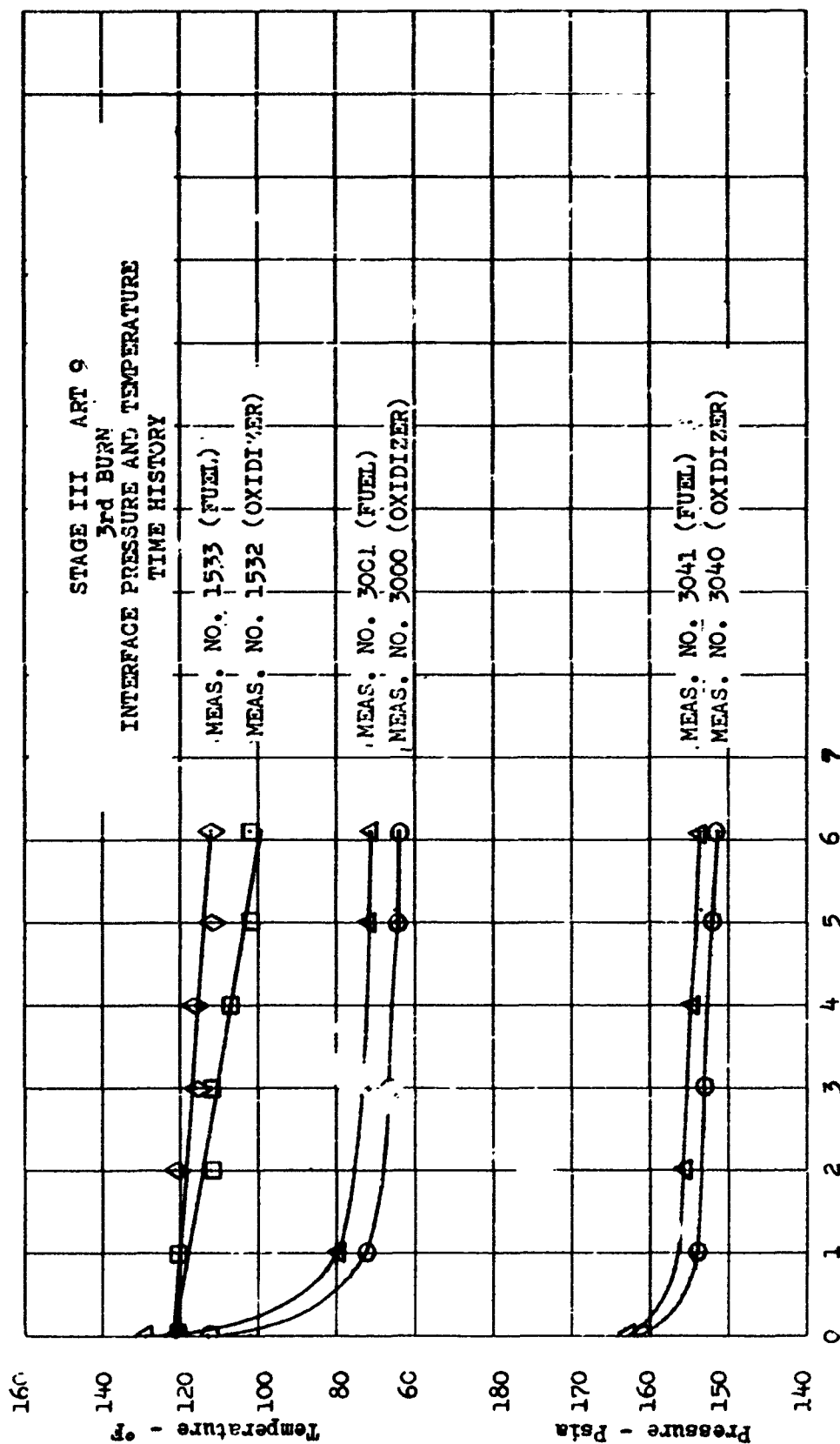
Time Fr. 1 - 138FS1 (13:58:34.412 Zulu) - Sec

FIGURE 84

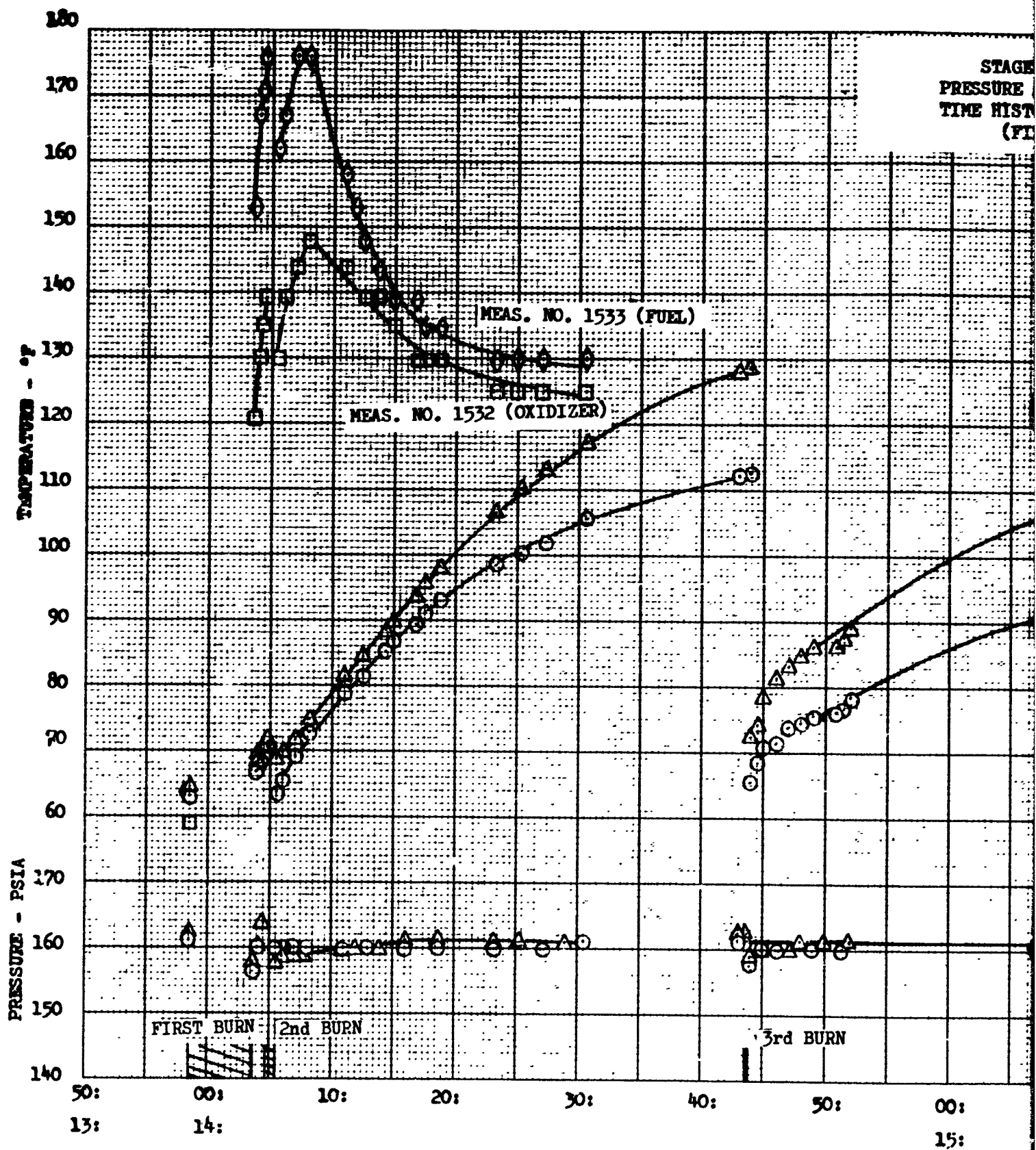


Time From 2-138FS1 (14:04:46.45 Zulu) - Sec

FIGURE 85



Time From 3 - 130751 (14:45:44.448 Zulu) - sec

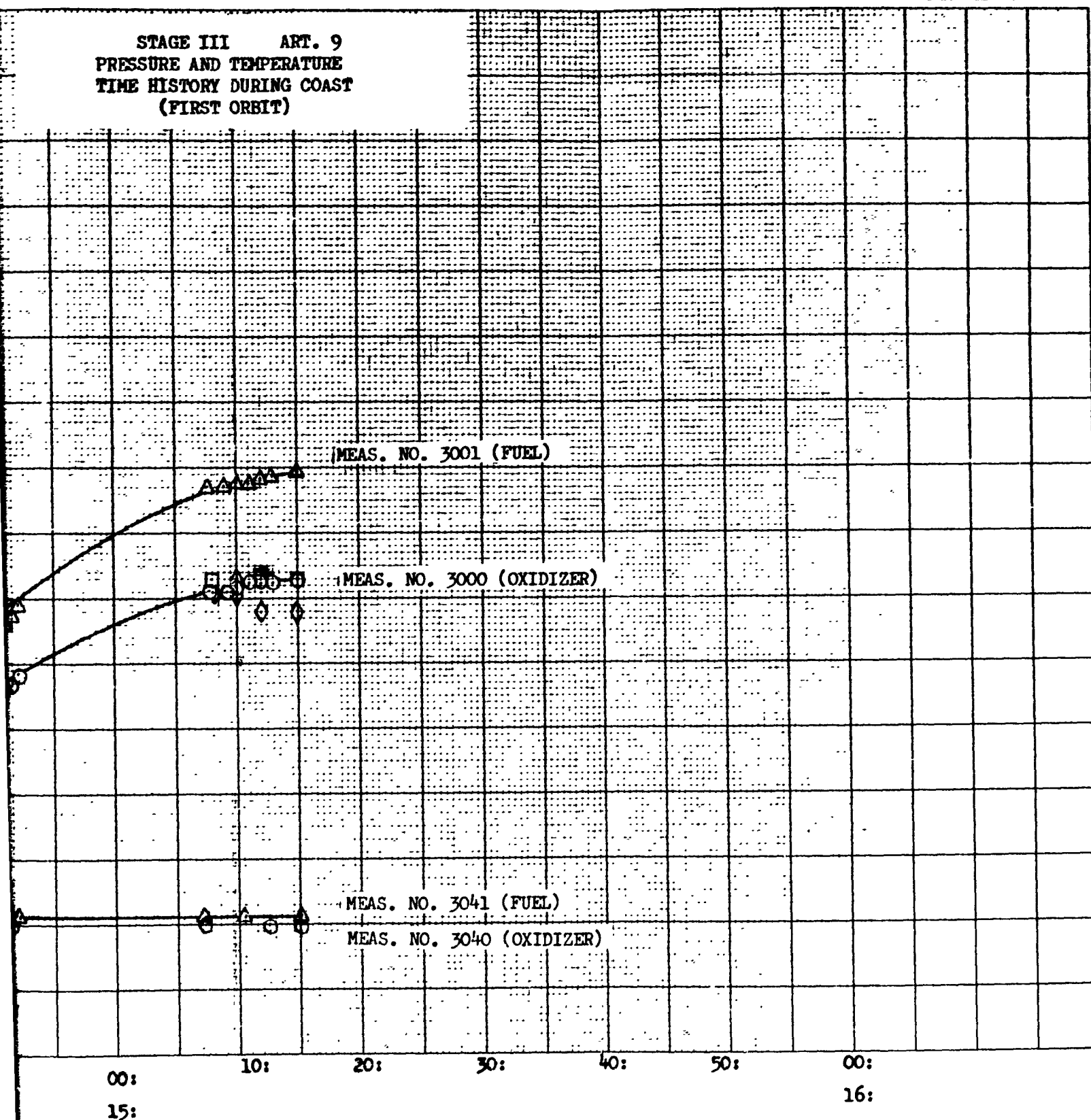


TIME OF DAY - ZULU (HR.-MIN.)



FIGURE 86

STAGE III ART. 9  
PRESSURE AND TEMPERATURE  
TIME HISTORY DURING COAST  
(FIRST ORBIT)



(HR.-MIN.)

2

### 3.2.1.7.3 Propellants - (Cont.)

The feedline surface temperatures under the insulation are measured for the oxidizer and fuel line by measurements Numbers 1532 and 1533, respectively. It should be emphasized that the ability of these measurements to record propellant temperatures is governed by the isolation from the environment and heat "soak-back" affected by the line insulation.

#### Pressures

The interface pressures during each burn confirmed the tank gas pressure profiles. The fuel pressure was less than predicted during the first burn due to reasons outlined under the Stage III Pressurization section. The profiles during the first burn were as expected. The second and third burn profiles were different from predicted due to the rapid gas pressure saturation at MOL Sim/Lab retro as outlined under the Pressurization section.

Minimum tank pressure control is noted to produce minimum interface pressures of 151-152 psi during each burn. Interface pressures during coast periods are more stable than on previous flights due to the rapid gas pressure saturation occurring at Gemini separation.

#### Temperatures

The interface temperatures were normal during each burn. First burn is essentially stable from  $FS_1$  to  $FS_2$  indicating minimum heating of the propellant in the feedline prior to burn and minimum stratification within the tank during burn. Second burn temperatures reflect minor heating in the feedline during coast which becomes stabilized approximately 10 seconds into the burn. Third burn temperatures reflect larger heating during the long coast; temperatures near mean bulk are reached at shutdown.

The feedline surface temperatures (measurement numbers 1532 and 1533) respond similarly to those noted for Article C11. The temperatures during the long burn (first burn on Article C9, second burn on Article C11) begin deviating from interface temperatures at approximately  $FS_1 + 80$  sec. This deviation reflects the time required for the engine heat to penetrate the insulation and effect the instrumentation. Since the interface propellant temperature does not reflect a temperature increase during this portion of the flight, it can be assumed that the

### 3.2.1.7.3 Propellants - (Cont.)

surface measurements do not record true propellant temperature during burn, but only an intermediate temperature between propellant and ambient environment. During the second and third burn these measurements do not reflect propellant temperatures due to the high residual heat in the insulation.

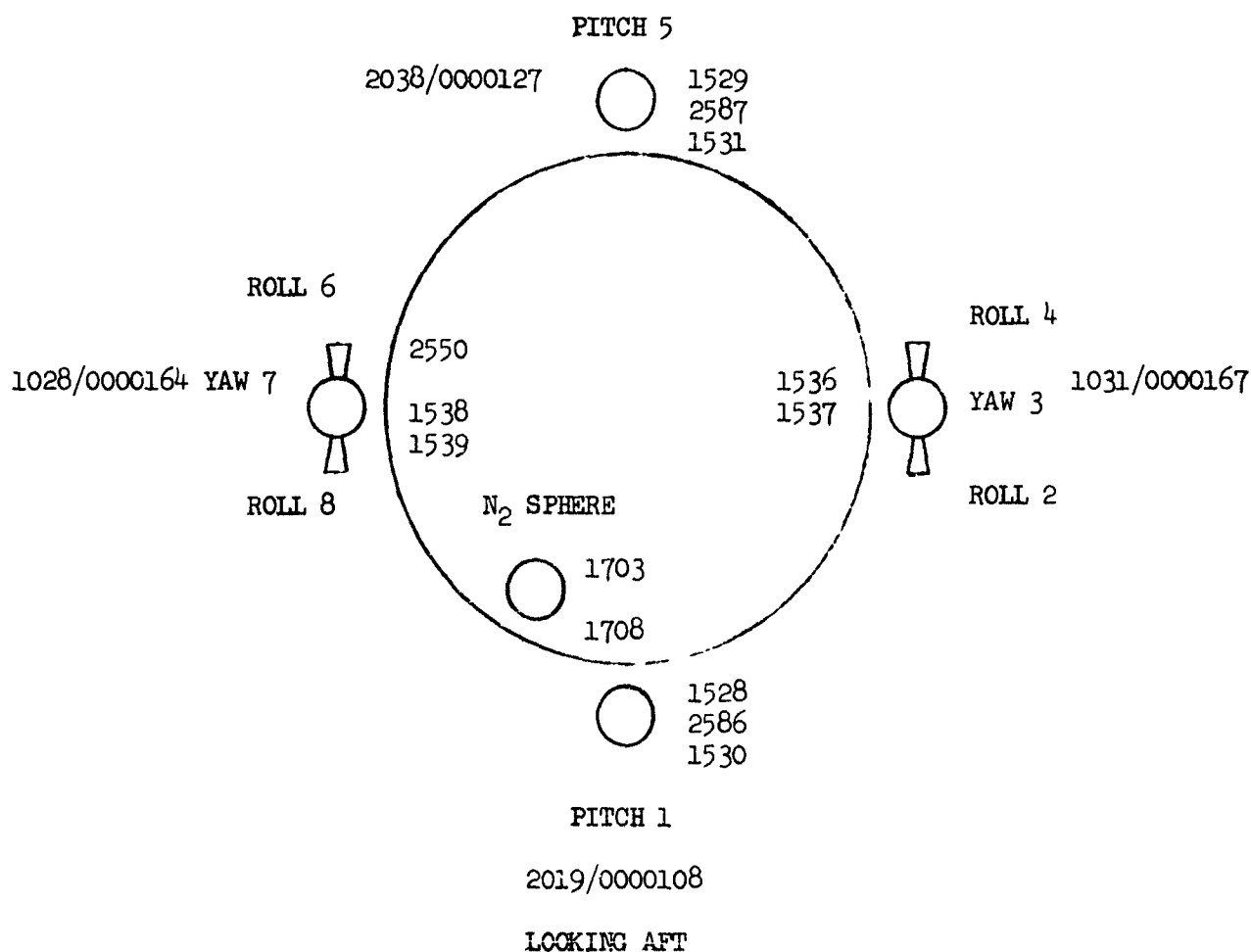
The temperatures during coast are shown in Figure 48. Equilibrium temperatures are noted to be similar to Article C11. Heating of interface temperatures and attendant heating then cooling of the surface temperatures are similar to Article C11. Maximum temperatures of approximately 110°F and 130°F are reached in the oxidizer and fuel interface temperatures, respectively. These values are well below the vaporization temperatures at existing pressures. The surface temperatures react similarly to those recorded on Article C11, reaching a maximum of 140°F and 180°F for oxidizer and fuel, respectively.

### 3.2.1.8 Attitude Control System

#### 3.2.1.8.1 Introduction

The Attitude Control System (ACS) utilizes 25 and 45 lb thrust engines to maintain vehicle attitude and perform required maneuvers. Due to the occurrence of a slight valve leakage on Article C11 the engine modules were subjected to 1500 freon cycles, 60 minutes of hot fire test with a reduced duty cycle and 300 additional freon cycles. This was followed by the acceptance tests and the ETR bench checks.

The following diagram describes the ACS engine utilization on article C9 and locates the instrumentation measurement numbers.



Instrumentation List

Number	Type	Location
1528	Temperature	P <sub>1</sub> - Oxidizer Line Midpoint
1529	Temperature	P <sub>5</sub> - Oxidizer Line Midpoint
1530	Temperature	P <sub>1</sub> - Injector
1531	Temperature	P <sub>5</sub> - Injector
1536	Temperature	Y <sub>3</sub> - Oxidizer Line Midpoint
1537	Temperature	Y <sub>3</sub> - Fuel Line Midpoint
1538	Temperature	Y <sub>7</sub> - Oxidizer Line Midpoint
1539	Temperature	Y <sub>7</sub> - Fuel Line Midpoint
1703	Pressure	N <sub>2</sub> - Pressurization Sphere
1708	Pressure	Regulated System Pressure
2550	Temperature	RY 6, 7, 8 - 3/8" Oxidizer Feedline
2586	Temperature	P <sub>1</sub> - Fuel Line Midpoint
2587	Temperature	P <sub>5</sub> - Fuel Line Midpoint

The engine performance data from the acceptance testing and the flight are presented in table 18.

### 3.2.1.8.2 Summary

The attitude control system successfully accomplished the specific mission functions as shown in Table 19 except for event number 21. Proper vehicle attitude was maintained for 6.12 hours of the planned 7 hour mission. A review of flight data has identified the following anomalies and their causes:

#### (1) Roll Engine Reduced Chamber Pressure

Reduced chamber pressure (See Table 20) occurred in all four roll engines after the first pass over Carnarvon. Excessive, nonexpected steady state firing on all Rocket Engine assemblies resulted in some throat erosion and excessive heat soak back into the propellant valves and lines causing two phase (liquid-vapor) oxidizer flow.

#### (2) ACS Guidance Backup Mode Saturation

The saturation of the ACS guidance backup mode (10 complete cycles) occurred over WTR 2nd pass. No evidence of any ACS engine leakage was found, i.e., chamber pressure, propellant line temperature drops, and/or unaccounted for propellant consumption. The ACS guidance backup mode was actuated because of the reduced effective thrust from the 45 lb engines due to plume impingement on the vehicle and electrical tolerances in the flight controls system. There were no ACS anomalies.

#### (3) Reduced Chamber Pressure in Yaw 7

Reduced chamber pressure in the Yaw 7 engine occurred over WTR (16:53:10GMT). This was caused by insufficient flow of oxidizer into the engine due to excessive line temperatures on that module. The boiling oxidizer reduced the liquid flow rate enough to cause a considerable reduction in chamber pressure. The excessive module temperatures were caused by the extensive use of both the Yaw 7 engine and the Roll 6 and 8 engines.

#### (4) Yaw 7 Chamber Pressure Ramps

Chamber pressure ramps on the Yaw 7 engine were observed over Pretoria 4th pass (19:09:30GMT) and Hawaii 4th pass (19:55:10GMT). These ramps could have been caused by either of the following:

TABLE 18  
ENGINE PERFORMANCE

ENGINE	FLIGHT DATA PC INSTRUMENT NUMBER	CHAMBER PRESSURE* (PSIA)			THRUST** (POUNDS)		
		ACCEPTANCE	RENO	FLIGHT	ACCEPTANCE	RENO	FLIGHT
P-1	1520	140.1	142.0	140.1	45.0	45.4	45.0
P-5	1521	142.0	140.0	140.2	45.1	44.7	44.7
Y3	1522	139.0	149.0	142.9	44.7	46.26	45.3
Y7	1523	145.0	143.0	146.8	45.12	44.8	45.4
R2	1524	156.0	158.0	153.8	24.8	24.8	24.5
R4	1525	153.0	156.0	140.0	24.2	24.8	21.6
R6	1526	153.0	156.0	147.7	24.2	24.7	23.3
R8	1527	153.0	153.0	151.2	24.3	24.3	24.0

\*P<sub>c</sub> Tolerance: Pitch & Yaw: 125 <sup>+15</sup> PSIA  
Roll: 150 <sup>+15</sup> PSIA  
Note: The Carnarvon Pass 1 data was used for chamber pressure level and may reflect some degradation on roll engines 4 & 6.

\*\*Thrust tolerance: Pitch & Yaw: 45-2.25 lbs  
Roll: 25 <sup>+1</sup> 1.25 lbs

TABLE 19  
ACS MISSION FUNCTIONS  
ARTICLE 9

ACS EVENT NO.	FLIGHT TIME AS GMT HOURS:MINUTES:SECTIONS	DESCRIPTION OF EVENT
0	13:50:42	Lift/off
1	13:58:21 to 13:58:34	Propellant Settling-1st T/S Burn
2	14:03:42 to 14:03:44	Shutdown burn-1st T/S Burn
3	14:03:45 to 14:04:11	Short Coast Control Mode
4	14:04:11	Gemini Separation
5	14:04:16 to 14:04:47	Pitch up & Propellant Settling -T/S 2nd Burn
6	14:05:29 to 14:05:31	Shutdown Burn - 2nd T/S Burn
7	14:43:32 to 14:43:44	Propellant Settling - 3rd T/S Burn
8	14:43:50 to 14:43:53	Shutdown Burn - 3rd T/S Burn
9	14:43:55 to 14:44:54	30° Pitch up Maneuver for OV1-6
10	14:45:36 to 14:46:11	Short Coast Control Mode -
11	14:46:13	OV-1-6 Separation
12	14:46:19 to 14:47:16	Pitch Down to Normal Attitude
13	14:47:17 to 14:47:52	Short Coast Control Mode
14	14:47:54	OV4-1 Transmitter Separation
15	14:47:55 to 14:48:11	Short Coast Control Mode
16	14:48:14	OV4-1 Receiver Separation



TABLE 19 (Cont.)

171

ACS EVENT NO.	FLIGHT TIME AS GMT HOURS:MINUTES:SECONDS	DESCRIPTION OF EVENT
17	15:09:02 to 15:19:42	1st De-Pitch
18	16:39:07 to 16:49:47	2nd De-Pitch
19	18:09:22 to 18:20:02	3rd De-Pitch
20	19:39:37 to 19:50:07	4th De-Pitch
21	20:51:00 (approximately)	Spin up maneuver*

\*Not accomplished due to ACS propellant exhaustion

- a. Small fuel valve leakage causing an ice plug to form in the throat. The pressure build up would force out the plug and the process would repeat itself.
- b. Raw fuel build up in the  $P_c$  sensing tube due to fuel-rich pulses seen earlier over WTR. The raw fuel, freezing on the thrust chamber side and boiling on the pressure transducer side, could also cause the ramps observed in the data.

(5) Propellant Exhaustion

The fuel supply was exhausted over Hawaii 4th pass (19:59:17GMT). The oxidizer was exhausted after that point and before Pretoria 5th pass (20:51:00GMT). Propellant depletion occurred as a result of excessive engine utilization. The complete mission would have been accomplished if the engine usage would have been as predicted. The additional ACS utilization was due to engine exhaust plume impingement forces acting on the vehicle skin causing reverse torques and reducing the effectiveness of the engines. Analysis indicates the reduction in effectiveness to be approximately 50%.

It should be noted that the ACS engine modules were operating out of their temperature specification limit (130°F max). The roll engines had exceeded both the maximum allowable total on time (60 sec) and the maximum allowable single steady state burn time (7 sec). Altitude control was maintained, however, until propellants were exhausted.

### 3.2.1.8.3 Discussion

The discussion that follows is concerned with the five problem areas as described in the foregoing section.

#### (1) Roll Engine Reduced Chamber Pressure

The following table shows the reductions in roll engine chamber pressure and the time at which they occurred:

TABLE 20  
ROLL ENGINE  $P_c$  HISTORY

STATION	GMT TIME	CHAMBER PRESSURE-PSIA			
		R2	R4	R6	R8
Antigua	14:00	155	152	148	156
Carnarvon	14:42	154	140	148	151
Hawaii 1st	15:08	80	112	110	142
Pretoria 2nd	15:58	50	--	94	--
WTR 2nd	16:53	70	--	110	--
Pretoria 4th	19:10	90	130	150	145
Hawaii 4th	20:02	100	140	155	150

From this table it can be seen that all the roll engines had some degradation in chamber pressure. Of the four roll engines only Roll #6 appears to have returned to its original level, indicating that the other engines experienced throat erosion. The main reason for the chamber pressure changes is oxidizer boiling in the propellant lines and valves of the roll engines. The hot propellant lines were caused by excessive heat soak back resulting from excessive engine usage. Table 21 lists the engine "on-time" for all the engines during the flight. By comparing the engine on times with the chamber pressure table the following conclusions can be reached:

TABLE 21  
ARTICLE 9 ENGINE TIME

STATION	START TIME	P1	P5	Y3	IN SECONDS Y7	R2	R4	R6	R8
BOOST THROUGH SHIP	13:52:20	47.96	31.65	36.31	38.28	5.69	32.57	32.63	5.95
COAST PERIOD	14:08:40	.85	-	.21	-	.04	-	.04	-
ASCENSION	14:11:05	1.90	1.48	1.61	0.41	.08	.08	.08	.08
COAST PERIOD	14:18:40	1.75	-	.41	-	.06	-	.06	-
PRETORIA 1ST	14:23:20	3.08	-	1.51	.20	.04	-	.04	-
COAST PERIOD	14:30:30	4.66	-	1.07	-	.18	.06	.18	.06
CARNAVON*	14:42:50	30.85	25.80	65.33	37.38	22.98	26.63	28.63	24.09
COAST PERIOD	14:50:20	5.83	-	1.51	-	.24	.06	.24	.06
HAWAII 1ST	15:07:40	16.42	3.46	3.91	-	.12	.12	.12	.12
COAST PERIOD	15:15:40	8.51	13.26	1.89	-	.24	.06	.24	.06
CAPE 1ST	15:31:40	.80	-	1.00	-	.06	-	.06	-
COAST PERIOD	15:34:25	7.82	0	2.00	-	.36	.12	.36	.12
PRETORIA 2ND	15:57:40	2.52	-	-	-	.12	-	.12	-
COAST PERIOD	16:05:40	35.35	16.72	8.68	-	.24	.08	.28	.08
WTR 2ND	16:53:10	1.83	-	.94	1.09	.06	-	.06	-
COAST PERIOD	17:07:40	11.42	-	3.5	-	.18	.04	.14	.04
PRETORIA 3RD	17:37:40	2.35	-	.50	-	.14	.04	.14	.04
COAST PERIOD	17:41:40	29.17	3.46	7.21	-	.6	.18	.6	.18
HAWAII 3RD	18:19:40	3.13	13.26	.60	-	.04	-	.04	-
COAST PERIOD	18:26:40	14.40	-	3.69	-	.48	.18	.48	.18
PRETORIA 4TH	19:09:30	2.76	-	.625	-	.08	.04	.08	.04
COAST PERIOD	19:17:00	33.90	16.72	7.81	-	.54	.18	.54	.18
HAWAII 4TH	19:55:10	1.05	-	.40	-	.12	.06	.12	.06
COAST PERIOD	20:02:20	-	-	-	-	-	-	-	-
TOTAL TIME		267.31	125.81	156.34	77.36	32.15	60.50	65.21	31.34
SEVEN MDS MODES			7.0	1.40					
CORRECTED TOTAL TIME			163.34	78.76					

\*ROLL ENGINES SHOWED DECAY IN PERFORMANCE AFTER THIS TIME IN FLIGHT. ROLL #2 80 PSIA - REMAINING APPROXIMATELY 120-130 PSIA.

### 3.2.1.8.3 Discussion - (Cont.)

- a. Roll Engine 2 exhibits the greatest chamber pressure loss. This engine is mounted with Yaw 3 which had 65 seconds of ontime over Carnarvon. This extremely high usage resulted in severe heat soak back to the module. The oxidizer line to Roll 2 is routed very close to the engine mount.\* This heat source coupled with high valve temperatures caused oxidizer boiling at least in the injector and very likely in the valve, resulting in decreased oxidizer flow and chamber pressure.
- b. Roll Engine 4 also exhibited a chamber pressure drop because it too is mounted with a yaw 3. In addition Roll 4 had extensive use earlier in the flight resulting in direct heat soak back from its own chamber adding to that coming from yaw 3.
- c. Roll Engine 6 exhibited a considerable chamber pressure drop due to high heat soak back and oxidizer boiling caused by extensive use earlier in the flight. In addition the Roll 6 oxidizer line is also routed close to the mount, thereby increasing the heat input to the propellant.\*
- d. Roll Engine 8 exhibited the least chamber pressure drop primarily because it had little use earlier in the flight. In addition, the Roll 8 oxidizer line is not routed in close proximity to the mount as it is on Roll 2 and Roll 6.\*

\*Note: The roll engines are mounted in a manner such that one propellant line is routed very close to the mount bracket. This results in relatively good head transfer to that line compared to the line routed away from the mount. As a result, one propellant to the 25 pound engines runs hotter than the other.

For the case where the fuel line is closest to the mount the added heat to the propellant has little effect. This is because of the low vapor pressure of the fuel as compared to the system operating pressure. For these engines, Roll 4 and Roll 8, the heat input resulting in oxidizer boiling must come primarily from soakback from their own chambers or the 45 pound chambers being conducted into the oxidizer valves.

### 3.2.1.8.3 Discussion - (Cont.)

For the case where the oxidizer line is closest to the mount the added heat to the propellant can have a very significant effect. The vapor pressure of oxidizer exceeds the system operating pressure above 212 degrees Fahrenheit. This results in oxidizer boiling in the valve in turn causing reduced oxidizer flow and chamber pressure. Although the primary heat source is still heat soakback from the chambers, the added heat from the mount can significantly aggravate the problem. This situation existed on Roll 2 and Roll 6.

#### (2) ACS Guidance Backup Mode Saturation

Three ACS Guidance Backup Mode cycles occurred over data stations; Ascension, Pretoria 1st and WTR 2nd. In all three instances the pulses were on Yaw 3 and Yaw 7 engines, with the out-of-tolerance offset towards the Yaw 7 side. The following table demonstrates the temperature,  $P_c$ , and consumption correlation for these three passes.

TABLE 22

PASS	Y <sub>7</sub> TEMPERATURES				Y <sub>7</sub> P <sub>c</sub>		LBS-CONSUMPTION	
	FUEL		OXIDIZER		O SHIFT		PROPELLANT	
	IN	OUT	IN	OUT	IN	OUT	N <sub>2</sub> SPHERE*	ENGINE OT
Ascension	78	85	82	91	-3.1	-3.1	1.0	.84
Pretoria(1st)	93	100	98	104	-3.1	-3.1	1.0	.74
WTR (2nd)	176	148	176	183	-3.1	-3.1	.5	.41

\*Accuracy within  $\pm .5$  lbs, due to T/M system granularity.

The only apparent discrepancy in the table is the drop in fuel line temperature over WTR. The reason for this drop is the reduced  $P_c$  phenomena which is discussed in the following paragraph. The remaining data supports the conclusion that no leak existed.

### 3.2.1.8.3 Discussion - (Cont.)

#### (3) Reduced Chamber Pressure in Yaw 7

Over WTR the  $P_c$  level of the Yaw 7 engine was reduced to between 60 and 80 PSIA. Figure 87 is a plot of a typical pulse over WTR. As seen in Figure 88, the oxidizer line temperature is approximately 180°F over Pretoria and WTR. The vapor pressure of oxidizer at 180° is 185 PSIA. The valve temperatures are normally about 25° warmer than the lines. The vapor pressure of oxidizer at 210°F is approximately 280 PSIA. The system pressure is at 290 PSIA so boiling is imminent in the valve. Cycling the valve open causes a momentary but significant pressure drop in the valve. This results in severe boiling in the valve and reduced oxidizer flow to the engine. Combustion in the chamber is very fuel rich and, along with the reduced mass flowrate, results in a lower chamber pressure. The line temperature behavior observed over WTR is consistent with the explanation, there being relatively little oxidizer flow and therefore little oxidizer line cooling and greater than nominal fuel flow and therefore considerable fuel line cooling.

#### (4) Yaw 7 Chamber Pressure Ramps

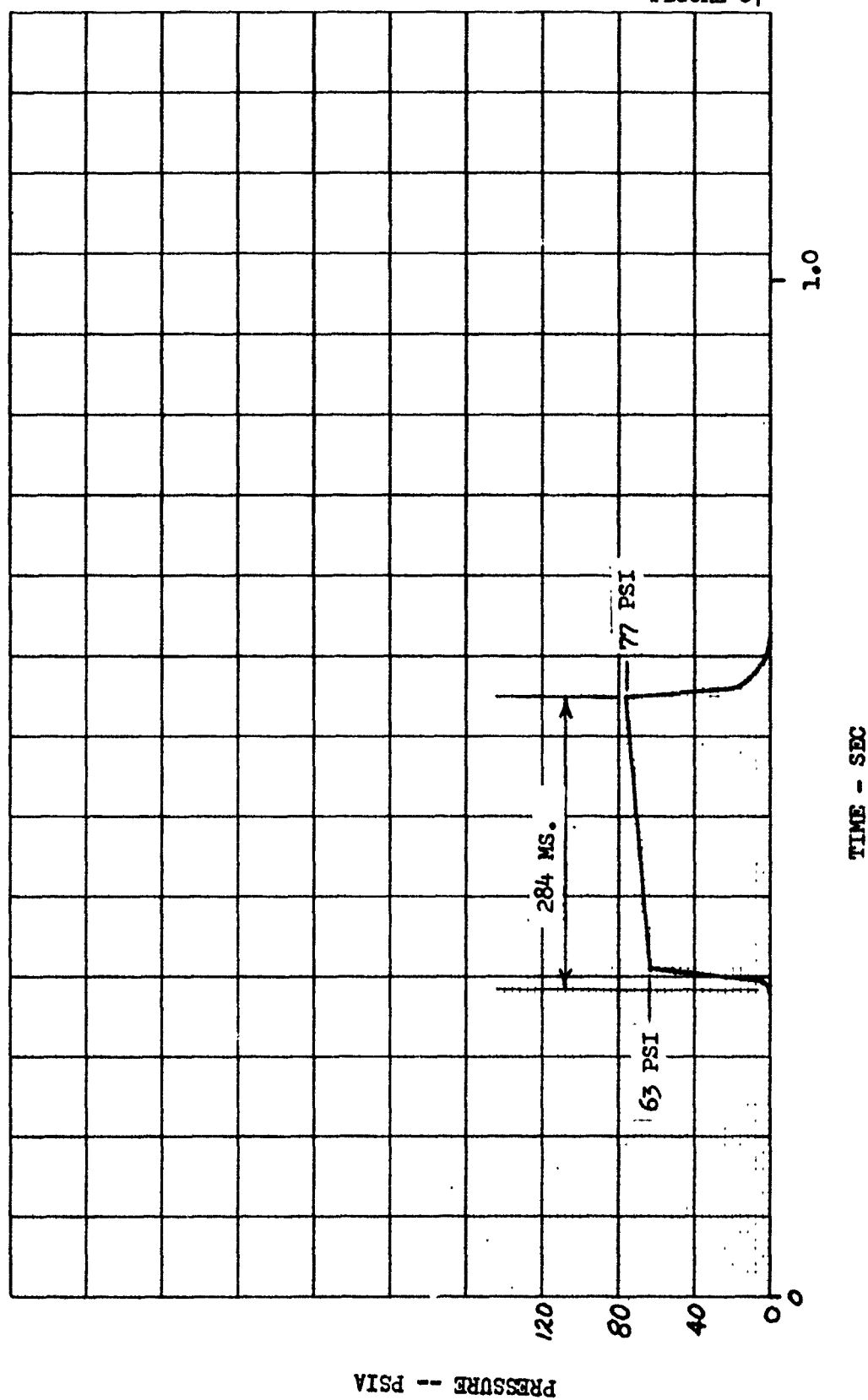
The four Yaw 7 chamber pressure ramps are plotted in Figures 89 and 90. Two possible explanations for these occurrences are as follows:

##### a. Small Fuel Leakage

The low flow rate fuel leak would flash to a three phase mixture as it passes through the chamber. The fuel ice and snow could eventually freeze over the throat creating a closed volume. As the volume fills with additional fuel it also begins to heat up from the warm engine. It is possible that the vapor pressure could be raised to the  $P_c$  levels indicated. Then a combination of heat and pressure could result in ejection of the throat ice plug. The process then repeats itself.

FIGURE 87

ARTICLE 9  
WTR - 2nd PASS  
YAW 7 - LAST PULSE - 16:57:26 HRS, GMT



PRESSURE -- PSIA

TIME - SEC



ARTICLE 9  
YAW 7  
PROPELLANT LINE TEMPERATURES

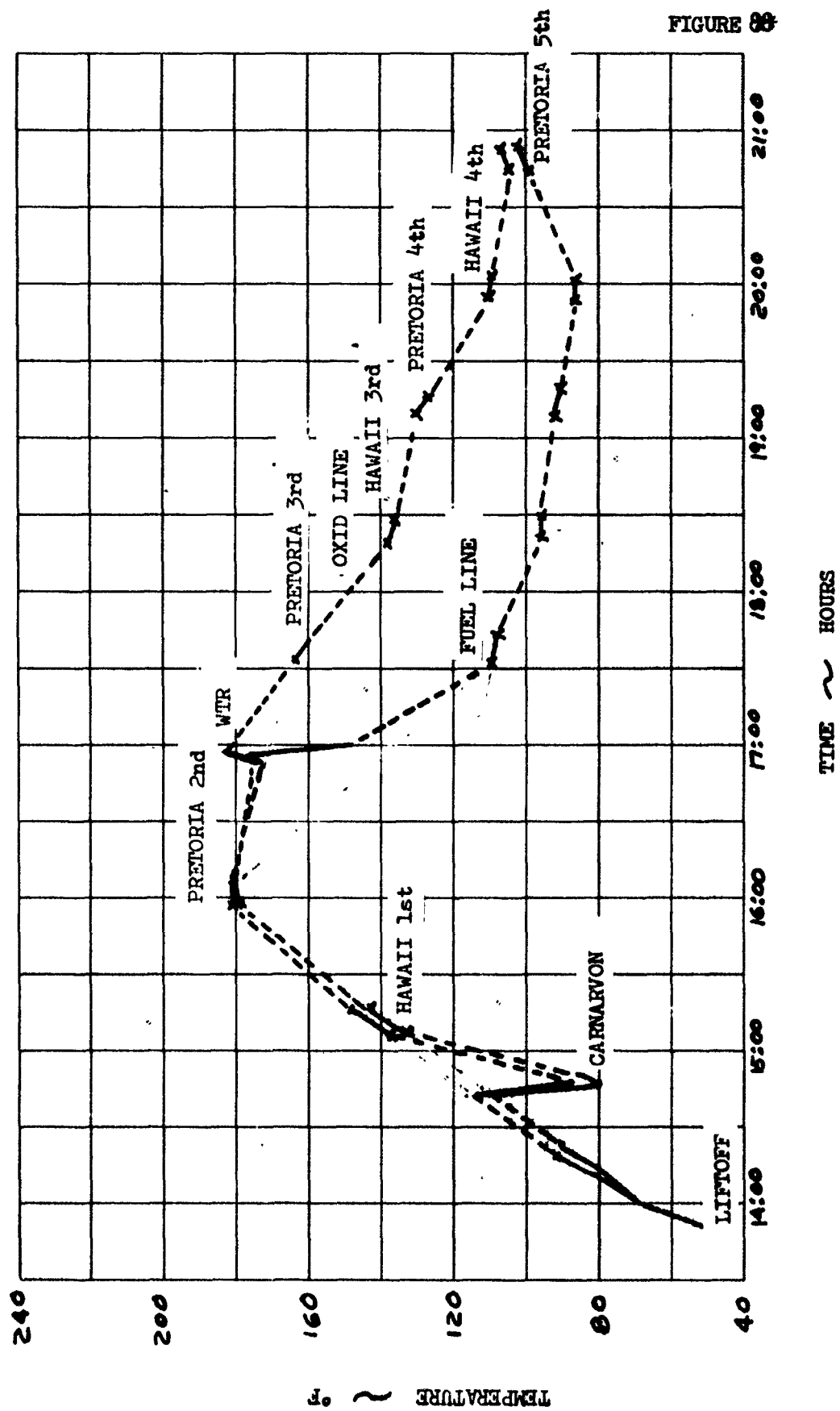


FIGURE 89

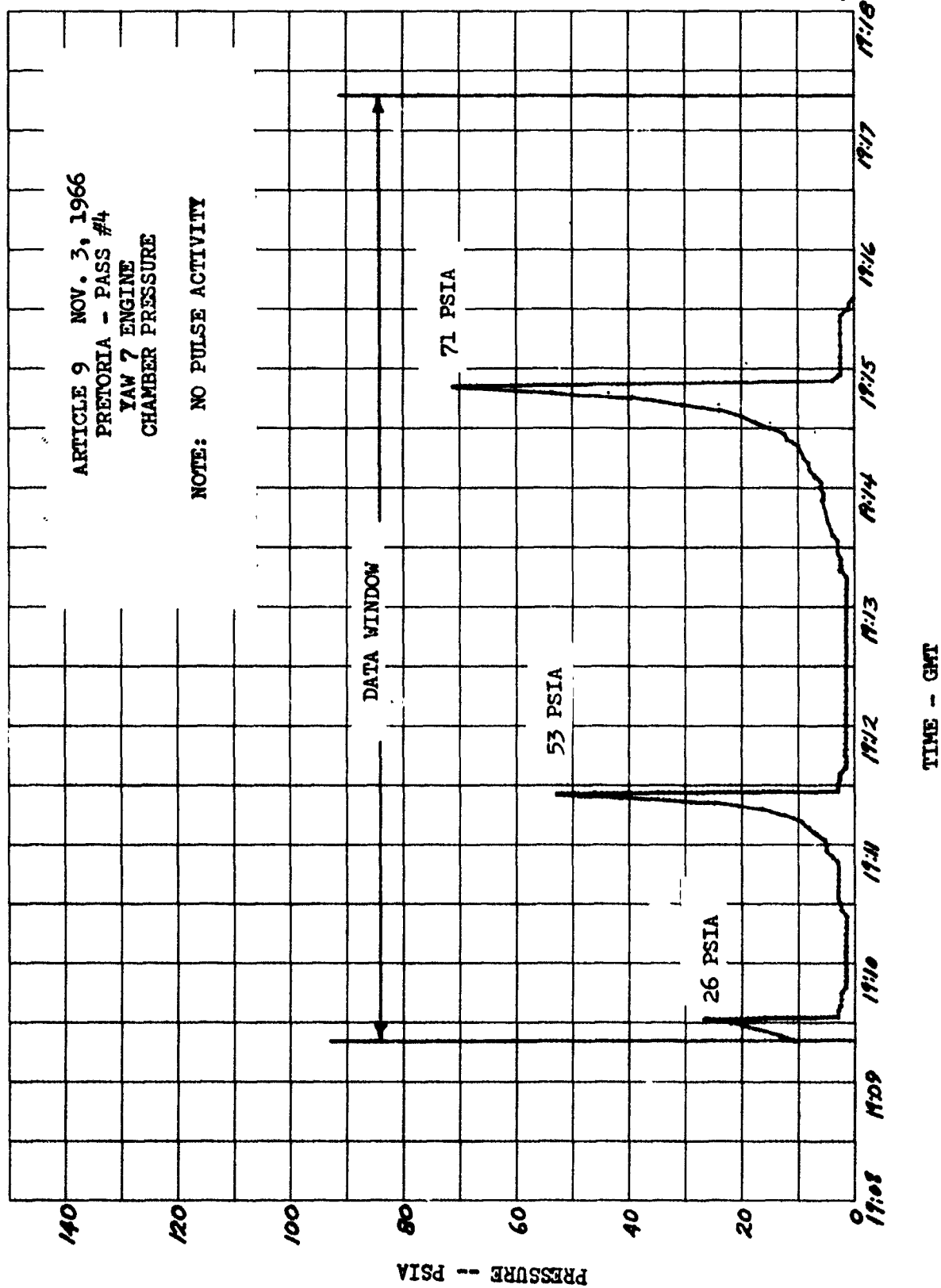
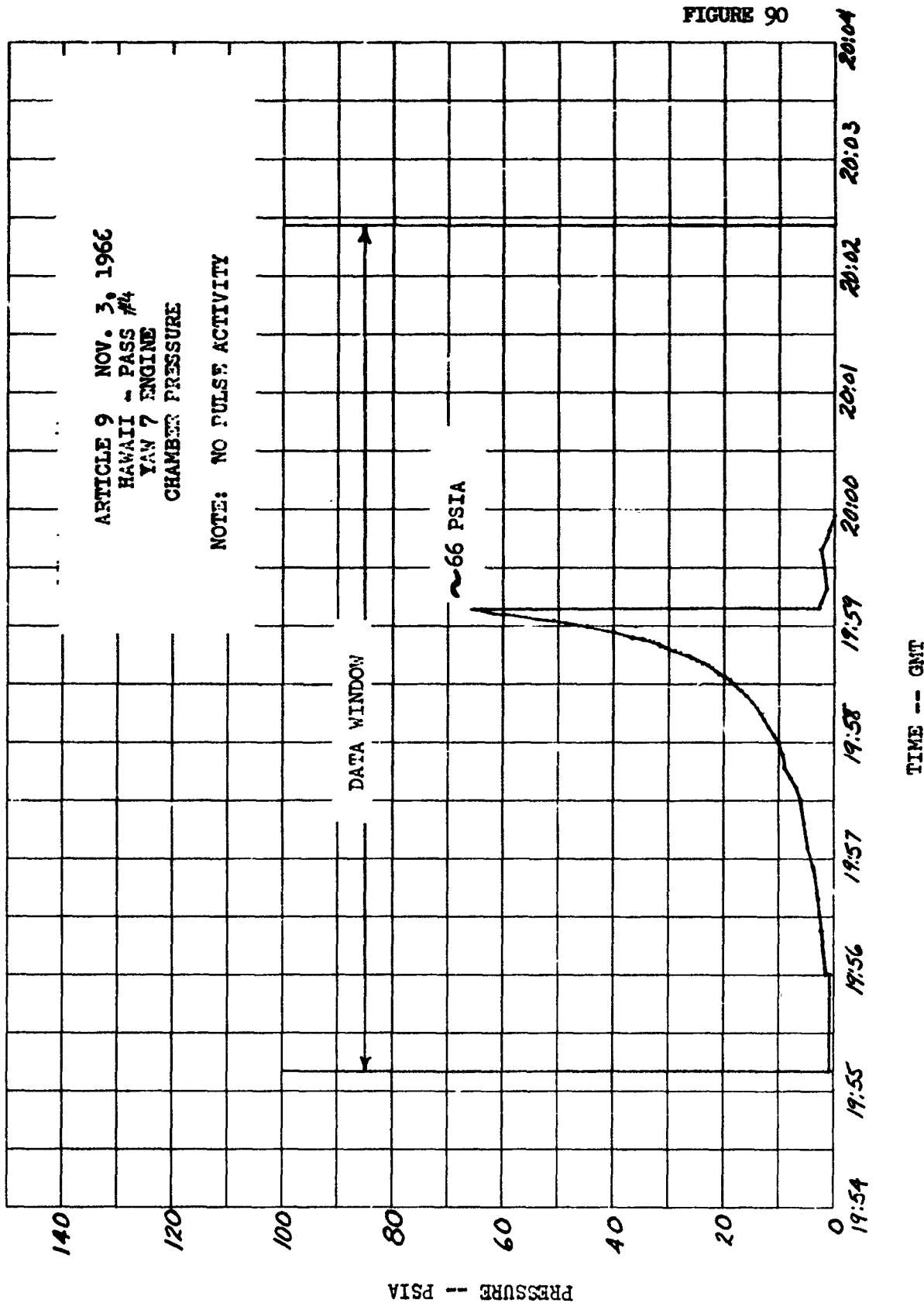


FIGURE 90



### 3.2.1.8.3 Discussion - (Cont.)

The factor that favors a small fuel leak is that the line temperature on Y7 continues to drop until propellant exhaustion and then begins to rise. The propellant consumption during Pretoria Pass 4 is impossible to calculate as the  $\text{GN}_2$  sphere pressure shifts only one data bit over the entire pass. This could represent between 0.1 pounds and 1.5 pounds of propellant. Overall propellant consumption figures are 111 pounds accounted for due to engine on time. The minimum usable load was approximately 121 pounds. This 10 pound difference could easily be accounted for by increased activity outside tracking stations. The ramp profile does not lend itself directly to the ice plug theory because the  $P_c$  rise would require a substantial rate of heat input. It is felt that if this rate were present the ice plug would melt out of the throat much faster. Another consideration is that the fuel line temperature did not reach the bulk temperature. This could be explained as thermal equilibrium, where the small flow rate is cooling the line as fast as the engines and mount are trying to heat it. However, significant cooling has been demonstrated at leakage rates estimated as low as 0.1 pounds per hour during hotfire testing.

#### b. $P_c$ Tube Phenomenon

The factor that favors the fuel ice, liquid and vapor in the  $P_c$  tube theory is the fact that fuel rich pulses occur over WTR 2nd pass. It is theorized that unburned liquid fuel could feed into the  $P_c$  tap during the very fuel rich pulses. The liquid fuel in the tube vaporizes on the transducer end due to residual heat in the mount and ablative material. The liquid on the thrust chamber end freezes because of its exposure to the space vacuum. The ice plug forms the liquid and vapor at the transduce end of the tube is heated causing an increase in the  $P_c$  reading. The ice plug is finally blown out and the process repeats itself. Using full vapor pressure data, the following temperatures would have had to have been achieved in the line.

### 3.2.1.8.3 Discussion - (Cont.)

1st ramp 26 PSIA 203°F

2nd ramp 33 PSIA > 250°F

3rd ramp 71 PSIA > 250°F

4th ramp 66 PSIA > 250°F

The 250° temperature appears to be quite feasible in view of the high propellant line temperatures. The only Yaw 7 pulses observed after Carnorvan are over WTR. It is possible that more pulses occurred during the ACS Guidance Backup Mode cycles. The more pulses that occur the more fuel is available to feed into the  $P_c$  tube. However, the pulsing adds heat and lessens the chance of ice forming in the  $P_c$  tube outlet close to the injector.

### (5) Propellant Exhaustion

Propellant exhaustion occurred over Hawaii fourth pass. Figure 91 is a plot of the Pitch 1 activity as that depletion occurs. The engine activity as shown in Table 21 when multiplied by engine flow rates yields the propellant consumption shown in Table 23. Figure 92 depicts the propellant consumption based on  $GN_2$  sphere pressure. Based on the factor of 1/2 for effectiveness due to plume impingement, the engine on times for the Pitch and Yaw engines would have been as shown below had not plume impingement effected the ACS control authority (note: during propellant settling and pitch roll mix the on-times would not have changed):

ENGINE	ON TIME	
	ACTUAL	COMPUTED W/O IMPINGEMENT EFFECTS
$P_1$	267.31	173.1
$P_5$	125.8	91.6
$Y_3$	163.34	129.0
$Y_7$	78.76	75.7
TOTAL	635.21	469.40

FIGURE 91

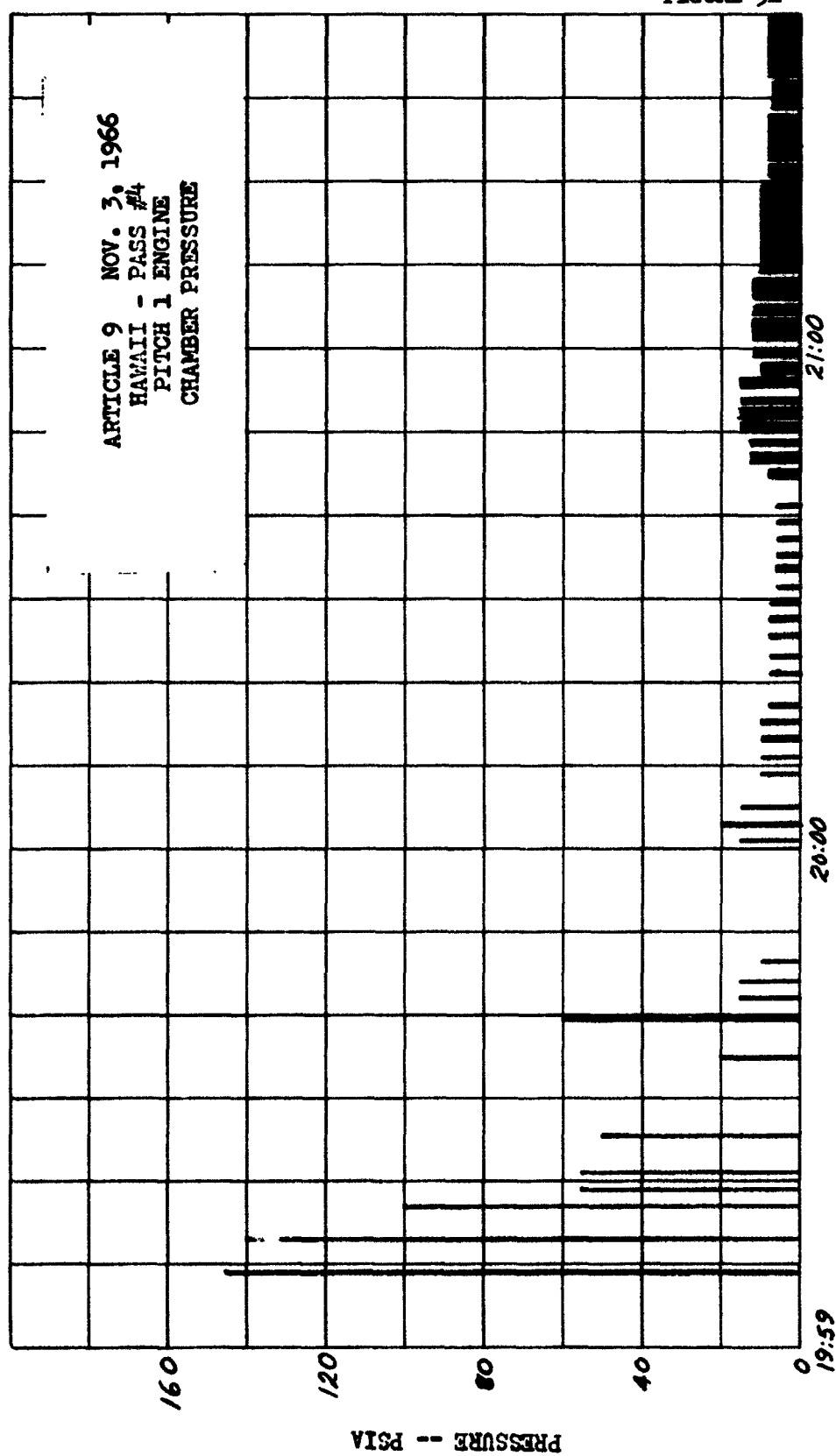


TABLE 21

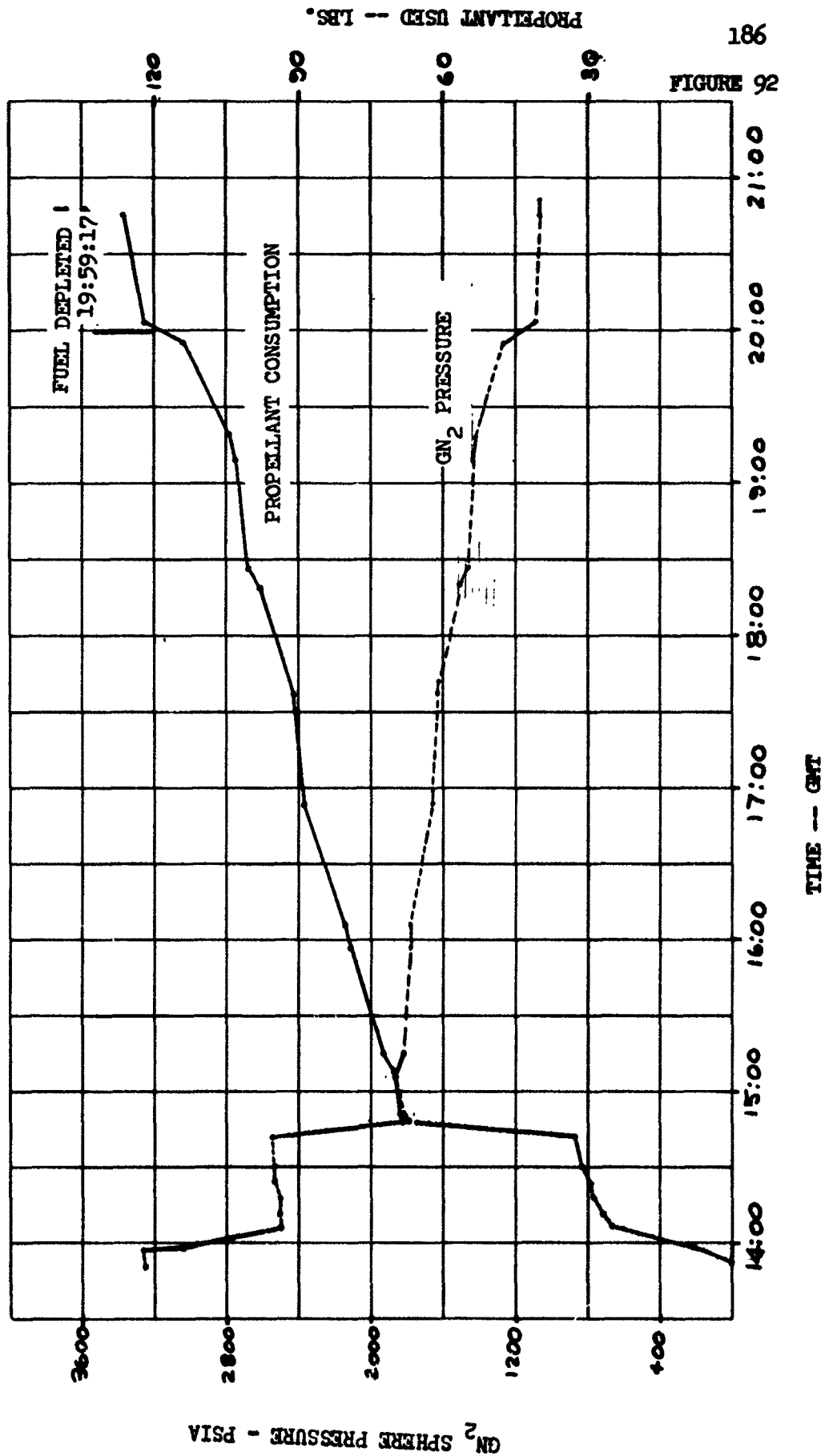
**MARTIN**  
 DENVER DIVISION

**ARTICLE 9**  
**Propellant Consumption Summary**  
**(Based on Engine On Times)**

Data Source	Amount LBS	Total LBS
Antigua thru Ship	29.49	29.49
Coast Period	.12	29.61
Ascension	.84	30.45
Coast Period	.22	30.67
Pretoria 1st	.74	31.41
Coast Period	.63	32.04
Carnarvon	32.55*	64.59
Coast Period	.94	65.53
Hawaii 1st	3.61	69.14
Coast Period	4.10	73.24
ETR 1st	.28	73.52
Coast Period	1.15	74.67
Pretoria 2nd	.40	75.07
Coast Period	9.75	84.82
WTR	.41**	85.23
Coast Period	2.36	87.59
Pretoria 3rd	.46	88.05
Coast Period	7.21	95.26
Hawaii 3rd	2.56	97.82
Coast Period	2.82	100.64
Pretoria 4th	.53	101.17
Coast Period	10.39	111.56
Hawaii 4th	.26	111.72
Coast Period	- 0 -	111.72
Pretoria 5th	- 0 -	111.72
	TOTAL -	111.72 lbs

\* Propellant Consumption does not take into account degraded roll engines.  
 \*\* No attempt made to calculate  $Y_7$  propellant usage during period of anomalous performance.

ARTICLE 9 -- GN<sub>2</sub> SPHERE  
PRESSURE & PROPELLANT CONSUMPTION





#### 3.2.1.8.3 Discussion - (Cont.)

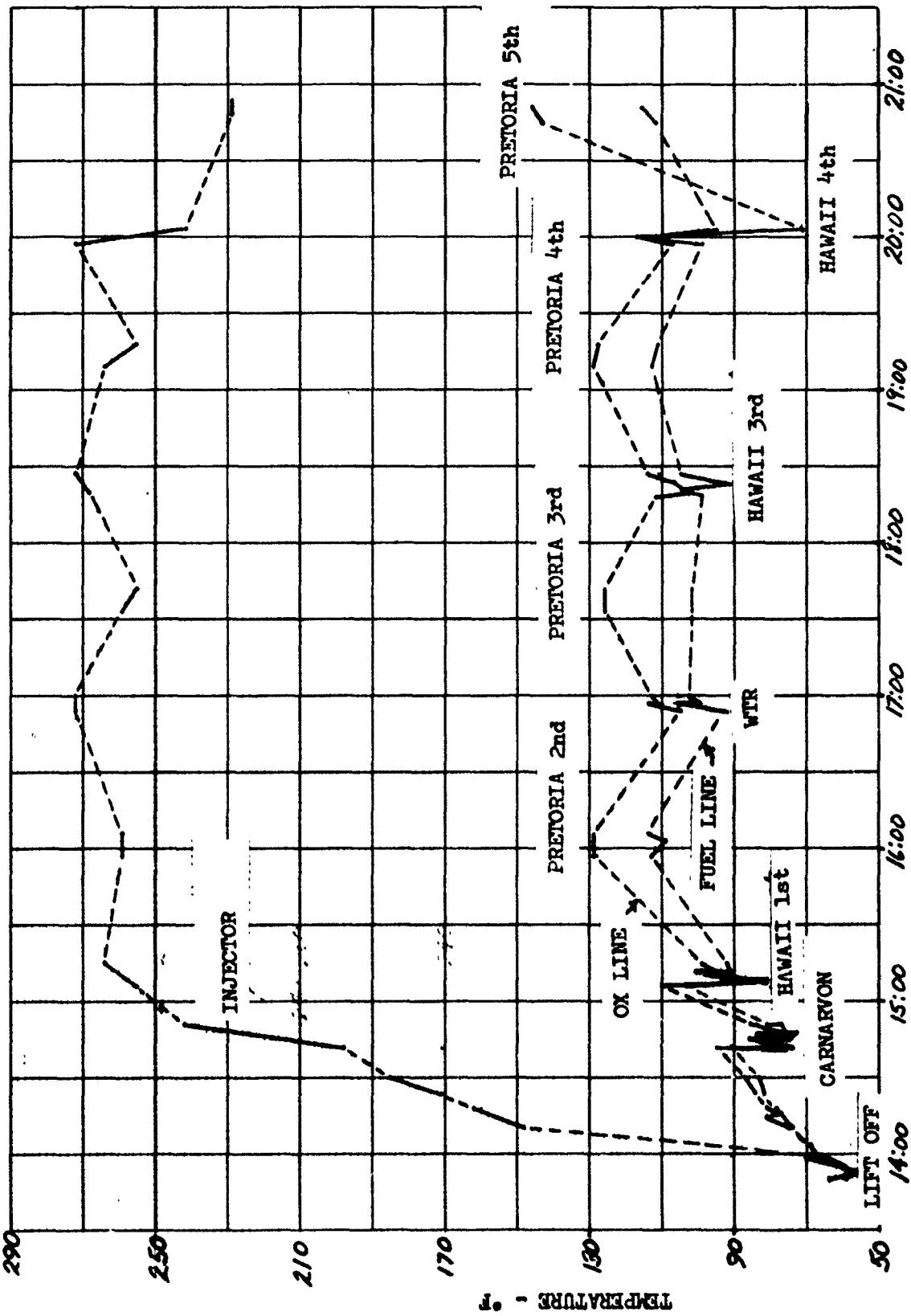
The total propellant consumption based on the computed column would be 86 pounds rather than 111.7 pounds. This would have left more than enough propellants to complete the mission. The calculated consumption (111.7 pounds) is approximately ten pounds less than the minimum usable load. However, the analysis is necessarily based on extrapolation of most of the coast data. Considering the possible sources of error in the extrapolation techniques, the calculated consumption and minimum usable load are in reasonable agreement.

#### 3.2.1.8.4 Conclusions & Recommendations

The Article C-9 ACS system performed remarkably well even though required to operate in excess of specification limits. It is felt that the test program used to prepare the ACS engines for flight is adequate. No change in this test program is recommended at this time.

FIGURE 93

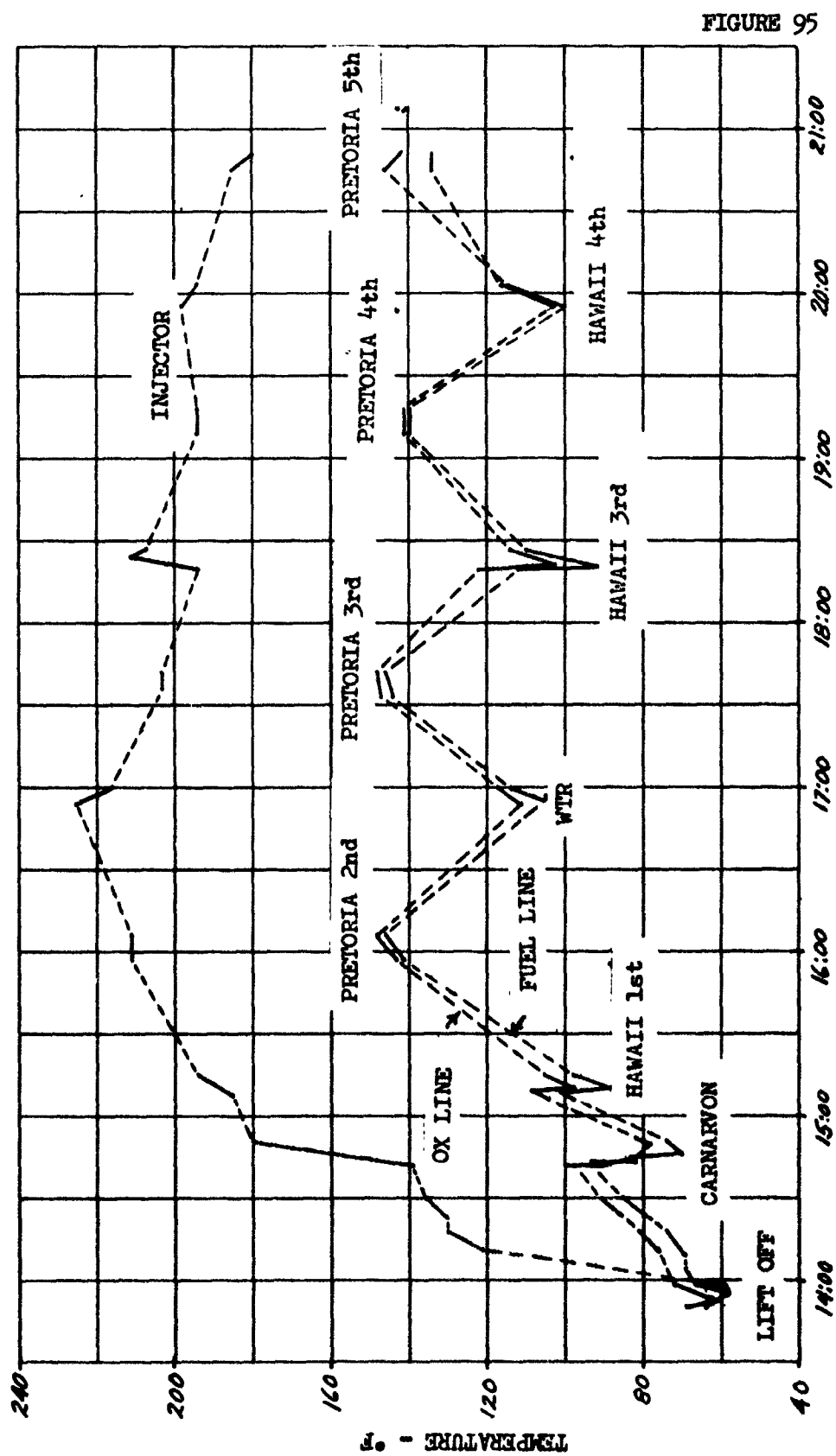
ARTICLE 9  
PITCH 1  
INJECTOR & PROPELLANT LINE TEMPERATURES



GMT TIME -- HOURS



ARTICLE 9  
PITCH 5  
INJECTOR & PROPELLANT LINE TEMPERATURES



**GET TIME -- HOURS**

### 3.2.2 Guidance and Controls

#### 3.2.2.1 Summary

The Flight Control System performance during the boost phase was normal with the exception of an actuator transient which was observed on Stage I subassembly 2 pitch actuator at Stage I shutdown. Transtage powered phases were also normal. At Gemini separation, the pitch up vehicle rate was less than predicted due to plume impingement from the retro rockets. The coast phases were characterized by extremely long ACS engine on times which were attributed to the reduced control torque resulting from the presence of large pitch and yaw ACS engine plume impingement moments. In addition, the ACS Guidance Backup Mode logic of the Guidance Computer program was utilized, in yaw, to pulse the ACS engines the programmed maximum number of cycles.

#### 3.2.2.2 Configuration

The Flight Control System configuration for Vehicle #9 differed from that of Vehicle #12 in that the autopilot gains and dynamics were completely revised to accommodate the longer and heavier payload (MOL-HSQ) and experiments. This also included an additional gain state for Stage I and quadratic filters for the Stage II pitch and yaw rate channels. In addition, the Stage II actuator attach points on the injector dome were modified to provide an increased moment arm from 10.04 inches to 14.00 inches (TIII-B Stage II configuration). This increased moment arm and the TIII-B sustainer actuators (PD46S0002-519) were used for increased stability. The TIII-B sustainer actuators had an increased stroke and incorporation of pressure feedback in the valve assembly to provide additional damping.

The coast control portion of the autopilot included capability of pitch roll mixing to augment the pitch thrust after Gemini separation in order to achieve a desired pitch up rate of 3 degrees/second.

#### 3.2.2.3 Data and Analysis

Review of the Vehicle #9 data indicates that the performance of the Flight Control System for all powered phases of flight was satisfactory. Control authority was significantly reduced during coast phase due to large unanticipated plume impingement moments resulting from the extreme forward location of the C.G. as a result of the MOL-HSQ vehicle configuration.

### 3.2.2.3.1 Stage "0"

Stage "0" start and liftoff transients were negligible. The lockout of the Guidance System ladder commands until liftoff plus 0.98 seconds occurred as programmed. The roll program was executed at L/O + 6.2, for a 3 second duration, at a rate of 2.4 degrees/second-clockwise, to roll the vehicle until the pitch plane of 107.25 degrees was attained. The steady state roll error during this time was 1.23 degrees. Pitchover maneuver began at L/O + 10.2 seconds with a rate of 1.4 degrees/second. Steering throughout the remainder of Stage "0" flight was moderate and remained well within limits.

#### Load Relief

The Lateral Accelerometer Sensing System (LASS) was employed during autopilot gain state #2 from L/O + 40.5 to L/O + 81.5 to provide structural load relief for periods of maximum aerodynamic pressures. The maximum accelerations during this interval were 0.238 g's and 0.143 g's in yaw and pitch respectively. The peak yaw acceleration and steering error of  $2.46^\circ$  during LASS operation closely correlated with the preflight wind recordings of 125 nautical miles per hour from the north at 40,000 feet. Upon termination of LASS operation, the Guidance System smoothly drove the error to null in yaw.

#### Stage O/I Staging

Guidance steering errors were small during Stage O I staging, the largest being -0.88 degrees in roll as a result of the normal roll moment imparted by separation of the solids. The roll rate reached a maximum of 1.5 degrees/second and returned to zero at separation plus 2 seconds.

### 3.2.2.3.2 Stage I

At Stage I start, the engines centered within less than 0.4 seconds as the turbine driven hydraulic pump brought hydraulic pressure up to normal operating level of 3000 psi. The absence of Guidance System rate limited gimbal commands 3 seconds after separation indicated a smooth transition from open loop to closed loop (explicit) steering. Steering errors were close to null for the remainder of Stage I flight.

### 3.2.2.3.2 Stage I - (Cont.)

#### Stage I Shutdown

At Stage I shutdown (L/O + 258.2) a transient was observed on the subassembly 2 pitch actuator ( $l_1$ ). In 10 milliseconds, T/M measurement #1233 indicated a spike of 2 degrees retract on the  $l_1$  actuator with several more spikes observed in less than 200 milliseconds. The pitch VDA output, T/M measurement #1258 indicated both positive and negative spikes at approximately the same time. The Stage I & II rate gyros showed the usual vibrations that occur at shutdown. Results of the investigation of the actuator disturbance is covered under paragraph 3.2.2.4.

### 3.2.2.3.3 Stage II

During Stage II flight, the guidance steering errors were extremely smooth. Closed loop steering began at 91FS1 + 4.3 seconds. Pitch up rate limiting of 0.9 degrees per second was required for the initial 4 seconds. Small pitch corrections were required to maintain the vehicle pitch-down rate until Stage II shutdown. Staging was very smooth and the maximum attitude errors between Stage II shutdown and first transtage ignition were -0.43 degrees, -0.37 degrees and + 0.35 degrees in pitch, yaw and roll respectively.

### 3.2.2.3.4 Stage III First Burn

At Stage III ignition, the steering errors in pitch and yaw were small, indicating the thrust vector was passing through the C.G. of the vehicle. Open loop guidance steering began at 138FS1 + 4.3 seconds with a 7 second pitch down rate limit. The vehicle pitch down rate of 1 degree/second reversed at 138FS1 + 12.5 seconds and the steering transient was nulled out within 3 seconds. The Guidance System entered pitch down rate limiting three additional times during this burn and correlate with programmed steering events for this mission.

### 3.2.2.3.5 Retro/Pitch-Up Maneuver

The Retro/Pitch-Up Maneuver performed immediately after Gemini separation did not occur as anticipated. It was predicted that a 2 degree/second pitch-up rate would be imparted to the vehicle due to the retro-fire. However, due to retro plume impingement, a pitch-down rate initially of 0.17 degrees/second which increased to a maximum of 0.547 degrees/second was observed.

### 3.2.2.3.5 Retro/Pitch-Up Maneuver - (Cont.)

The vehicle experienced a pitch-down torque of approximately 1650 ft-lbs for 2.5 seconds. The ACS, which also employed pitch/roll mixing to augment the pitch-up thrust, performed as expected considering the pitch-down torque. Figure 96 shows the commanded, expected and actual pitch attitude history during this maneuver.

### 3.2.2.3.6 Stage III - Second Burn

Pitch and yaw errors again were extremely small prior to main engine ignition, indicating again that the thrust vector alignment with the vehicle C.G. was very good. At ignition plus 4.4 seconds, Guidance closed loop steering commenced resulting in a small pitch transient. After the damping out of the initial transient, steering became moderate, although, due to the much higher autopilot gains for the MOL-HSQ configuration and the derived rates, the travels appeared to be somewhat more active than those of previous flight plans.

### 3.2.2.3.7 Stage III - Third Burn

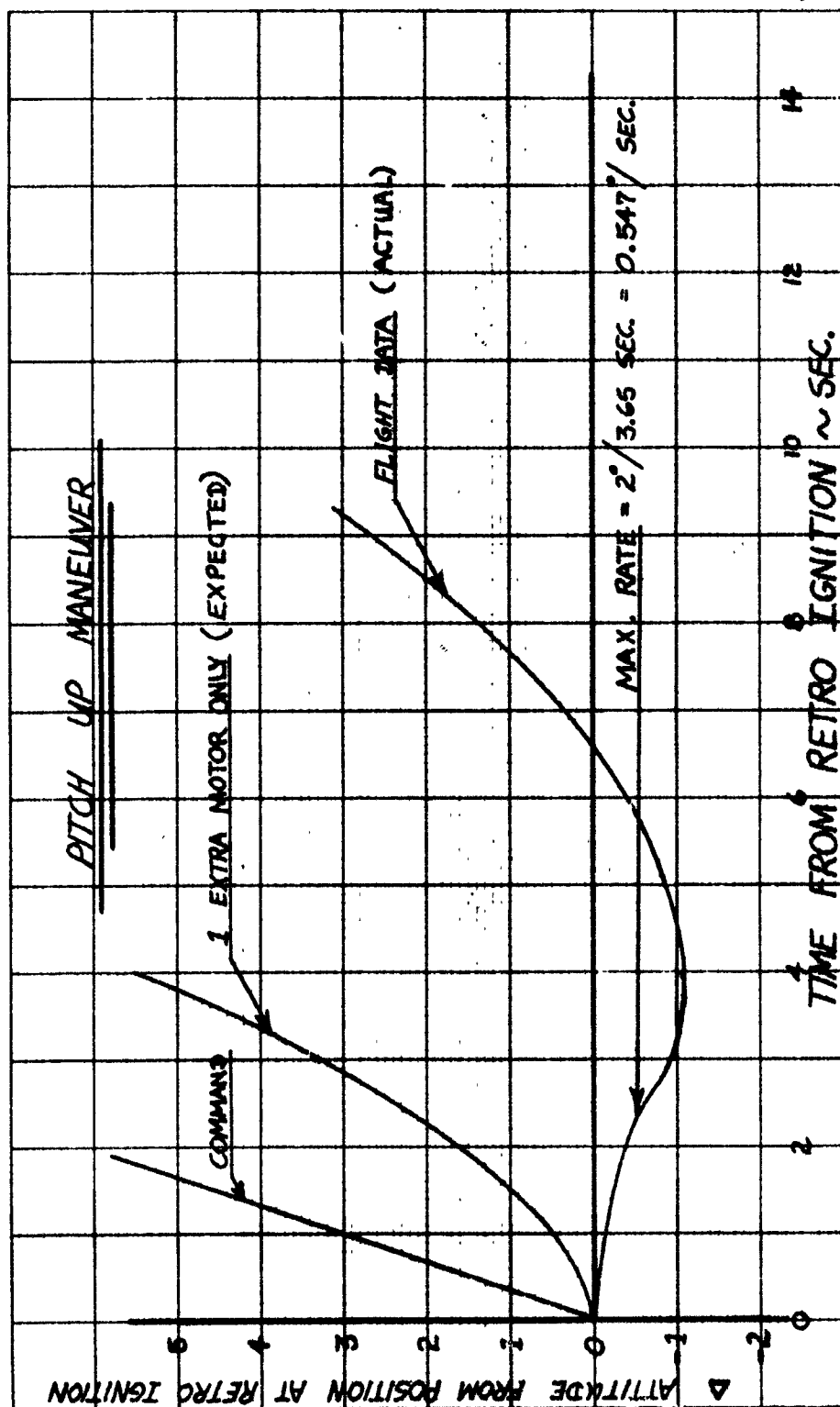
Third burn duration was only 9 seconds. Errors at main engine ignition were virtually non-existent. Actuator travels were very smooth up until shutdown.

### 3.2.2.3.8 Attitude Control System Operation

Analysis of the ACS data during the coast periods showed the ACS Guidance Backup Mode (GBUM) was utilized to pulse the ACS engines for the programmed maximum number of cycles. The first two cycles were during the transfer orbit over Ascension Island and Pretoria, and both GBUM's pulsed the yaw nozzles. From the Guidance computer word (NACS) count, it is known that two cycles of GBUM ACS pulsing occurred between Pretoria pass 1 and Hawaii pass 1. Likewise, one cycle of GBUM pulsing occurred between Hawaii pass 1 and ETR pass 1. Also, two cycles of the pulsing occurred between ETR pass 1 and Pretoria pass 2, and the last three cycles occurred between Pretoria pass 2 and South Vandenberg AFB pass 2. The three periods of observed GBUM ACS pulsing were verified to have occurred on the yaw engines. The yaw attitude errors during these periods displayed near identical characteristics. The yaw error exceeded the -3.1 degree level for the required 10 seconds prior to each GBUM ACS pulsing cycle.



FIGURE 96



### 3.2.2.3.8 Attitude Control System Operation - (Cont.)

During analysis of the data, it became obvious that actual engine-on-time was much greater than that which was predicted. Results of an ensuing study revealed that the plume of the aft pointing ACS engines ( $N_1$ ,  $N_3$ ,  $N_5$  and  $N_7$ ) impinge upon the missile skin with a force of approximately 8 lbs. This force acts normal to the missile skin at approximately station 140. Referring to Figure 97, note that the measured change in yaw attitude rate is a factor of 2 less than the anticipated change in rate based on a knowledge of engine on time, thrust and inertia. Therefore, an impingement which degraded the control capability of the ACS was implied. Since the impingement reduces the control capability of a pulse from an aft pointing engine by approximately 2, it would be expected that engine on time would increase by a factor of 2. Flight data has verified this contention. Impingement effects are not noticeable on the roll nozzle orientation. Therefore, the net impingement effect in Pitch during pitch/roll mixing was very small.

The occurrence of all available GBUM's during this flight may be attributed to the ACS plume impingement which resulted in the reduction of control torques in pitch and yaw. Referring to Figure 98, it is observed that after the first GBUM cycle, the system excursion is again beyond the sensing level. The dotted line depicts the no-impingement trajectory which indicates clearly that an additional GBUM cycle would not have been triggered.

No GBUM cycles occurred in pitch or roll. Impingement does not affect the roll ACS engines and therefore was not a problem. The roll steering error indicated that the vehicle roll attitude was being controlled by the first one shots which are set at  $\pm 1.85$  degrees. The pitch steering error illustrated that ACS variable pulses (four pulses occurring approximately every 90 seconds) maintained the pitch vehicle attitude between  $-2.5$  degrees and  $-3.3$  degrees. In the pitch channel, the guidance command function changes state every few seconds to maintain a "belly-down" vehicle attitude. Therefore, the system was not allowed to maintain a value of error above the sensing level for the required 10 seconds. While this effect did not prevent the vehicle pitch attitude error from attaining the sensing level, it did cause the sensing level timer to be reset before a GBUM cycle could be issued.

YAW ATTITUDE VS. TIME (PRE 1<sup>ST</sup> PASS)

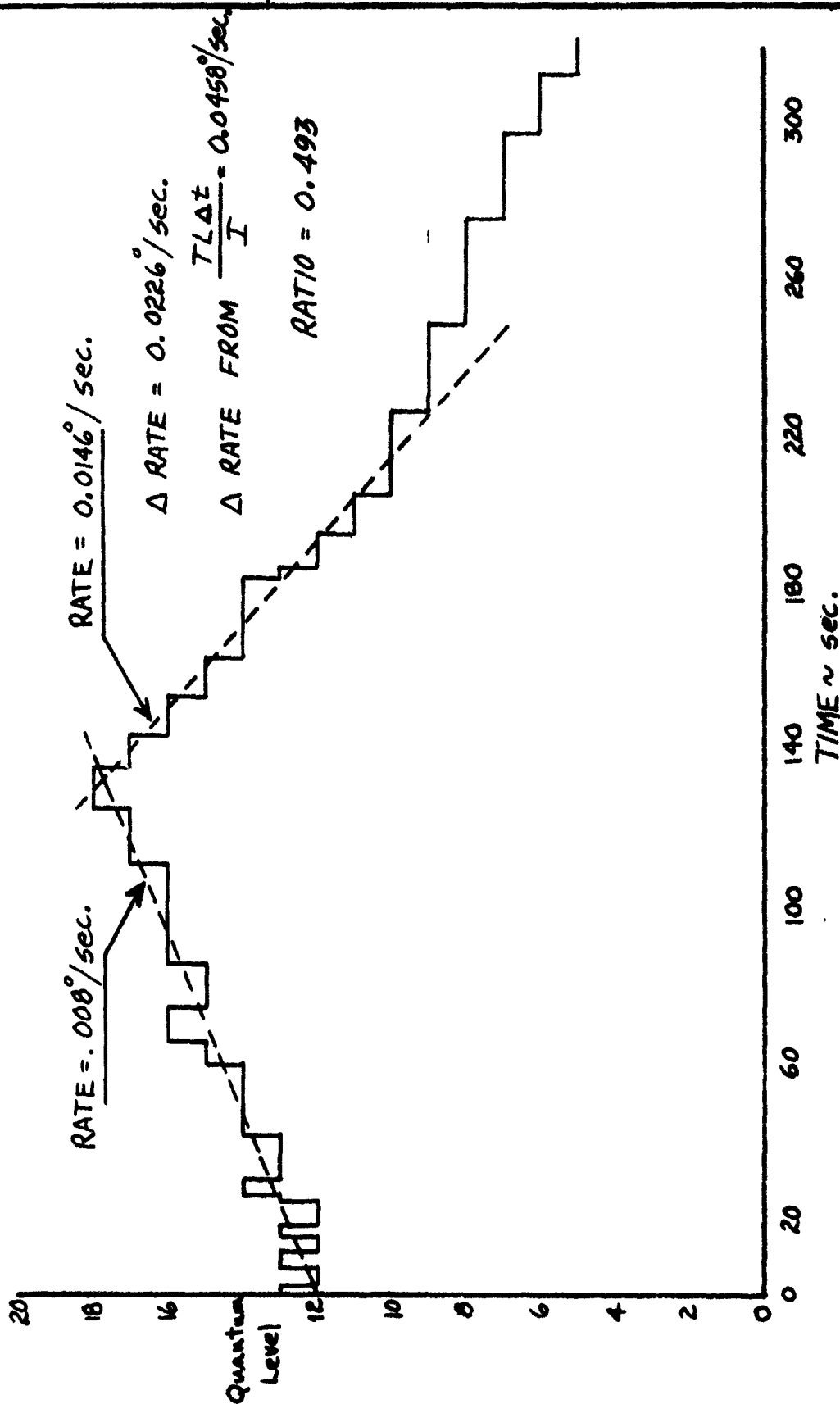
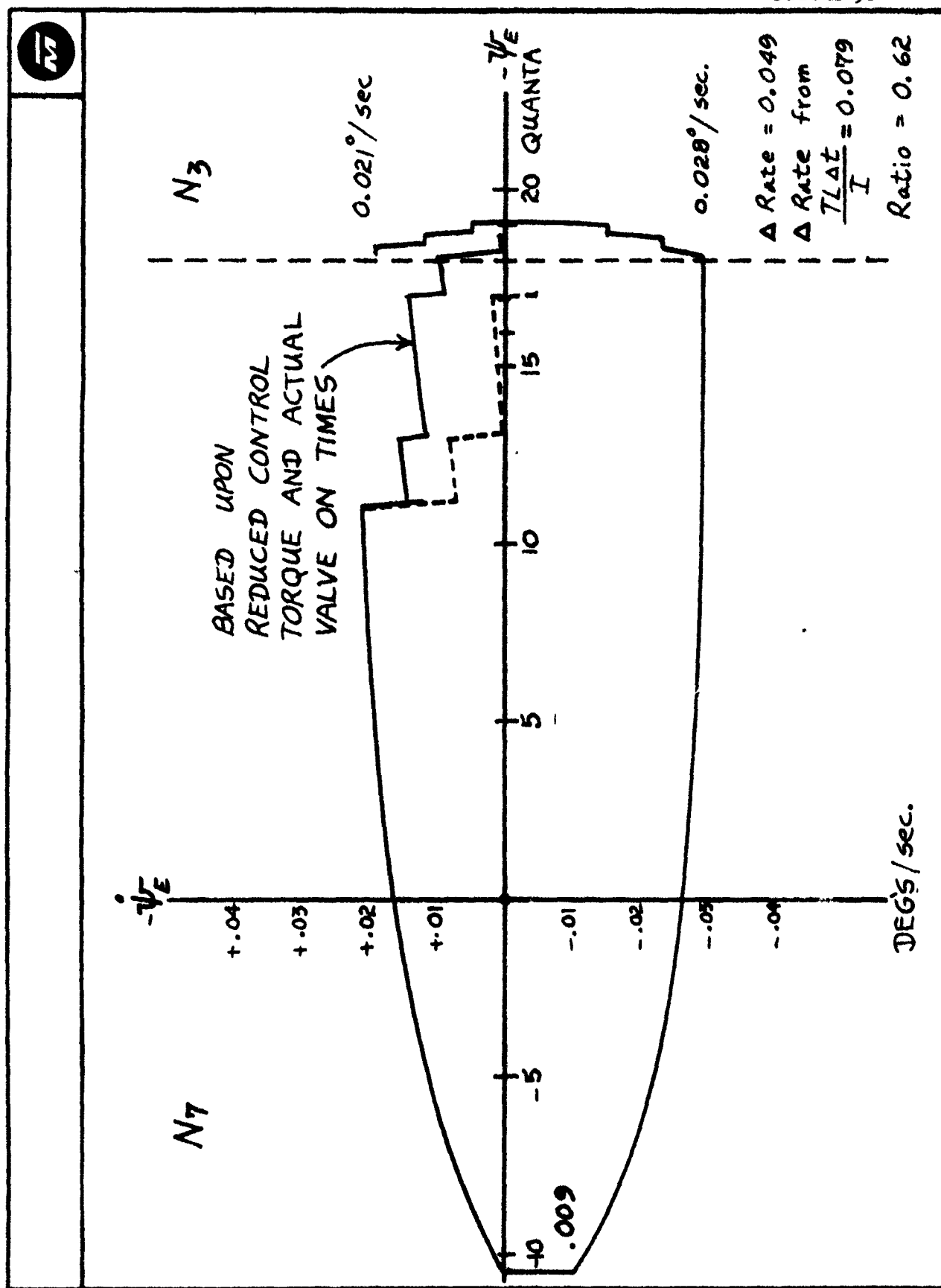


FIGURE 97

FIGURE 98



### 3.2.2.3.8 Attitude Control System Operation - (Cont.)

Analysis of steady state coast data has not indicated any unexpected torques. Speculation in some areas arose concerning possible unknown torques occurring in the yaw plane during the first pass over ETR (L/O + 6060 to 6225 seconds). The speculation arose because of N<sub>3</sub> engine on times which were inconsistent with calculated responses due to PTC torque alone. Further investigation has disclosed that the system was not operating in a steady state condition, but rather was damping out a transient. It is known that GBUM cycles occurred immediately prior to data acquisition (L/O + 6060 seconds). Therefore, it is concluded that the N<sub>3</sub> activity was due entirely to damping of the transient induced by the previous GBUM cycle.

No variable pulse output was obtained when the steering errors increased from the 15th to the 16th quantum level in pitch and yaw for the Vehicle #9 autopilot. However, this is well within hardware mechanization tolerances and is not considered anomalous.

### 3.2.2.4 Special Considerations

Investigation of the subassembly #2 pitch actuator disturbance at 87FS2 referred to on page 193 has revealed the following:

(1) The actuator is incapable of forcing the engine with observed rates indicated in actuator travels. The maximum velocity limit of the actuator is 33.2 degrees per second. In order for the actuator to have moved 2 degrees in 10 milliseconds, the actuator velocity would have been 200 degrees per second.

(2) Subassembly #1 pitch actuator (4<sub>1</sub>) shows absolutely no disturbance at this time.

(3) The pitch Valve Drive Amplifier (VDA) is common to both the 1<sub>1</sub> and 4<sub>1</sub> actuators.

(4) The actuator cannot respond to the observed VDA signals.

(5) No other actuator showed an oscillation at this time.

#### 3.2.2.4 Special Considerations - (Cont.)

(6) Oscillations in the actuator data precedes the VDA data oscillations.

(7) Assuming a constant force for 10 milliseconds, the torque required to move the engine 2 degrees is 140,000 ft-lbs.

(8) The distance from the edge of the engine bell to the gimbal pad is 6.17 ft. A side force of 22,690 lbs at the end of the bell would have been required.

(9) The calculated actuator differential pressure during this transient is 27,670 psid.

(10) AC Electronics reported no unusual shocks or vibrations on the Guidance System parameters at this time. However, environmental accelerometers located in the Stage I engine compartment (on the vehicle longeron and on the S/A 2 gimbal pad) indicated vibration levels at 2.5 to 10 g's.

(11) Vehicle #7 flight shows a similar anomaly at Stage I shutdown and is presently under investigation.

#### 3.2.2.5 Conclusions

(1) The Flight Control System did steer and maintain stable control of the vehicle's attitude and trajectory during SRM, Stage I, Stage II, and Stage III flight. (Primary Objective).

(2) The Stage I, Stage II and Stage III hydraulic systems performance was satisfactory. All parameters were within the specification limits (Secondary Objective).

(3) The Flight Control System maintained stable control of the vehicle during coast phases (Primary Objective) until ACS propellants were depleted as a result of the reduction in control torque from plume impingement.

(4) The ACS system performed as would have been expected, had impingement effects been considered. No evidence of unexpected torques or any other anomalies have been identified at this time.

### 3.2.2.5 Conclusions - (Cont.)

(5) No derived rate pulse output was obtained at the -16 quantum level ( $2.8^\circ$ ) in Pitch and Yaw for the Vehicle #9 autopilot. However, this is well within hardware mechanization tolerances and is not considered an anomaly.

(6) The Lateral Acceleration Sensing System (LISS) operated satisfactorily during the Max Q Region (Secondary Objective).

(7) The unexplained actuator transient at Stage I engine shutdown is still under investigation. The transient does not appear to be Flight Control System self-induced.

### 3.2.3 A/B Electrical and MDS

#### 3.2.3.1 Summary

The airborne Electrical System performed satisfactorily through the entire mission time duration of seven (7) hours. This was the longest mission thus far in the TIIIC test program and is in excess of the 6.75 hour limit for which the power systems were designed.

#### 3.2.3.2 Configuration

The electrical system was of the basic configuration including: (a) current shunts to monitor all power systems except TPS and T & FS, (b) current shunts installed to monitor the Transtage Bi-propellant valves and heaters, (c) the Malfunction Detection System (MDS), and (d) an additional motor-driven-switch incorporated in the power transfer system to deactivate the CIPS, IGS, APS and IGS Arming Busses at approximately T + 25,200 seconds (7 hours) from Lift-off.

#### 3.2.3.3 Data and Analysis

##### 3.2.3.3.1 Accessory Power System (APS)

Meas. No. 1100 (APS Bus Voltage) - The APS bus voltage varied from about 27 to 29.5 volts, with about 0.75 volts peak-to-peak noise, throughout the flight. The specification bus limit is 26 to 31 VDC. The APS bus was showing about 29.5 volts at 20:50:41, which is just a few seconds short of the 7 hour transtage power deactivation time. Data acquisition ending at 20:50:41 did not cover the power deactivation event. (Lift-off occurred at 13:50:42.2)

Meas. No. 1117A (APS current) - The current drawn by the APS equipment varied from about 16.5 amps at lift-off (this is about 4.5 amps higher than that observed on vehicle no. 11 due to additional MDS load) down to 8 and 9 amps during the coast periods. Pulses of 4 to 5 amps (on top of the nominal 8 to 9 amps) lasting from 1/4 second to several seconds in duration were observed. These pulses were due to the pulsing of the ACS nozzles during Pitch-Roll-Mixing, Propellant Settling and normal vehicle attitude control maneuvers. One ACS maneuver of particular significance was the extended pitch up operation required to correct the residual pitch down rates following MOL/HSQ Lab ratro firing. APS current pulses continued in response to ACS demands throughout the coast period until depletion of the attitude control system propellants.



#### 3.2.3.3.1 Accessory Power System (APS) - (Cont.)

It has been established that ACS propellants were depleted at the end of the 4th pass over Hawaii at approximately 20:02:23. From this point on, the appropriate "correcting" ACS nozzles remained energized since no correcting action could take place. Under this condition, the APS current load was 12 amps until the 7 hour transtage power deactivation event.

#### 3.2.3.3.2 Continuous Instrumentation Power System (CIPS)

Meas. No. 1106 (CIPS Voltage) - The CIPS bus voltage varied between 28.5 and 30 volts from power transfer through the flight duration. Specification bus voltage limit is 26 to 31 VDC. The CIPS bus was assumed to be de-energized at the time of Transtage Power Deactivation at T + 25,200 sec. (7 hours).

Meas. No. 1118A (CIPS Current) - The current drawn by the instrumentation equipment was 6.2 to 7.8 amps throughout the flight.

#### 3.2.3.3.3 Switched Instrumentation Power System (SIPS)

Meas. No. 1107 (SIPS Voltage) - The SIPS bus voltage varied between 27.5 and 28.2 volts from power transfer throughout the flight. Specification bus voltage limits is 26 to 31 VDC.

Meas. No. 1119A (SIPS Current) - The current drawn by the instrumentation equipment varied between 21 and 21.5 amps throughout the flight when the equipment was switched on.

#### 3.2.3.3.4 Transient Power System (TPS)

Meas. No. 1102 (TPS Voltage) - The TPS bus voltage remained within limits during steady state conditions. The TPS battery satisfactorily started the hydraulic pump three times and supplied approximately 28 volts during the pump run periods. The battery also supplied sufficient power for all experiment ordnance and all MOL/HSQ Simulated Lab ordnance requirements.

#### 3.2.3.3.5 Inertial Guidance System (IGS)

The IGS batteries provided 23.5 to 24 amps to the IGS equipment throughout the flight until approximately the end of the fourth pass over Hawaii. At this time, due to the depletion of ACS propellants, the inertial platform was gimballed against its stops. This caused an increase in the torquing current to the gimbal torquers. This increase in torquing current caused the IGS current to increase from the nominal 23.5 amps to about 38 amps. This condition remained until the transtage power deactivation time, where it is assumed that the IGS bus was deactivated at about T+25,200 seconds (7 hours).

#### 3.2.3.3.6 Malfunction Detection System (MDS)

All MDS rate outputs (pitch, yaw, and roll) remained within the specified limits and provided satisfactory data at lift-off, staging, engine ignition and at other major events. The MDS pitch rate output verified the pitch down and the counteracting pitch up by the attitude control system which occurred at vehicle retrofire following Gemini separation.

#### 3.2.3.3.7 Stage II Instrumentation System

Meas. No. 1105 (Stg. II IPS Voltage) - The Stage II IPS bus voltage varied between 28.5 and 29 volts during the applicable portion of flight. Specification bus limit is 26 to 31 VDC. There was no random variation of the voltage after Stage II separation as has occurred on previous flights. This vehicle was modified by adding protection to the aft end of the instrumentation conduit to shield the wiring from the retro-rocket flame impingement. Apparently this modification eliminated the random voltage variations observed on prior flights.

Meas. No. 1120A (Stage II IPS Current) - the current drawn by the Stage II IPS equipment was approximately 26 amps through SRM flight and about 24 amps through Stage II flight. There was no random variation of the current after Stage II separation as observed on previous flights apparently as a result of the modification described above.

#### 3.2.3.4 Special Considerations

The transtage bi-propellant valve monitor provided verification data of the valve operation. The bi-propellant valve heater (which would turn on only if a leaky valve existed) did not turn on during any flight data acquisition period. The vent tube heater drew approximately 0.5 amps from power transfer (T-31 sec) to Transtage Power Deactivation.

The data indicated that the transtage propellant tank pressurization system operated in the correct sequence and the current drawn by the solenoids was normal.

As indicated by the successful Gemini separation and successful operation of the MOL/HSQ Lab functions, the vehicle sequence system, as modified for the MOL/HSQ Lab functions, performed as designed.

### 3.2.4 Tracking and Flight Safety Subsystems

#### 3.2.4.1 Summary

Telemetry measurements and information from ETR indicates that satisfactory operation was obtained from the Glotrac rate transponder, the pulse transponder and the two command receivers during flight of Vehicle C-9.

During the time that the Grand Turk command destruct transmitter (CDT) carrier was on, the two command receiver AGC's had anomalies like those experienced at WTR on TIIIB-2.

#### 3.2.4.2 Configuration

The subsystem consisted of the following major components:

- a. Glotrac Pulse Transponder (Motorola)
- b. Glotrac Rate Transponder (Azusa Type "G")
- c. Two Command Receivers (manned mode, 3.5 sec. delay)
- d. Glotrac RF System
- e. Command RF System
- f. Destruct System (ISDS in manned mode, 3.5 sec. delay)
- g. Telemetry Passive RF System (multiplexers, antenn., and junctions)

NOTE: RF coax switches were not used on Vehicle 9.

#### 3.2.4.3 Data and Analysis

##### 3.2.4.3.1 Glotrac Rate Transponder

Measurement No. 1014 and information from ETR indicates that satisfactory operation and tracking was obtained from the "G" type transponder. The approximate time Glotrac data was obtained is as follows:

### 3.2.4.3.1 Glotrac Rate Transponder - (Cont.)

<u>Station</u>	<u>Data Acquisition Time Periods</u> (seconds from lift-off)
Azusa Mk. II	-1800 to + 528
	+5731 to +6038
Atlantic Field	+ 147 to + 501
Burmuda	+ 255 to + 675
Jupiter	+ 27 to + 495
G.B.I.	+ 42 to + 576
	+5810 to +6285
Eleuthra	+ 74 to + 582
	+5806 to +6309
Grand Turk	+ 182 to + 703
	+5908 to +6440
Antigua	+ 363 to + 699

### 3.2.4.3.2 Glotrac Pulse Transponder

Information from ETR indicates that satisfactory operation and tracking was obtained. The approximate time pulse tracking data that was obtained are as follows:

<u>Station</u>	<u>Data Acquisition Time Periods</u> (seconds from lift-off)
Cape (Station 1.16)	0 to + 415
PAFB (Station 0.18)	+ 11 to + 534
Merritt Is. (Station 19.18)	+ 11 to + 520
	+ 5,738 to + 6,218
G.B.I. (Station 3.16)	+ 64 to + 365
(Station 3.18)	+ 74 to + 540
Grand Turk (Station 7.18)	+ 225 to + 704
Antigua (Station 91.18)	+ 417 to + 831
Ascension (Station 12.16)	+ 1,245 to + 1,660
(Station 12.18)	+ 1,360 to + 1,956
Pretoria (Station 13.16)	+ 2,009 to + 2,383
	+ 7,661 to + 8,111
	+12,849 to +13,878

### 3.2.4.3.3 Command Receivers

Measurements 1002, 1006 and 1008 indicated that satisfactory command control coverage was maintained. The following ground transmitter handovers were recorded on Command Receiver AGC measurements and verified with ETR.

### 3.2.4.3.3 Command Receivers - (Cont.)

<u>Station</u>	<u>Carrier on (Zulu)</u>	<u>Carrier Off (Zulu)</u>
Cape	1327:29	1352:25
G.B.I.	1352:24	1355:25
Grand Turk	1355:24	1358:26
Antigua	1358:24	1404:34
		1405:31

### 3.2.4.3.4 Telemetry RF System

Listed below are times and stations of telemetry data acquisition. Satisfactory operation of the telemetry RF system was obtained:

<u>Station</u>	<u>Time</u>
Tel IV (Launch)	13:49:30/13:52:50
G.B.I. (Launch)	13:52:20/13:58:40
Antigua (Launch)	13:56:24/14:04:38
Ship (RIS)	14:01:38/14:08:09
Ascension	14:11:04/14:18:42
Pretoria (Pass #1)	14:23:13/14:30:35
Carnarvon	14:41:33/14:50:43
Barking Sand (Pass #1)	15:06:35/15:15:16
Hawaii (Kokee Partk) (Pass #1)	15:06:35/15:15:16
Tel IV (Pass #1)	15:31:35/15:34:28
Pretoria (Pass #2)	15:57:43/16:05:35
Barking Sands (Pass #2)	T/M Off
Hawaii (Kokee Park) (Pass #2)	T/M Off
SVAFB (Pass #2)	16:53:30/16:59:01
Pretoria (Pass #3)	17:33:38/17:41:37
Barking Sands (Pass #3)	18:19:48/18:26:43
Hawaii (Kokee Park) (Pass #3)	18:19:48/18:26:43
Pretoria (Pass #4)	19:09:21/19:17:17
Barking Sands (Pass #4)	19:55:10/20:02:25
Hawaii (Kokee Park) (Pass #4)	19:55:00/20:02:25
Pretoria (Pass #5)	20:45:03/20:50:41

### 3.2.4.4 Special Evaluation

#### 3.2.4.4.1 Command Receiver AGC Anomalies

During the period that the Grand Turk command destruct transmitter (CDT) was on the air, TLM measurements 1002 and 1006 showed the following voltage anomalies over a 2 second period (approx.)

3.2.4.4.1 Command Receiver AGC Anomalies - (Cont.)

	<u>1002</u>	<u>1006</u>
1355:56	2.1 VDC to 1.5 VDC to 1.8 VDC	2.0 VDC to 1.6 VDC to 1.8 VDC
1356:18	2.1 VDC to 1.8 VDC to 2.15 VDC	2.0 VDC to 1.75 VDC to 2.0 VDC

The observed Command Receiver AGC anomalies on Vehicle C-9 were similar to those observed on Vehicle TIIIB-2. In both cases the drop in Command Receiver AGC voltage coincided with signal strength data received from ground stations at both ranges during the two flights (C-9 and B-2). Similar variations are seen on telemetry received signal strengths. It is concluded that the Command Receiver AGC and telemetry received signal strength variations are a direct function of the individual ground station radar antenna control system. The radar system controls both the telemetry receiving antenna position and the range safety transmitting antenna position. Radar hunt will result in variations of the slaved antenna positions and therefore cause variations in received signal strengths. Command Receiver AGC received signal strength on C-9 flight was still substantially greater than the range minimum requirements even during the period of fluctuations.

The signal strength at the command receivers went from 550 microvolts to 100 microvolts (approx.) or -55 dbm to -68 dbm which is at least 32 db above the 1.0 micro volt sensitivity of these command receivers.

3.2.4.5 Conclusion

Satisfactory operation was obtained from the Tracking and Flight Safety subsystems and vehicle antenna systems during the flight of vehicle SSLV5-9.

### 3.2.5 Airborne Instrumentation System

#### 3.2.5.1 Summary

The airborne instrumentation system performance was nominal throughout the Article 9 mission.

#### 3.2.5.2 Configuration

A total of 344 measurements were programmed for this flight and distributed as follows:

- Transtage PCM/FM System - 153 measurements
- Stage II PCM/FM System - 176 measurements
- Stage II SSB/FM System - 15 measurements

In addition to the telemetered data, two recoverable cameras were flown on this vehicle to evaluate SRM/core separation.

#### 3.2.5.3 Data and Analysis

##### 3.2.5.3.1 Instrumentation System

All measurements of instrumentation system parameters indicated nominal performance of the system. The regulated power supplies, PCM encoders, SSB modulator, transmitters and airborne cameras performed within design specifications.

##### 3.2.5.3.2 Other Systems

Two temperature monitors on the transtage engines which utilize Aerojet supplied end instruments failed during flight. These two measurements are as follows:

- Meas. No. 3077 - Temperature Nozzle Flange Outboard S/A4: Thermocouple appears to open up at 14:02:25

- Meas. No. 3081 - Temperature Nozzle Exit S/A4: Thermocouple appears to open up at 14:03:41.



#### 3.2.5.3.3 Special Considerations

The erratic data from the Stage II PCM which has been experienced on past flights at Stage II/III separation was not evident on this vehicle. It is concluded that the added protection from retro-rocket flame impingement provided at the aft end of the instrumentation conduit was probably the contributing factor in this improvement and it has been recommended that this modification be employed on future vehicles.

### 3.2.6 Vehicle Environmental Analysis

#### 3.2.6.1.1 Summary

Fluid Dynamics instrumentation acquired data in the areas of skin temperatures, surface pressures, compartment pressures and heating rates. Data evaluation is primarily in the area of boost phase.

Vehicle 9 flight demonstrated no measurement anomalies in Fluid Dynamics instrumentation and no measurements exceeded success criteria. The aeroheating environment was significantly lower for this flight than for previous flights. Aeroheating indicator was  $84 \times 10^6$  lb/ft-sec. as compared to  $98 \times 10^6$  for Vehicle 11. Skin temperatures were generally  $50^\circ$  to  $100^\circ$  lower than for previous flights. Step "zero" base heating environment was very consistent with previous flights and compartment venting was normal.

#### 3.2.6.1.2 Data and Analysis

Figures 99, 100 and 101 present typical representative data in the areas of aeroheating, base heating and compartment venting respectively. Comparison is made with Vehicle 11.

Table 24 is a general listing of aerothermal measurements on this flight and Figures 102 thru 126 are time histories of those measurements.

All measurements are considered consistent with the vehicle trajectory with the exception of Meas. No. 2238, Retro Fairing Temperature (Figure #114). This measurement is considered questionable, there being no suitable explanation for the noted temperature drop at approximately 108 seconds. Shock at this time from Stage I ignition may have separated the thermocouple from its mounting structure while retaining a junction.

#### 3.2.6.1.3 Special Evaluation

Special evaluations were conducted in two areas. The first was an evaluation of possible transtage skin burn through resulting from the extended operation of roll attitude control nozzles at Gemini separation. The second was an investigation of forces on the vehicle resulting from impingement of both retro-motor and ACS exhaust plumes upon adjacent structure.

Figure 127 is a time history plot of transtage skin temperatures in the vicinity of the ACS nozzles. These measurements show no indication of a skin burn-through.

Computation of forces due to plume impingement effects were based on empirical data collected by NASA and by AEDC. These data were extrapolated to meet the conditions of the retro motor and ACS pitch nozzles and yielded impingement forces of 177 lbs for the retro motor and 8 lbs for the ACS nozzles. Clustering effects of the retro motors were considered to be insignificant in view of the relatively large distances between the retro motors. The analyses assumed conical shaped pressure distribution as indicated by the references. The report numbers referred to are listed below:

1. NASA TND-2326 (Cold Jet)
2. AEDC TDR 63-214 (Hot Jet)
3. AEDC TDR 63-247 (Hot Jet)
4. AEDC TN 60-223 (Cold Jet)

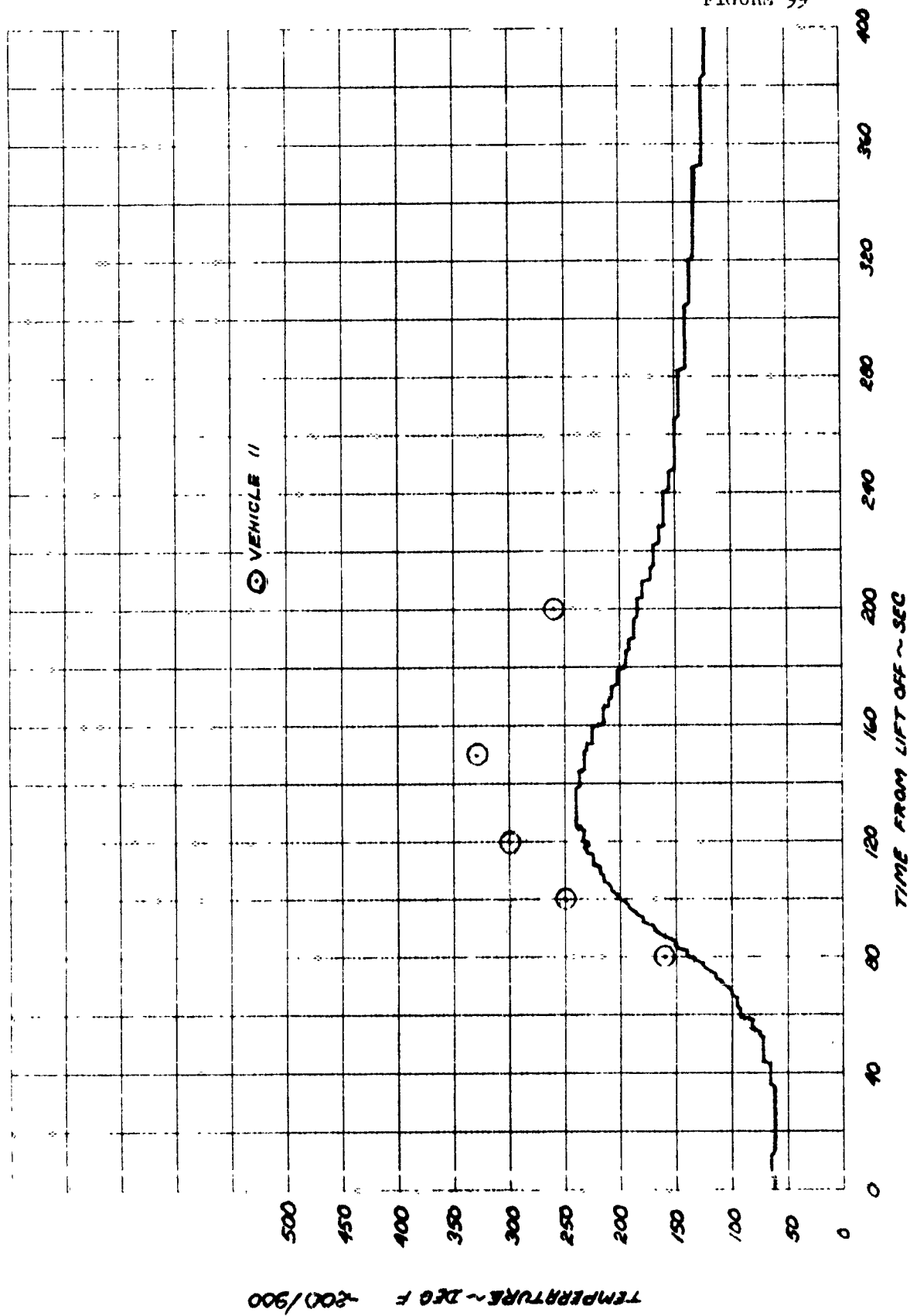
TABLE 24  
SLV 9 AEROTHERMAL MEASUREMENTS LIST

<u>Meas. No.</u>	<u>Description</u>	<u>Range</u>
STAGE I		
2224	Press Compt 1B	0/15
2236	Temp Stringer Vent Area	0/1000
2244	Press Base 210 Deg Stage I	0/20
2251A	Press Dif Acr Ht Shd Vent Area 90 Dg	-1/1
2252	Press Diff Acr Heat Shd Base 90 Deg	-1/1
2253	Press Diff Acr Heat Shd Sde Stn 1250 90 deg	-1/1
2254A	Press Dif Acr TCA Closure S/A 1	-1/1
2255	Press Inside TCA S/A 1	0/20
2255	Press Inside TCA S/A 1	0/20
2283	Temp Aft Frame Inside 73 Deg Sta 1225	0/1000
2662	Temp Outside Base Heat Shd 90 Deg	0/1000
2663	Temp Inside Heat Shd Stn 1300 90 Deg	0/1000
2664	Temp Inside Heat Shd Stn 1300 180 Deg	0/1000
2666C	Total Cal Heat Shd Base 135 Deg	0/15
2667C	Conv Cal Heat Shd Base 135 Deg	0/10
STAGE II		
2205	Press Diff Across Skin 180 Deg	-5/5
2206	Press Diff Across Skin 270 Deg	-5/5
2207n	Press Compt 2A	0/2

TABLE 24 - (Cont.)  
SLV 9 AEROTHERMAL MEASUREMENTS LIST

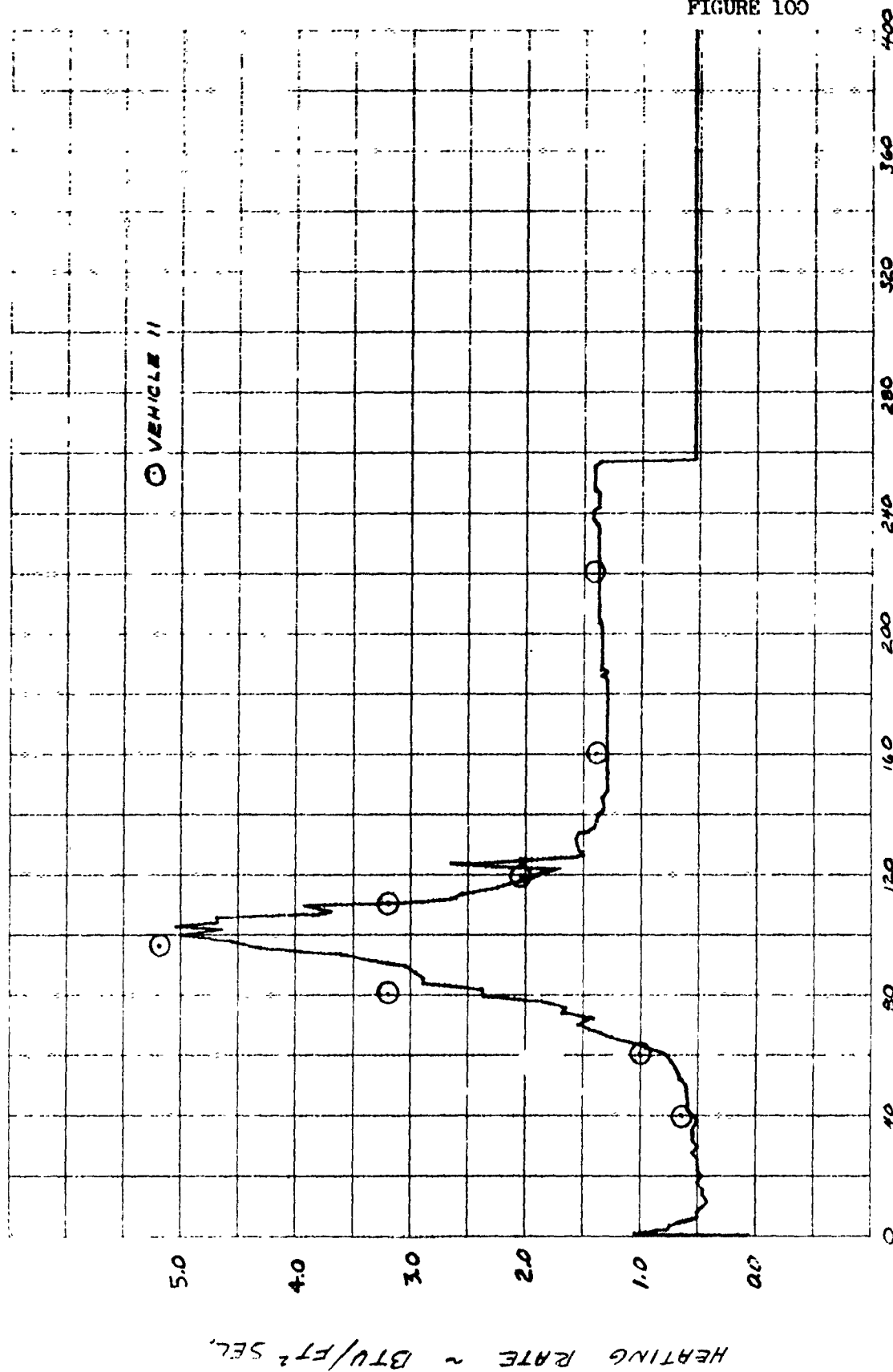
<u>Meas. No.</u>	<u>Description</u>	<u>Range</u>
2208	Temp Shock Impingement Sta 445 WL60	0/1000
2209	Temp Shock Impingement Sta 400 WL60	0/1000
2210	Press Diff Across Vehicle 0-180 Deg	-10/10
2211	Press Diff Across Vehicle 90-270 Deg	-10/10
2212	Press Compt 2B	0/15
2213	Press Buffet	-5/5
2214	Press Buffet	-5/5
2215	Press Buffet	-5/5
2216	Press Buffet	-5/5
2217	Temp Shock Impingement Sta 490 WL60	0/1000
2219	Temp Shock Impingement Sta 490 Target	0/1000
2221D	Press Compt 2C	0/2
2237	Temp Skin Front of Retro, Stg II	0/1000
2238	Temp Skin on Retro Fairing, Stg II	0/1000
2246	Temp Shock Impingement Sta 360 WL60	0/1000
TRANSTAGE		
2239	Temp Skin Sta 112 90 Deg Off Tgt	-200/900
2240	Temp Skin Sta 117 10 Deg Off Tgt	-200/900
2241	Temp Skin Sta 117 105 Deg Off Tgt	-200/900
2242	Temp Skin Sta 117 190 Deg Off Tgt	-200/900

FIGURE 99



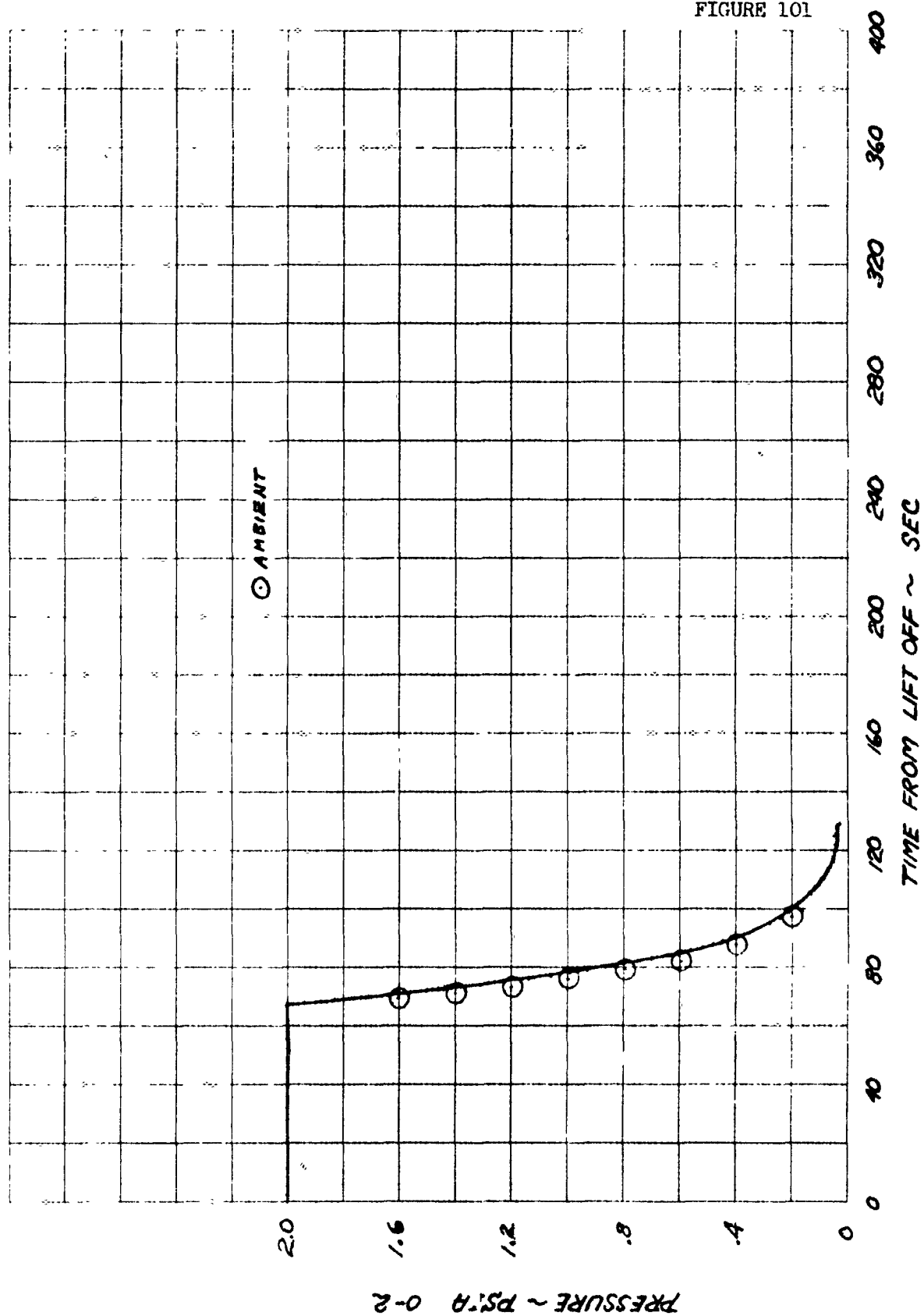
SLV-9 TEMP SKIN, STATION 117, 10° OFF TARGET MEASUREMENT NO. 2240

FIGURE 100



SLV-9 CONV. CAL. HEAT SHIELD BASE 135° MEAS. NO. 2667C

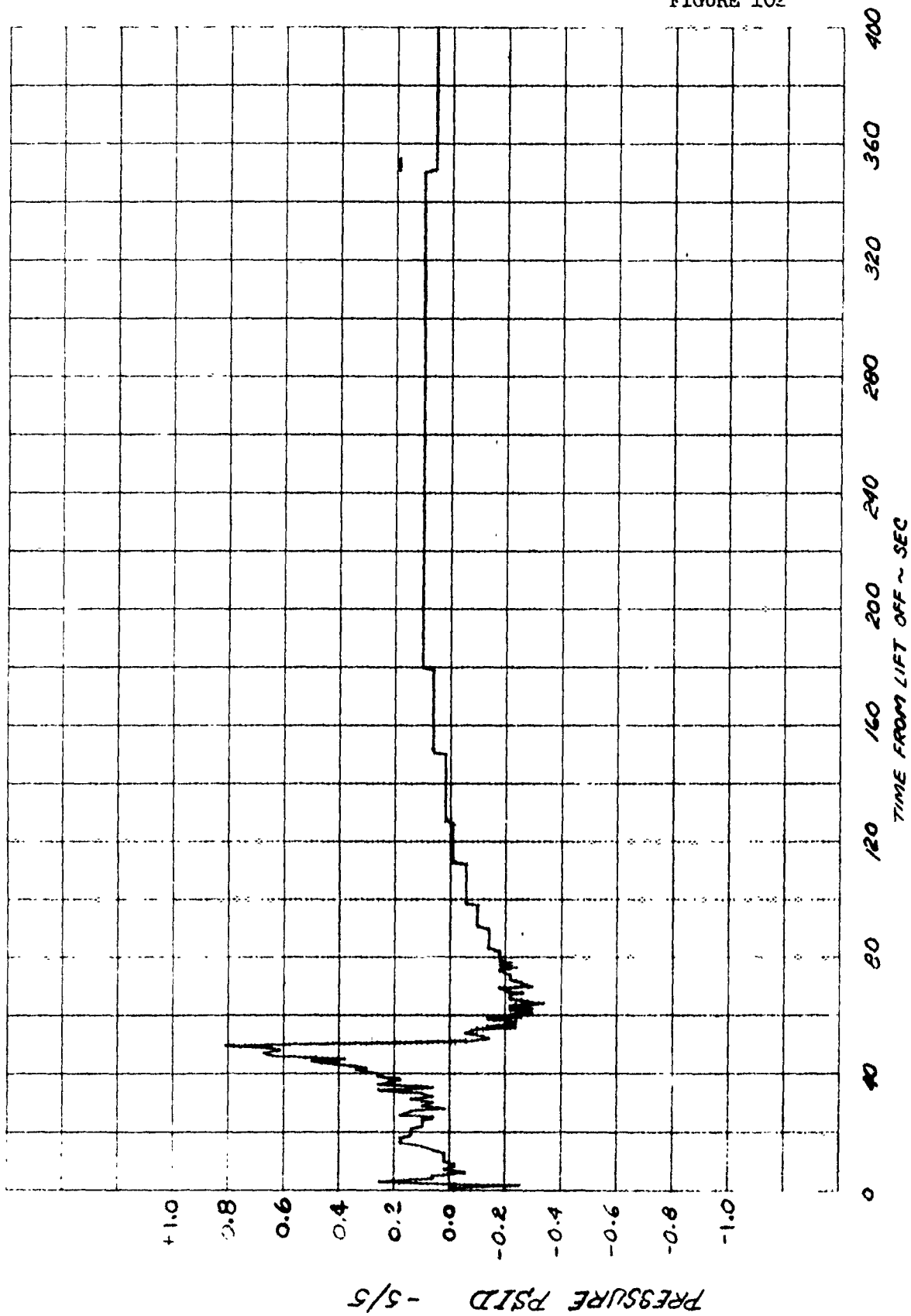
FIGURE 101



SLV-9 PRESSURE COMPARTMENT 2A MEASUREMENT NO. 2207D

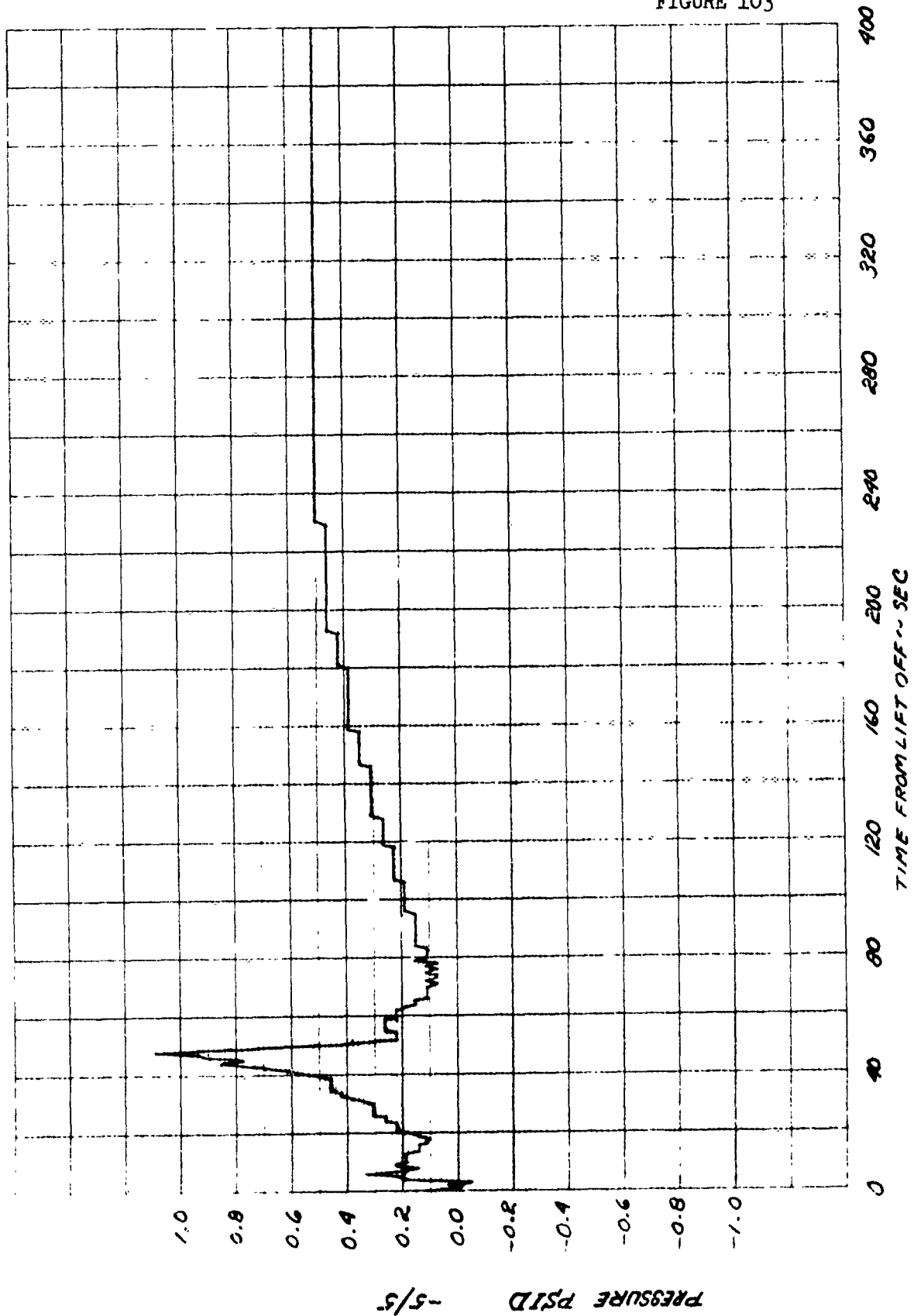


FIGURE 102



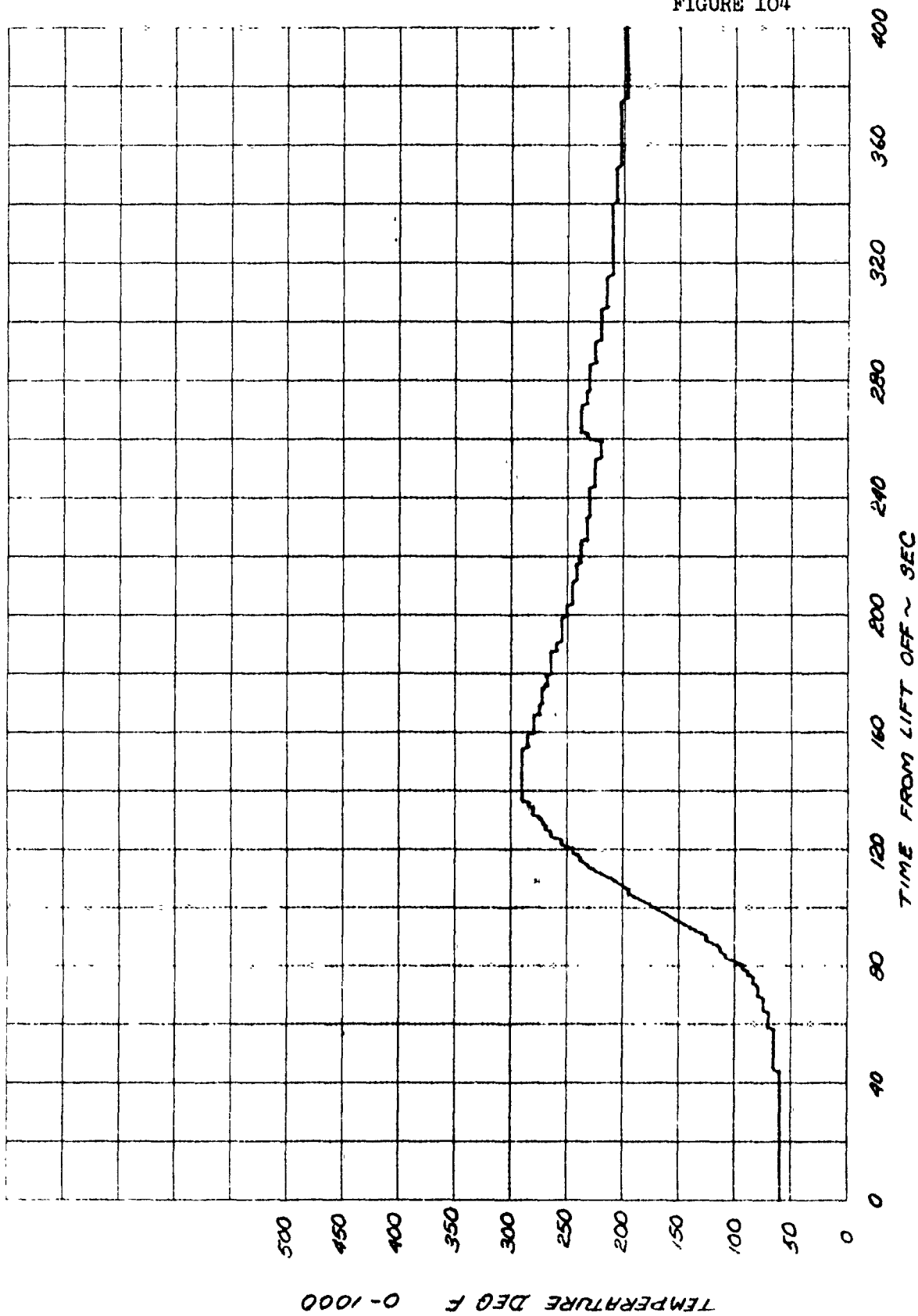
SLV-9 PRESS DIFF ACROSS SKIN 180 DEG MEASUREMENT NO. 2205

FIGURE 103



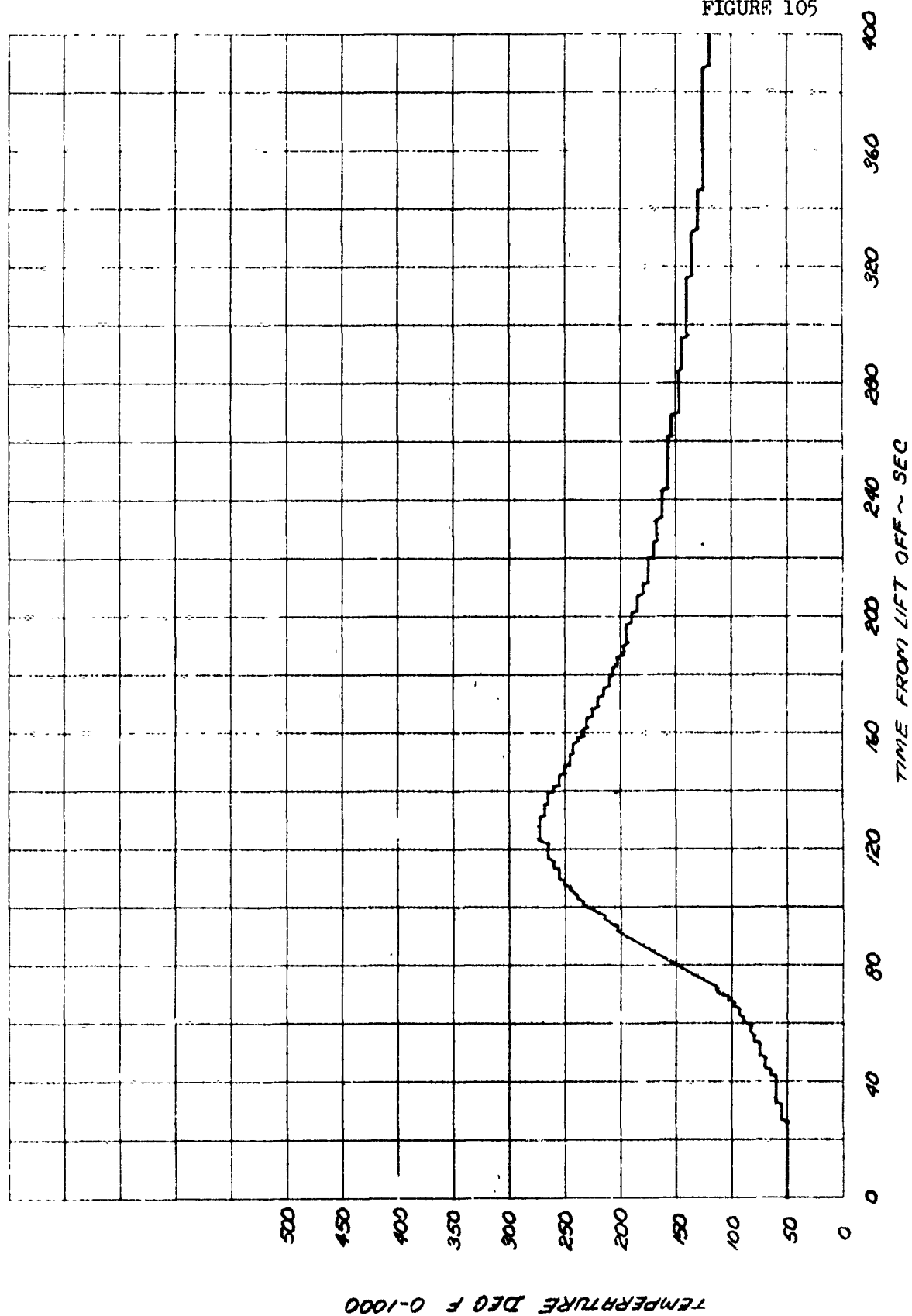
SLV-9 PRESS DIFF ACROSS SKIN 270° MEASUREMENT NO. 2206

FIGURE 104



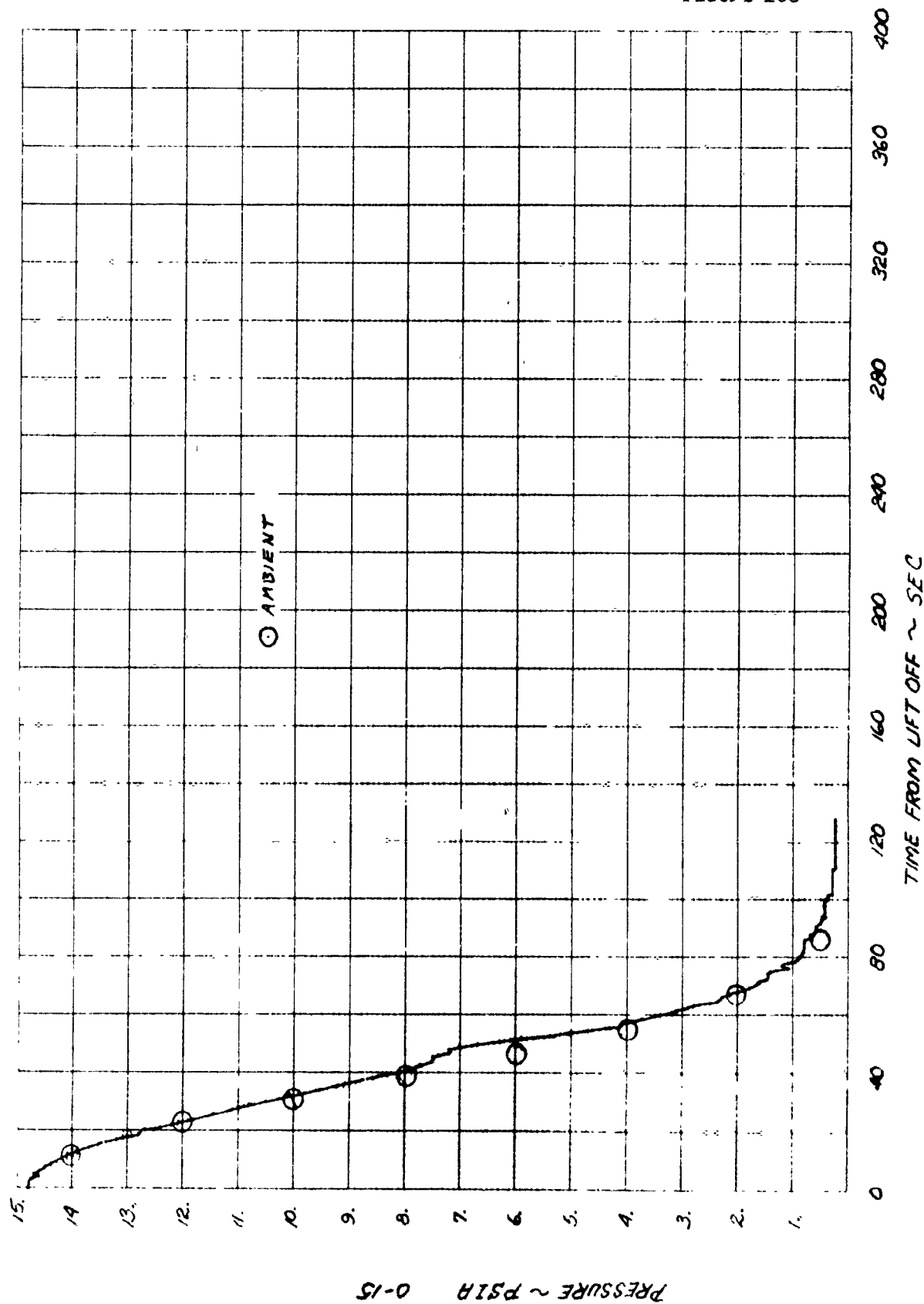
SLV-9 TEMP SHOCK IMPINGEMENT STATION 445 WL 60, MEASUREMENT NO. 2208

FIGURE 105



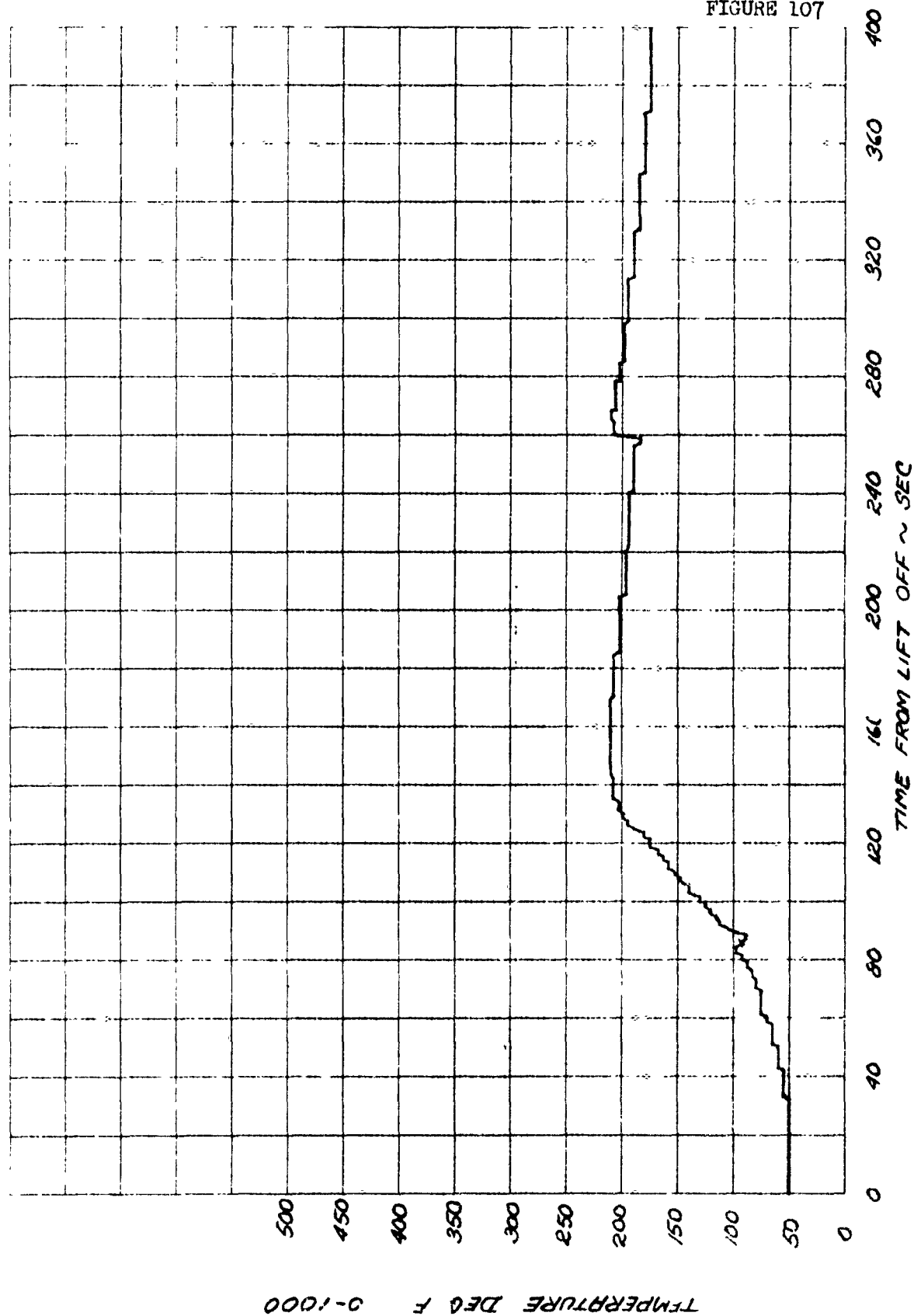
SLV-9 TEMP SHOCK IMPINGEMENT STATION 400 WL60, MEASUREMENT NO. 2209

FIGURE 106



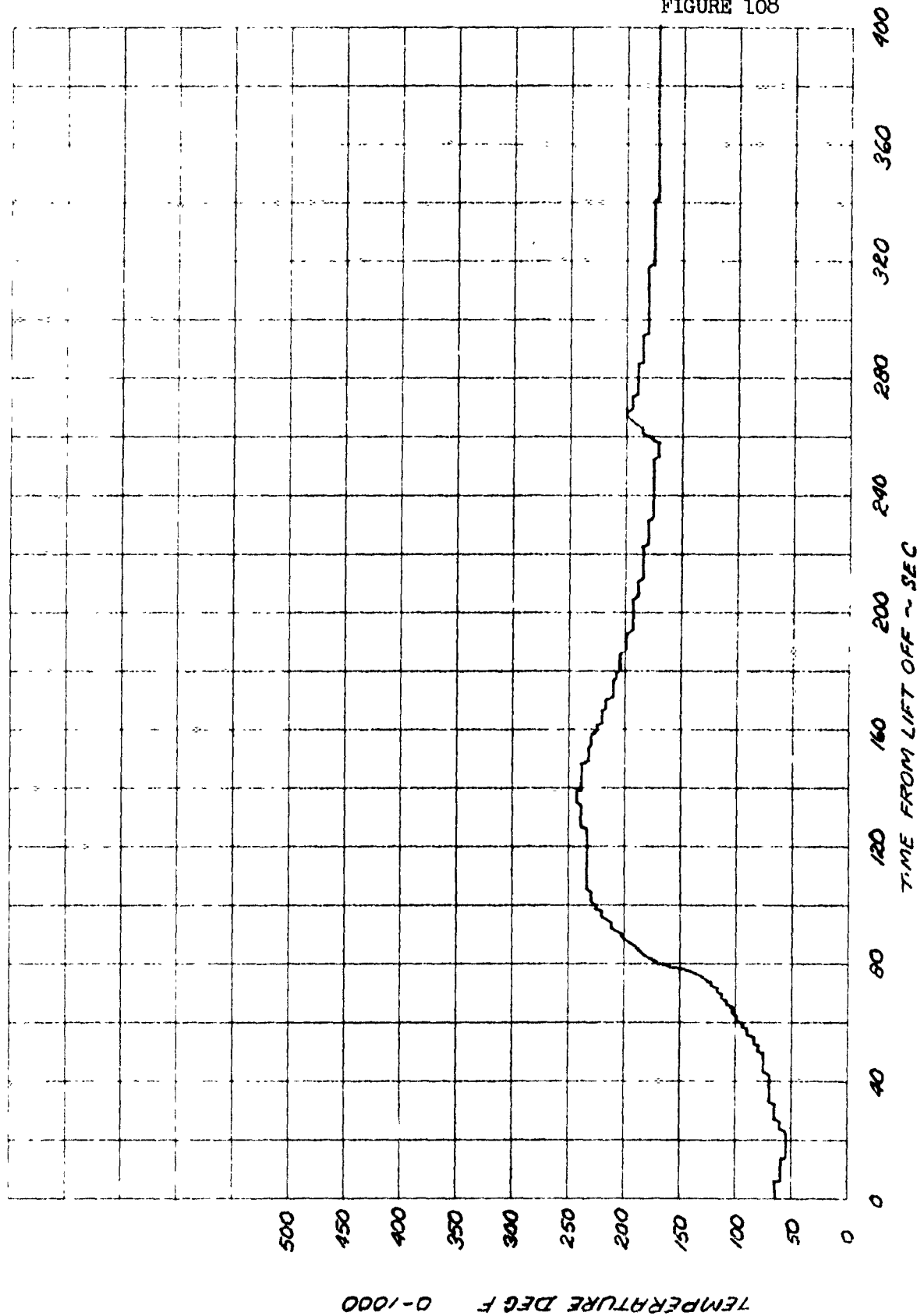
3.4-9 PRESSURE COMPARTMENT 2B MEASUREMENT NO. 2812

FIGURE 107



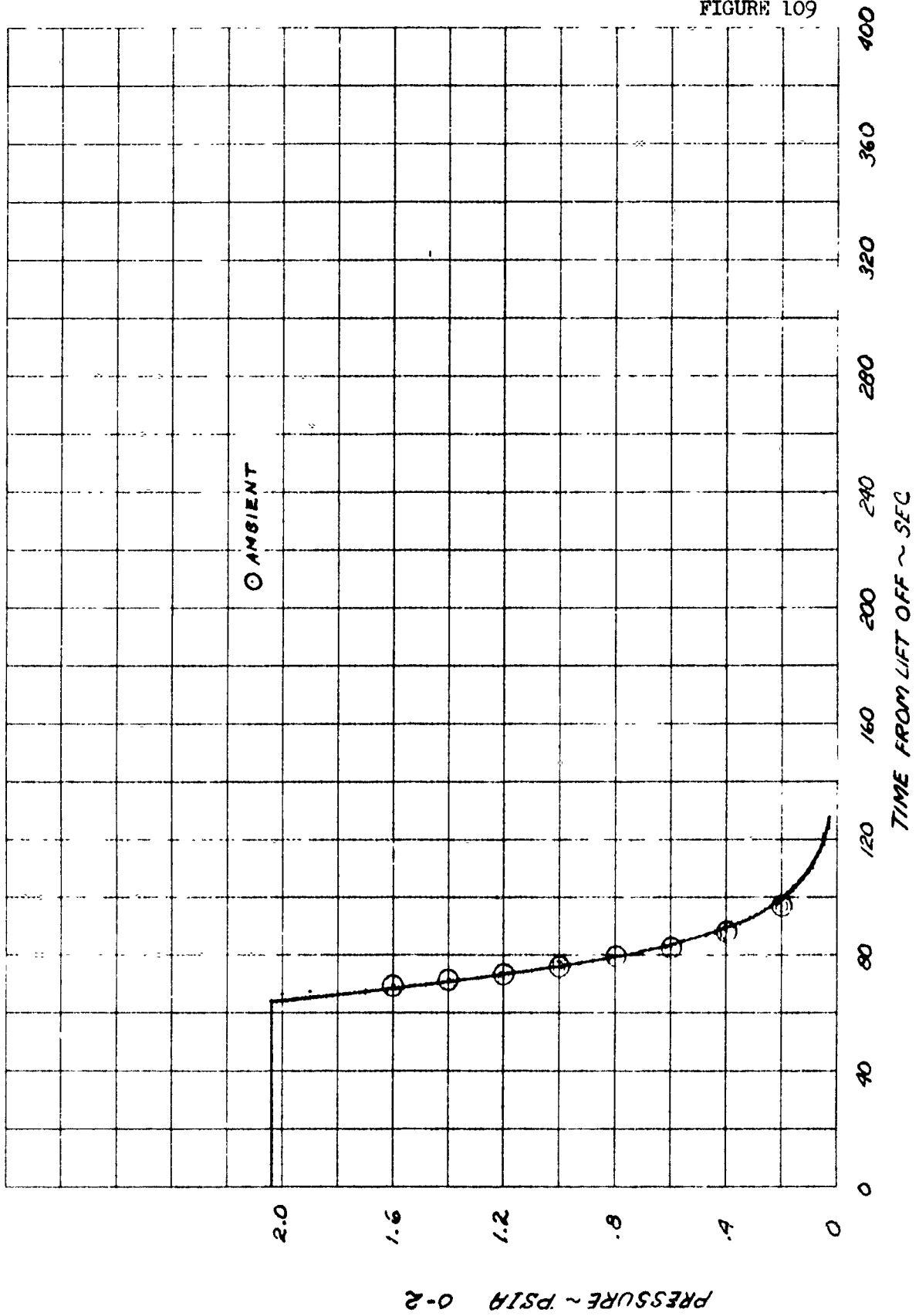
SLV-9 TEMP SHOCK IMPINGEMENT STATION 490 WL 60 MEASUREMENT NO. 2217

FIGURE 108



SLV-9 TEMP SHOCK IMPINGEMENT STA 490 TARGET MEASUREMENT NO. 2819

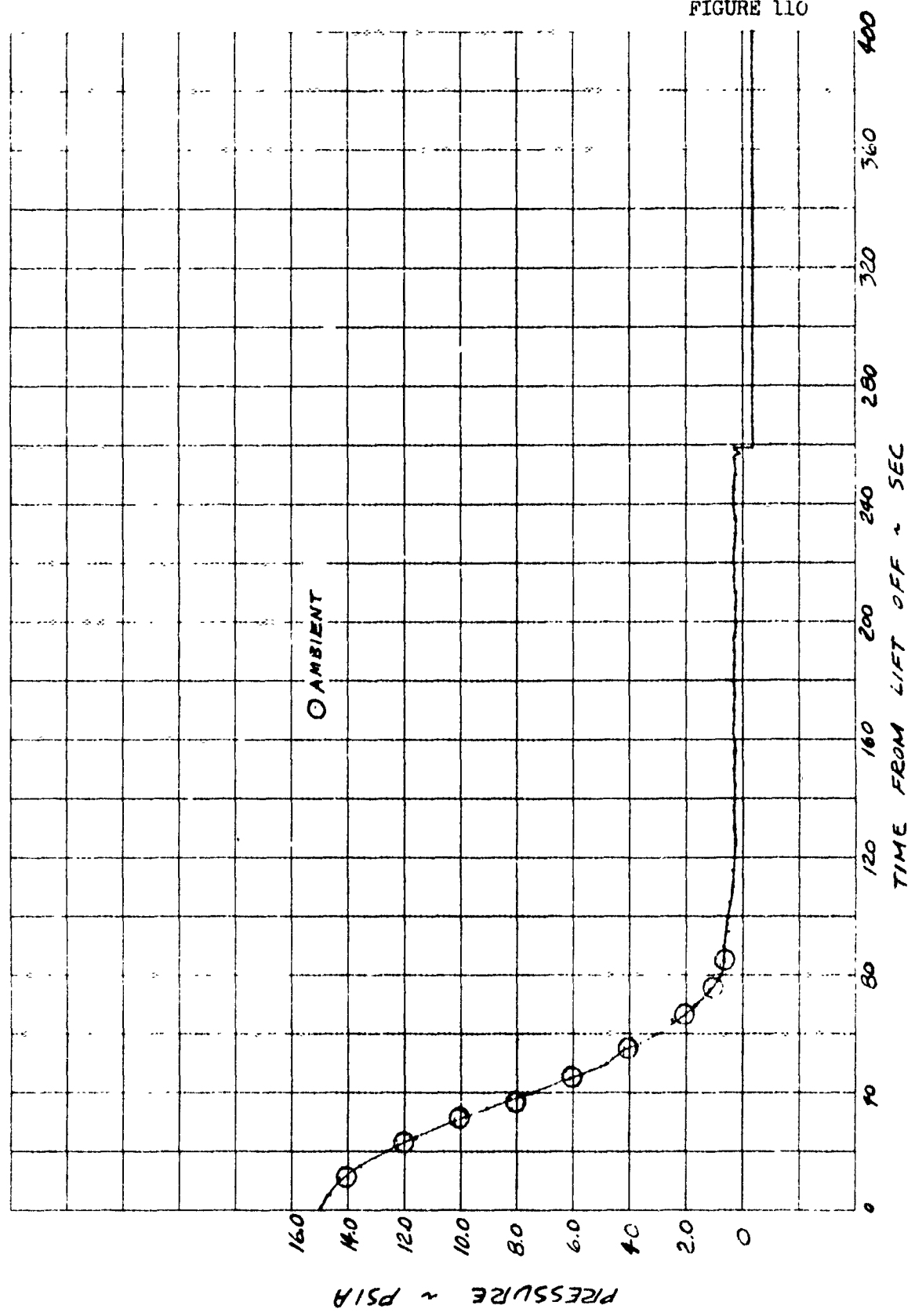
FIGURE 109



SLV-9 PRESSURE COMPARTMENT 2C MEASUREMENT NO. 2221 D



FIGURE 110



SLV-7 PRESS. COMPT. 1B MEASUREMENT NO 2224

FIGURE 111

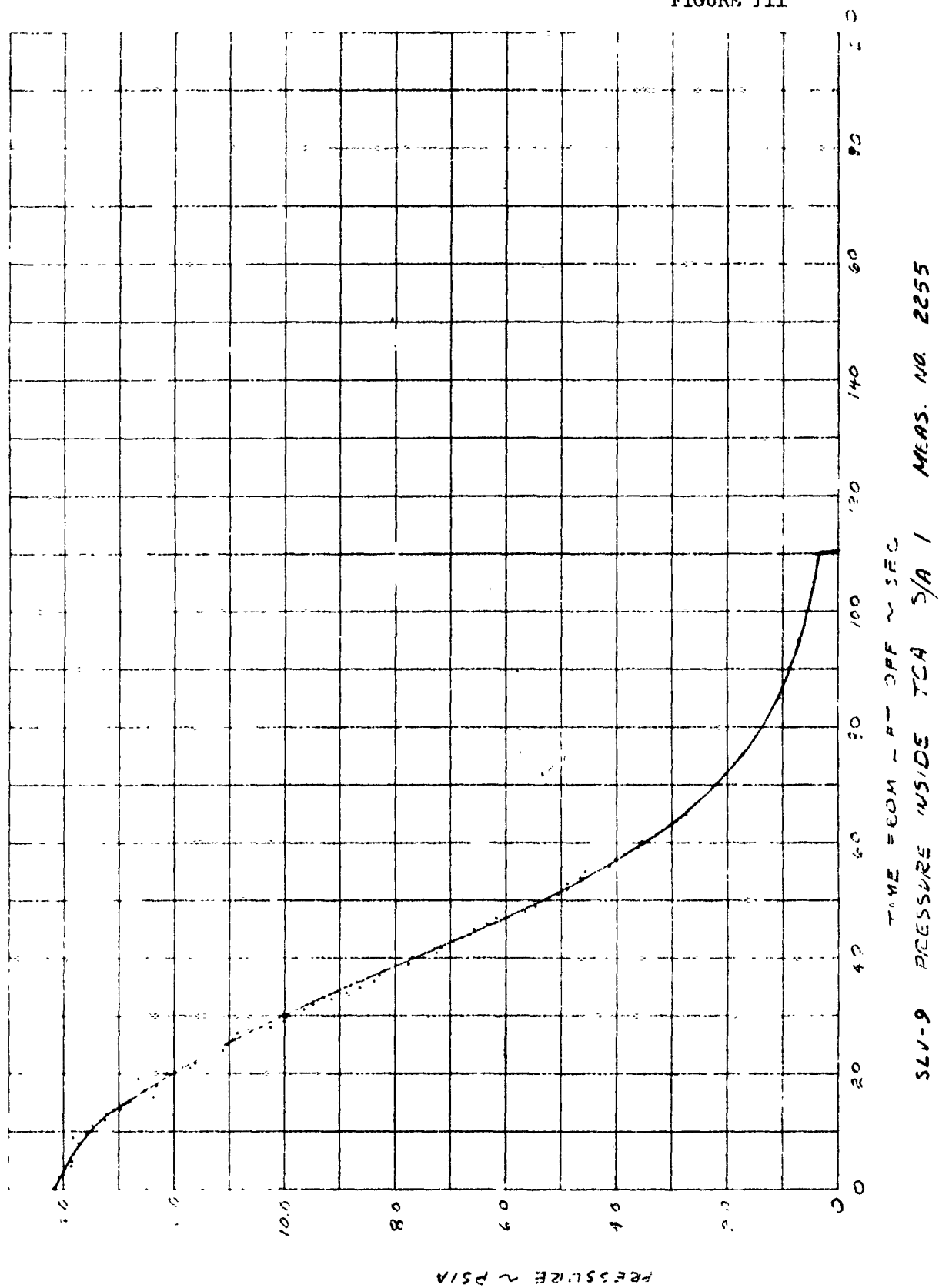
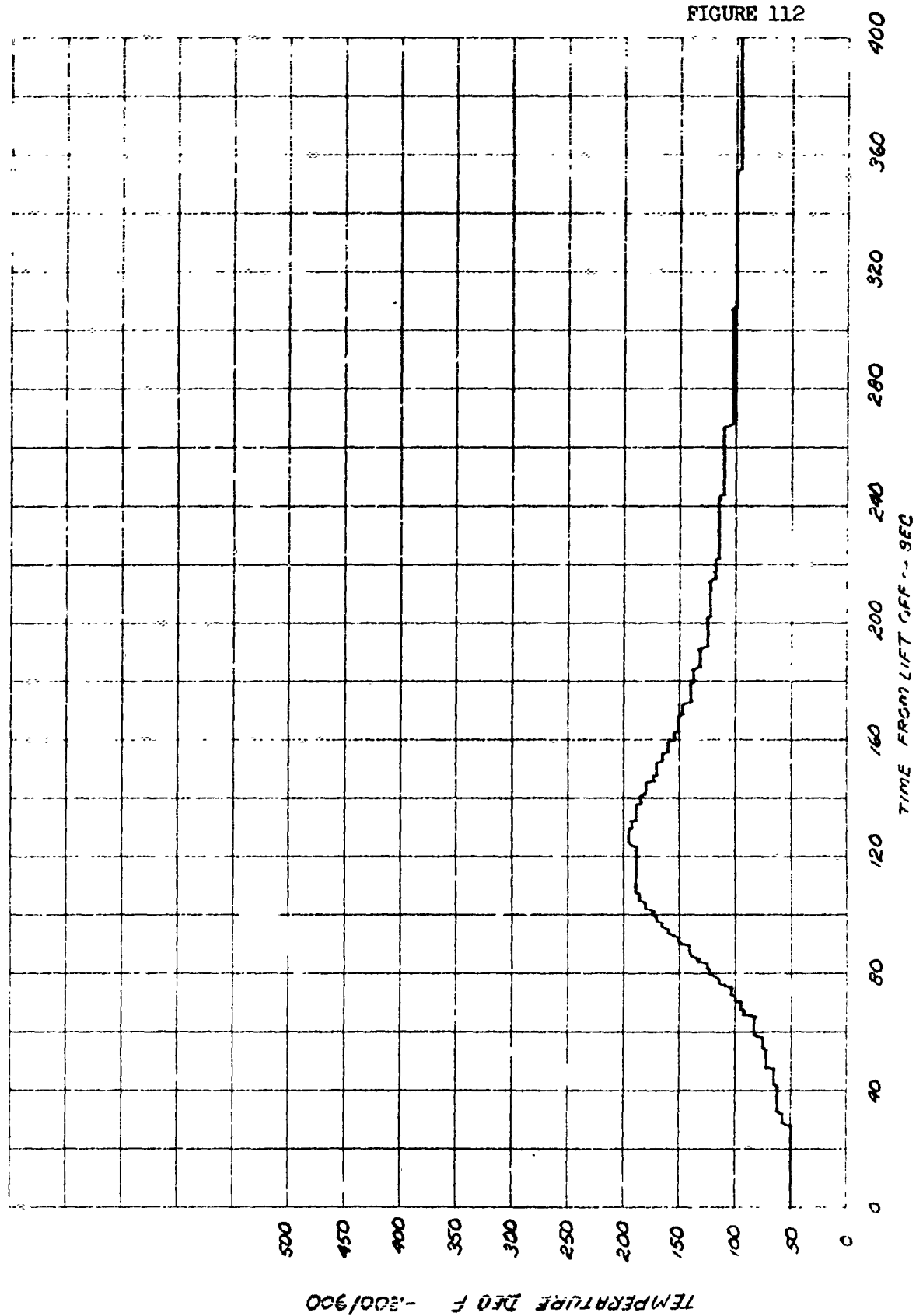
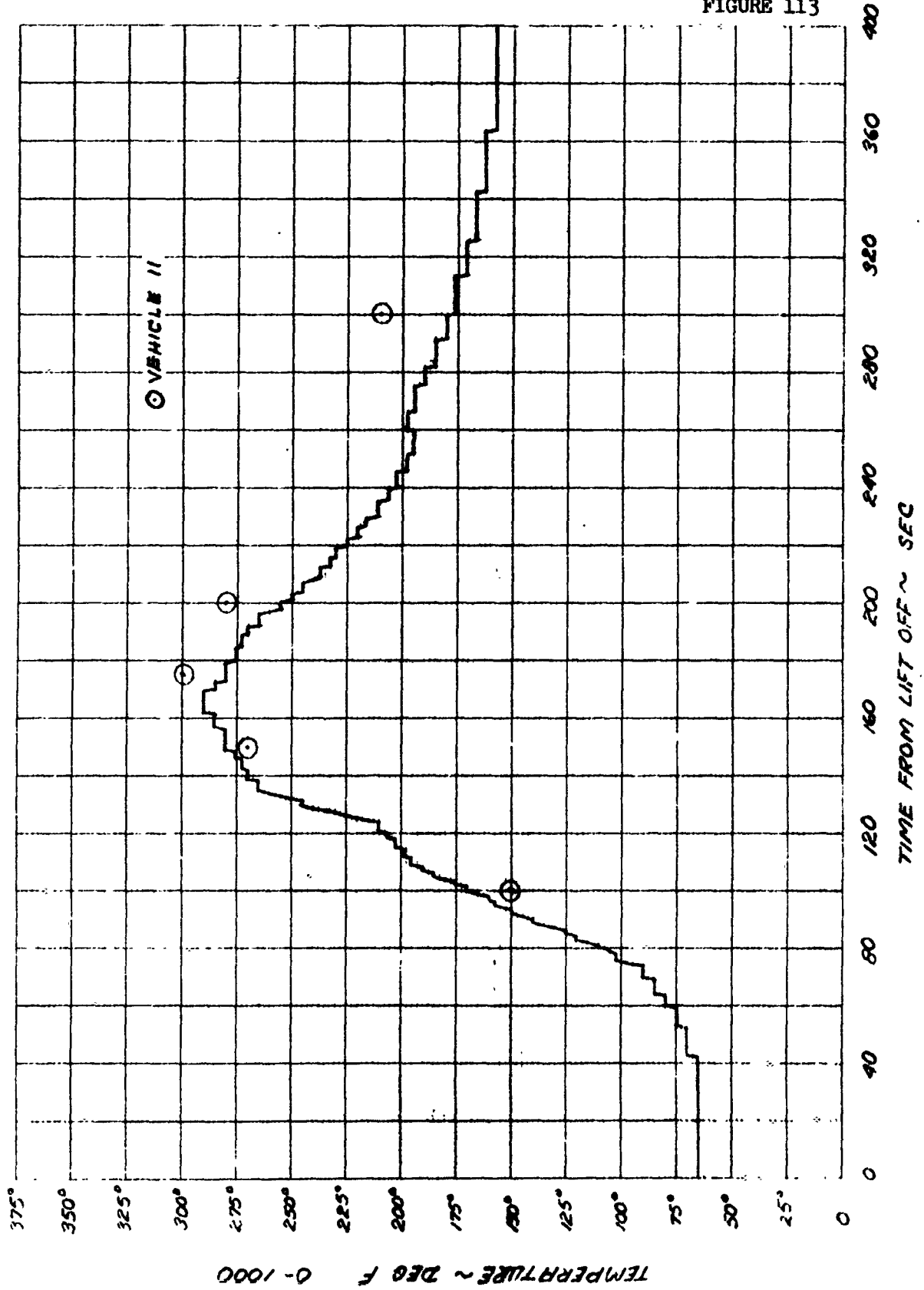


FIGURE 112



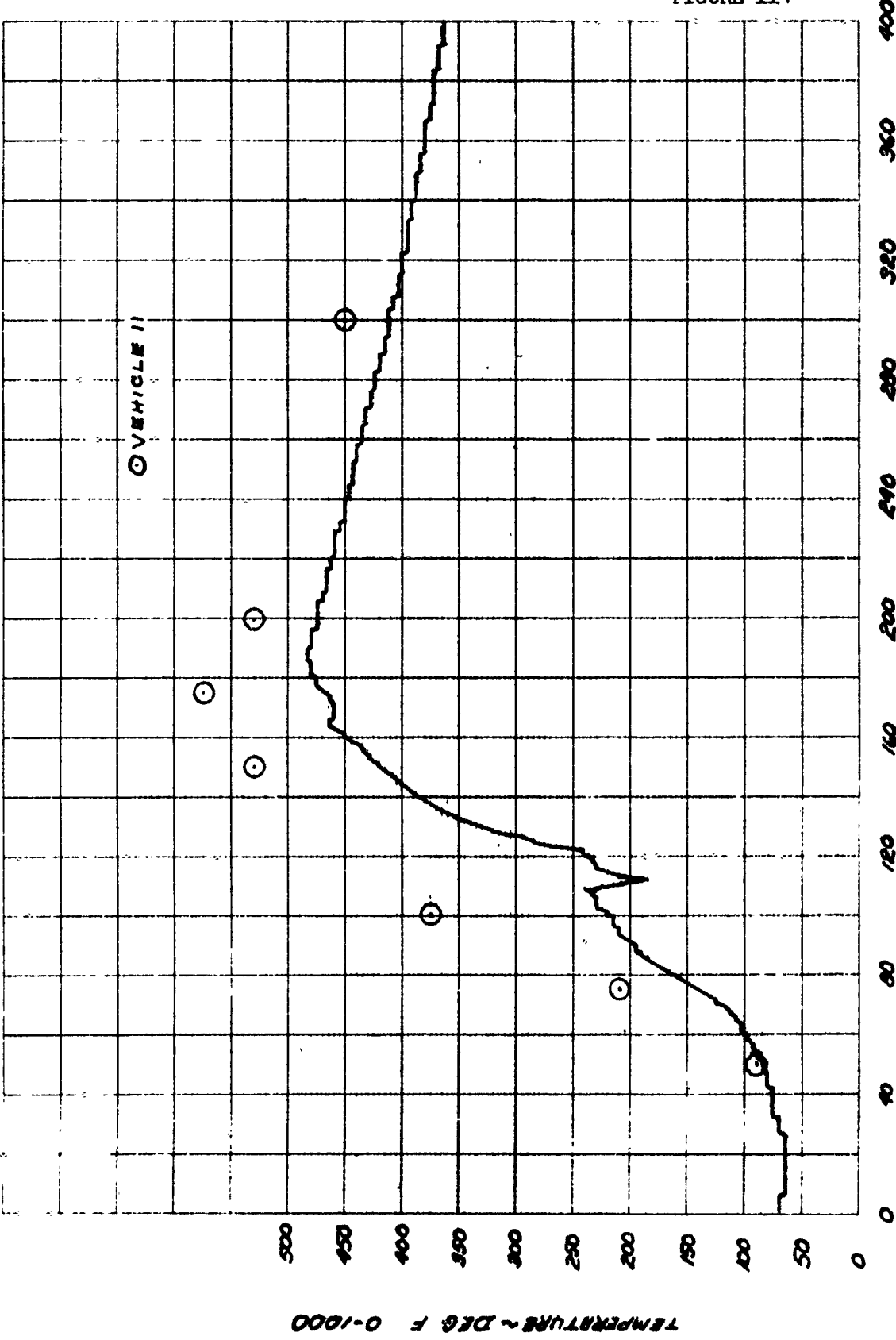
SLV-9 TEMP SKIN, STATION 117 190° OFF TARGET MEASUREMENT NO. 2242

FIGURE 113



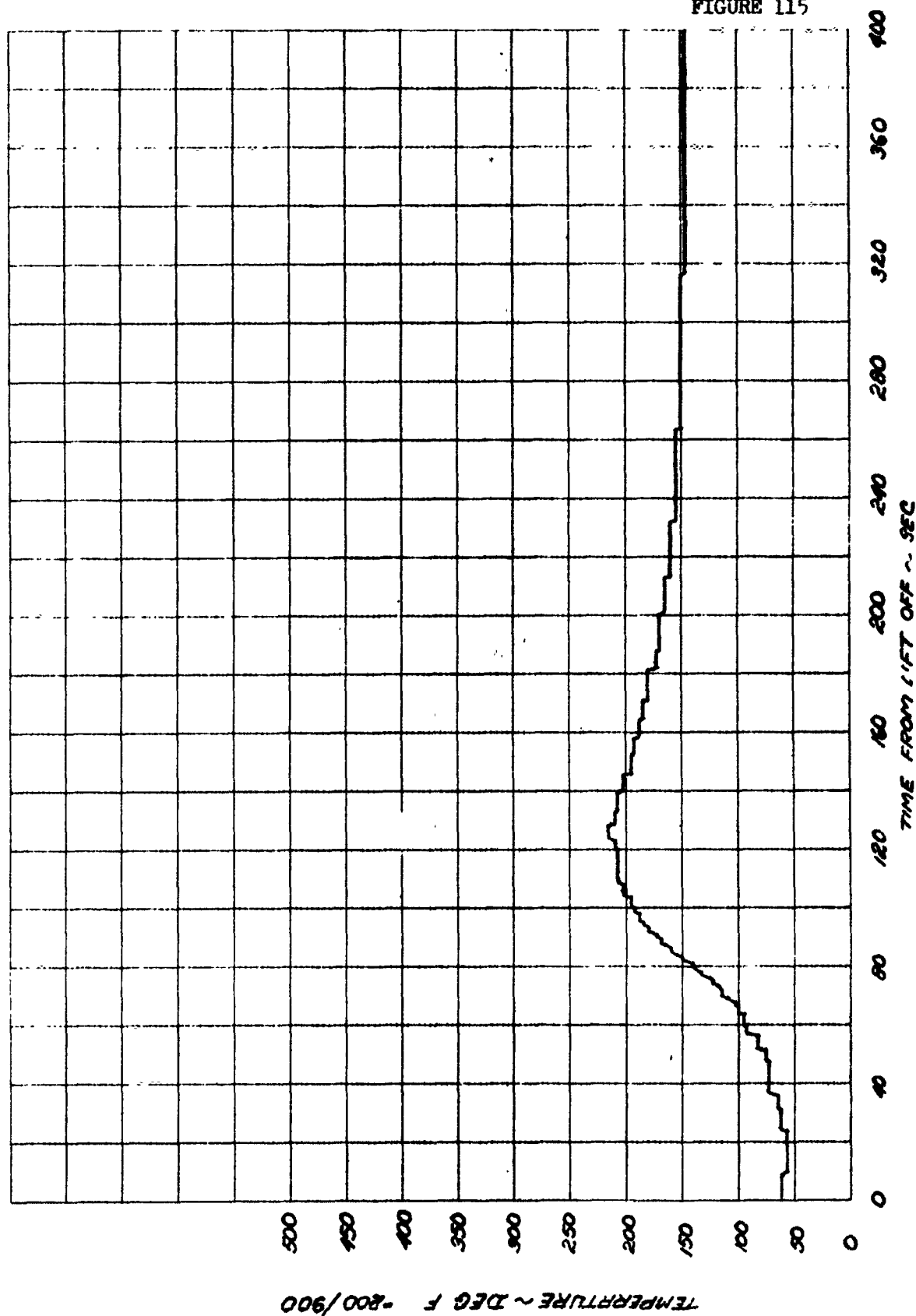
SLV-9 TEMP SKIN FRONT OF RETRO, STG II MEASUREMENT NO. 2237

FIGURE 114



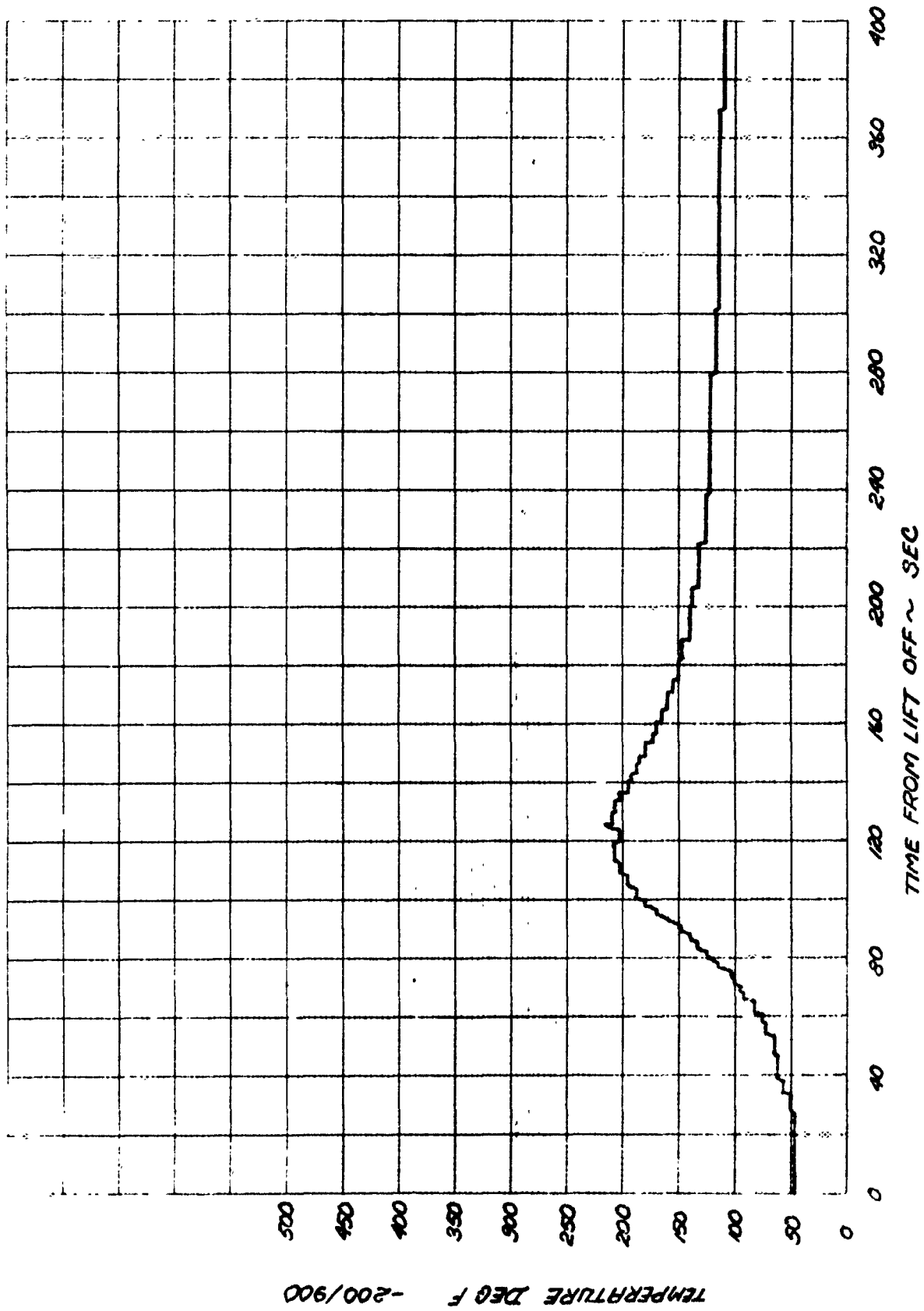
SLV-3 TEMP SKW ON RETRO FIRING, STB II MEASUREMENT NO. 2238

FIGURE 115



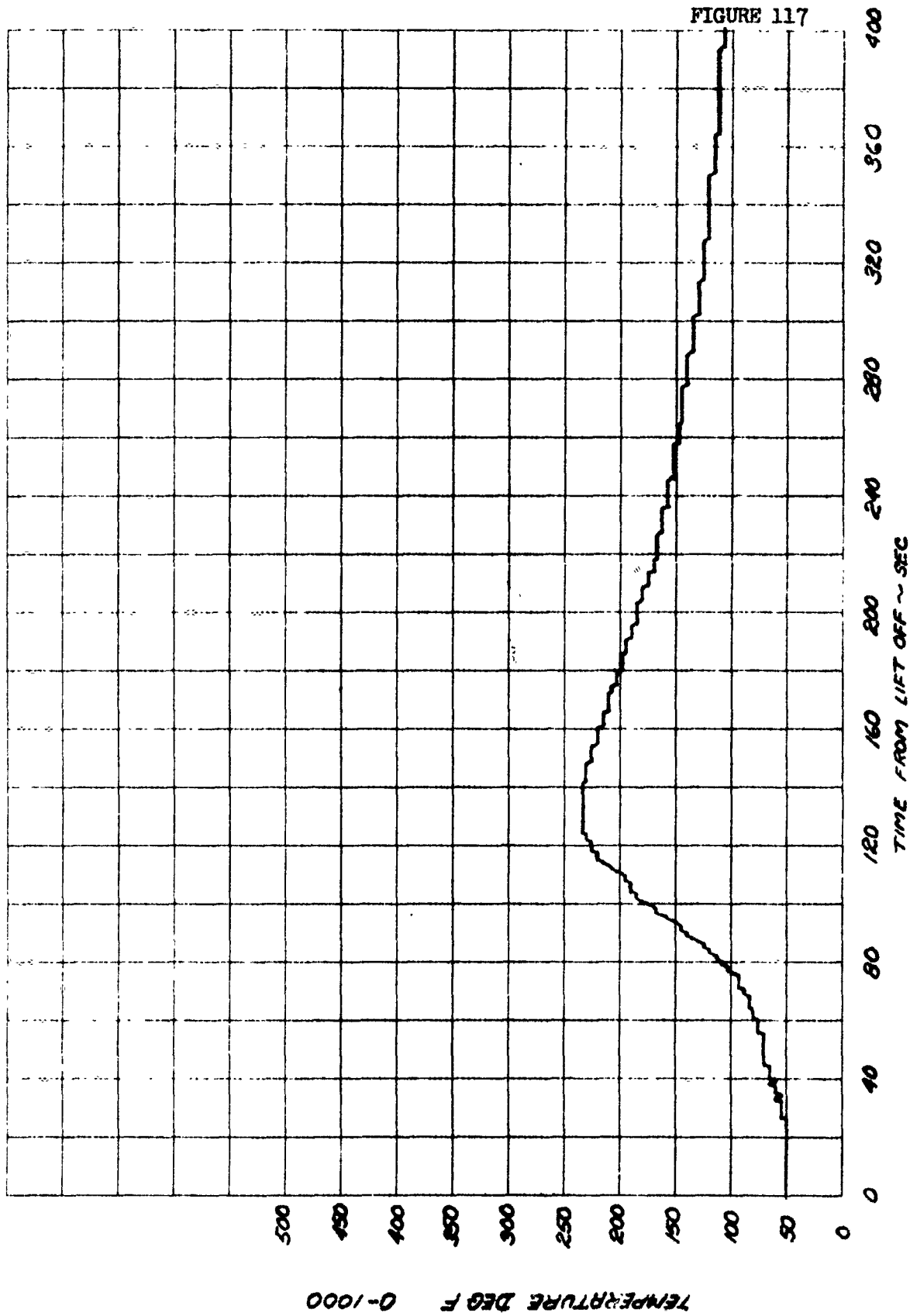
SLV-9 TEMP SKIN, STATION 112. 90° OFF TARGET MEASUREMENT NO. 2239

FIGURE 116



SLV-9 TEMP SKIN, STATION 117 105° OFF TARGET MEASUREMENT NO. 2241

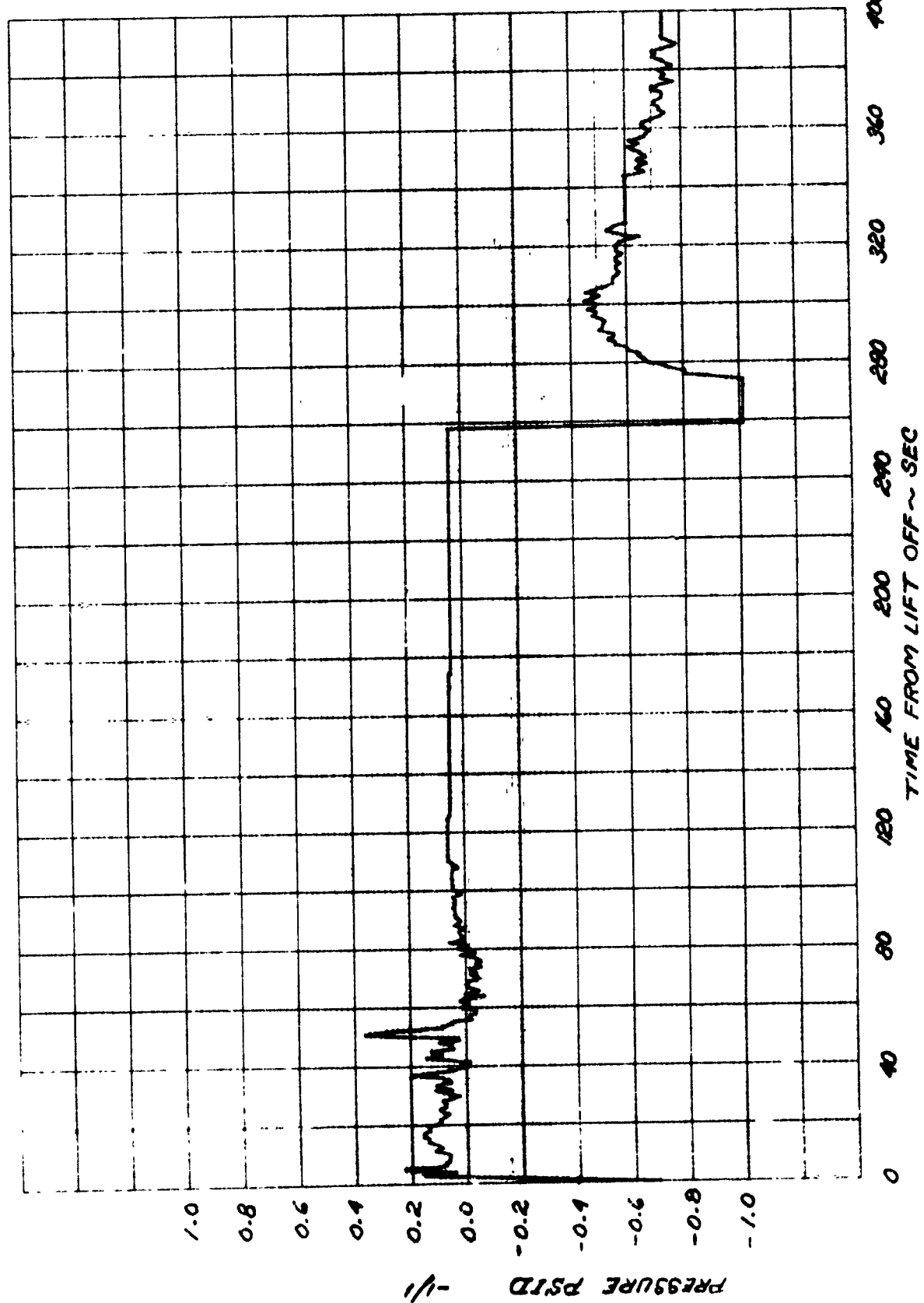
FIGURE 117



SLV-9 TEMP SHOCK IMPINGEMENT STA 360 WILCO MEASUREMENT NO. 2246

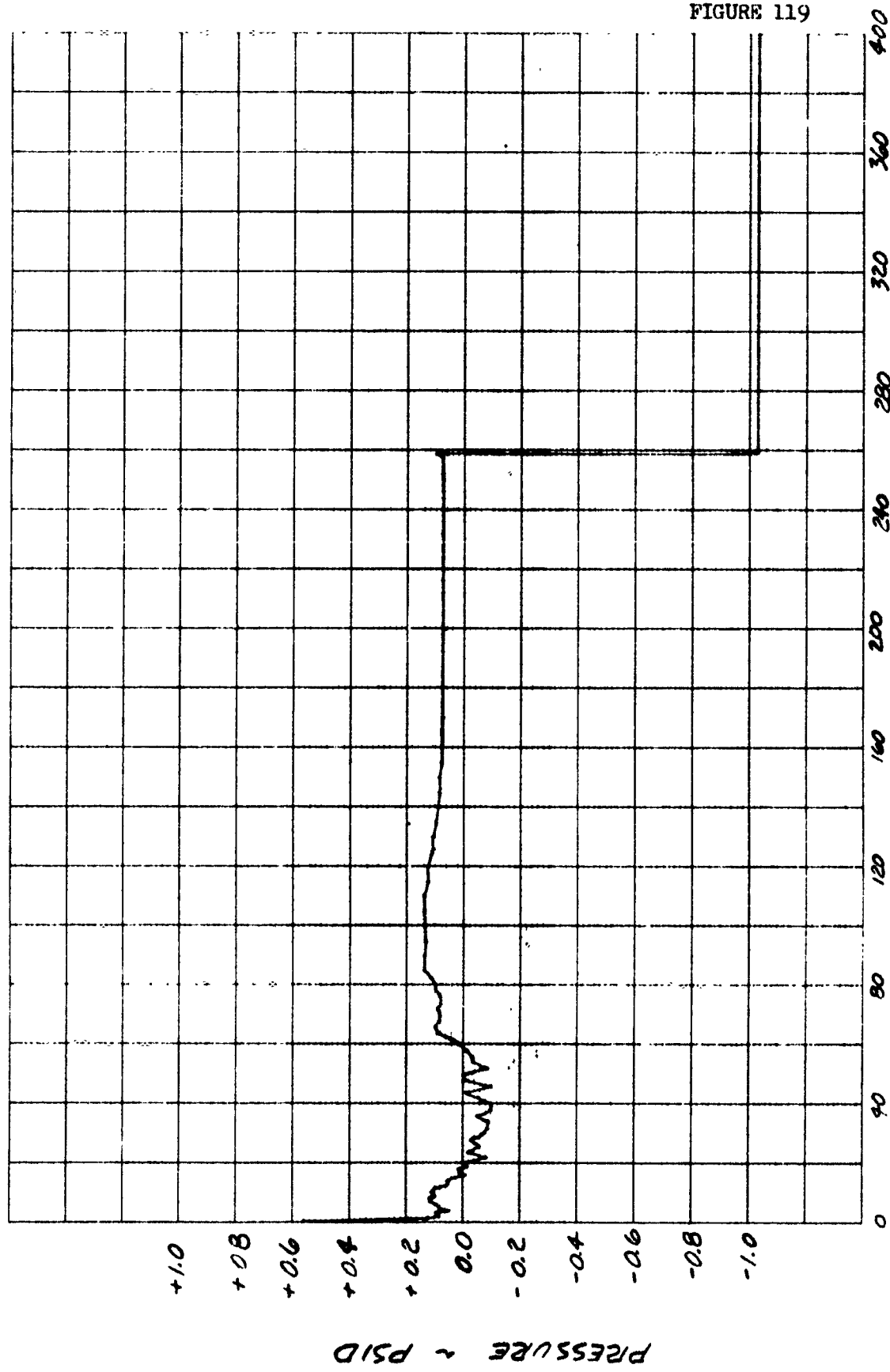


FIGURE 118



SLV-9 PRESS DIF ACR HT SHD VENT AREA 90 DEG MEASUREMENT NO. 2251A

FIGURE 119

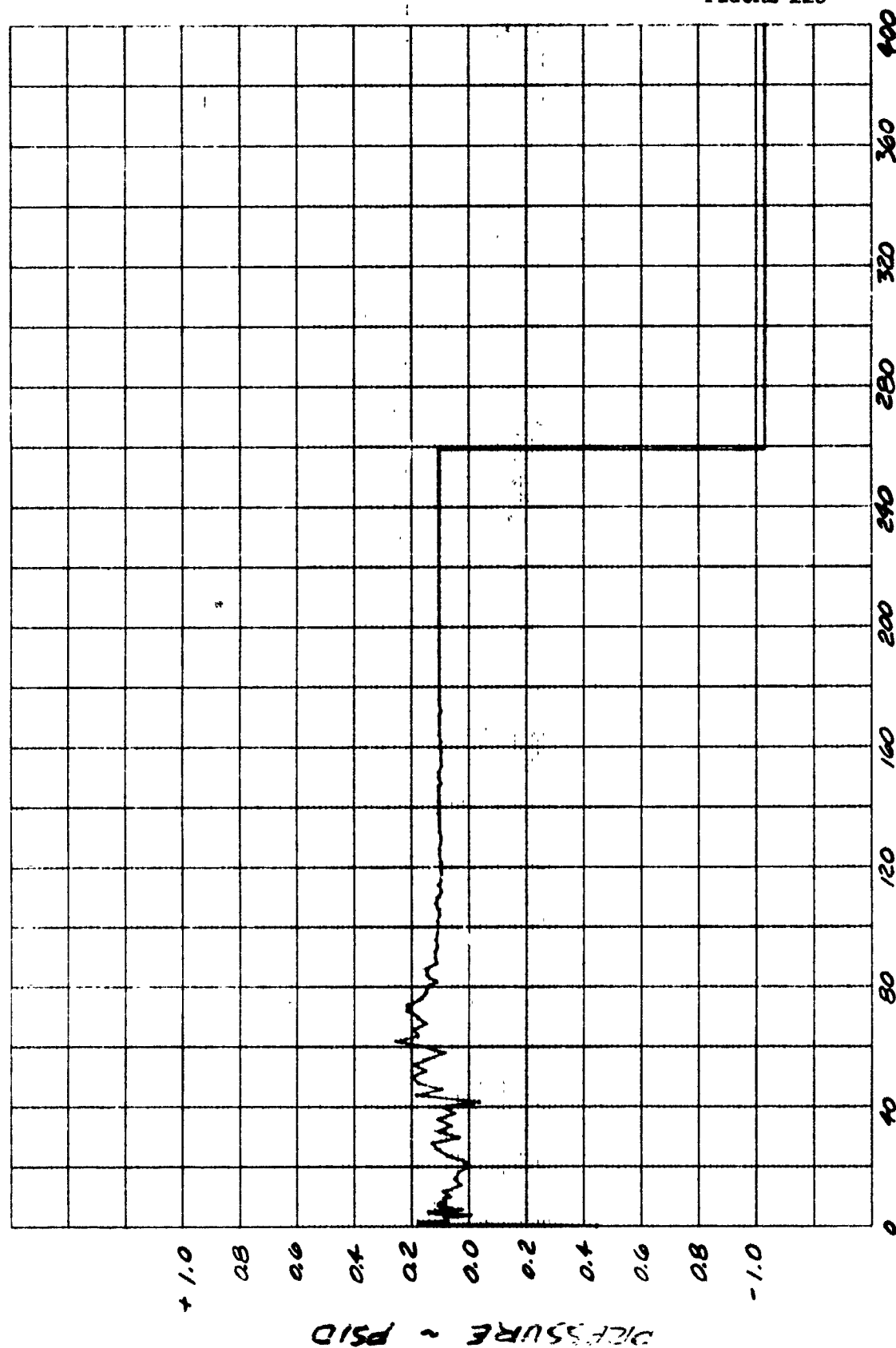


TIME FROM LIFT OFF ~ SEC.

PRESS DIFF ACROSS HEAT SHIELD BASE 90° MEASUREMENT NO 2252

PRESSURE ~ PSID

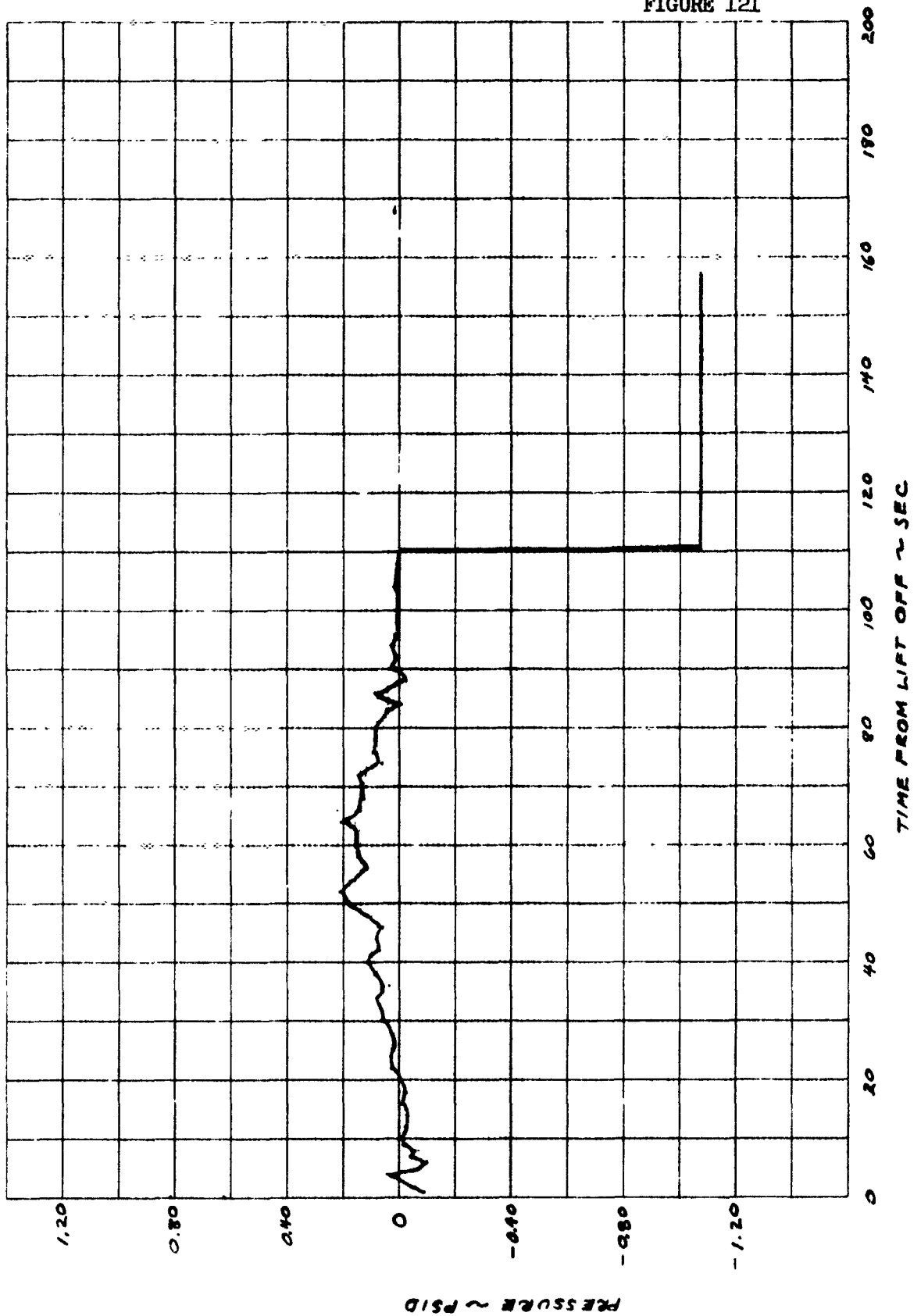
FIGURE 120



TIME FROM LIFT OFF ~ SEC.

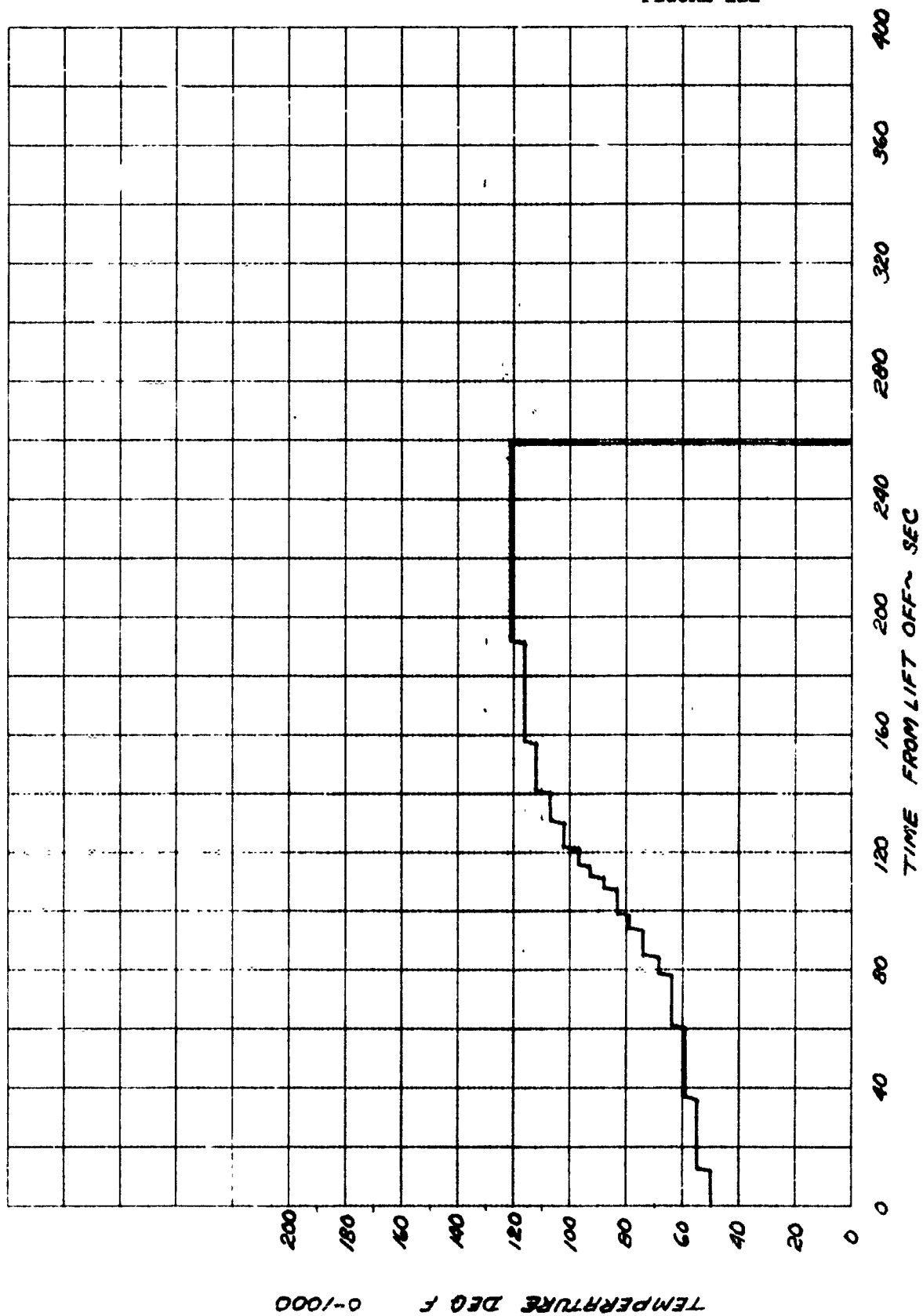
PRESS. DEF ACC HEAT SHIELD SDE STN 1250 90' MEAS. NO. 2053

FIGURE 121



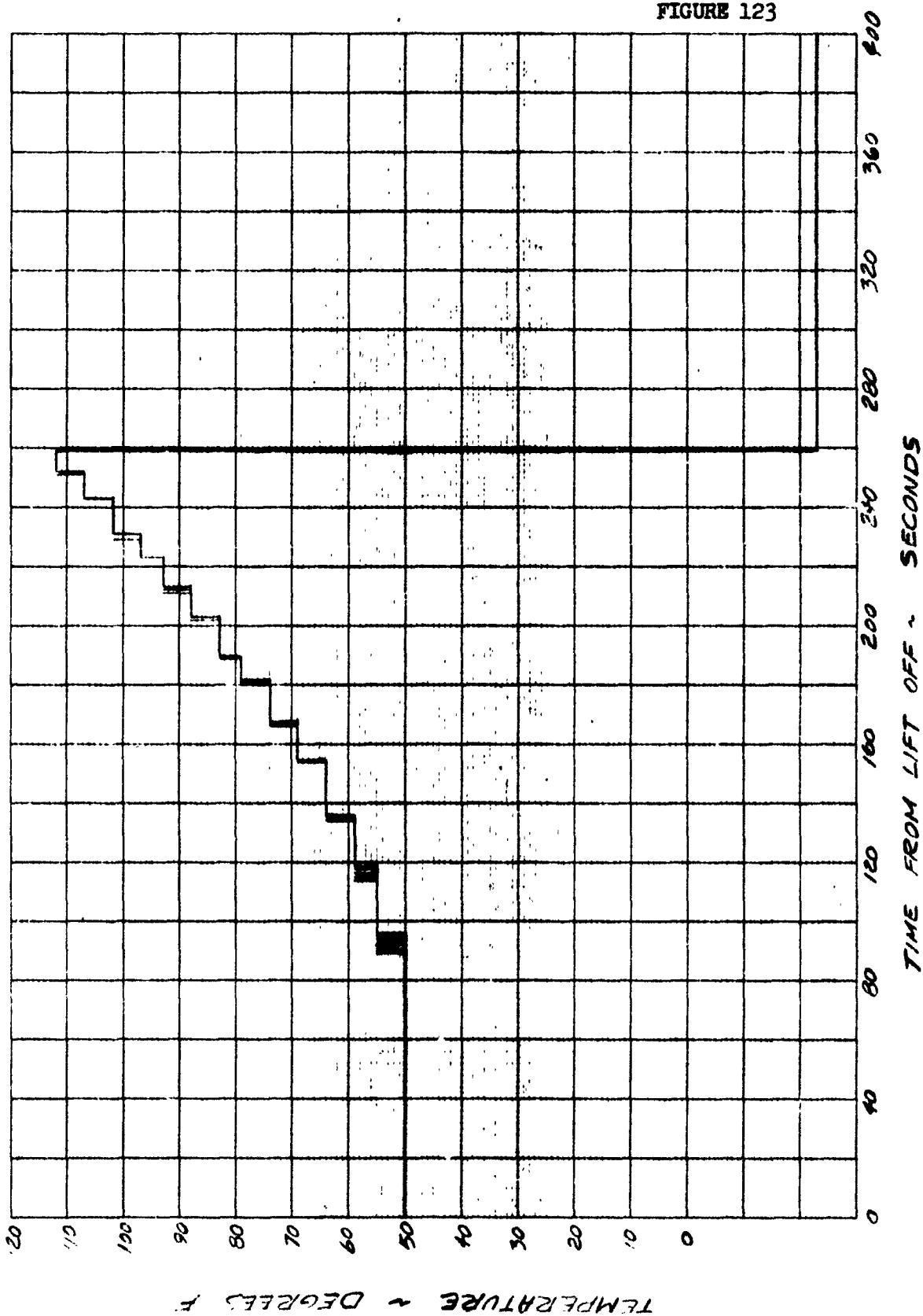
SAV-9 PRESSURE DIFF. ACR. TGA CLOSURE, S/A 1 MEAS. NO. 2254A

FIGURE 122



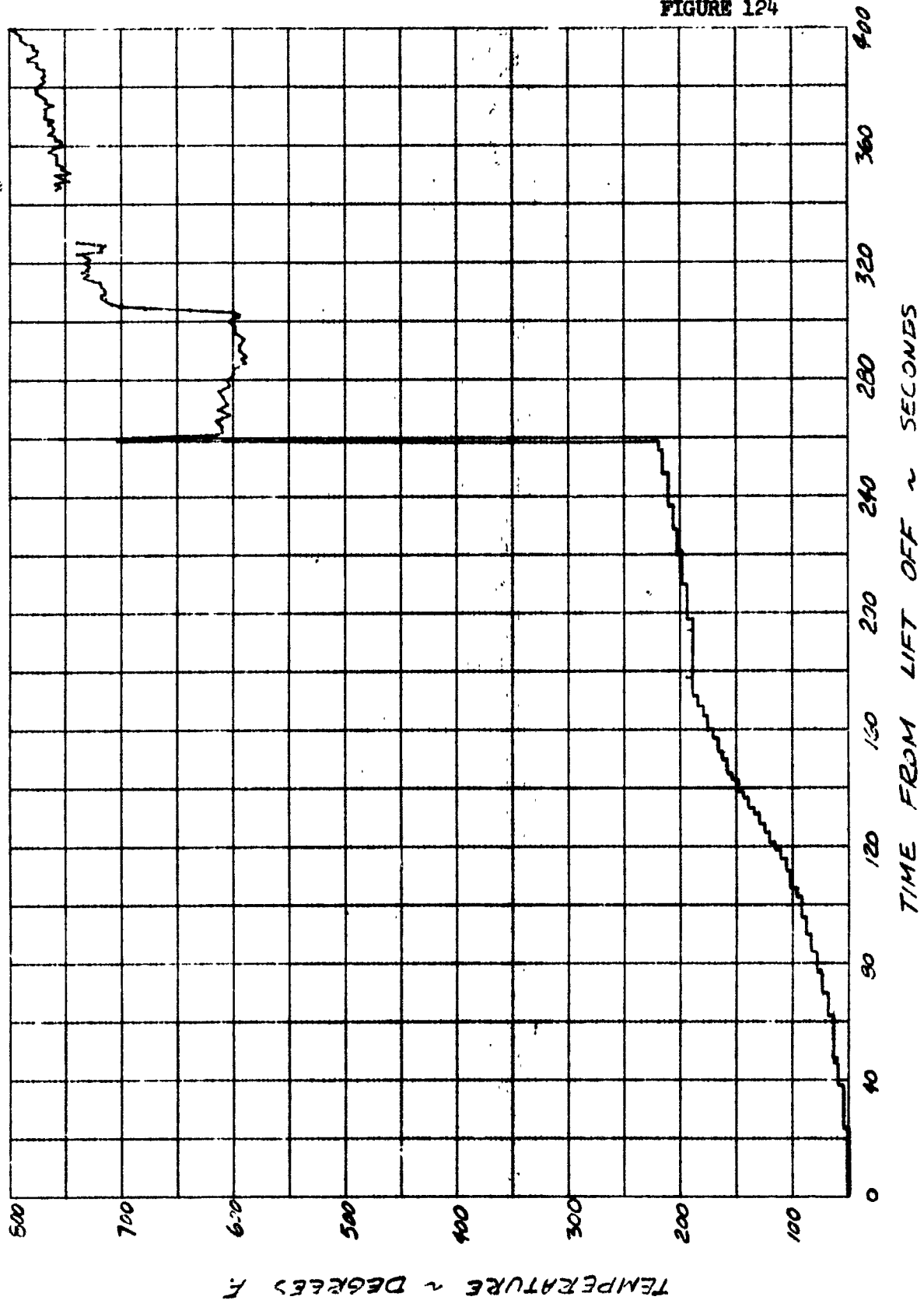
TEMP AFT FRAME INSIDE 73 DEG STATION 1225 MEASUREMENT NO. 2283

FIGURE 123



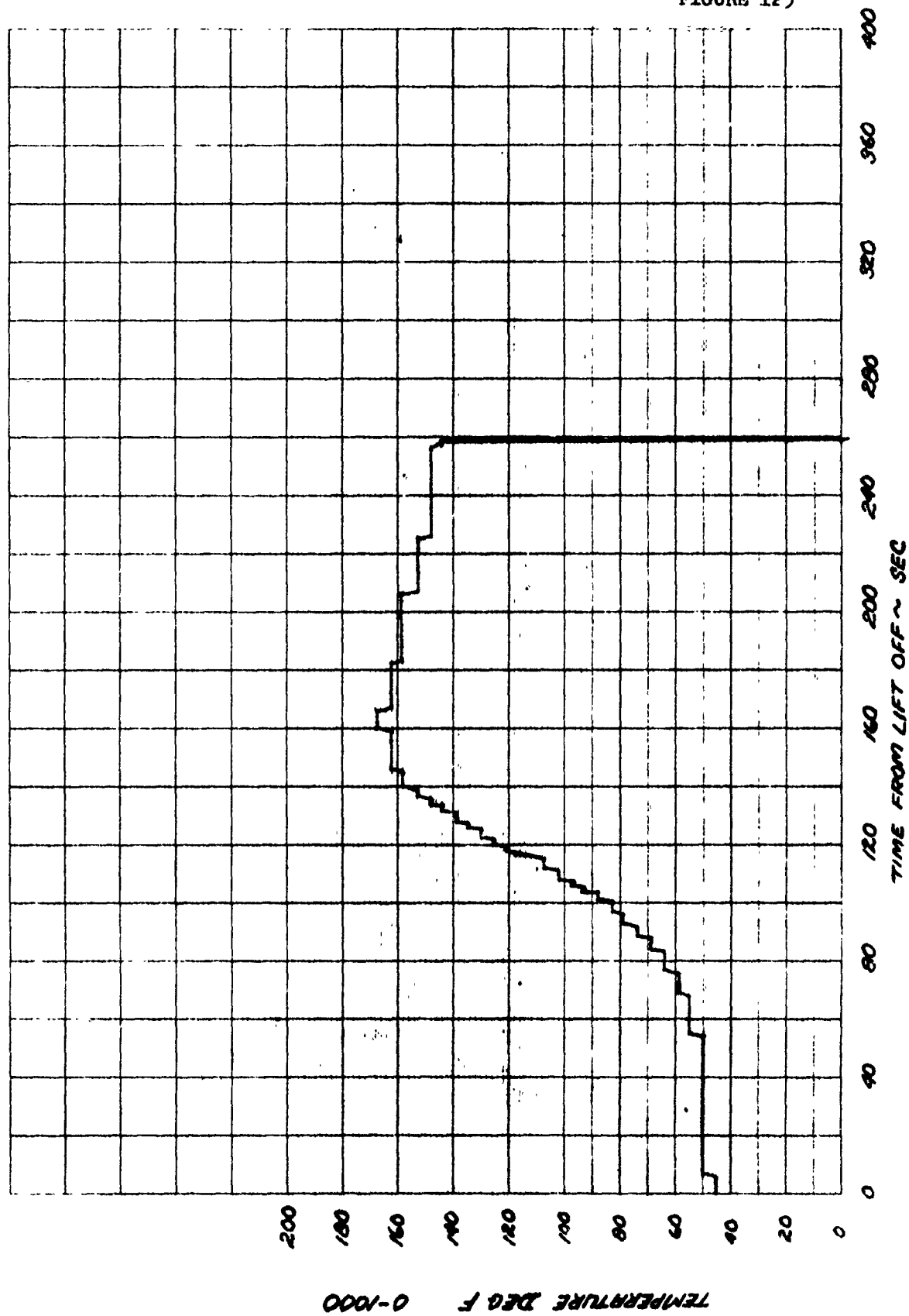
TEMPERATURE OUTSIDE BASE HEAT SHIELD 90° MEASUREMENT NO. 2662

FIGURE 124



TEMPERATURE INSIDE HEAT SHIELD STN 1300 90° ~ MEAS NO. 2663

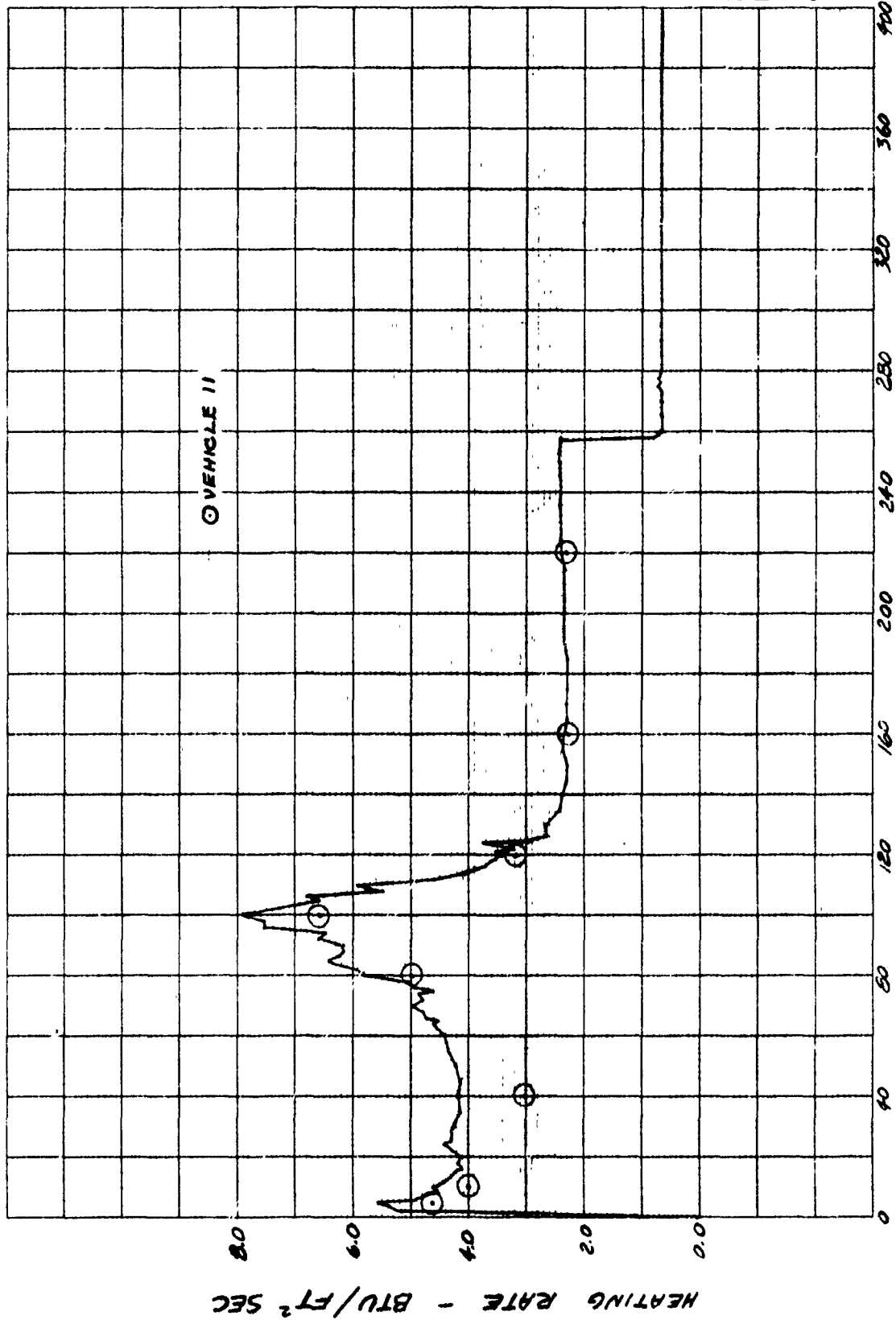
FIGURE 125



SLV-9 TEMP INSIDE HEAT SHD STATION 1300 180° MEASUREMENT NO. 2664

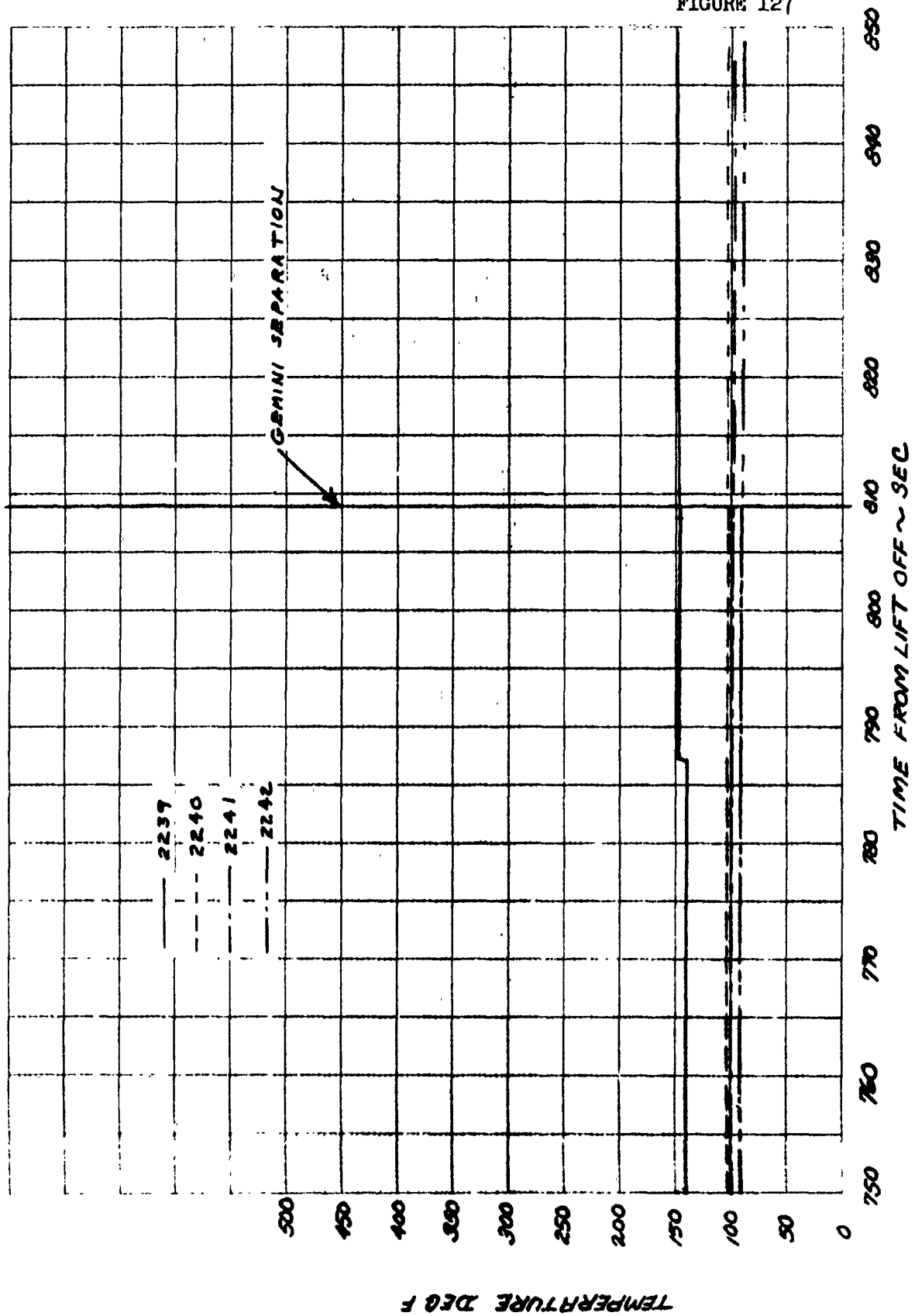


FIGURE 126



TIME FROM LIFT OFF ~ SEC.  
 SALV-9 TOTAL CALORIMETER HEAT SHIELD BASE 135° MEAS. NO. 2666C

FIGURE 127



### 3.2.6.2 Vibration and Acoustic

#### 3.2.6.2.1 Summary

Fourteen environmental vibration measurements and one acoustic measurement were acquired during the launch and flight of Vehicle 9 with the airborne single side band instrumentation system. Sixteen vibration and one acoustic measurement were recorded during the launch with the fly-away landline system. Three acoustic measurements were taken at launch facility locations using the ground landline instrumentation. Good quality data was generated from all the measurements programmed and acquired with the three data acquisition systems.

#### 3.2.6.2.2 Data and Analysis

The maximum vibration and acoustic levels recorded with the single side band instrumentation system during the launch, transonic, and maximum dynamic pressure periods of the flight are tabulated in Table 25. The design assurance test specification overall vibration/acoustic level applicable to the area at which the transducer was located also is listed for each measurement. The maximum overall levels recorded with the 100-ft. fly-away landline and ground landline instrumentation system during the launch phase of the flight are given in Table 26. Corresponding specification overall levels are shown for each of the measurements listed.

#### Vibration Data

As is evident from the data shown in Table 25, the maximum, overall acceleration levels of all the measurements acquired, except one, were considerably lower than the corresponding design assurance test specification overall levels. Measurement No. 2610 exhibited an overall level of 55.5 Grms during the transonic period of the flight, whereas the specification overall level is 40.1 Grms. This measurement was recorded on the Compartment 1A airframe at the location of the solid state switches, on the ring frame at station 508, between stringers 31 and 32. The same measurement on Vehicle C-4 exhibited a maximum level of 28 Grms. During the Vehicle C-7 flight a maximum level of 46 Grms was measured on the airframe at station 508 at stringer 2A in the area of the SRM outrigger tie point. A higher level normally would be expected at the location of Measurement No. 2610 since the effects of aerodynamic buffeting of the SRM nose cone are greater at that point and the airframe structure weight is less than that in immediate area of the outrigger tie point.

### 3.2.6.2.2 Vibration Data - (Cont.)

Therefore, the higher level recorded on the Vehicle C-9 flight is considered to be more in agreement with the Vehicle C-7 measurement at the outrigger tie point than the level recorded on Vehicle C-4. Whether or not the vibration environment at the location of Measurement No. 2610 exceeded those to which the equipment installed in that area has been qualified will be determined when random vibration spectral analyses of the measurement have been completed and appropriate test spectra comparisons have been performed.

### Acoustic Data

Reference to Table 25 shows that the maximum overall acoustic (sound pressure) level recorded at the vehicle skin surface at Compartment 1A during the launch period was 152 db, which is equal to the acoustic specification overall level for that compartment. During the transonic period of flight the level reached a maximum of 163.6 db which is greater than the specification level. The transducer is located in vehicle quadrant III, 120 degrees off target, at station 567, which is a point at which the noise resulting from SRM nose cone buffeting is at a high level. During the flight of Vehicle C-11 a maximum acoustic level of 158 db was recorded at the Compartment 1A surface at a position on butt line 0 at station 572. This is the position at which minimum noise would be expected in the station zone of the two subject measurements. To this extent, the two measurements are in agreement with each other. Further, the higher than predicted acoustic environment measured at this compartment correlates with the higher vibration environment observed. Measurement No. 2632 recorded inside Compartment 1C exceeded the compartment design acoustic level of 154 db during the launch. The maximum overall level measured was 163.5 db. The same measurement obtained on Vehicle C-4 had a maximum value of 158 db.

Since there are no items of equipment in either of Compartments 1A or 1C which are considered directly sensitive to an acoustic environment, the higher than specification levels recorded have no effect on the qualification status of the equipment in these compartments. This equipment has been qualified to compartment vibration specifications.

### 3.2.6.2.3 Conclusions and Recommendations

From the examination of the data and the reduction of the time history (RMS) analyses of the vibration and acoustic measurement recordings acquired during the launch and flight, it

#### 3.2.6.2.3 Conclusions and Recommendations - (Cont.)

is concluded that good quality, usable data were obtained from all of the measurements programmed. The vibration environments measured were within pertinent specification ranges in all but one area. The acoustic environments measured in two vehicle areas exceeded pertinent specification ranges, but this poses no equipment problems.

Spectral analyses will be conducted for that vibration measurement which exhibited higher than specification vibration levels and the qualification status of the equipment in the area of this measurement will be reviewed with reference to the measured environment. In the event that an equipment item has not been qualified to vibration levels as high as that measured, it is recommended that its performance under the flight environment be thoroughly investigated.

TABLE 25  
VEHICLE 9 SINGLE SIDE BAND VIBRATION/ACOUSTIC MEASUREMENTS

Meas. No.	Compt.	Location	Axis	Overall Acceleration/SPL			DAT Spec.	Comments
				Launch	Transonic	Max. Q		
				<u>Grms</u>	<u>Grms</u>	<u>Grms</u>		
2553	3A	Guidance Truss Between MGC & Relays	Long	1.3	1.1	1.7	16.7	
2555	3A	Guidance Truss at IMU Long & DCU Common Mounting	Long	0.8	0.8	1.1	16.7	
2558	3A	Equipment Truss at MDP Mounting	Long	1.4	1.0	0.7	16.7	
2594	3A	Equipment Truss at Motor Driven Switch Mounting	Long	1.4	1.1	0.9	16.7	
2560	3B	Oxidizer Tank Top on Pressure Switch Mounting Plate	Long	3.3	1.8	1.0	31.6	
2610	1A	Airframe at Solid State Switches, Quad IV, Sta. 508	Long	16.0	55.5	24.8	40.1	

TABLE 25 - (Cont.)  
VEHICLE 9 SINGLE SIDE BAND VIBRATION/ACOUSTIC MEASUREMENTS

Meas. No.	Compt.	Location	Axis	Overall Launch	Acceleration/SPL Transonic	Max. Q	DAT Spec.	Comments
2569	1B	Fuel Tank Dome on MDS Underpressure Switch Mounting Plate	Perp	18.7	8.0	8.9	35.7	2.8 Grms - Stage I Flight
2571	1B	Airframe at Destruct Battery Mounting	Tang	9.2	4.4	3.7	43.5	
2577	1C	Booster Engine SA #1 on Gimbal Pad	Long	2.1	0.9	0.8	48.7	10.0 Grms - Stage I Flight
2623	1C	Airframe at Mounting of Electrical Umbilical Connector ICIE	Radial	16.8	3.8	4.6	45.0	3.7 Grms - Stage I Flight
4271	S1A	TVC Tank on Destruct Mechanism	Tang	2.1	1.6	1.9	52.4	
4101	S1B	TVC Electrical Package	Perp	11.9	10.9	13.4	46.2	13.1 Grms - Lift-off + 17 Sec.
4107	S1B	TVC Injector Valve Feed	Para	4.0	4.7	7.8	46.2	

TABLE 25 - (Cont.)  
VEHICLE 9 SINGLE SIDE BAND VIBRATION/ACOUSTIC MEASUREMENTS

Meas. No.	Compt.	Location	Axis	Overall Acceleration/SPL Launch	Transonic	Max. Q	DAT Spec.	Comments
4113B	S1B	SRM Staging Rocket (Aft)	Prep	7.0	3.7	1.7	46.2	
2630	1A	SPL, Skin Surface, 120° off Target, Quad III. Sta. 567		<u>DE</u>	<u>DB</u>	<u>DB</u>	<u>DB</u>	
				152	163.6	153.5	152	



TABLE 26  
VEHICLE 9 FLY-AWAY LANDLINE VIBRATION/ACOUSTIC MEASUREMENTS

Meas. No.	Compt.	Location	Axis	Overall Accel./SPL Launch	DAT Spec.	Comments
2554	3A	Guidance Truss Between MCC & Relays	Lateral	<u>Grms</u> 1.7	<u>Grms</u> 16.7	
2556B	3A	Guidance Truss Between IMU & DCU, on Common Mounting	Vert	1.0	16.7	
2559B	3A	Equipment Truss at MDP Mounting	Lateral	3.2	16.7	
2595	3A	Equipment Truss at Motor Driven Switch Mounting	Lateral	2.8	16.7	
2561B	3B	Oxidizer Tank Top on Pressure Switch Mounting Plate	Lateral	2.3	31.6	
2515	2B	Instrument Truss on Destruct Initiator & Amplifier Chassis Panel	Long	4.2	10.5	
2516B	2B	Instrument Truss on Destruct Initiator & Amplifier Chassis Panel	Lateral	3.2	10.5	

TABLE 26 - (Cont.)  
VEHICLE 9 FLY-AWAY LANDLINE VIBRATION/ACOUSTIC MEASUREMENTS

Meas. No.	Compt.	Location	Axis	Overall Accel./SPL Launch	DAT Spec.	Comments
2611	1A	Airframe at Solid State Switches, Quad III, Sta. 508	Radial	10.3	40.1	
2612	1A	Airframe at Solid State Switches, Quad III, Sta. 508	Tang	5.2	40.1	
2617B	1B	Airframe at Solid State Switch Panel Mounting	Long	7.9	43.5	
2618	1B	Airframe at Solid State Switch Panel Mounting	Radial	21.1	43.5	
2619	1B	Airframe at Solid State Switch Panel Mounting	Tang	22.1	43.5	
2572B	1C	Airframe at Electrical Staging Disconnect, on Forging, Quad III, Sta. 1224	Long	21.4	45.0	
2573B	1C	Airframe at Electrical Staging Disconnect, on Forging, Quad III, Sta. 1224	Radial	13.0	45.0	
2622	1C	Airframe at Mounting of Electrical Umbilical Connector ICIE	Long	12.6	45.0	

TABLE 26 - (Cont.)  
VEHICLE 9 FLY-AWAY LANDLINE VIBRATION/ACOUSTIC MEASUREMENTS

Meas. No.	Compt.	Location	Axis	Overall Accel./SPL Launch	DAT Spec.	Comments
2624	1C	Airframe at Mounting of Electrical Umbilical Connector ICIE	Tang	14.5	45.0	
2632	1C	SPL, Internal, near Airframe, Quad III, Sta. 1204		<u>DB</u>	<u>DB*</u>	*Design Values
8003		SPL, AGE Building Wall, Near Door		163.5	154	
				142.5	140	141.6 DB - Corrected for noise per Meas. 8005
8004		SPL, AGE Van Side Wall		133.1	140	
8005		SPL, Capped Microphone Beside Meas. 8003 Microphone		135.4	116	

### 3.2.6.3 Structural Dynamics

#### 3.2.6.3.1 Data Evaluation

A summary of the structural dynamic measurements obtained during the T-III-C - 9 flight is presented. No problem areas were detected on this flight.

Several structural dynamic accelerometers were located on Vehicle C-9; three on the Stage I airframe and four in the transtage, mounted on the equipment truss. Data were obtained on the Stage I and Stage II measurements throughout the applicable boost period. Data on the four transtage measurements were obtained from lift-off through Gemini separation. In general the data were of good quality with minimum noise observed.

The maximum unfiltered levels were experienced, in most cases, during the lift-off phase. Other period of flight were also of interest, however. Table 27 indicates pertinent levels associated with the seven accelerometers. In addition, the guidance accelerometers located in compartment 2B (measurements 1251A and 1252A) are also included for comparison purposes.

Table 27  
Measured Flight Accelerations

Location	Measure- ment	Orientation	Range (g's)	Flight Condition	
				Liftoff (g's O-P)	Transonic (g's O-P)
Equipment Truss	2300	Longitudinal Compartment 3A	10.0	2.0	0.8
Equipment Truss	2301	Vertical Compartment 3A	2.5	2.2	0.8
Equipment Truss	2302	Lateral Compartment 3A	2.5	1.2	0.4
Equipment Truss	2400	Longitudinal Compartment 3A	2.5	1.0	0.63
Stage I (Airframe)	2303	Longitudinal Compartment 1C	10.0	2.1	0.68

**Table 27 - (Cont.)  
Measured Flight Accelerations**

Location	Measure- ment	Orientation	Range (g's)	Flight Condition	
				Liftoff (g's O-P)	Transonic (g's O-P)
Stage I (Airframe)	2304	Lateral Compartment 1C	2.5	1.4	0.8
Stage I (Airframe)	2305	Vertical Compartment 1C	2.5	1.5	0.42
Stage II	1251A	Pitch Compartment 2B	1.0	0.4	0.42
Stage II	1252A	Yaw Compartment 2B	1.0	0.5	0.28

There was some indication of POGO early in Stage I flight (0.3 g PP at approximately 9 cps, measurement no. 2400). No sustained longitudinal oscillation occurred however. Stage I shutdown dynamics were smooth, with slight indication of some first mode bending. First mode bending was not observed during the pitch-over phase.

The transient acceleration levels were considered normal with no anomalies detected. There was no indication of the post-SECO anomalies following Stage II engine shutdown.

#### **3.2.6.3.2 Conclusions**

The flight was exceptionally smooth, with no abnormalities observed in the seven measurements listed.

First mode response, usually seen with light payloads, was not observed.

There was no apparent increase in buffeting data using the Gemini payload, versus payload fairings used on previous flights.

### 3.2.6.4 System Dynamics

#### 3.2.6.4.1 POGO Evaluation

Pre-flight stability analysis conducted in early 1966 predicted MOL/HSQ vehicle configuration pogo instability in the time interval 95 sec to 140 sec of Stage I flight. Post flight analysis based on measured suction pressures and structural mode frequencies predicted instability in the time interval 112 sec to 132 sec of Stage I flight. Subsequent review of Vehicle C-9 flight data from guidance system torque current measurements revealed a sustained oscillation at approximately 0.1g zero to peak level corresponding to the mode A frequency in the time interval 90 sec to 115 sec of Stage I flight. The observed oscillatory acceleration amplitude was only 20% of the amplitude expected from correlations between degree of predicted amplitude and expected oscillatory acceleration levels. No explanation can at this time be made for the differences between the observed and expected acceleration level except to observe that data scatter is quite large on Titan III flights from which the correlation technique is derived.

Presence of the simulated MOL cannister as part of the structural configuration should not have had any appreciable effect on the oscillatory acceleration level. The cannister contained no structural anomalies which in any way could have increased system damping or reduced model gain as acceleration amplitudes increased.

Analysis is currently being performed to determine whether the degree of predicted instability can be reduced by an alternate interpretation of test data used to compute propellant feed system natural frequencies. The alternate interpretation of feed system frequencies should predict a more stable POGO configuration.

#### 3.2.6.4.2 Gemini Separation Analysis

The unexpected vehicle pitch down rates and attitude which resulted from the retro fire operation following Gemini separation can be satisfactorily explained by an analysis of the phase impingement forces applied to the vehicle by the retro motors.

#### 3.2.6.4.2 Gemini Separation Analysis - (Cont.)

It was first determined from films that the retro motors were properly located on the MDL Sim Lab, i.e., 3 motors opposite target and 2 motors on target. It was also determined that all motors fired satisfactorily. The maximum longitudinal acceleration expected during retro operation was  $3.9 \text{ ft/sec}^2$ , using batch firing test valves for retro thrust, and no propellants being accelerated. Guidance data indicated a  $3.9 \pm .4 \text{ ft/sec}^2$  maximum. The 2.5 g accelerometer on the transtage indicated a  $3.5 \pm .3 \text{ ft/sec}^2$  maximum. At the end of retro burn time the expected velocity increment was  $7.65 \text{ ft/sec}$ , using batch values for retro impulse and propellants accelerated. Guidance data indicated  $8.0 \pm .5 \text{ ft/sec}$  and the 2.5 g accelerometer indicated  $7.5 \pm .7 \text{ ft/sec}$ . From this data is concluded that all five retro-rockets fired.

Sometime during retro action, the transtage propellants will collect at the forward ends of the tanks. The time at which they do so depends on where they were at retro ignition. The rotation of the vehicle had little effect on the relative motion of the propellants inside the tanks. Depending on the propellant location, the average torque necessary to produce the pitch-down motion during retro action was between  $-610$  and  $-500 \text{ ft/lbs}$ ,  $\pm 140 \text{ ft/lb}$  due to data reading inaccuracies. (Positive torque is defined as nose up.)

The former value corresponds to propellants at the tank aft ends, and at the forward end for the latter. These torques account for a residual rate at retro ignition of about  $0.04 \text{ deg/sec}$ . Using batch values for retro-rocket thrust, and the vehicle mass properties, the retro-rockets alone would produce a torque of  $+2740 \text{ ft/lb}$ , independent of longitudinal propellant location. The ACS would produce a torque of  $+930$  to  $+1000 \text{ ft/lb}$  with propellants aft and forward respectively. All these torques were calculated assuming the propellant cg is @ W.L.60. Nominal plume impingement forces described in the Fluid Dynamics section would result in torques of  $-130$  to  $-140 \text{ ft/lb}$  from ACS, and  $-3700$  to  $-3460 \text{ ft/lb}$  from the retro-rockets, propellants aft and forward respectively. The net value of these torques is  $-160 \text{ ft/lb}$  for propellants aft, and  $140 \text{ ft/lb}$  for propellants forward, leaving  $450$  to  $640 \text{ ft/lb}$  of nose-down torque unexplained. This unexplained torque could result from a 12 to 18% larger plume impingement than the nominal quoted in the Fluid Dynamic section which is within the

#### 3.2.6.4.2 Gemini Separation Analysis - (Cont.)

estimated accuracy of  $\pm 20\%$ , or from the propellant cg being located @ W.L. 72 to 77 (58 to 86% of maximum distance from W. L. 60). Other factors that could contribute a portion of the unexplained torque are uncertainties in predicted mass property characteristics and in thrust vector alignments and magnitudes.

The vehicle attitude history after retro-action was quite close to what would be expected with normal ACS operation, propellants moving back from the forward end of the tanks, and ACS plume impingement forces acting. This would indicate the anomaly occurred only during retro-rocket action.

An examination of telemetered skin temperatures do not indicate any skin burn through near the retro-rockets or the ACS motors at any time.

In conclusion, the attitude history of the vehicle following Gemini separation can be satisfactorily explained by the action of the 8 rocket motors plume impingement and possibly some motion of transtage propellant relative to their tanks.



### 3.2.7 Payload

#### 3.2.7.1 MOL/HSQ Objectives

The primary objective of Vehicle C-9 flight event concerning the payload was to inject the Gemini B Heat Shield Qualification (HSQ) vehicle into a high-heating re-entry trajectory to verify the Gemini heat shield as modified to accommodate the Manned Orbiting Laboratory (MOL) crew transfer method. The secondary objectives of ascent environment for the Orbiting Vehicle Structure and structural integrity and control capability of the Titan IIIC with a MOL-type payload are reported in sections 3.2.2 and 3.2.6 of this report.

After injection of the HSQ vehicle into the required ballistic trajectory, the transtage was to perform a pitch-up maneuver and power the MOL Simulated Laboratory into a transfer trajectory having an apogee of 160 nautical miles. Power was to have been applied again upon achieving apogee to circularize the orbit at that altitude. Following successful orbit circularization, the vehicle was to perform a 30 degree pitch-up maneuver, eject the OV1-6 satellite, perform a 30 degree pitch-down maneuver and eject the OV4-1T and the OV4-1R satellites in sequence. In this same general time period the scientific experiments contained in the MOL Simulated Laboratory were to have been activated. Upon completion of four orbital revolutions transtage power was to have been disabled while experiment activity and data acquisition was to continue for thirteen days. The command system was to remain active until battery depletion. A time sequence of events may be found in section 3.1.3 of this report.

#### 3.2.7.2 Payload Definition

The payload may be briefly defined as follows:

Gemini Spacecraft, refurbished GT-2 previously flown to qualify Gemini A heat shield, and modified for crew transfer through the heat shield. This spacecraft has a boiler plate adapter to mate it to the Simulated Laboratory and active subsystems to enable spacecraft separation, re-entry, recovery, and acquisition of pertinent experimental data during flight and re-entry phases.

### 3.2.7.2 Payload Definition -(Cont.)

Simulated Laboratory, fabricated from a surplus Titan II Stage I oxidizer tank to approximate outboard profile, mass properties, and structural characteristics of the MOL and furnished with independent telemetry, power distribution, command control, and experiments.

Simulated Laboratory experiments are categorized as follows:

- (1) Serviced by the boost phase instrumentation system and completed prior to orbit inject: Protuberance.
- (2) Passive, requiring no range operations support: Paint pattern and corner reflectors.
- (3) Ejectable: OV1-6 and OV4-1 receiver and transmitter.
- (4) Active on-orbit and serviced by the Simulated Laboratory command and data handling subsystems: Zero-G propellant gaging, Heat Transfer Test Capsule (HTTC), Fuel Cell, Bio-Cell, Orbis-Low (Command only, contained radio frequency system supported by experimenter), and two Micro-meteoroid Detectors (MMD).

#### 3.2.7.2.1 Detail Description

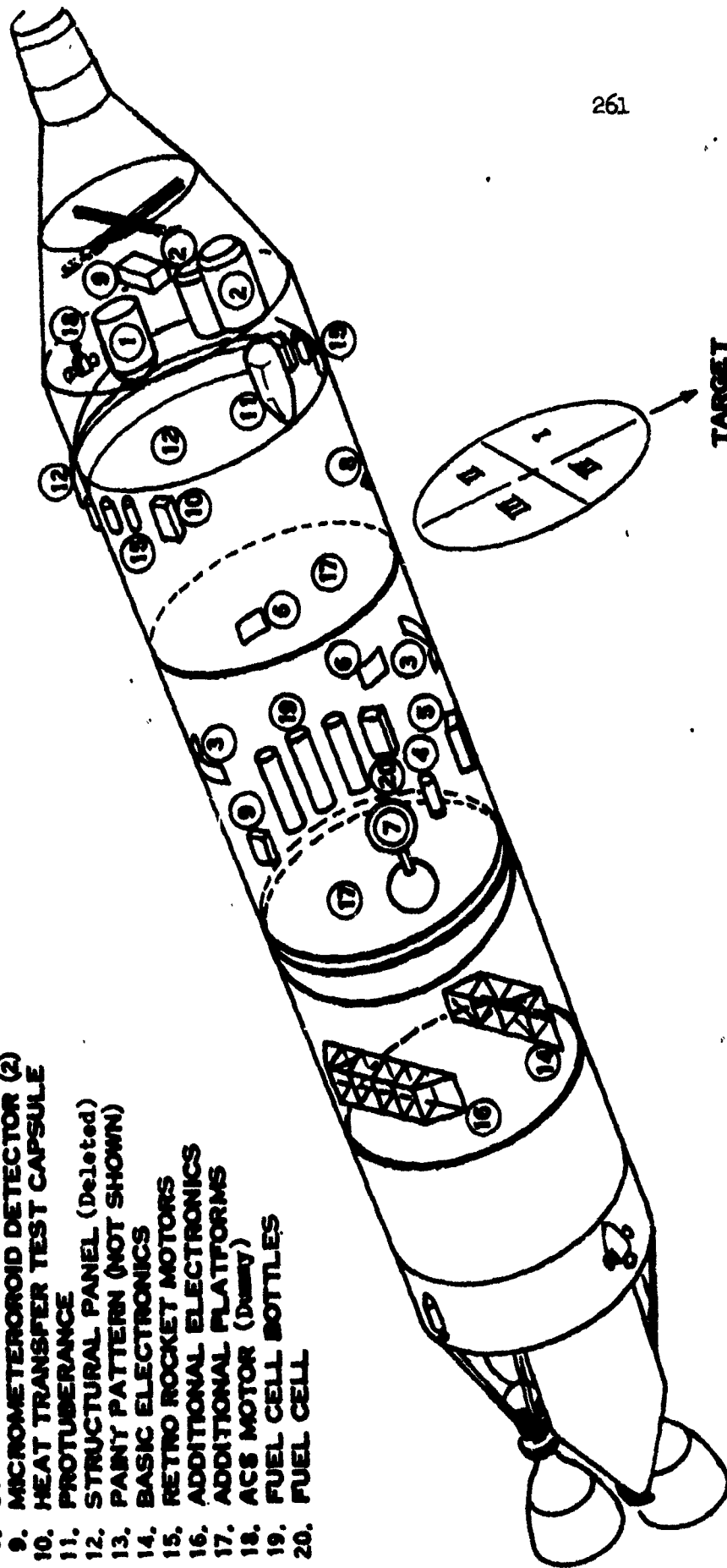
Total payload weight forward of vehicle station 77 is approximately 20,000 pounds with an overall length of 50.2 feet. The general arrangement of the vehicle and experiments is depicted in Figure 128.

#### Spacecraft

The spacecraft structure comprises two major portions - the adapter module and the re-entry module. The adapter module, in addition to providing the mechanical and electrical interface with the laboratory, contains the spacecraft coolant umbilical and a portion of the spacecraft instrumentation system. The complete adapter module remains with the laboratory after spacecraft separation.

The re-entry module is approximately 11 feet in height, with a 7 1/2 foot diameter at the convex heat shield end. The

1. OV-1
2. OV-4
3. T/M ANTENNA
4. BNO CELL
5. ORBS LOW
6. COMM. CONT. ANTENNA
7. ZERO "G" PROPELLANT GAUGING
8. CORNER REFLECTOR (18)
9. MICROMETEROID DETECTOR (2)
10. HEAT TRANSFER TEST CAPSULE
11. PROTUBERANCE
12. STRUCTURAL PANEL (Deleted)
13. PAINT PATTERN (NOT SHOWN)
14. BASIC ELECTRONICS
15. RETRO ROCKET MOTORS
16. ADDITIONAL ELECTRONICS
17. ADDITIONAL PLATFORMS
18. ACS MOTOR (Dummy)
19. FUEL CELL BOTTLES
20. FUEL CELL



261

TARGET

General Arrangement

FIGURE 126

### 3.2.7.2.1 Detail Description - (Cont.)

heat shield crew transfer hatch is approximately 26 inches in diameter. Its edge is located 8 inches from the heat shield/spacecraft mold line.

The re-entry module comprises three sections. The recovery section contains the parachute area. The reaction control system (RCS) section, located between the recovery section and the conical section, contains the hypergolic bipropellant propulsion system which furnishes re-entry attitude control. The conical section is the major portion of the re-entry module. It includes the heat shield and houses most of the functional spacecraft systems equipment.

#### Simulated Laboratory

The Simulated Laboratory consists of a Titan II, Stage I oxidizer tank with a forward skirt, which mates with the Gemini conical adapter. Structural additions have been provided to support electrical power, instrumentation and command control systems, plus eleven scientific experiments.

#### Scientific Experiments

##### (1) Fuel Cell (Air Force Aero Propulsion Laboratory)

A hydrogen-oxygen fuel cell is to be tested by utilizing a resistive load bank. This experiment is internally mounted in the Simulated Laboratory and consists of an Allis-Chalmers 200 watt fuel cell and Martin furnished support equipment. Experiment startup is effected by sequentially initiating fuel supply flow, purging the cell, and applying external loads (after verification that operating voltage has been reached). Thermal control is achieved through utilization of heaters and louvered radiators. Periodic purges during operation are automatically provided; however, additional manual purges may be required dependent upon cell performance. On-orbit operation for a minimum of 50 hours is required. Actual experiment duration will be approximately 100 hours.

### 3.2.7.2.1 Detail Description - (Cont.)

Fuel flow initiation, nominal start-up purges and heater controls are programmed by the Simulated Laboratory sequencer. Module on-off commands and manual purge controls are available via the Simulated Laboratory command subsystem. Experiment data is handled by the Simulated Laboratory PAM telemetry system, real time and stored.

#### (2) Micrometeoroid Detector (Air Force Cambridge Research Laboratory)

This experiment consists of two sensor packages, each having the capability of measuring velocity, mass, and changes of micrometeoroids in the near earth region. One sensor package is mounted in the forward skirt area oriented to be exposed along the velocity vector and the other is mounted in the aft tank area oriented away from target. Both sensors are protected during the boost phase by doors. Experiment activation is effected with application of Simulated Laboratory power to experiment instrumentation and upon opening of the protective doors. A minimum of 6 days of on-orbit operation is required.

Experiment control is provided by the Simulated Laboratory sequencer. Instrumentation parameters are introduced into the Simulated Laboratory orbital data system.

#### (3) Zero "G" Propellant Gaging (Air Force Rocket Propulsion Lab)

The purpose of this experiment is to test two acoustic gaging systems mounted in separate storage vessels. Two pressure vessels, interconnecting piping, and acoustic gaging instrumentation constitute the experiment. Measurements from each tank during Zero "G" conditions were to be compared to pre-calculated values. On-orbit operation of the experiment is limited to periodic activation of the electronics.

Application of power to experiment electronics is cycled with real time Simulated Laboratory telemetry. Data handling support is provided by the Simulated Laboratory T/M subsystems.

### 3.2.7.2.1 Detail Description - (Cont.)

#### (4) Heat Transfer Test Capsule (HTTC) (Air Force Aero Propulsion Lab)

In this experiment molten metal is pumped from a boiler to a space radiator to measure the effects of Zero "G" environment on heat transfer characteristics. The unit is externally mounted under a fairing with a hinged door covering the radiator. Heater power is applied prelaunch to assure molten metal conditions on orbit. The protective door is opened between second and third transtage burns, and the pump started during third transtage burn. Life of the experiment is three hours following pump start.

Experiment support, data handling and controls are provided by Simulated Laboratory sequencer and data handling subsystems.

#### (5) Bio-Cell (Air Force School of Aerospace Medicine)

Frozen, dried biological organisms are to be introduced to a liquid nutrient by a laboratory discrete signal early in the orbit phase. Their reproduction rate in a Zero "G" environment was to be monitored by a lamp-photocell unit and telemetered via the Simulated Laboratory PAM data link. Experiment life will end within six hours.

#### (6) ORBIS - Low (Air Force Cambridge Research Laboratories)

The ORBIS-Low experiment consists of three transmitters (5.006, 10.004, and 30.012 MC), and a 35 ft extendable antenna. Ionospheric sounding by measuring RF transmission to the ground of three different frequencies was to be accomplished.

Antenna extension is commanded by the Simulated Laboratory sequencer. Transmitter On-Off controls are provided by the Simulated Laboratory real time command subsystem. RF reception and all measurements are to be made by the experimenter.

### 3.2.7.3.1 Detail Description - (Cont.)

#### (7) OVL-6 (Office of Aerospace Research)

The OVL-6 is a complete, self-supporting satellite containing several experiments, power, telemetry, and command subsystems. It is ejected from the Simulated Laboratory shortly after orbit circularization in accordance with sequencer program. Simulated Laboratory T/M will include indication of separation and monitor of the eject signal.

#### (8) OV4-1 (Office of Aerospace Research)

The OV4-1 experiment consists of two complete, self-supporting satellites, each with independent power, telemetry and command subsystems. Both satellites are to be ejected from the Simulated Laboratory shortly after OVL-6 ejection. Eject signals and sequencing are provided by the Simulated Laboratory sequencer. Separation monitor and eject signal data channels are included in Simulated Laboratory PAM telemetry.

#### (9) Paint Pattern (Air Force Avionics Laboratory)

The paint pattern is a passive experiment. It consists of a pattern of black and white paint, exhibiting particular optic and thermal characteristics, applied to the Simulated Laboratory. Ground tracking studies will be conducted by the experimenter. Participation in the experiment is not required of AFIRD. The experimenter requires vehicle position predictions. (provided via PFOAR).

#### (10) Corner Reflectors (Air Force Avionics Laboratory)

Eighteen reflectors externally mounted are to be used as targets for earth based laser beams. The experiment is passive.

#### (11) Protuberance (MOL Program Office)

A representative attitude control nozzle assembly is mounted on the Simulated Laboratory. A fiberglass fairing which could house that assembly is mounted diametrically opposite on the vehicle. Temperature and heat flow data is to be gathered during the ascent phase from each protuberance to assess the requirement for a protective fairing. The experiment is completed during the power flight phase of the mission.

### 3.2.7.2.2 MOL/HSQ Electronic Systems

The basic requirements for the boost and orbital missions are listed in Table 28 by experiment or basic HSQ contract item. The composite of these requirements resulted in a vehicle with three telemetry links, a command system, three individual power systems, on-board magnetic tape storage, and a ten-step programmer controlled by the transtage computer.

#### Telemetry and Data Storage System

Three types of telemetry were used in the Simulated Laboratory: Pulse Code Modulation (PCM), Single Sideband (SSB), and Pulse Amplitude Modulation (PAM). The PCM and SSB systems are the same type as those used in the TIIIC booster and were only used during the boost phase. Upon orbit injection these were shut down and the PAM system was turned on to handle experiment data. The PAM system consists of two commutators, a time-reference generator, a two-channel tape recorder, a four-channel subcarrier oscillator assembly, a ten watt transmitter, and signal conditioning devices.

Normal operation of the system on-orbit is as follows: When the vehicle is "in sight" of a ground station the telemetry transmitter is commanded on, permitting reception of real time PAM data. The tape recorder may now be commanded to reproduce, permitting simultaneous reception of real time and tape recorder stored data. When loss of usable signal is imminent, the telemetry transmitter is commanded off returning the tape recorder to the record mode. Upon acquisition of the next ground station the above data retrieval sequence may be repeated.

A back-up telemetry mode exists whereby under command control, PAM data may be telemetered from orbit through the SSB booster transmitter. This provided protection against the loss of orbital data due to a failure of the prime ten watt transmitter.

#### Command Control

A fully redundant command receiver and decoder system exists in the vehicle. The command receiver responds to ten of the twenty Inter Range Instrumentation Group (IRIG) tones used to frequency modulate the range transmitter. The tones are combined into pairs by the decoder so that two specific tones are always required to execute a command. One of the tone pairs is unique in that it serves as an address specifically



TABLE 28  
EXPERIMENTS & BASIC HSQ REQUIREMENTS

Item	Orbit Req.	Approx Dur From L/O	Ordnance Req	Data Real Time	Storage	Sim-Lab Type Data	Approx. Power	Comments
Gemini Cap- sule HSQ	Balistic Trajec- tory	14 Min	Separ- ation	PCM	N/A	Sound Pres- sure, Abso- lute, Press- sure, Strain Guage, Sep- aration	N/A	Ordnance Power supplied by capsule thru sim-lab sequencer
Basic HSQ (Sim-Lab)	Boost Phase	14 Min	N/A	PCM	N/A	Absolute Pressure, Temp.	N/A	+10 VDC Transponder power supplied by Sim-Lab.
Protuber- ance	Boost Phase	53.5 min.	N/A	PCM	N/A	Temp., Calori- meter	N/A	+10 VDC Transponder power supplied by Sim-Lab.
OV-1	Ejected at Sim. Lab Orbit Injection	N/A	Separ- ation	PAM	PAM	Separation enable and ejected	N/A	Ordnance Power supplied by Sim- Lab.
OV-4 T&R	Ejected at Sim- Lab Orbit Injection after OV-1	N/A	Separ- ation	PAM	PAM	Separation enable and ejected	N/A	Ordnance power supplied OV-4 routed through Sim-Lab sequencer.
Zero-G Pro- pellant Guaging	Boost & with Sim-Lab Orbit of 160 n mi circular	40 through 6 days on-orbit	N/A	PCM PAM	N/A	Volume, Temp., Pressure	+25 VDC 90W	PCM data during boost & data with real time PAM operation
Structural Panel								Deleted

TABLE 28 - (Cont.)  
EXPERIMENTS & BASIC HSQ REQUIREMENTS

Item	Orbit Req.	Approx Dur From L/O	Ordnance Req	Data Real Time	Storage	Sim-Lab Type Data	Approx. Power	Comments
Orbits Low	On-orbit with Sim-Lab, 160 n. mi. circular	10 days on- orbit	Door opening Antenna extend	N/A	N/A	Antenna extended, Door full open	+25 VDC 16W Avg.	Operation under Sim-Lab ground command control
Fuel Cell	On-Orbit with Sim-Lab, 160 n. mi. circular	50 hrs min 100 hrs goal	H <sub>2</sub> & O <sub>2</sub> supply valves	PAM	PCM	Temp., H <sub>2</sub> , O <sub>2</sub> , H <sub>2</sub> O Pressures, Fuel cell voltage purge	+25 VDC 200W HTR 13W control 5W purge	HTR power for L/O + 4 hrs, control & purge power as re- quired.
MMD (2 units)	On-orbit with Sim-Lab, 160 n. mi. circular	6 days on-orbit	door openings	PAM	PAM	Micrometer- roid veloc- ity, polar- ity, ampli- tude, micro- phone, doors full open	+25 VDC 5W/unit	
HTTC	Boost & on- orbit with Sim- Lab, 160 n. mi. circular	4 hours	door opening	PCM PAM	PAM	Pressure, Temp., Acceler- ation	+28 VDC 850 W +25 VDC 325W	PCM data-pressure & Temp. PAM-pressure, Temp., & acceleration
B10-Cell	With Sim-Lab 160 n. mi. cir- cular for 8 hrs	N/A	N/A	PAM	PAM	Organism growth rate, temp.	+25 VDC 1.25W	
Paint Pattern								Passive
Corner Reflectors								Passive

### 3.2.7.2.2 MOL/HSQ Electronic Systems

for MOL/HSQ. The command system will not accept any other command unless it is preceded by the vehicle address. A timer in the decoder arms the command busses for 15 seconds when a vehicle address is received. Only commands received during that period are accepted by the vehicle. Totally, the vehicle can accept 15 commands of which three are spares (Refer to Table 29).

#### Antennas

Two command antennas (identical to the TIII destruct antennas) are used on opposite sides of the vehicle. The power splitter which couples energy from each antenna to each command receiver is also a TIII device which provides isolation such that a single malfunction will not make the system inoperative.

The two telemetry antennas are identical to the TIII system used on Stage II of the booster.

#### Power Systems

Three individual power systems are used on the vehicle. They are:

- (1) A pair of 28 volt TIII 60 ampere hour batteries supplying the booster telemetry system.
- (2) An identical pair of batteries to those mentioned above to supply the 1000 watt HTTC heater loads.
- (3) A pair of Gemini-type 25 volt 400 ampere hour batteries used to power the orbital data system and most of the experiments.

The 28 volt bus system is regulated at 25 to 31 volts and the 25 volt system is regulated over a 22 to 29 volt range. A power distribution and switching system under a combination of program and command control is used to produce ten significantly different configurations of the power system in flight.

#### Program Control

A 21-relay sequencer under guidance computer control provides the necessary programmed discretes during the first seven hours of flight. All but one relay in the

TABLE 29  
COMMAND FUNCTIONS

270

<u>Command Number</u>	<u>IRIG Tone Channels</u>	<u>Function</u>
1	4 + 10	a) Spacecraft Address b) Lo-Power T/M On c) Zero-G Propellant Gauging Electronics On
2	6 + 7	Recorder to Playback Mode
3	6 + 8	a) Recorder to Record Mode b) T/M Off c) Zero-G Propellant Gauging Electronics Off
4	6 + 13	Transtage Power Shutdown Enable
5	6 + 14	a) Fuel Cell On b) Fuel Cell Purge On
6	7 + 8	Fuel Cell Purge Off
7	7 + 13	ORBIS - Low On
8	7 + 14	Orbital Data System On
9	7 + 15	Spare
10	8 + 13	a) Hi-Power T/M On b) Lo-Power T/M Off
11	8 + 14	ORBIS - Low Off
12	13 + 14	Fuel Cell Off
13	13 + 15	Orbital Data System Off
14	6 + 15	Spare
15	14 + 15	Spare

### 3.2.7.2.2 MOL/HSQ Electronic Systems - (Cont.)

sequencer is redundant to provide maximum reliability, specifically with dual bridge-wire ordnance devices. Sequencer outputs are paralleled where only a single activation device is used.

### 3.2.7.3 Launch Preparations

The effectiveness of the electrical checkout performed at the Denver Vertical Test Fixture (VTF) was seriously compromised as a result of the requirement to delay installation of the scientific experiments until arrival of the vehicle at the Eastern Test Range (ETR). This resulted in an unusual number of problems which were required to be worked at ETR. Routine installation and test functions performed at ETR in preparation for launch are listed in table 30.

Numerous interference problems were encountered during ballast installation. Modifications were required to mounting hardware, Sim Lab structure, and the ballast itself before the installation was completed. The structural panel experiment was deleted from the mission as a result of questionable integrity of the concept and the possible adverse impact on the flight. Serious fit problems were encountered during installation of the corner reflectors. The problem was finally resolved by machining the male threads on the corner reflector units. Use of N306A lubricant was approved for use as required.

#### 3.2.7.3.1 Experiment Preparations

The following delineates pertinent factors associated with launch preparation of several of the scientific experiments.

TABLE 30

## MOL/HSQ SIM LAB INSTALLATION AND TEST HISTORY

ETR

1. Sim Lab Arrival - VIB	18 August
2. Receiving - Insp. Completed	20 August
3. Fuel Cell Pallet Installation	22 August
4. Protuberance Installation	22 August
5. Fuel Cell Installed	25 August
6. Ballast Installation Complete	26 August
7. Sim Lab Mated to Core Vehicle	29 August
8. Power Application	31 August
9. Zero-G Propellant Gaging Exp. Installed	31 August
10. Orbis-Low Transmitter Installed	31 August
11. Bio-Cell Installed	31 August
12. Subsystem Tests Completed	18 September
13. VIB CST Performed	19 September
14. Vehicle Moved to SMAB	21 September
15. Vehicle Arrival - P-40	27 September
16. OV4-1 Satellites Installed	2 October
17. OVI-6 Satellite In-Place	2 October
18. Gemini Spacecraft Installed	3 October
19. Gemini Electrical Mating	12 October
20. HTTC Installed	12 October
21. P-40 Baseline CST	13 October
22. EMC Testing	19 October
23. Umbilical Drop Test	21 October
24. Launch CST Completed	28 October
25. Corner Reflectors Installed	30 October

### 3.2.7.3.1 Experiment Preparations - (Cont.)

#### Zero-G Propellant Gaging

An experiment requirements change dictated that pressurization of the spheres was to be deleted. This necessitated replacement of the upper-sphere transducer to a component having a range of 0.25 psia. A decision not to transfer propellant while in flight required capping and stowing of the connector and harness to the solenoid valve. Finally, propellant volumes were changed to three (3) gallons in the upper sphere and fifteen (15) gallons in the lower sphere. The electronics package was modified by incorporating a filter at Acoustics.

After completion of the launch CST, the experimenter requested additional testing. The retest was carefully controlled because electrical connectors were disconnected during the test. In accomplishment of the retest, 28 volt power to the experiment was inadvertently shorted to ground causing the fuse to the experiment to open. This fuse was located in a potted fuse block containing nine fuses. The fuse block was replaced and sufficient testing was performed to assure that all affected systems were operating properly.

#### Heat Transfer Test Capsule

During the Electro-Magnetic Compatibility (EMC) test, the time required for the HTTC to reach operating temperature was longer than anticipated. The experiment was removed for bench checks and an open fuse was found in the upper boiler heater circuit and was replaced.

#### OV-4 Satellites

Preflight checks revealed improper resistance in a component. The component was replaced and the checks were successfully completed. The CST results were not affected by this change.

#### 3.2.7.4 Flight Performance

##### 3.2.7.4.1 Booster Flight Phase

The fuel cell heaters were energized using ground power three hours before liftoff in order to achieve normal operating temperature. The airborne power supply continued to heat the unit after liftoff until the three-hour cutoff power switch was opened. At this time the unit bootstrapped to supply its own heater power.

HTTC heater power was applied 70 minutes prior to liftoff. The measurements indicated that the lower boiler was maintained at approximately 700 degrees at liftoff while the upper boiler appeared to be maintained at 450 degrees Fahrenheit.

The maximum temperature observed at the protuberance experiment during the first eight minutes of flight was 225°F at T+118 seconds.

Calorimeter maximums of 1.4 Btu/square feet-second occurred between T+83 and T+90.5 seconds. Laboratory structure temperatures (maximum skin temperature of 190°F at T+118 seconds) and pressures (maximum pressure differential of 4.5 psi at T+39 seconds) appeared normal.

The telemetry system operated continuously from liftoff until booster system shutdown. One measurement, a protuberance platinum thermometer, was lost during this period. The vehicle sequencer programmed functions occurred as planned initiating such events as retrorocket ignition, Orbit-Low and HTTC door opening, activation of Bio-Cell and MMD, and shutdown of the booster telemetry system. Refer to Table 1 for detail flight sequence of events.

The Gemini Spacecraft was successfully injected into the planned re-entry trajectory. Table 2 presents the observed and predicted trajectory parameters. Sim Lab backoff and reorientation for the transfer maneuver to orbit did not occur as predicted. Instead of the pitch-up rate at retro termination, a pitch-down rate was observed. This required more than the predicted attitude control system operation. Details of this anomaly may be found in section 3.2.2 of this report. Final circular orbit was achieved as planned.



### 3.2.7.4.2 On-Orbit Operations

#### Sim Lab Electronics

After initiation over Carnarvon the orbital telemetry system operated by ground Command Control for the next six consecutive days. During orbit number 92 the system was shutdown with power supplied to the Orbis-Low experiment. Approximately 12 days and 14 days after orbit injection, the telemetry system was activated to obtain vehicle status. The 14th day activity also provided a check of the 50 watt backup transmitter. The system performance was satisfactory and complied with design requirements. The system was again activated at approximately T+30 days and was found to be operating properly. Considering a total of 126 data channels, one channel (fuel cell purge indication) appeared to have been lost.

Sequencer operation satisfied all design requirements by initiating such events as: orbit power transfer, satellite ejection, fuel cell experiment initiation, MMD door opening, Orbis Low antenna deployment HTTC shutdown, and finally complete power shutdown of the transtage.

The on-board command system responded to and executed all commands transmitted by ground control throughout the mission. All of the 12 usable commands were exercised as dictated by mission requirements.

Table 31 presents a brief overall status of the performance of the scientific experiments. The following are more detailed results of a few of the experiments.

#### OV4-1 Satellites

The orbital parameters achieved were very close to those that were predicted. It was initially predicted that only one antipodal condition would be acquired during the satellites orbital lifetime. However, to the delight of the experimenter, three such antipodal conditions had been achieved as of 19 December. Communication has been accomplished when the transmitter and receiver were antipodal. Current prediction (as of 20 December) for satellite re-entry is 14 January for OV4-1R and 24 January for OV4-1T.

#### HTTC Experiment

The experiment is not functioning as planned because of loss of the upper boiler heater. Review of the data received indicates pump start was achieved. The

TABLE 31 SCIENTIFIC EXPERIMENT RESULTS

<u>EXP.</u>	<u>RESULTS</u>	<u>REMARKS</u>
LAB SUPPORT EQUIPT	SUCCESS	
ORHIS--LOW	FAILURE	NOT DRAWING ANY LOAD CURRENT
OV-4	UNQUALIFIED SUCCESS	COMMUNICATION ACHIEVED WHEN TRANSMITTER AND RECEIVER WERE ANTIPODAL
OV-1	UNQUALIFIED SUCCESS	INTERNAL EXPS ACTIVATED/ OR EJECTED
ETTC	QUALIFIED SUCCESS	UPPER BOILER DID NOT HEAT PROPERLY
ZERO "G" PROP. GAUGING	APPARENT SUCCESS	EXPERIMENTER STILL EVALUATING DATA
PAINT PATTERN	SUCCESS	PHOTOGRAPHS OBTAINED
CORNER REFLECTORS	NO DATA TO DATE	LASER NOT YET DELIVERED
BULK CELL	UNQUALIFIED SUCCESS	OPERATED APPROX 120 HRS
PROTECTORANCE	UNQUALIFIED SUCCESS	
BIO CELL	APPARENT SUCCESS	EXPERIMENTER STILL EVALUATING DATA
MND	APPARENT FAILURE	EXCESSIVE NOISE EXPERIMENTER STILL EVALUATING DATA

#### 3.2.7.4.2 On-Orbit Operations - (Cont.)

experimenter is reviewing the data in detail to determine if useful information has been obtained despite the failure.

##### Fuel Cell

Experiment activation was successfully accomplished and performance was entirely satisfactory. During the 11th revolution, approximately 17 hours after liftoff, one cell reversed and the voltage dropped to approximately 26 volts. By the 18th revolution, the voltage was down to 24.5 volts. The experimenter requested a 10 second manual purge be accomplished each revolution for the remainder of the mission. The fuel cell was shut down during the 32nd revolution for two minutes as planned. Upon successful re-start it was decided to continue the experiment until depletion or failure caused termination. By revolution 88, approximately 120 hours of near normal operation, the fuel cell had removed itself from the load due to low voltage. Indications are that if a method were available to reheat the cell, the experiment could have continued successfully for another 120 hours as only half the gas supply had been used.

##### Orbital Test Support

Orbital support of the OV4-3 satellite (Sim Lab) was provided by ETR, acting as the lead range, in response to PFOAR, the range user. Participating stations were Tel 2 and Tel 4 of CKAFS, Ascension, Antigua, Carnarvon, Hawaii, Johnson Island, and West Coast WTR sites. Martin Company provided a test conductor and a planning and evaluation team on an around-the-clock basis in support of PFOAR.

Range activities consisted of interrogation of the satellite for data acquisition purposes, (real time and airborne stored), execution of requested experiment peculiar commands, and readout of status data for relay to Martin and Experimenter analysts. Martin Company participation consisted of data analysis, overall mission and individual overpass planning, and coordination of experimenter requirements.

#### 3.2.7.4.2 On-Orbit Operations - (Cont.)

Real time data interrogations and readouts of the airborne data recorder were implemented during the initial six days of the mission, (Phase 1), in such a way as to maximize recovery of stored data within the limitations of Range capability to support. During this phase a total of 43 readouts were conducted resulting in acquisition of 100.4 hours of data. A total of 37.2 hours of mission data was lost due to geographical limitations of the range, and support conflicts with OV4-1 and OV1-6 satellites and the impending Gemini 12 mission. Phase 1 was commanded to completion by deactivation of the orbit data system 5 days 18 hours and 35 minutes after launch (Orbit 91).

It was intended that during the following 10 days of the mission (Phase 2), the orbit data system would remain deactivated and performance of the Orbis Low experiment would be completed. However, due to apparent failure to command the Orbis Low experiment on, the system was reactivated to repeat the Orbis Low on command, dump the airborne recorder and evaluate subsystem status on orbits 183, 214, 215 and 230. A successful readout via the back-up T/M transmitter was accomplished during this period.

Following verification of an unsuccessful orbis low experiment, Phase 3 of the mission (continuation of data recovery until power depletion) was initiated on the L+22nd day. Phase 3 support by the range was implemented on a low priority basis with day time passes only being scheduled. Following each daily series of passes the orbit data system was being deactivated to conserve power.

Throughout the flight, booster and MOL Sim Lab support was completely satisfactory and in no way was contributory to the unsuccessful experiments.

### 3.3 GROUND EQUIPMENT

#### 3.3.1 Mechanical AGE

##### 3.3.1.1 Summary

All Mechanical AGE Systems and hardware performed normally during the launch of Vehicle C-9. These include the Propellant, Pressurization, Umbilical, Air Conditioning, and Water Systems.

##### 3.3.1.2 Configuration

Normally, the Mechanical AGE Systems configuration does not change from launch to launch except as authorized by approved EDCS's. In the launch of Vehicle C-9, however, several changes were made to accommodate the Gemini and MOL experiments. These were as follows:

##### 3.3.1.2.1 Umbilical Systems

###### Air Conditioning, MOL

The Air Conditioning System was extended from the normal payload interface to a new and higher interface with the MOL Lab. The system functioned normally.

###### Gemini B Umbilicals

A completely new system was designed and installed in the LC-40 Umbilical Tower for the purpose of disconnecting and retracting the two Gemini B umbilicals; one water and one electrical. This system consisted of lanyards, booms and actuating equipment on the Umbilical Tower.

##### 3.3.1.2.2 Pressurization Systems

Vehicle C-9 Pressurization Systems configuration was identical to previous vehicles with the following systems added to service Gemini B and the MOL experiment.

###### Gemini B Nitrogen Supply

A 3400 PSIG nitrogen supply was installed to supply Gemini B (MAC) with a pressure source for J-Box purging and pneumatic tool operation.

### 3.3.1.2.2 Pressurization Systems - (Cont.)

#### Gemini B Vent

A vent system was designed and installed from the MAC Propellant Metering Units to the existing TIII Vent System at LC-40.

#### Zero G Experiment

A 240 PSIG nitrogen supply system was designed and installed to provide for sphere pressurization in the Zero G experiment.

#### HTTC Experiment

A 23 PSIG nitrogen system was designed and installed to provide a heater cooling purge.

#### Fuel Cell Experiment

A 0 to 2200 PSIG helium system was designed and installed at the VIB and at LC-40 to provide leak and functional checks as well as blanket pressure for the Fuel Cell experiment.

#### Configuration Summary

All pressurization systems described above performed normally during Vehicle C-9 launch.

### 3.3.1.3 Data and Analysis

#### 3.3.1.3.1 Propellant Transfer Systems

##### Oxidizer Loading

Oxidizer loading was accomplished on Sunday 30 October 1966. Prover runs were completed successfully and without incident (Table 32). The ACS tank was loaded normally as were Stage I, II, III and the TVC tanks. For tabulated loading data refer to Table 33. All level sensor checks made during loading were satisfactory. For results see Table 34.

TABLE 32  
 PROVER RUNS - VEHICLE C-9 LAUNCH  
 % ACCURACY

Oxidizer, 10/30/66

	50 GPM	100 GPM	200 GPM
FM-1 to prover	-.22	+.02	+.10
FM-2 to prover	-.27	+.18	+.25
Spread	.05	.16	.14

(Allowable to prover  $\pm$  .43)

(Allowable spread  $\pm$  .45)

Fuel

FM-1 to prover	-.12	-.14	-.21
FM-2 to prover	-.10	-.18	-.21
Spread	.02	.04	.00

(Allowable to prover  $\pm$  .32)

(Allowable spread .32)

TABLE 33  
VEHICLE 9 LAUNCH  
PROPELLANT LOADING STATEMENT

STAGE	DESIRED LOAD	GROUND BIAS	FLOWMETER PRESET	FMC-1	FLOWMETER READINGS FMC-2	FM-1	FM-2	METER SPREAD	*TEMP. OF
I Oxid.	13664	42.27	13706.27	13695.87	13706.78	13696	13707	.08	82
II Oxid.	3493	12.83	3505.83	3506.28	3506.05	3506	3506	.00	82.5
III Oxid.	1142.50	11.30	1160.80	1161.31	1161.02	1161	1161	.00	83.3
TVC-1	1126.76	36.32	1163.08	1163.68	1163.35	1163.5	1163	.04	83.5
TVC-2	1126.76	12.52	1139.28	1139.68	1138.99	1139.5	1139.5	.09	83.1
I Fuel	11276	27.40	11303.40	11301.56	11303.88	11301.5	11303.5	.02	62.5
II Fuel	3196	9.39	3205.39	3205.86	3205.61	3206	3205.5	.02	81
III Fuel	939.30	9.71	949.01	949.16	949.61	949	949	.00	82.7
ACS	DESIRED LOAD-LBS.	TEMP °F	DESIRED LOAD-GAL.	GROUND GALLONS	METER PRESENT	METER READING			
Oxid.	77.4	68	6.4188	0.1519	6.5707	6.5752			
Fuel	48.4	71	6.4309	0.1519	6.5828	6.5884			

\*Stage I and II temperatures are read from a transducer located in the vehicle tanks. Stage III and TVC-1 and 2 have no airborne temperature probes; these values represent the temperature in the ground system at the end of loading.



TABLE 34  
VEHICLE C-9 LAUNCH  
LEVEL SENSOR CHECK DATA

STAGE	SENSOR	ALLOWABLE MIN.	SENSOR VOL. MAX.	TEMP. OF	FLOWMETER FMC-1	READINGS FMC-2
I Oxid.	High Point	12620.36	12821.79	82.0	12698	12712
II Oxid.	High Point	3235.00	3290.42	82.5	3244	3245
III Oxid.	Low Point	130.65	145.42	83.0	131	131
I Fuel	High Point	10532.83	10685.08	62.5	10561	10563
II Fuel	High Point	2953.59	3000.75	81.0	2969	2961
III Fuel	Low Point	166.45	176.80	83.0	170	170

### 3.3.1.3.1 Propellant Transfer Systems - (Cont.)

#### Propellant Temperature

All propellant tanks except Stage I fuel were loaded with propellant at ambient temperature. At the completion of loading, all temperatures were in the low 80° range. The day prior to launch, a cold front reached the launch area resulting in a drop in the propellant temperatures. The following data show the variation that occurred in the propellant temperature.

STAGE	PROPELLANT	LOADED TEMP °F	LIFT-OFF TEMP. °F
I	Oxid.	82.0	64.0
II	Oxid.	82.5	63.5
I	Fuel	62.5*	57.9
II	Fuel	81.0	63.6

\*Conditioned to this value

### 3.3.1.3.2 Pressurization Systems

No pressurization problems were experienced during the launch of Vehicle C-9. Refer to Table 35 for data on Vehicle tank pressures.

#### ACS Nitrogen Sphere

The ACS nitrogen sphere pressure dropped from the final topping pressure of  $3335 \pm 40$  PSIG to 3270 PSIG and remained at this level until lift-off. The pressure drop occurred after umbilical disconnect and is attributed to the dropping ambient temperature. The sphere pressure was still well above the lower launch limit of  $2780 \pm 30$  PSIG and did not cause a problem.

TABLE 35  
VEHICLE 9 LAUNCH  
TANK PRESSURES

TANK	UPPER LAUNCH LIMIT	LOWER LAUNCH LIMIT	PRESSURE PRIOR TO P/V OPEN	PRESSURE @ L/O
Stage I Fuel	28.98 psia	24.53 psia	27.3 psia	26.9 psia
Stage I Oxid.	41.92 psia	37.75 psia	38.9 psia	38.1 psia
Stage II Fuel	55.98 psia	50.78 psia	52.6 psia	52.2 psia
Stage II Oxid	53.92 psia	49.52 psia	51.1 psia	50.7 psia
ACS Nitrogen Sphere		3325 psig @ 0500 EST 3270 psig @ 0600 to 0815 EST		
Stage III Helium Sphere		3620 psig @ 0500 EST 3600 psig @ 0600 to 0815 EST		

### 3.3.1.3.2 Pressurization Systems - (Cont.)

#### Stage I Oxidizer Tank Pressure

A similar pressure drop, attributed to the ambient temperature, was experienced in the Stage I Oxidizer Tank. This situation was corrected by repressurizing the tank at approximately 0705 EST, November 3rd.

### 3.3.1.3.3 Umbilical Systems

Data review indicates that all umbilicals disconnected normally during the launch of Vehicle C-9. The electrical umbilical sequence of separation was as follows:

<u>UMBILICAL</u>	<u>TIME AFTER LIFT-OFF</u>
LB1E	40 Ms.
RB1E	60 Ms.
1C1E	100 Ms.
2B1E	150 Ms.
3A1E	160 Ms.
3A2E	160 Ms.
2C1E	180 Ms.
3A3E	180 Ms. *

\*Estimated based on data furnished by ACSP which indicates an accuracy of 0.1 sec.

### 3.3.1.3.4 Air Conditioning Systems

The Air Conditioning Systems for the Core, the Lab and the Vans functioned normally during the pre-launch activities and the launch of Vehicle C-9.

### 3.3.1.3.5 Mechanical Installations

#### Water Systems

The Water Systems performed satisfactorily and met all design objectives. For this launch, activation of the upper umbilical tower water system was delayed to prevent wetting of the corner reflector experiment on the MOL Lab. This delay caused no increase in tower structure or installation launch damage. Future Titan IIIC launches will also incorporate this delay to preclude the possibility of getting undesirable water on payloads prior to lift-off.

#### 3.3.1.3.5 Mechanical Installations - (Cont.)

##### Electrical Connector Restraining System

After failure of the restraining clamps during Vehicle C-12 launch, an energy absorbing restraining system was designed and installed at LC-40. The new system performed very well and met all design objectives during the C-9 launch.

##### Stand Damage

Launch damage to the mechanical AGE systems was minor; no engineering changes will be required.

#### 3.3.1.4 Conclusions and Recommendations

The Mechanical AGE systems performed without incident for this flight. No recommendations are considered necessary as a result of the data evaluation.

### 3.3.2 Electrical AGE

#### 3.3.2.1 Summary

The AGE performed per design all through countdown and launch. Modifications to VPDC, LPFDC and Power Supply cabling per MOL/HSQ requirements functioned satisfactorily.

#### 3.3.2.2 Configuration

Equipment was modified for MOL/HSQ requirements and was configured per ECP changes M40001, C40009, C40018 and C40020. Basic difference from vehicle 12 configuration was the absence of M01483, vehicle weight savings change which reduced power transfer sequence considerably, and power distribution and transfer functions to be compatible with the Gemini re-entry capsule, simulated lab, and experiments.

#### 3.3.2.3 Data and Analysis

Review of AGE electrical system performance during the Vehicle C-9 launch event confirmed satisfactory operation with no anomalies.

#### 3.3.2.4 Special Evaluations

##### 3.3.2.4.1 SRM/SDS battery heater power transfer during countdown.

##### Problem Description and Evaluation

During countdown of Vehicle 9 there were a number of extended holds which necessitated reapplication of SRM battery heater power to bring terminal voltages up to optimum levels. This is a manual operation utilizing a circuit breaker on the VPDC. After the T-count hold was cleared the circuit breaker was turned off per procedures at the time of pad evacuation.

An additional hold was encountered after pad evacuation due to a cold front moving into the area which again reduced the SRM battery voltages to a marginal level.

Experience with the SRM batteries and terminal voltage characteristics of primary cell batteries confirm marginal voltage possibilities after extended soaking in below normal temperature ambients.

## 3.3.2.4.1 (Cont.)

Resolution and Recommendation

A change was considered which would call for removal of the Battery Heater Power during the terminal count and automatic reapplication in the event of a hold (return to ground power). However, it was decided that the change was unnecessary in view of relatively low probability of having SRM battery voltage drop below minimum prelaunch levels. Holds longer than those experienced during Vehicle C-9 countdown coupled with ambient temperatures as low as those experienced in the countdown would be required before battery voltage would drop to the minimum level. This combination is considered remote and therefore no corrective action was deemed necessary.

3.3.2.4.2 Possibility of damage to the electrical AGEProblem Description and Evaluation

In previous launches efforts have been expended toward guiding the fall of the SRM umbilicals during liftoff to prevent their hitting the engine bell. On Vehicle C-9 the lanyard did not break and the umbilicals faced up into the exhaust blast of the SRMs. There are reports of visual display of arcing, shorting and burning at the end of the umbilical connectors. Post-flight analysis of the equipment noted ten (10) circuit breakers opened in the VPDC. Circuit analysis revealed the following:

- a) Some circuits which must have shorted did not have open breakers.
- b) Some of the circuits were open and could not have shorted until reset of the T&FS and CMG.
- c) Shorting existed on both SRM umbilicals.
- d) Cape review of DRS indicated most circuit breakers opened or had opened by T + 10 minutes.
- e) All circuits were circuit breaker isolated except SRM dump start which comes off VPDC readiness bus and is removed on CMG reset.

## 3.3.2.4.2 (Cont.)

Contact with Cape personnel indicated no damage to the AGE or GIE but assurance of such will require a wire-to-wire check throughout the van and post-mod testing after removal of the MOL/HSQ mod and updating to the vehicle 13 configuration.

Analysis of interconnections indicates the smallest wire and, hence, most likely point for a wire failure to be in the umbilical or between the transporter J-box and the umbilical. Efforts to obtain any assurance that there is no damage in the GIE have failed due to lack of testing capability while vans are being modified.

Resolution and Recommendations

Analysis and Cape contacts fail to reveal any equipment damage due to shorting although final assurance will not be available until retesting is completed, probably in January.

Possible remedial action is being evaluated.



SSD-CR-66-707

Addendum A  
Contract AFO4(695)-150  
CORE & VEHICLE POSTFLIGHT WEIGHT DATA  
(MOL-HSQ PAYLOAD)  
(Vehicle 9)

December 1966

Prepared by  
TITAN III WEIGHT CONTROL UNIT

Approved by

J. N. Miles  
TITAN III WEIGHT CONTROL UNIT

R. K. Hall  
TITAN III PROPULSION

MARTIN COMPANY  
DENVER, COLORADO

SSD-CR-66-707

## FOREWORD

This report is submitted and satisfies the requirements of Line Items IN-4, IN-14 and 3C-04 and is submitted as an Addendum to 1K-62 of Contractor Specification SSS-TIII-010-DND (Rev. 3) dated 15 April 1963, and DSCN's 1 through 155 as incorporated in Item 1, Exhibit A, Task 5.13 of Contract AFO4(695)-150.

CONTENTS

A-111

	<u>Page</u>
Foreword . . . . .	A-ii
Introduction . . . . .	A-1
Reasons for Change . . . . .	A-2
Performance Weight Summary . . . . .	A-5
Liquid Propellant Inventory . . . . .	A-9
MOL-HSQ Payload . . . . .	A-12
Ejected Items . . . . .	A-13
Mass Property Data, Stage 0, 1, 2 Operation . . . . .	A-14
Mass Property Data, Stage 3 Operation . . . . .	A-17

# INTRODUCTION

This report presents post-flight mass property data for Titan IIIC Vehicle 9. The data is based primarily on that presented in Weight and Balance Status Report SSD-CR-66-591, and differs only in changes incorporated in the field subsequent to that report.

Solid Rocket Motor (SRM) Data has been extracted from ER-UTC-66-120, Weight and Balance Status Report. Performance data has been taken from JHC:124:66:2, SRM 11 & 12 post-flight weight data.

Payload data has been taken from Martin Internal Document TM 0436/20-0005, MOL-HSQ Specification Weight Compliance Demonstration Report.

Mass Property data for Stages 0, 1 and 2 are reproduced from Weight and Balance Status Report (Preflight) SSD-CR-66-591 as vehicle changes reported here are not of appreciable significance. Due to the abnormal ACS operation and pitch-up anomaly, transtage in-flight mass property data was re-verified by the following checks:

1. HSQ actual weighing and longitudinal C.G. data were reviewed.
2. HSQ above Station 77 and transtage 3-Axis inflight mass property calculations were rerun with the post-flight propellant data incorporated.
3. The transtage dry actual weight and C.G. data were reviewed.
4. Field modifications to the transtage and HSQ were evaluated and the results incorporated in the mass properties run.
5. Identification of HSQ misalignment on the stand was made with proper adjustments incorporated in the mass property data.

The results of this investigation indicated no significant changes in mass properties. The table below presents mass properties for the transtage/MOL-HSQ at the point in time immediately after Gemini separation at which the pitch-up anomaly occurred. The post-flight data incorporates the actual propellant load while the preflight data represents that load detailed in Weight and Balance Status Report, SSD-CR-66-591. Both assume propellants are bottomed in the tanks. Studies indicate that for the case in which the propellants are in the top of the tank there is a 15 inch shift forward in longitudinal C.G.

Transtage and MOL-HSQ Payload Less Gemini	Weight (Lbs.)	C.G.			Moment of Inertia		
		X	Y	Z	Roll	Pitch	Yaw
		(Sta.)			(Slug - ft <sup>2</sup> )		
Preflight	25,407	-35.8	-.4	59.4	11,262	203,945	204,378
Post-flight	25,327	-36.8	-.1	60.0	11,177	203,104	203,509
MOL-HSQ ONLY							
Preflight	20,383	-218.0	-.6	58.9	9,035	122,562	122,568
Post-flight	20,335	-218.1	-.7	59.5	8,990	121,644	121,654

ACS consumption is reproduced from the preflight report.

TABLE 2  
REASON FOR CHANGE  
DRY WEIGHT  
MOL-HSQ P/L

A-2

GFP	<u>ΔWT.(lbs)</u>	<u>M.S.(in.)</u>
Fuel Cell, calculated to actual	+14.02	-99.0
Signal Conditioner, remove	-20.34	-126.7
OV-4 Transmitter, calculated to actual	+10.40	-319.5
OV-4 Receiver, calculated to actual	+ 4.90	-319.5
Separation Safe & Arm Box, calculated to actual	+ 7.75	-319.5
HTTC Experiment, calculated to actual	+17.00	-234.0
Zero "G" Prop. Gauge Exp., calculated to actual	-16.00	-105.9
Antenna, calculated to actual	+ 0.14	-104.5
Fwd. Micro Meteoroid Detector, cal. to actual	- 1.13	-234.5
Side Micro Meteoroid Detector, cal. to actual	- 1.13	-234.5
Corner Reflector, calculated to actual	- 2.40	-176.1
Retro Motor Assembly, calculated to actual	+ 0.33	-265.6
Panel Assemblies, remove	-37.02	-270.0
TOTAL	(-23.48)	(-101.6)
Ballast		
Ballast Bar, machine to fit	- 5.20	- 98.7
Ballast Bar, machine to fit	- 5.05	-108.1
Ballast Bar, machine to fit	- 6.75	-117.6
Ballast Bar, machine to fit	- 6.65	-127.0
Ballast Bar, machine to fit	- 2.10	-136.0
TOTAL	(-25.75)	(-115.8)
Ship Separate		
Battery, calculated to actual	- 2.51	58.0
Battery, calculated to actual	- 3.26	55.5
Cable Cutter Cartridge, Install	+ 0.70	---
Time Delay Relay Installation	+ 1.06	---
TOTAL	(- 4.01)	(81.4)
Gemini + Adapter, predicted to actual	(5.0)	(-399.9)
TOTAL	((-48.24))	((-63.4))

## REASONS FOR CHANGE

## VEHICLE 9

## DRY WEIGHT

Step I Post-Flight Total	(72.0)
*Spec. Compliance Total	(71.4)
*Recode 12 Separation Studs 80801B50040-023	+ 8.1

## From Step II to Step I

*Recode 12 Separation Washers 50A7C 1216A	+ 1.0
---	-------

## From Step II to Step I

*Step I Splice Bolt Delta	+ .5
*Step I Destruct Charge Delta PD60S0135-501	- .7
*Step I Destruct Initiator Delta PD64S0336-513	- 1.0
*Explosive Bolt Installation Delta PD26S0022-011	- .3
*Step O to Step I Separation Device (Outrigger) Delta PD33S0007-005	+ 3.4
*Step O to Step I Separation Device Hardware Delta 80802B50027-001,-003,-005	+ 4.5
Installation of Frame on Engine Covers	- 1.6
*Insulating Tape Delta	+ 3.6
*Start Cartridge Air Conditioning System Delta	- 1.1
*Installation of Eager Pak	+ 1.5
*Addition of Staging Camera	+ 58.8
Boattail Instrumentation Addition	+ 2.2
*Step O to Step I Separation Device Hardware Delta 80802B50027-009,-011,-013	- 1.0
*Misc.	- 5.0
Step II Post-Flight Total	(65.6)
*Spec Compliance Total	(65.6)
*Recode 12 Separation Studs 80801B50040-023	- 8.1

## From Step II to Step I

*Recode 12 Separation Washers 50 A7C1216A	- 1.0
---	-------

## From Step II to Step I

*Recode 8 Separation Studs 80801B50040-021	+ 5.4
--	-------

## From Step III to Step II

*Recode 8 Separation Nuts PD33S0007-005	+ 6.2
---	-------

## From Step III to Step II

*Recode 8 Separation Washers 50A7C1216A	+ 1.2
---	-------

## From Step III to Step II

*Step II Destruct Charge Delta PD60S0135-501	- 1.7
--	-------

## Step II (cont'd)

*Step II Destruct Initiator Delta PD64S0336-513	- 1.0
*Ablative Skirt & Attachment Hardware	+ 6.5
*Start Cartridge Air Conditioning System Delta	- 1.4
*Installation of Eager Pak	+ 1.5
*Addition of Staging Camera	+57.6
*Misc.	+ .4

Step III Post-Flight Total	(-16.6)
----------------------------	---------

*Spec. Compliance Total	(-15.7)
-------------------------	---------

*Recode 8 Separation Nuts PD33SC007-005	- 0.2
---	-------

From Step III to Step II

*Recode 8 Separation Studs 80801B50040-021	- 5.4
--	-------

From Step III to Step II

*Recode 8 Separation Washers 50A7C1216A	- 1.2
---	-------

From Step III to Step II

*Step III Destruct Charge Delta PD60S0135-501	- 1.5
---	-------

*Step III Destruct Initiator Delta PD64S0336-513	- 1.0
--	-------

Installation of Nozzle Extension Kits	- 1.4
---------------------------------------	-------

*Removal of Electrical Connectors	- 1.0
-----------------------------------	-------

*Thermal Insulation Blanket Delta	- 5.0
-----------------------------------	-------

Installation of IGS/PTC	+ 1.4
-------------------------	-------

Installation of IGS/MGC	- .5
-------------------------	------

*Installation of ACS Pitch Engines	- 1.2
------------------------------------	-------

*Installation of ACS Roll/Yaw Engines	- 2.3
---------------------------------------	-------

*Installation of ACS Roll/Yaw Engine Covers	+ .5
---	------

*Installation of Glotrac Transmitter	+ .8
--------------------------------------	------

*Add Nut Plates to T/S Doors	+ 2.0
------------------------------	-------

*Add Measurement to ACS Engine	+ 3.3
--------------------------------	-------

*Misc.	+ 2.1
--------	-------

\*Specification compliance item

**624A PERFORMANCE WEIGHT SUMMARY**

PAGE \_\_\_\_\_

**VEHICLE ON. 9 (CONFIG. "C")**

DATE \_\_\_\_\_

REPORT Post Flight

ITEM	STEP WEIGHT SUMMARY					
	STEP 0	STEP I	STEP II	STEP III		STEP IV
				IIIa	IIIb	
BODY	22,910	7,674	3,346	156	368	
SEPARATION AND DESTRUCT	2,715	395	241	88	166	
PROPULSION	109,239	3,942	1,560	1975	6	
POWER GENERATING	1,242	278	234	65	245	
ORIENTATION CONTROL	21,212	238	175	119	253	
GUIDANCE		28	27		895	
ENVIRONMENTAL CONTROL	1,241	213	52	97	14	
INSTRUMENTATION OPERATING	756					
ENGINE HEAT SHIELD		1,233				
GROWTH ALLOWANCE						
WEIGHT EMPTY	159,315	14,001	5,635	2,500	1,947	
TELEMETERING	1,745	636	761	113	540	20,359
PAYLOAD						
PAYLOAD FAIRING						
DEVIATION		-125	-100		-30	
UNACCOUNTABLE VARIATION		-116	-156		+22	
SPECIAL PAYLOADS						
FIELD MODIFICATIONS		+72	+66	-16		-48
STAGING CAMERAS		198	175			
INCORPORATION OF DESIGN CHANGES			+50		-26	
DRY WEIGHT TOLERANCE						
DRY WEIGHT	161,060	14,668	6,431	5,050		20,311
PRESSURE GAS	2,976	28	10	52	4	
LUBRICANT		17	5			
IGNITER	176	9	3			
IGS COOLANT AND GAS					23	
ATTITUDE CONTROL					125	
PROPELLANTS						
LIQUID PROPELLANTS		251,235	66,631	21,090		24
SOLID PROPELLANTS	844,390					
TVC INJECTANT	27,361					
STEP WT. LOADED	1,035,963	265,957	73,080			20,335
				26,344		
LOADED WT. STAGE 0	1,421,679					



VEHICLE NO. 9

FLIGHT PLAN \_\_\_\_\_

ITEM	STEP WEIGHT SUMMARY					STAGE WEIGHT SUMMARY
	STEP 0	STEP 1	STEP 2	STEP 3	STEP 4	
Loaded Wt. Stage 0	1,035,963	265,957	73,080	26,344	20,335	1,421,679
Igniter Charge	-176					
Start Propellant	-282					
Engine Bleed & Leakage						
Weather Seal - Nozzle	-120					
Step Wt. Liftoff	1,035,385	265,957	73,080	26,344	20,335	
Liftoff Wt. - Stage 0						1,421,101
Nominal Steady State Prop	-809,390					
TVC Injectant	-19,679					
Ablative Material	-9,020					
Engine Bleed & Leakage		-29	-7			
Step Wt. - End Web Action	197,296	265,928	73,073	26,344	20,335	
Stage 0 Wt. - End Web Action						582,976
Solid Propellant	-18,058					
TVC Injectant	-82					
Step Wt. Stg. 1 FS-1	179,156	265,928	73,073	26,344	20,335	
Stg. 0 Wt. Stg. 1 FS-1						564,836
Solid Propellant	-12,673					
TVC Injectant	-277					
Ablative Material	-24					
Engine Heat Shield		-291				
Stage 1 Igniter Charge		-9				
Stage 1 Start Propellant		-242				
Stage 1 Steady State Prop.		-8,850				
Step Wt. Mid Point	166,182	256,536	73,073	26,344	20,335	
Stage 0 Wt. Mid Point						542,470
Solid Propellant	-3,977					
TVC Injectant						
Stg. 1 Steady State		-9,092				
Step Wt. Stg. 0 Jettison	162,205	247,444	73,073	26,344	20,335	
Stage 0 Wt. at Jettison						529,401
Step 0 Jettison Wt.	-162,205					
Step Wt. Stage 1 Separation		247,444	73,073	26,344	20,335	
Stage 1 Wt. at Separation						367,196
Nominal Steady State		-231,228				
Engine Bleed		-12	-10			
Staging Cameras		-58	-57			
Step Wt. Stg. 1 End Eff. Burn		16,146	73,006	26,344	20,335	
Stage 1 Wt. - End Eff. Burn						135,831
Shutdown Propellant		-146				

VEHICLE NO. 9

FLIGHT PLAN NO.

PAGE

A-7

REPORT PostFlight

ITEM	STEP WEIGHT SUMMARY					STAGE WEIGHT SUMMARY
	STEP 0	STEP I	STEP II	STEP III	STEP IV	
STEP WT. - STAGE I BURNOUT		16,000	73,006	26,344	20,335	
STAGE I WT. AT BURNOUT						135,685
STEP I BURNOUT WT.		-16,000				
STEP WT. - STAGE II START			73,006	26,344	20,335	
STAGE WT. AT START						119,685
IGNITER CHARGE START PROPELLANT			-3 -183			
STEP WT. - STAGE II START EFF. BURNING			72,820	26,344	20,335	
STAGE II WT. - START EFF. BURNING						119,499
NOMINAL STEADY STATE PROPELLANT ENGINE BLEED AND LEAKAGE ABLATIVE MATERIAL			-65,470 -8 -58			
STEP WT. STAGE II END EFF. BURNING			7,284	26,344	20,335	
STAGE II WT. - END EFF. BURNING						53,963
SHUTDOWN PROPELLANT TAILOFF			-98			
STEP WT. - STAGE II BURNOUT			7,186	26,344	20,335	
STAGE II WT. AT BURNOUT						53,865
STEP II BURNOUT WT. BOTTOMING PROPELLANT			-7,186	-8		
STEP WT. AT STAGE III START				26,336	20,335	
STAGE III WT. - START 1st BURN PERIOD						46,671
START PROPELLANT				-5		
STEP WT. AT STAGE III START 1st BURN				26,331	20,335	
STAGE III WT. AT START 1st BURN						46,666
NOMINAL STEADY STATE PROPELLANT ABLATIVE MATERIAL				-16,526 -26		
STEP WT. AT STAGE III END 1st BURN				9,779	20,335	
STAGE III WT. AT END 1st BURN						30,114
SHUTDOWN PROPELLANT				-8		
STEP WT. AT STAGE III START 1st COAST				9,771	20,335	
STAGE III WT. AT START 1st COAST						30,106
Elect Gemini ATTITUDE CONTROL PROPELLANT IGS COOLANT Fire Retro Rockets				-8 -1 -24	-4,730	

VEHICLE NO. 9 FLIGHT PLAN NO. \_\_\_\_\_REPORT POSTFLIGHT

ITEM	STEP WEIGHT SUMMARY					STAGE WEIGHT SUMMARY
	STEP 0	STEP I	STEP II	STEP III	STEP IV	
STEP WT. AT STAGE III END 1st COAST				9,762	15,581	
STAGE III WT. - END 1st COAST						25,343
BOTTOMING PROPELLANT START PROPELLANT				-11 - 5		
STEP WT. AT STAGE III START 2nd BURN				9,746	15,581	
STAGE III WT AT START 2nd BURN						25,327
NOMINAL STEADY STATE PROPELLANT ABLATIVE MATERIAL				-2,302 - 3		
STEP WT. AT STAGE III END 2nd BURN				7,441	15,581	
STAGE III WT. AT END 2nd BURN						23,022
SHUTDOWN PROPELLANT				- 8		
STEP WT. AT STAGE III START 2nd COAST				7,433	15,581	
STAGE III WT. AT START 2nd COAST						23,014
ATTITUDE CONTROL PROPELLANT IGS COOLANT				- 6 - 1		
STEP WT. AT STAGE III END 2nd COAST				7,426	15,581	
STAGE III WT. END 2nd COAST						23,007
BOTTOMING PROPELLANT START PROPELLANT				- 8 - 5		
STEP WT. AT STAGE III START 3rd BURN				7,413	15,581	
STAGE III WT. AT START 3rd BURN						22,994
NOMINAL STEADY STATE PROPELLANT ABLATIVE MATERIAL				-306		
STEP WT. AT STAGE III END 3rd BURN				7,107	15,581	
STAGE III WT. AT END 3rd BURN						22,688
SHUTDOWN				- 8		
STEP WT. AT STAGE III START 3rd COAST				7,099	15,581	
STAGE III WT. AT START 3rd COAST						22,680
ATTITUDE CONTROL PROPELLANT IGS COOLANT / EJECTION OF SATS.				- 56 - 16	-987	
STEP WT. AT STAGE III BURNOUT				7,027	14,594	
STAGE III BURNOUT WEIGHT						21,621
STEP III BURNOUT WT.						
STEP WT. - STAGE 4						
STAGE 4 WEIGHT						

PAGE \_\_\_\_\_

DATE \_\_\_\_\_

REPORT \_\_\_\_\_

# 624A LIQUID PROPELLANT INVENTORY

## CONFIGURATION C

## VEHICLE 9

FLIGHT PLAN NO. \_\_\_\_\_

		STEP I	STEP II	STEP III
1. ENGINE NUMBER		6241010	6242015	6243026 6243027
2. AVERAGE INFLIGHT MIXTURE RATIO		1.959 (1)	1.797 (1)	1.94 (1)
3. PROPELLANT TEMPERATURE*	FUEL	63.0	65.3	68.
	OXID.	67.3	65.6	66.
4. PROPELLANT DENSITY	FUEL	56.55	56.48	---
	OXID.	90.26	90.39	
5. MAXIMUM LOADABLE VOLUME	FUEL	N/A	N/A	N/A
	OXID.			
6. NOMINAL PROPELLANT LOADED, LBS.	TOTAL	251235	66631	21090
	FUEL	85387 (2)	24209 (2)	7121
	OXID.	165848 (2)	42422 (2)	13969
7. PROPELLANT EXPENDED BEFORE LIFTOFF	TOTAL	0	0	0
	FUEL	0	0	0
	OXID.	0	0	0
a. ENGINE BLEED	FUEL	0	0	0
	OXID.	0	0	0
b. ENGINE LEAKAGE	FUEL	0	0	0
	OXID.	0	0	0
c. START CONSUMPTION, 87FS1 TO TCPS	FUEL	N/A	N/A	N/A
	OXID.			
d. HOLD DOWN CONSUMPTION, TCPS TO LIFTOFF	FUEL	N/A	N/A	N/A
	OXID.			
8. PROPELLANT ABOARD AT LIFTOFF	TOTAL	251235	66631	21090
	FUEL	85387	24209	7121
	OXID.	165848	42422	13969
9. PROPELLANT EXPENDED DURING PREVIOUS STAGE OPERATION	TOTAL	29	17	0
	FUEL	28	17	0
	OXID.	1	0	0
a. ENGINE BLEED, STAGE 0 OPERATION	FUEL	28	7	0
	OXID.	0	0	0
b. ENGINE LEAKAGE, STAGE 0 OPERATION	FUEL	0	0	0
	OXID.	1	0	0
c. ENGINE BLEED, STAGE I OPERATION	FUEL	N/A	10	0
	OXID.		0	0
d. ENGINE LEAKAGE, STAGE I OPERATION	FUEL	N/A	0	0
	OXID.		0	0

\*ENTIRE PROPELLANT LOADING IS HIGHLY DEPENDENT ON TEMPERATURE

PAGE \_\_\_\_\_

REPORT \_\_\_\_\_

		STEP I	STEP II	STEP III
10. PROPELLANT ABOARD AT FS 1	TOTAL	251206	66614	21090
	FUEL	85359	24192	7121
	OXID.	165847	42422	13969
11. ENGINE LEAKAGE DURING STAGE OPERATION	TOTAL	12	8	0
	FUEL	11	7	0
	OXID.	1	1	0
12. TOTAL AVAILABLE USABLE PROPELLANT	TOTAL	250072 (4)	66196 (5)	21056 (6)
	FUEL	84900 (4)	24029 (5)	7118 (6)
	OXID.	165172 (4)	42167 (5)	13938 (6)
a. START CONSUMPTION	FUEL	41 (3)	51 (3)	6 (3)
	OXID.	201 (3)	132 (3)	9 (3)
b. STEADY STATE	FUEL	84119 (4)	23435 (5)	6508
	OXID.	164971	42035	12626
c. SHUTDOWN CONSUMPTION	FUEL	146	98	9 (3)
	OXID.	0	0	15 (3)
d. TAIL OFF (PRIOR TO STAGING)	FUEL	N/A	---	N/A
	OXID.	N/A	N/A	N/A
e. FUEL BIAS	FUEL	N/A	N/A	N/A
	OXID.	N/A	N/A	N/A
13. TOTAL NON-USABLE PROPELLANT	TOTAL	1122	410	34
	FUEL	448	156	3 (3)
	OXID.	674	254	31 (3)
a. PROPELLANT VAPOR RETAINED	FUEL	108	63	3
	OXID.	500	191	31
b. TRAPPED ABOVE INTERFACE	FUEL	43 (3)	64 (3)	0
	OXID.	0	25 (3)	0
c. TRAPPED BELOW INTERFACE	FUEL	297 (3)	29 (3)	0
	OXID.	174 (3)	38 (3)	0
14. OUTAGE	TOTAL	514 (F)	445 (F)	135 (OX)
15. NOMINAL PROPELLANT CONSUMED DURING STAGE OPERATION	TOTAL	249558	65751	19173 (7)
a. STEADY STATE PROPELLANT	TOTAL	249170	65470	19134 (7)
b. TRANSIENT PROPELLANTS	TOTAL	388	281	39
16. PRESSURIZATION SYSTEM INERT GAS	TOTAL	28	10	52
	FUEL	16	6	3
	OXID.	12	4	4
	SPHERES	N/A	N/A	45

TITAN III PROPULSION UNIT 0441

PREPARED BY: G. B. Bester - BachmanAPPROVED BY: W. G. ThomasDATE: 12/4-66

- (1) Based on level sensor readings.
- (2) Average of flow meter readings.
- (3) Assumed same as preflight prediction with appropriate temperature corrections.
- (4) Includes 514 lb. of fuel outage.
- (5) Includes 445 lb. of fuel outage.
- (6) Includes 595 lb. of fuel residual and 1153 lb. of oxidizer residual plus 135 lb. of oxidizer outage.
- (7) Excludes 595 lb. of fuel residual and 1153 lb. of oxidizer residual.

## MOL/HSQ Payload

<u>Martin Responsibility</u>	(11,885)	(-115.0)	( -2.9)	( 58.4)
Basic Structure	5,592	-110.0	+0.7	58.8
Experiment Support	2,385	-201.2	-13.3	62.8

## Structure &amp; System

Instrumentation, Electrical and Guidance	1,730	-9.5	-1.2	63.5
Ballast	2,178	-117.1	-2.1	48.4

GFE	( 8,450)	(-363.2)	( 3.9)	( 59.7)
Gemini & Adapter	6,410	-400.1	0.0	58.7
OV-1	490	-307.6	17.5	77.5
OV-4 Transmitter	317	-318.9	17.6	40.3
OV-4 Receiver	379	-320.0	-18.5	41.5
Protuberance	97	-302.0	59.0	29.0
HTFC	90	-234.0	51.0	100.0
Micrometeroid Detector, Fwd	5	-367.0	-15.0	65.0
Micrometeroid Detector, Side	5	-102.0	-7.7	119.3
Orbis Low Transmitter	3	-104.0	8.0	4.0
Orbis Low Antenna	3	-104.0	8.0	4.0
Corner Reflectors	61	-176.1	-4.7	62.7
Bio Cell	3	-103.4	53.0	56.0
Zero "G" Propellant Gauge	439	-105.9	38.0	82.0
Fuel Cell	47	-99.0	-25.0	17.0
Resolution Paint Pattern	25	-96.5	0.0	60.0
Simulated ACS	26	-302.0	-56.5	92.0

## Total Payload

Wt = 20,335	$I_x = 41,650,000 \text{ lb-in}^2$
X = -218.1	$I_y = 563,576,000 \text{ lb-in}^2$
Y = -0.07	$I_z = 563,624,000 \text{ lb-in}^2$
Z = 58.9	

EJECTED ITEMS

<u>Item</u>	<u>Wt.</u>	<u>X</u>	<u>Y</u>	<u>Z</u>	<u><math>I_x</math></u> <u>(lb-in<sup>2</sup>)</u>	<u><math>I_y</math></u> <u>(lb-in<sup>2</sup>)</u>	<u><math>I_z</math></u> <u>(lb-in<sup>2</sup>)</u>
Gemini	4730	-415.6	0.0	57.9	3,428,198	7,718,191	7,273,446
OV-1	437	-309.8	17.5	77.5	34,284	68,105	72,274
OV-4 Trans.	255	-320.2	17.6	40.3	7,958	17,172	17,800
OV-4 Rec.	308	-321.3	-18.5	41.5	12,615	16,522	17,370
Stage I Camera	58	954.8	-63.0	90.0	1,04	2,736	2,736
Stage II Camera	57	364.6	58.9	26.0	404	2,848	2,848
Stage I Eng. Cover	291	1350.0	0.0	60.0	385,965	315,481	70,918



## MASS PROPERTY DATA

DATE: \_\_\_\_\_

VEHICLE 79

PAYLOAD \_\_\_\_\_

REPORT \_\_\_\_\_

Point Description	Weight	CG X Y   Z	Roll Io Slug Ft <sup>2</sup>	Pitch Io Slug Ft <sup>2</sup>	Yaw Io Slug Ft <sup>2</sup>
Stage 0 Prior to Lif* Off	1,421,638	829.1 .1   60.0	4,037,582	25,596,543	29,059,571
Stage 0 10 Sec	1,325,276	828.9 .1   60.0	3,674,036	24,338,620	27,471,693
Stage 0 20 Sec	1,228,810	827.9 .1   60.0	3,313,387	23,129,190	25,931,316
Stage 0 30 Sec	1,136,910	825.7 .1   60.0	2,970,070	22,046,422	24,538,138
Stage 0 40 Sec	1,051,682	821.4 .1   60.0	2,650,526	21,113,557	23,318,026
Stage 0 50 Sec	971,393	815.7 .1   60.0	2,343,467	20,300,011	22,233,274
Stage 0 60 Sec	894,814	809.2 .1   60.0	2,044,266	19,522,784	21,194,473
Stage 0 70 Sec	820,767	801.7 .1   60.0	1,755,518	18,796,873	20,218,720
Stage 0 80 Sec	749,467	794.0 .1   60.0	1,473,575	18,120,212	19,301,536
Stage 0 90 Sec	680,364	785.6 .1   60.0	1,196,613	17,474,419	18,422,071
Stage 0 100 Sec	612,390	776.2 .1   60.0	917,369	16,837,759	17,553,955
Stage 0 EWAT	583,507	772.3 .1   60.0	798,295	16,593,027	17,211,365
Stage 0 FS-1	564,121	769.8 .1   60.0	717,720	16,416,222	16,967,009
Stage 0 Midpoint	541,782	767.9 .1   60.0	664,244	16,225,754	16,732,695
Stage 0 Jettison	530,152	767.6 .1   60.0	653,045	16,156,169	16,654,257
Stage 1 90% Steady State	360,257	676.3 .1   60.0	26,498	11,330,425	11,333,613
Stage 1 80% Steady State	335,251	667.7 .1   60.0	26,381	11,118,234	11,125,671
Stage 1 70% Steady State	310,370	665.7 .1   60.0	26,380	10,858,225	10,861,346

## MASS PROPERTY DATA

DATE: \_\_\_\_\_

VEHICLE #9

PAYLOAD \_\_\_\_\_

REPORT \_\_\_\_\_

Point Description	Weight	CG X		Roll Io Slug Ft <sup>2</sup>	Pitch Io Slug Ft <sup>2</sup>	Yaw Io Slug Ft <sup>2</sup>
		Y	Z			
Stage 1 60% Steady State	285,488	.1	60.0	26,380	10,523,614	10,526,735
Stage 1 50% Steady State	260,606	.1	60.0	26,380	10,083,837	10,086,958
Stage 1 40% Steady State	235,725	.1	60.0	26,380	9,503,699	9,506,820
Stage 1 30% Steady State	210,843	.2	60.0	26,380	8,711,249	8,714,370
Stage 1 20% Steady State	185,962	.2	60.0	26,380	7,619,681	7,622,801
Stage 1 10% Steady State	161,081	.2	60.0	26,380	6,077,124	6,080,244
Stage 1 Shutdown	136,176	.2	60.0	26,380	3,756,373	3,759,492
Stage 1 Burnout	135,846	.2	60.0	26,380	3,696,820	3,699,940
Stage 2 Start	119,929	.4	59.9	18,254	1,385,589	1,388,610
Stage 2 100% Steady State	119,743	.4	59.9	18,254	1,385,165	1,388,185
Stage 2 90% Steady State	113,146	.4	59.9	18,254	1,362,435	1,365,456
Stage 2 80% Steady State	106,554	.4	59.8	18,253	1,335,042	1,338,063
Stage 2 70% Steady State	99,960	.5	59.8	18,253	1,301,340	1,304,360
Stage 2 60% Steady State	93,368	.5	59.8	18,253	1,260,631	1,263,650
Stage 2 50% Steady State	86,775	.5	59.8	18,252	1,210,831	1,213,851
Stage 2 40% Steady State	80,181	.6	59.8	18,252	1,149,547	1,152,566
Stage 2 30% Steady State	73,589	.6	59.8	18,251	1,074,329	1,077,347
Stage 2 20% Steady State	66,996	.7	59.8	18,250	980,235	983,253

**A-16**

### MASS PROPERTY DATA

**DATE:**

VEHICLE #9

**PAYLOAD** \_\_\_\_\_

## REPORT

[illegible]

A-17

## MASS PROPERTY DATA

DATE: \_\_\_\_\_

## STAGE 3 OPERATION

VEHICLE 9

PAYLOAD \_\_\_\_\_

REPORT POSTFLIGHT

Point Description	Weight	CG X Y   Z	Roll Io Slug Ft <sup>2</sup>	Pitch Io Slug Ft <sup>2</sup>	Yaw Io Slug Ft <sup>2</sup>
Stage III Start 1st Burn	46,666	-13.2 1.0   59.9	14,660	457,143	460,160
Stage III 75% 1st Burn	42,497	-25.0 .8   59.9	13,980	442,494	444,932
Stage III 50% 1st Burn	38,360	-35.5 .5   59.8	13,302	440,078	441,130
Stage III 25% 1st Burn	34,222	-63.9 .2   59.8	12,621	384,569	385,525
Stage III End 1st Burn	30,106	-96.3 -.2   59.8	11,936	328,055	328,348
Stage III Start 2nd Burn	25,327	-36.8 -.1   60.0	11,177	203,104	203,509
Stage III 50% 2nd Burn	24,145	-47.0 -.4   60.0	10,990	190,891	191,109
Stage III End 2nd Burn	23,014	-58.8 -.6   60.0	10,800	176,506	176,533
Stage III Start 3rd Burn	22,994	-59.0 -.6   60.0	10,198	176,364	176,391
Stage III End 3rd Burn	22,680	-62.4 -.6   60.0	10,747	171,125	172,100
Stage III Eject OV-1	22,171	-57.6 -1.0   59.7	10,679	166,158	166,130
Stage III Eject OV-4 Trans.	21,926	-54.7 -1.2   59.9	10,638	162,420	162,399
Stage III Eject OV-4 Rec.	21,680	-50.9 -.9   60.2	10,593	157,644	157,620
Stage III Burnout	21,621	-51.3 -.9   60.2	10,586	157,411	157,389

CON/.

**SUPPLEMENTARY**

**INFORMATION**

MARTIN MARIETTA CORPORATION

CONTRACT NO. AF 04(695)-150

COPY NO.  
DATE 13 March 1967**DOCUMENT CHANGE INSTRUCTION**

FORM DEN 1016-02 (2-64)

ENCLOSURE: Rev. 1, Pages 213A, 213B, 215A, 215B, 244A, 244B, and 244C.

TITLE: SSLV-5 No. 9 Post Firing Flight Test Report (Final Evaluation Report) and MOL-EFT Final Flight Test Report (U) SSD-CR-66-707

## INSTRUCTIONS:

The purpose of this revision is to include additional MOL payload environmental analysis which was not available when the document was originally published.

Insert the enclosed pages in sequence following the corresponding basic pages of the report.

REFERENCE: CDRL Line Items IK-62 and 3C-4

FILE THIS PAGE IN THE FRONT OF THE DOCUMENT TO INDICATE THE LATEST CHANGE.

#### 3.2.6.1.4 Payload Thermal Analysis

Seventeen payload temperatures were reduced and compared to pre-flight predictions. Forward skin temperatures were within two (2) degrees of the aeroheating predictions during boost phase. Fuel cell cover temperatures compared within ten (10) degrees of those predicted during the free pitch and roll orbital coast.

The configuration of the MOL Sim Lab environmental instrumentation which was reduced for this analysis are shown in Tables 24A and 24B. Figure 127A shows the skin temperature locations in reference to the paint pattern.

The pre-flight analysis included a thermal model of the laboratory, experiments, and equipment of the lumped mass node type. This analysis resulted in predictions of maximum temperatures for the orbital and boost phases of the flight.

Table 24A lists the outer skin temperatures recorded during the boost phase. The maximum temperatures which were predicted were within two (2) degrees of those experienced in flight. Measurements 0204 and 0205 reached 182°F at T + 120 and 160 seconds respectively which compared with the predicted temperature of 180°F. Measurements 0201, 0202, and 0203 were 30 to 40°F cooler than the predicted 170°F. Figure 127A presents the skin paint pattern and Figures 127B and 127C present the skin temperature data obtained to T + 53 minutes. Figure 127B presents the skin temperatures on an expanded scale for easier interpretation of the aeroheating effects.



3.2.6.1.4 Payload Thermal Analysis (Cont'd)

Tables 2<sup>4</sup>B and 2<sup>4</sup>C present the fuel cell temperature descriptions and the data obtained. Measurements 6114 through 6116 were located on the outer fuel cell cover. These temperatures were expected to stabilize in a band of  $75 \pm 3^{\circ}\text{F}$  during the fuel cell operation. Flight data indicated (ref. Table 2<sup>4</sup>C) that the cover temperatures stabilized in a band of  $83 \pm 9^{\circ}\text{F}$ . Measurement 6117 located under the fuel cell on stringer 3 was about  $10^{\circ}\text{F}$  higher than the predicted temperature for the skin in that area. However, since this was essentially a bracket temperature, an elevated temperature would be expected. Fuel cell operating temperatures were within expected temperature limits. The data included in Table 2<sup>4</sup>B was presented as single-point data because it was found to be nearly constant over the data acquisition period of about six (6) minutes for each pass.

In conclusion, the thermal performance of the skin and fuel cell temperatures was found to agree with the preflight predictions. The thermal model may be relied upon to closely predict aeroheating environment for future flights of similar payload configurations.

Table 24A

## MOL Skin Temperature Description

Meas. No.	Description	Location	Paint
0201	Temperature-Lab Forward Skirt Skin	Station-308 170° From TGT	Black
0202	Temperature-Lab Forward Skirt Skin	Station-324 10° From TGT	Black
0203	Temperature-Lab Forward Skirt Skin	Station-309 10° From TGT	Black
0204	Temperature-Lab Tank Skin	Station-270 350° From TGT	Iridite
0205	Temperature-Lab Tank Skin	Station-350 350° From TGT	Gemini Adapter
0206	Temperature-Lab Aft Skirt	Station-8 10° From TGT	Alum. Paint

Table 24B

## Fuel Cell Temperature Description

Measurement No.	Description	Location Station
6108	Fuel Cell Water Outlet	-112.5 BTW STR 6-7
6109	Fuel Cell Load Radiator	
6110	Fuel Cell External #1	
6111	Fuel Cell External #2	
6112	Fuel Cell External #3	-112 F.C. Cover
6113	Fuel Cell External #4	
6114	Fuel Cell Structural #1	
6115	Fuel Cell Structural #2	
6116	Fuel Cell Structural #3	-112 F.C. Cover
6117	Fuel Cell Structural #4	-117 STR 3 Under F.C.

215B  
Rev 1

Table 24C

Flight Fuel Cell Temperatures

Pass	1	12	14	28	32	58	76	89	92	434
Time	15:32:25	07:40:00	10:56:00	09:26:43	14:12:40	06:31:02	08:18:52	05:15:40	08:21:20	18:29:40
Date	11-03-66	11-04-66	11-04-66	11-05-66	11-05-66	11-07-66	11-08-66	11-09-66	11-09-66	11-30-66
Measurement No.										
6108	85	112	110	110	105	108	107	33	31	44
6109	55	35	35	35	50	50	43	60	32	65
6110	189	192	192	194	194	195	194	Fuel	Cell	Off
6111	197	195	196	197	196	200	198	↓	↓	↓
6112	194	189	190	192	192	197	199	↓	↓	↓
6113	190	187	189	191	191	195	196	↓	↓	↓
6114	77	92	90	87	83	83	80	34	29	48
6115	82	92	91	87	84	85	85	40	33	50
6116	77	88	83	83	76	75	75	40	30	49
6117	57	43	38	38	49	25	33	20	21	30

Figure 127A  
MOL HSQ Exterior Finish  
and Skin Temperature Location

STA	TGT						205*		
-327	↓	* 202							
		* 203							
		B* 201							
-292.8		A	C	A	C	A	204*		
-241.9		B		B		B	C		
-196.7		A		A		A			
-157.1		B		B		B			
-123.2		A		A		A			
- 94.9		B		B		B			
- 72.3		A		A		A			
- 55.3		B		B		B			
- 44.0		A		A		A			
- 38.3									
- 25.0		B							
		D							
		*206							

77

Finish Code:

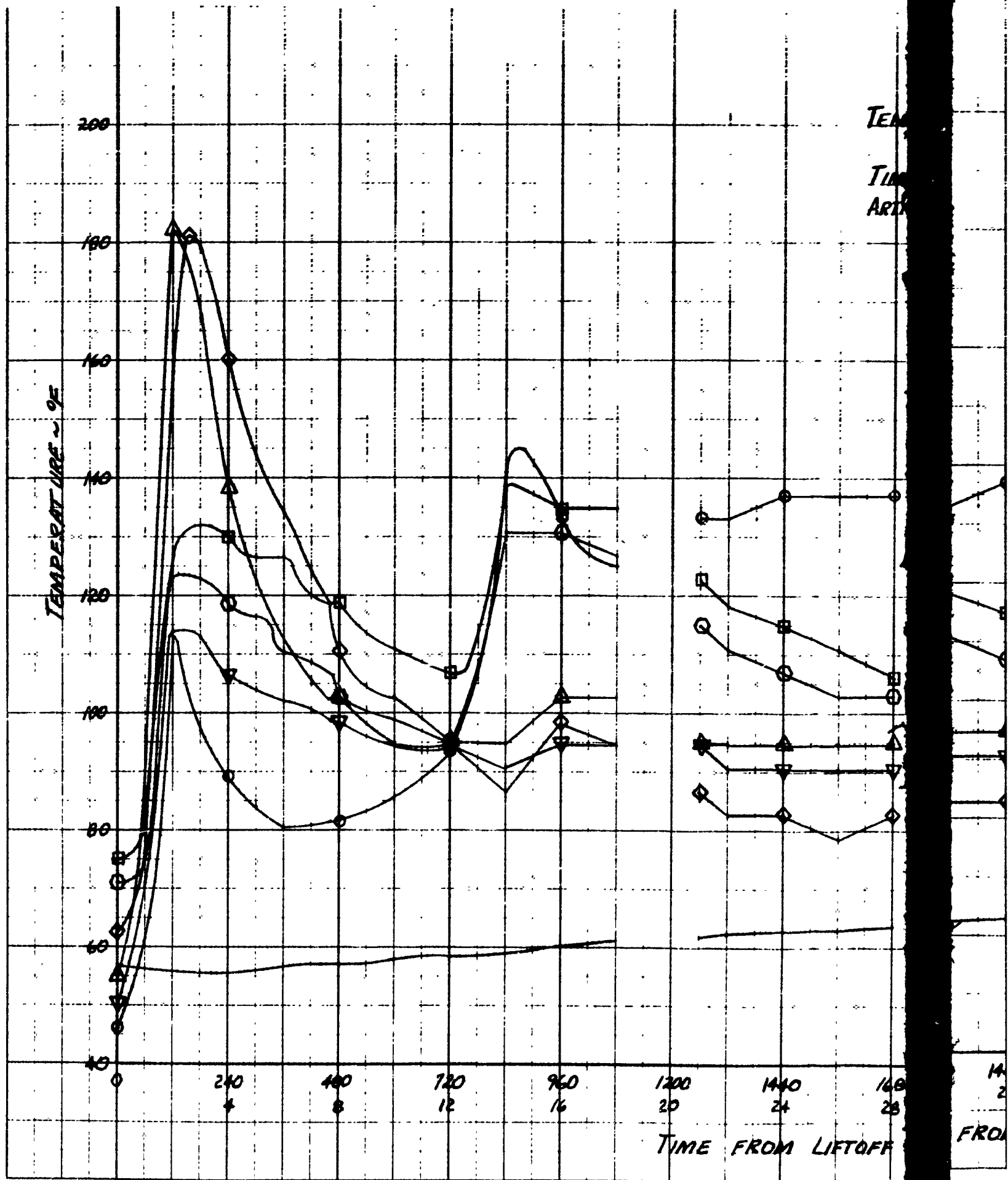
A ~ White Paint  
B ~ Black Paint  
C ~ Iridite  
D ~ Aluminum

Finish 603 MMSK 227-A  
Finish 604 MMSK 227-B  
Finish 198  
Finish 715 MMSK 453 Type -1

Antenna Covers not shown



1



2

244C  
Rev. 1

Figure 127C

TEMPERATURE  
VS  
TIME FROM LIFTOFF  
ARTICLE 9 PAYLOAD - MQL

		TEMP	LAB	FWD	SKIRT	SKIN	STEAM
○ ~	201						-308 ~ 170
□ ~	202	"	"	"	"	"	-324 ~ 187
○ ~	203	"	"	"	"	"	-309 ~ 167
△ ~	204	"	"	TANK	SKIN		-278 ~ 350
◇ ~	205	"	"	"	"		-350 ~ 350
▽ ~	206	"	"	AFT	SKIRT		8 ~ 167
- ~	207	"	"	AIR	TANK		

